

Optimisation of Microbial Fuel Cells (MFCs) through bacterial-robot interaction



Pavlina Theodosiou

Faculty of Environment and Technology

University of the West of England, Bristol

This dissertation is submitted for the degree of

Doctor of Philosophy

I would like to dedicate this thesis to my best friend and partner, for her loving support and encouragement over the past years that kept me going even in the most difficult times. Without you, by my side, I am sure I would not have been here!

Thanks for everything!

Declaration

I declare that the work in this dissertation was carried out in accordance with the requirements of the University's Regulations and Code of Practise for Research Degree Programmes and that it has not been submitted for any other academic award. Except where indicated by specific reference in the text, the work is the candidate's own work. Work done in collaboration with, or with the assistance of, others is indicated as such. Any views expressed in this dissertation are those of the author.

Pavlina Theodosiou

01/09/2019

Acknowledgments

This thesis would not have been possible without the inspiration and support of a number of wonderful individuals, my thanks and appreciation goes to all of them for being part of this journey and making this thesis possible.

Firstly, I would like to express my sincere gratitude to my Director of Studies Prof. Ioannis Ieropoulos for the continuous support, for his patience, motivation, and immense knowledge. His guidance helped me in all the time of research and writing of this thesis. Yanni, I could not have imagined having a better advisor and mentor for my Ph.D. study.

Besides my DoS, I would like to thank another two equally important people that have helped me immensely throughout this journey, my supervisors Prof. John Greenman and Dr. Jonathan Winfield for their insightful comments and encouragement. I am sincerely and heartily grateful to the whole of my supervisory team for their support, guidance and for their hard questions which helped me to widen and view my research from various perspectives and have shaped me to the researcher I have become. My sincere thanks also go to Prof. Chris Melhuish for creating such an inspiring laboratory and research facility to work, learn and grow.

I thank my fellow colleagues, both current and past, at the Bristol Bioenergy Centre (BBiC). In particular, Dr. Xavier-Alexis Walter, Dr. Iwona Gajda, Dr. Carlo Santoro and Dr. Irene Merino-Jimenez for the stimulating discussions and for the constant help. Dr. Ben Taylor for his support during the initial stages of the EVOBLISS project. Dr. Jiseon You for her friendship and for all

the fun we have had in the last four years. I would like to thank also Dr. David Patton for his help in SEM and EDX analysis. Also, special thanks go to the technical team that has assisted me throughout the course of this study, in particular, Andrew Stinchcombe and Arjuna Mendis who have helped me immensely with the EvoBot. Without the precious support of the whole of BBiC team, it would not have been possible to conduct this research.

Also, I thank my EVOBLISS collaborators for their support, encouragement, and guidance throughout the project. In particular, special thanks goes to Prof. Kasper Stoy and Assistant Prof. Andres Faina from the IT University of Copenhagen., Prof. Martin Hanczyc and Silvia Holler from the University of Trento and Prof. Harald Horn, Dr. Michael Wagner and Dr. Florian Blauert from Karlsruhe Institute of Technology (KIT).

I would like to express my gratitude to the European Union's Future and Emergent Technologies Programme for funding this work under Grant Agreement No 611640 (EVOBLISS Project). Without their financial support, this work would not have been possible.

Last but not the least, I would like to thank my family for encouraging me in all of my pursuits and inspiring me to follow my dreams, I am forever indebted to them for giving me all these opportunities. I am especially grateful to my parents Konstantina and Mario who always believed in me and invested in my future despite life's hardships, and to my brother Evro for supporting me spiritually throughout this journey and my life in general.

“The role of the infinitely small in nature is infinitely great.”

— Louis Pasteur

Abstract

For over 100 years, Microbial Fuel Cells (MFCs) have been developed as eco-friendly alternatives for generating electricity via the oxidation of organic matter by bacteria. In the early 2000s, collectives of MFCs were proven feasible energy providers for low-power robots such as Gastrobot and EcoBots. Even though individual MFC units are low in power, significant progress has been achieved in terms of MFC materials and configurations, enabling them to generate higher output levels. However, up to this date, MFCs are produced and matured using conventional laboratory methods that can take up to three months to bring the MFCs to their maximum power aptitudes.

In this work, an approach to use a low-cost (£1.5k) RepRap liquid handling robot called EvoBot was employed with the aim to bring the MFCs to their maximum power ability in a shorter time span. Initially, the work focused on establishing an interface and interconnection between the living cells (in the MFC) and the robotic platform, and investigating whether the MFC voltage can trigger a feedback loop feeding mechanism. It was shown that the robot successfully matured the MFCs in 6 days and, they were also 1.4 times more powerful than conventionally matured MFCs (from 19.1 mW/m² to 26.5 mW/m²).

This work took a rounded approach in improving the overall MFC performance. 3D-printable materials that can be produced from EvoBot were in-

investigated for fabricating MFCs. MFCs employing these printable materials had almost 50% improved power output (from 66 μ W to 130 μ W) compared to the ones based on conventional, fluorinated materials. Furthermore, Evo-Bot was able to improve the fuel supply frequency and composition using evolutionarily algorithms. For the first time, this project has demonstrated that the fabrication and maintenance of MFCs can be automated using a dedicated robotic system which can result in optimised power generation of MFCs.

Contents

Contents.....	xii
List of Figures.....	xv
List of Tables.....	xix
Nomenclature.....	xxi
Chapter 1 Introduction.....	1
1.1 Overview.....	1
1.2 Thesis outline.....	2
Chapter 2 Background.....	5
2.1 Microbial Fuel Cells.....	5
2.1.1 Chronological development.....	5
2.1.2 Operation.....	10
2.1.3 Applications.....	34
2.2 MFC relevance to EVOBLISS project.....	43
2.3 Aims and Objectives.....	47
Chapter 3 General Materials and Methods.....	48
3.1 Electrode Materials.....	48
3.1.1 Anode Electrode.....	48
3.1.2 Cathode Electrode.....	49
3.2 Membranes and Preparation.....	51
3.2.1 Cation exchange membranes (CEM).....	51
3.2.2 Kilned Terracotta Clay membranes.....	52
3.3 MFC designs.....	53
3.3.1 Analytical type MFCs.....	53

3.3.2	Small-scale MFCs	55
3.4	Inoculum and Feedstock	56
3.4.1	Activated Sludge.....	57
3.4.2	Tryptone Yeast Extract	57
3.4.3	Urine	57
3.5	Mode of feeding	58
3.5.1	Batch mode	58
3.5.2	Continuous flow	58
3.6	Operational conditions	59
3.6.1	Practical challenges	59
3.7	Data capture	59
3.8	Calculations	59
3.9	Polarisation experiment	60
3.10	Conductivity and pH measurements	61
3.11	Chemical Oxygen Demand (COD) analysis	61
3.12	Scanning electron microscopy (SEM).....	62
3.13	Energy-dispersive x-ray (EDX) spectroscopy.....	62
3.14	Experimental data	62
3.15	Conclusions.....	63
Chapter 4	3D-Printable core materials for MFCs.....	64
4.1	3D-printing and its impact on MFC research.....	65
4.2	Air-dry 3D-printable membrane electrode assembly.....	67
4.2.1	Specific Materials and Methods	69
4.2.2	Results and discussion.....	74
4.2.3	Connection with EvoBot	96
4.3	Printable substrate/ carbon energy source.....	101
4.3.1	Specific Materials and Methods	102
4.3.2	Results and Discussion	104
4.3.3	Connection with EvoBot	114
4.4	3D-Printable Cathode Electrode.....	116
4.4.1	Specific Materials and Methods	116
4.4.2	Results and discussion.....	120
4.4.3	Connection with EvoBot	130
4.5	Conclusions and future work.....	131

Chapter 5	EvoBot and MFCs	135
5.1	The making of EvoBot.....	136
5.1.1	Characteristics	138
5.1.2	Scope	141
5.2	Phase I - Interface and interconnection	142
5.2.1	Specific Materials and Methods	143
5.2.2	Results and discussion.....	145
5.3	Phase II – Optimisation of substrate parameters	149
5.3.1	Specific Materials and Methods	150
5.3.2	Results and discussions.....	154
5.4	Phase III – Adaptation / Chemostat-like operation.....	162
5.4.1	Specific Materials and Methods	163
5.4.2	Results and discussion.....	166
5.5	Phase IV - Evolutionary experiment	169
5.5.1	Specific Materials and Methods	170
5.5.2	Results and discussion.....	172
5.6	Phase V - EcoBot-II behavioural experiments powered by the EvoBot-matured MFCs	183
5.6.1	Specific Materials and Methods	185
5.6.2	Results and discussion.....	187
5.7	Conclusions	198
Chapter 6	Conclusions and Further work.....	199
6.1	Executive summary	199
6.2	General discussion and conclusions	200
6.3	Novelty of the project	204
6.4	Future work.....	205
6.5	List of publications from this thesis	207
References	209
Appendix A	239
A.1	Details of the evolutionary algorithm	239
A.2	EcoBot-II 2018 edition.....	240

List of Figures

Figure 2.1 - Quantitative analysis of the literature focusing on “microbial fuel cell/s”	6
Figure 2.2 - Drawing illustration of Galvani's experiment on “animal electricity” using frog legs.	7
Figure 2.3 - Re-drawn version of the Microbial Fuel Cell prototype as created by Allen and Bennetto in 1993.	10
Figure 2.4 - Schematic representation of a Microbial Fuel Cell showing the reduction and oxidation (Redox) processes in each compartment.	11
Figure 2.5 – Stages of an electroactive biofilm formation on conductive surfaces.	14
Figure 2.6 - Schematic representation of direct (A & B) and indirect (C) electron transfer between bacterial cells and anode electrodes.	16
Figure 2.7 - Photographic evidence of electrically conductive nanowires.	17
Figure 2.8 - Microbial growth curve in a batch (closed) system.	19
Figure 2.9 - Examples of different MFC designs with different housing materials.	33
Figure 2.10 – MFC powered autonomous robots in chronological order until 2015.	42
Figure 2.11 – EvoBot robotic workstation.	44
Figure 3.1 - Photos of the two mainly used types of air-breathing cathode electrodes in this study.	51
Figure 3.2 - In-house preparation technique for custom made clay membrane “kilned clay”.	53
Figure 3.3 - Analytical type MFC with a liquid chemical cathode.	54
Figure 3.4 - 3D printed small-scale MFCs.	56

Figure 4.1 - Photographs of the four cut-to shape (25 cm ²) membrane materials.	70
Figure 4.2 - Photographs of the MFC setup.....	71
Figure 4.3 - ED-X analysis results data of the chemical elements between the four tested types of membranes.....	76
Figure 4.4 - SEM images at three different magnification of the MEA side surface coated with the graphite ink (cathode side).	78
Figure 4.5 - Resistivity of the MEA and hardness of the membrane.	81
Figure 4.6 - Power generation recorded in the first 15 days of operations....	84
Figure 4.7 - Power generation over 70 days operations (n=3)	88
Figure 4.8 - Polarisation results [A] voltage vs current curve and [B] power curve. (n=3)	91
Figure 4.9 - COD reduction results and power output at the time of sampling.	93
Figure 4.10 - Cost analysis of the membranes.....	95
Figure 4.11 - EvoBot RepRap 3D-printer.	97
Figure 4.12 - Universal paste extruder mounted on a heavy payload module on the EvoBot robotic head.	100
Figure 4.13 - The process of 3D printing membranes.....	100
Figure 4.14 - MFC design and set-up.	103
Figure 4.15 - Power profile of the inoculation process and initial feeding of the twelve MFCs.....	108
Figure 4.16 - Time profile of MFC's after feeding with soft materials for the first time.	110
Figure 4.17 - Average power production of MFCs after feeding with different soft materials.....	112
Figure 4.18 - Area under curve (AUC) of the full experiment [A] and the starvation period [B].	112
Figure 4.19 - Power curves produced after two months operation on a fixed load of 2.7 k Ω	114
Figure 4.20 – Photographs of the three different cathode electrodes used in this study.....	118
Figure 4.21 – Time-lapse photography of the manual extrusion of the PTFE-free/alginate based cathode electrode on the membrane of an assembled MFC.	118

Figure 4.22 - Manually extruded PTFE-free alginate electrode 0, 2 and 24 hours after extrusion, showing the electrode settling and solidifying (air-drying).	119
Figure 4.23 – Temporal power output of the MFCs employing different cathode electrodes.	125
Figure 4.24 - Overall calculated area under the curve, presented in Joules, based on the temporal power output data.	126
Figure 4.25 – Polarisation results of the three types of MFCs examined. (n=3)	127
Figure 4.26 – Linear sweep voltammetry results of the three cathode electrodes (250 mV/S) (n=3).	129
Figure 4.27 - Time-lapse photographs of the EvoBot extrusion of the PTFE-free/alginate based cathode electrode on a ceramic MFC membrane.	131
Figure 5.1 - Graphical representation of the chemostat method/biofilm continuous culture reactor for culturing bacterial cells.	138
Figure 5.2 - Overview of the actuation and experimental layer of the robot.	140
Figure 5.3 - Experimental set-up of Phase I: Interface and Interconnection experiment.	144
Figure 5.4 - Screen capture of the voltage increase.	148
Figure 5.5 – Layout of Phase II experiment on EvoBot platform.	151
Figure 5.6 – Phase II experimental set up on EvoBot.	154
Figure 5.7 – Indicative power output from one of the MFCs (MFC2) fed by the EvoBot with sodium acetate.	155
Figure 5.8 – Power output profile of the [A] EvoBot maintained and [B] manually maintained MFCs for a time period of two weeks.	157
Figure 5.9 – Temporal power output of [A] acetate, [B] lactate and [C] cellulose fed MFCs, at different concentrations, via the EvoBot.	160
Figure 5.10 – Modified Nanocure® printed MFCs for Phase III.	165
Figure 5.11 – Improved EvoBot based on the Chemostat approach for Phase III experiments.	167
Figure 5.12 – Python generated graph based on the power output of the MFCs fed with casein.	168
Figure 5.13 – OCV of 24 individually fed MFCs inoculated by EvoBot with activated sludge.	173

Figure 5.14 – Temporal voltage output of the three groups of MFCs during the adaptation period.	174
Figure 5.15 – Fitness evolution over each generation	177
Figure 5.16 – Percentages of each feedstock per generation based on the algorithm recipes.	178
Figure 5.17 – Average (n=3) temporal voltage output of Group A MFCs as they responded to each generation recipe.....	180
Figure 5.18 – Average (n=3) temporal voltage output of Group B MFCs as they responded to each generation recipe.....	181
Figure 5.19 – Average (n=3) temporal voltage output of Group C MFCs as they responded to each generation recipe.....	182
Figure 5.20 – Modified small-scale MFCs (2018 ed.).....	186
Figure 5.21 – Treated and untreated carbon veil electrode and their resistance.	186
Figure 5.22 – OCV voltage from [A] the 8 MFCs plugged on EvoBot compared to [B] the ones on the bench.....	188
Figure 5.23 - Temporal voltage behaviour of the MFCs maintained manually and fed once a day (batch-mode feeding).	191
Figure 5.24 – Temporal voltage behaviour of the MFCs maintained by the EvoBot robot and based on different threshold values under 2.7 k Ω load...	192
Figure 5.25 – Long-term temporal voltage behaviour of the manually maintained MFCs.	194
Figure 5.26 – Mean (n=8) polarisation results gathered on the 6th day of operation.	196
Figure 5.27 – Summary graph comparing existing literature data from EcoBot-II 2006 edition MFCs to EcoBot-II 2018 edition MFCs.....	197

List of Tables

Table 1 Advantages and disadvantages of the most commonly used anode electrode materials on MFCs.	25
Table 2 Alternative materials tested as membranes for Microbial Fuel Cells.	30
Table 3 Breakdown of the experimental scheme followed through the entire duration of the experiment.	74
Table 4 Adaptation period feeding schedule for MFCs on Group A and B..	173
Table 5 Average (n=3) comparative data from the membrane investigations on small-scale (6,25 mL) MFCs as presented in Ieropoulos <i>et al.</i> , 2010.....	185

Nomenclature

3D	Three-dimensional
A	Ampere
AC	Activated Carbon
ACCV	Activated Carbon - Carbon Veil
ACSS	Activated Carbon – Stainless Steel Mesh
BBiC	Bristol Bioenergy Centre
BRL	Bristol Robotics Laboratory
CAD	Computed Aided Design
CEM	Cation Exchange Membrane
COD	Chemical Oxygen Demand
DC	Direct current
ECOBOT	Ecological Robot
EDX	Energy Dispersive X-Ray
EET	Extracellular Electron Transfer
EET	Extracellular Electron Transfer
EPS	Extracellular Polymeric Substances
EVOBOT	Evolutionary Robot
GA	Genetic Algorithms

GDL	Gas Diffusion Layer
HRT	Hydraulic Retention Time
HRT	Hydraulic Retention Time
LSV	Linear Sweep Voltammetry
MEA	Membrane Electrode Assembly
MFC	Microbial Fuel Cell
MPL	Micro Porous Layer
MPT	Maximum Power Transfer
OCP	Open Circuit Potential
ORR	Oxygen Reduction Reaction
PEM	Proton Exchange Membrane
$R_{ext.}$	External Resistance
S	Siemens
SD	Standard Deviation
SHE	Standard Hydrogen Electrode
SS	Stainless Steel
TYE	Tryptone and Yeast Extract
V	Volts
W	Watts
WW	Waste water
Ω	Ohms

Chapter 1 Introduction

1.1 Overview

Nowadays robotic systems and artificial intelligence are changing the way we interact with the world around us. Robotic systems can be considered as one of humankind's greatest accomplishments, with manufacturers developing robots that make our life easier. Already, robots exist in our households (e.g. iRobot vacuum cleaner and Amazon Alexa), and our interaction with them improves our everyday tasks.

Many scientific and technological advancements that can be traced back to the beginning of the 1st century, have contributed to the development of robotics as we know it today. Since the introduction of the first human-like robot (ELEKTRO) in 1939, many notable discoveries showcasing the robotic progress have been made. In particular, the creation of the two "turtle robots", Elmer and Elsie, developed by W. Grey Walter in 1948 opened the way to the field of autonomous robots. These two robots were able to perform phototaxis and find their charging station before running out of battery. In the past 80 years, robotics and disciplines associated with robotics (i.e. Artificial Intelligence) have come such a long way that now many individuals, industries and research areas are benefiting from these advances.

Unlike robots, Microbial Fuel Cells (MFC) were invented more than 100 years ago and have not faced the same trajectory in success. MFCs are energy transducers that convert liquid organic matter into electricity through microbial digestion and respiration. MFCs have been successfully incorpo-

rated into field trials and laboratory based trials around the world for powering among others; LED lights, gadgets and sensors. Despite some advancements especially over the past 30 years, research still relies on conventional and outdated methods for maintaining these systems. More specifically the low power of the MFC units (power output in μW and mW) along with the long time they require for maturing (inoculation) and reaching maximum power output levels, are a hindrance to the advancement of the technology.

However, robotic automation might be an innovative approach to advance MFC research, and the technology itself, even further. This approach has been explored as part of the EVOBLISS project, an EU funded interdisciplinary project, which sponsored this PhD work. The main apparatus of the project was EvoBot, a customisable liquid handling robot, which was trialled as an automated maintenance platform to carry out MFC experiments. This thesis therefore investigates the contention that:

By responding to changes in MFC voltage, the EvoBot platform can mature and maintain the MFC systems whilst optimising their power output.

1.2 Thesis outline

Chapter 2 presents a literature review survey addressing the background of MFC technology from its invention until now. This is followed by a breakdown of the various MFC components, detailing their role in the system and the pioneering advancements up to date. Then an overview of the relevant MFC practical applications to date is given, highlighting the development of MFCs for low-power autonomous robots. Finally, the chapter brings into context the

relevance of MFCs to the EVOBLISS project and outlines the research aims and objectives.

Chapter 3 presents the materials and methods employed throughout the thesis including the make-up of MFCs, peripherals used and analysis methods. This chapter acts as a reference point to the experimental work carried out in the following empirical chapters.

Chapter 4 reports on the suite of experiments carried out to develop and investigate 3D-printable materials as novel MFC components. This chapter is divided into three subsections that describe the main three elements of focus; separators and membrane electrode assemblies (MEAs), substrates and cathode electrodes. Concomitantly with the power output analysis, this chapter will discuss the economics of MFCs and how the cost effective materials tested here can lead to a widely affordable MFC that could cost £1 per unit.

Chapter 5 starts with the history behind EvoBot and describes the characteristics and abilities of the robot. Then, the series of five interactive experiments are presented, highlighting the interaction between EvoBot robot and MFCs and how these lead to the improved power output of the latter. **Chapter 6** summarises the findings of the study, outlines the novelty of the project and identifies directions for future research. In an effort to standardise the results, the specific advancements towards the MFC technology made through this study (in terms of price and performance) are highlighted in the executive summary. Furthermore, even though this is beyond the scope of this thesis, in this chapter the power output of the advanced MFCs is compared against the power requirements of the EvoBot. This approach aims to inform future studies by putting into context the power requirements of a robot such EvoBot and the power output of the MFCs themselves. Final-

ly, this chapter also includes a list of publications derived from work presented in this thesis.

Chapter 2 Background

This chapter aims to present a background overview of the Microbial Fuel Cell (MFC) technology, through a literature review, starting from its creation and leading to noteworthy breakthroughs, providing an explanation for the principles of operation. The chapter then finishes with an overview of MFC practical applications.

2.1 Microbial Fuel Cells

Microbial Fuel Cells (MFCs) are bio-electrochemical transducers that use the catalytic activity of microorganisms to convert chemical energy (stored in organic matter) into electricity (Bennetto, 1990). MFCs can utilise a vast collection of organics including organic waste, due to the diverse metabolism of the bacterial communities within the MFC system (Pant *et al.*, 2010). This characteristic has led into a rapidly expanding international interest around the subject of MFCs for its potential to treat wastewater and harvest green energy (Gajda *et al.*, 2016; Ahn and Logan, 2010).

2.1.1 Chronological development

Even though the MFC research interest has bloomed over the recent 20 years, as reflected from the number of publications around the subject (**Figure 2.1**), it was, in fact, more than 100 years ago that the fundamental MFC concept was first reported by Potter (Potter, 1911).

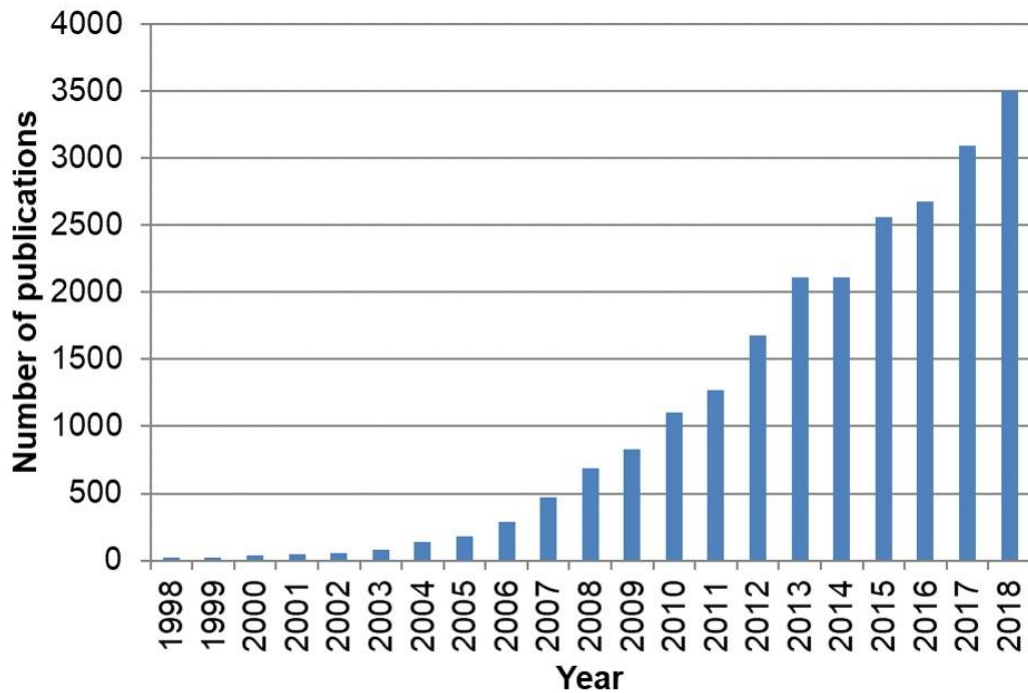


Figure 2.1 - Quantitative analysis of the literature focusing on “microbial fuel cell/s”.

(Google Scholar, January 2019).

In his pioneering study, Potter was the first to exploit the microbial ability of decomposing organic matter and liberating electrons. In the aforementioned study, he managed to produce 0.3-0.5V of electrical energy using *Saccharomyces cerevisiae* (baker's yeast) and pure culture of *Escherichia coli*, grown on platinum electrodes (Potter, 1911). Although Potter with his discovery established the stepping stones for microbial electricity, historically the first ever mention of bioelectricity occurred in the 18th century by Luigi Galvani who proved the flow of electrons in biological organisms and demonstrated this using dead frog legs (**Figure 2.2**) (Whittaker, 1910).

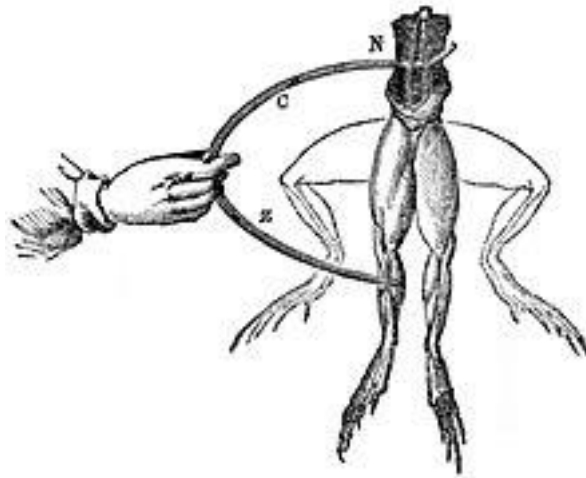


Figure 2.2 - Drawing illustration of Galvani's experiment on “animal electricity” using frog legs.

This experiment proved that electrons could flow in biological organisms. In his experiment, Galvani plugged a zinc wire with the muscle of the leg, and a copper wire with the nerves and showed that when the two wires are connected an instantaneous convulsion takes place (Wells, 1859).

Potter's discovery was underappreciated at the time, perhaps due to the negligible amount of power (units of nanoWatts) that his MFC prototype produced. Even when 20 years later Cohen managed to produce more than 35 V, by connecting MFCs in series (Cohen, 1931), still there was not a lot of interest in the technology. The years that followed recorded the *nadir* of the MFC research. However, that attitude changed in the 1960s when the National Aeronautics and Space Administration (NASA) wanted to assess MFC applications in space missions (Canfield, Goldner and Lutwack, 1963). Despite the promising technology, the understanding around fuel oxidation and MFC reactions were limited back then, thus, the outcome from this work was not enough to encourage NASA to continue the studies.

Even though NASA's attempt to utilise MFCs for its explorations proved unsuccessful at the time, the fact that it even attracted their attention fuelled the MFC research and many breakthroughs followed. A key set of findings came from Allen and Bennetto's research in the 1980s. This gave new insights into the technology by demonstrating a better capability from MFCs, to produce power, which could be greatly enhanced with the use of synthetic electron mediators (Bennetto, 1990). Their approach made possible the extraction and transfer of electrons from bacterial cells, which were otherwise incapable of directly transferring electrons, to the anode electrode. Even though it was shown through this study that synthetic mediators can accelerate the electron transfer process within the anode, it was an unsafe approach due to toxicity and instability issues of the synthetic mediators (Allen and Bennetto, 1993). Regardless, this study led to the development of the widely used "analytical type MFC" design which has been extensively used in MFC research since then, and inspired the development of the MFCs of today (**Figure 2.3**).

Contemporary of Bennetto's work, Habermann and Pommer designed MFCs which were able to treat two types of wastewaters (sewage and landfill effluent) continuously for 5 years (Habermann and Pommer, 1991). Their MFCs were based on sulphate-reducing bacteria species *Desulfovibrio desulfuricans* which were forming sulphide as a metabolic by-product after reducing the sulphate found in wastewater (sulphate was used as the end terminal electron acceptor). Subsequently, the sulphide was then anodically oxidised to electrons and sulphate (Habermann and Pommer, 1991). Thus this study showed that in this type of MFCs the sulphate / sulphide redox couple acted as soluble electroactive metabolite (mediator) between the bacterial cells and the electrode surface, eliminating the need to add exogenous synthetic mediators.

A few years later Bond and Lovley (2003) reported that some microbes can directly transfer electrons to the anode. These bacteria were named as “anodophiles” or “anodophilic organisms” due to their ability to attach to the anodic electrode and use it as an electron acceptor. In 2005 another type of direct electron transfer was reported and this time it was through the construction of bacterial conductive extracellular appendages (bacterial “nanowires”) (Reguera *et al.*, 2005). These discoveries led to the creation of mediator-less MFC for electricity generations and encouraged the continuation of the research around MFC systems without the need for exogenous mediators that required constant replenishing; this marked the start of a modern era for MFCs. The mediator-less / direct electron transfer (DET) will be discussed in more detail in the following section **2.1.2.1**.

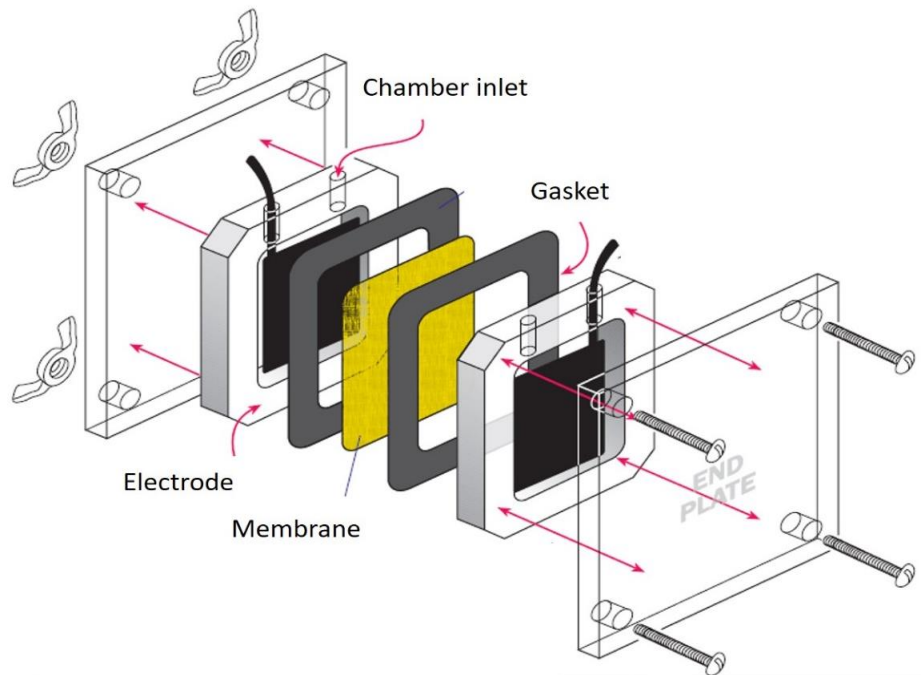


Figure 2.3 - Re-drawn version of the Microbial Fuel Cell prototype as created by Allen and Bennetto in 1993.

This design is the foundation of the development of the “analytical type” MFC that has been used extensively in MFC research up to now. (Allen and Bennetto, 1993) – Illustrations Copyright© Dean Madden, 2001 - NCBE, University of Reading.

2.1.2 Operation

Structurally, MFCs consist of two electrodes, a positive cathode and a negative anode, which are separated by a semi-permeable membrane such as a cation exchange polymeric based membranes or a salt bridge (**Figure 2.4**). Microorganisms are inoculated into the anodic compartment and are growing as a biofilm on the electrode. A biofilm is a syntrophic consortium of bacteria which can grow on different surfaces. Within that consortium of bacteria, in the anode compartment, the electroactive organisms are the ones capable of oxidising the substrate by electron abstraction. The electrons are released to

the anode electrode either directly, or indirectly (using natural or synthetic chemical mediators) (Gralnick and Newman, 2007). The biofilm formation within an MFC is of great importance as without a biofilm, the harvesting of electrons from bacteria will not be possible. Biofilms will be described in detail in section 2.1.2.1. The anodic and cathodic electrodes are connected by an external circuit, which allows the flow of electrons from the anode to the cathode side. Here, the reduction of oxygen occurs as will be explained in section 2.1.2.2.2 (Figure 2.4).

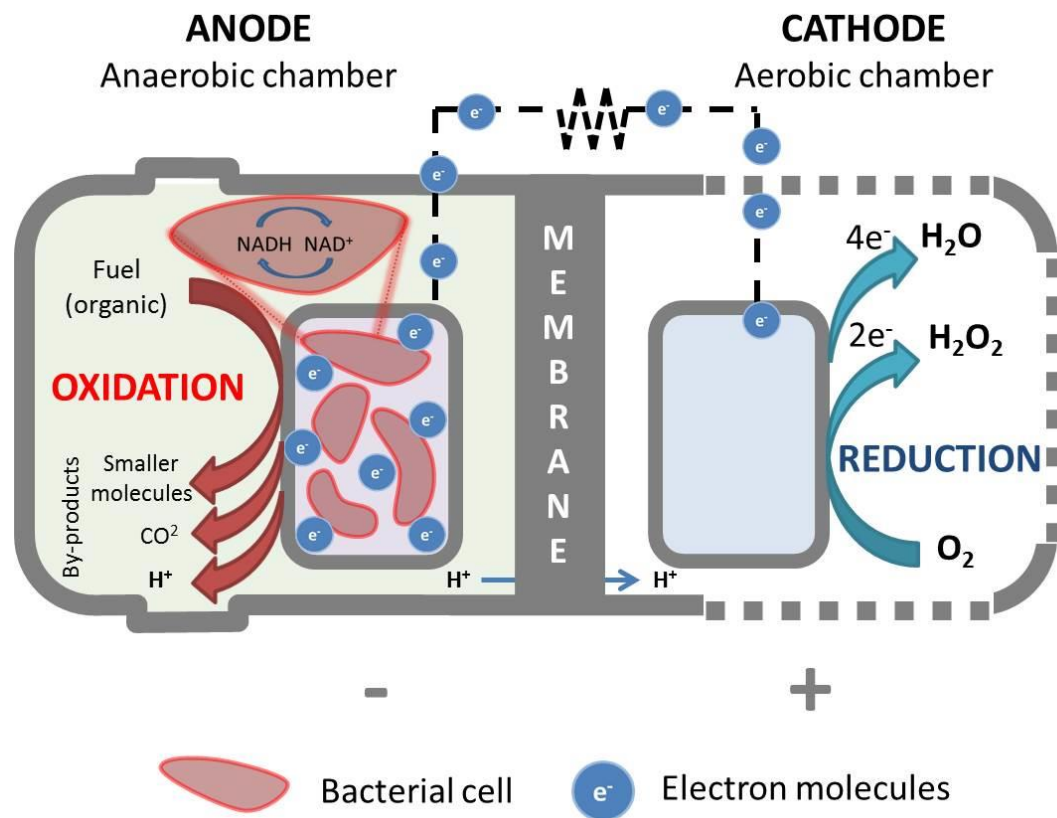


Figure 2.4 - Schematic representation of a Microbial Fuel Cell showing the reduction and oxidation (Redox) processes in each compartment.

2.1.2.1 The microcosm within an MFC system

Microorganisms can be nutritionally classified based on; their source of energy (chemical [*chemo-*], light [*photo-*]), their source of electrons (organic [*organo-*]), inorganic [*litho-*]) and their source of carbon (organic [*hetero-*], inorganic [*auto-*]-*trophic*). Microbial cells within an MFC acquire their energy, electrons, and carbon through the oxidation of organic molecules. This ability has given them the name of *chemoorganoheterotrophs*.

During the oxidation process (**Figure 2.4**), microbial cells obtain energy which is stored chemically in the form of adenosine triphosphate (ATP) and enables cell growth and multiplication (Willey, Sherwood and Woolverton, 2009). Also through their metabolic pathways, bacteria release electrons that are transferred to NAD^+ , reducing it to $\text{NADH} + \text{H}^+$. Subsequently, NADH molecules donate the electrons to facilitate electron-requiring processes in the cells (i.e. synthesis of cellular components) (Comeau, 2008). However, there is a net amount of electrons that is harvested by MFCs and is turned into electricity. This process continues indefinitely as long as there is an electron donor (organic matter) and an electron acceptor present. The latter is needed in order to receive the electrons and close the exchange loop.

In the case of aerobic metabolism, this electron acceptor will be dissolved oxygen. However, for anaerobic respiration, this will be an alternative end-terminal electron acceptor compound such as nitrate, sulphate, organic acids or carbon dioxide, with the exception of anodophiles that may use solid phase electron acceptors such as metal oxides or conductive materials. The latter is the case for microbes in MFC systems where electrons are transferred from external electron donors (carbon energy sources) to external electron acceptors (conductive surfaces), this process is described as *extra-cellular electron transfer* (EET) (Haluk and Jerome, 2015).

Bacteria cells within an MFC anodic environment can be found both living in a planktonic state (free-floating) and/or as part of a biofilm which has been defined as:

“a structured community of bacterial cells enclosed in a self-produced polymeric matrix and adherent to an inert or living surface “
(Costerton, Stewart and Greenberg, 1999)

As mentioned above, the key element in an MFC system is the biofilm formation on the anode electrode (**Figure 2.5**), composed of microorganisms with current generating abilities known as anodophiles or anodophilic. In the literature, these biofilms, due to their capabilities, are often referred to as electroactive or electrochemically-active biofilms (Haluk and Jerome, 2015).

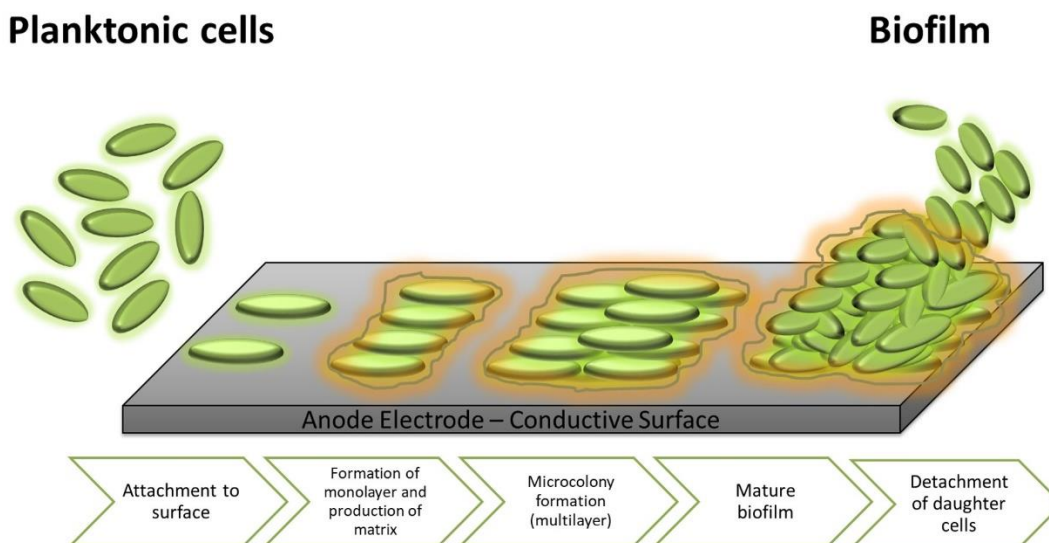


Figure 2.5 – Stages of an electroactive biofilm formation on conductive surfaces.

Free-floating bacterial cells (planktonic) attach to and grow on a surface, producing extracellular polymers that facilitate attachment and matrix formation. Initially they form monolayers which then become multilayers as the biofilm grows, until a full mature biofilm is formed. As the cells multiply and divide, some of them detach from the biofilm (daughter cells) and can then go on to produce other biofilms.

The biofilm-forming microorganisms can achieve electron transfer to the anode electrode through three different mechanisms which are illustrated in **Figure 2.6** and can be categorised as direct and indirect electron transfers (Patil, Hägerhäll and Gorton, 2012). Anodophilic organisms achieve direct transfer of electrons either by direct contact of the outer membrane of the bacterial cell with the surface of the anode electrode (via the cytochrome *c* membrane proteins) (**Figure 2.6A**), or through electrically conductive nanowires (molecular pili) which are connected to those cytochromes (**Figure 2.6B**) (Reguera *et al.*, 2005). The latter has been observed in studies with the model organisms *Shewanella oneidensis* (MR-1) (Beveridge *et al.*, 2009),

proving the ability of those cells to establish physical electrical connection with neighbouring cells or electrodes (**Figure 2.7**). Apart from anodophilic or anodophiles, in the literature these bacteria have been also described as “electroactive” (Dulon *et al.*, 2007), “exoelectrogenic” (Logan, 2009), “electricigens” (Yousaf *et al.*, 2017), “exoelectrogens” (Kumar *et al.*, 2015), “electrogenic”(Feng *et al.*, 2009) and “anode-respiring” (Torres, Kato Marcus and Rittmann, 2007).

Indirect or mediated electron transfer facilitates the transfer of electrons outside of bacteria cells via the oxidation and reduction (redox) of artificial (exogenous) mediators or via microbe secreted (endogenous) mediators also known as electron shuttles (**Figure 2.6C**). This is the only way non-anodophilic bacteria can donate electrons outside of their cell as their outer membrane consists of lipids, peptidoglycans, and lipopolysaccharides that act as insulator which prevents electron flow (Reguera *et al.*, 2006). To be efficient, artificial mediators (e.g. methylene blue, neutral red) need to have the following characteristics; i) be capable of achieving physical contact with the electrode, ii) be electrochemically active, iii) have similar redox potential to the substrate, iv) be stable in both the oxidised and reduced form and v) be soluble in aqueous systems in order to pass through or get absorbed by the bacterial cytoplasmic membrane (Allen and Bennetto, 1993; Park and Zeikus, 2000). However, as mentioned above, exogenous mediators have many disadvantages over endogenous ones, due to their toxicity and constant need for replenishment. Endogenous mediators (e.g. sulphide) are excreted by the bacteria itself, as secondary metabolites, they are constantly synthesised (do not require any replenishment) and their production can be regulated based on the biocatalytic activity of the anodic microorganisms. Moreover, metabolites produced by electroactive species such as *Pseudomonas* can enable non-electroactive to achieve EET (Pham *et al.*, 2008)

which emphasises on the importance of using a mixed culture of bacteria in inoculating and operating MFCs for achieving higher power output levels (Nevin *et al.*, 2008).

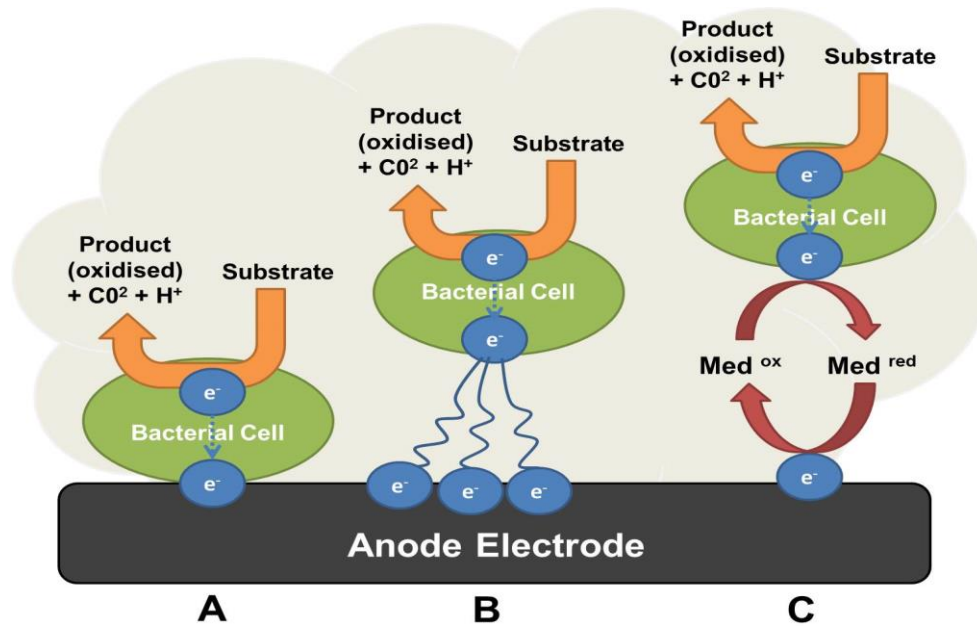


Figure 2.6 - Schematic representation of direct (A & B) and indirect (C) electron transfer between bacterial cells and anode electrodes.

A. Direct electron transfer via membrane-bound c-cytochrome proteins **B.** Direct transfer through conductive pili or nanowires **C.** Indirect/mediated transfer via artificial (exogenous) or microbe secreted (endogenous) mediators.

Knowledge on biofilm formation and electron transfer mechanisms enable researchers to take an educated decision regarding the type of bacteria that their MFC will employ and the type of mediators. This needs to be decided at the beginning of the study as it will dictate the inoculation process, as explained below. Throughout the whole duration of this study, the MFCs were operating without any artificial mediators, as a mixed inoculum was used.

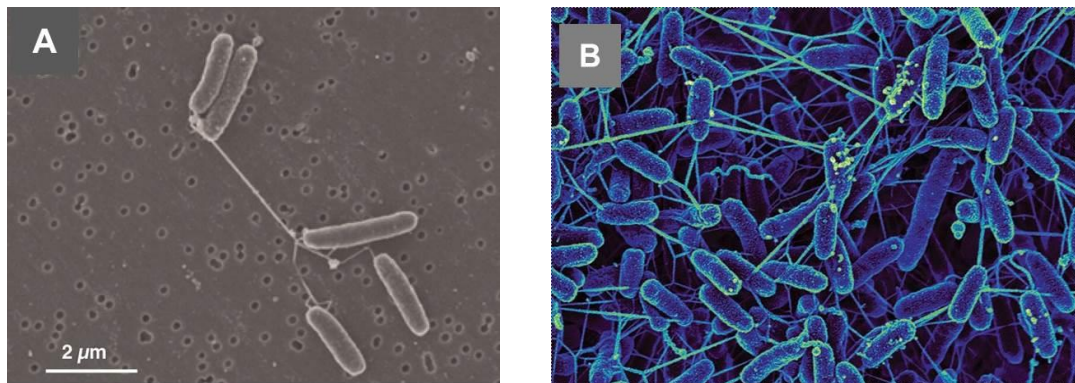


Figure 2.7 - Photographic evidence of electrically conductive nanowires.

A. SEM image of the wild-type strain *Shewanella oneidensis* (MR-1)ⁱ (Beveridge *et al.*, 2009). Copyright© National Academy of Sciences **B.** Image of a *Shewanella oneidensis* biofilmⁱⁱ. The electron-conducting nanowires extend the length of the bacterium and form an electric circuit within the biofilm and the electron acceptor. (Alivisatos *et al.*, 2015). Copyright© U.S Department of Energy

2.1.2.1.1 Inoculation

Inoculation of the microorganisms in the anodic compartment of an MFC is the crucial process that initiates the selection of the electroactive microbial community and the formation of the electroactive biofilm. The source of bacteria is equally crucial but differs among studies. Some studies employ monoculture organisms such as *Shewanella oneidensis* (Ringeisen *et al.*, 2006) and *Geobacter sulfurreducens* (Katuri *et al.*, 2010) whereas others employ a mixed culture of organisms sourced from activated sludge which consists of a diverse community of bacteria (Rulkens, 2008).

The latter is the source of inoculum that has been used throughout this study as its' mixed consortium of bacteria have been proven to exhibit both direct electron transfer and endogenous mediated electron transfer; and because biocatalytically it is more versatile than monocultures (Fernandez *et al.*, 1999; Snaird *et al.*, 1997; Watanabe *et al.*, 1998).

2.1.2.1.2 Feeding modes and bacterial growth

Following the inoculation process, the bacteria need to be supplied with substrate rich in carbon energy sources in order to survive and thrive. In MFC operations there are two frequent modes of feeding used, batch feeding (a close system) and continuous feeding (an open system). During the batch feeding mode, the substrate is replaced when depleted. In contrast, in continuous feeding, the substrate is supplied constantly with the use of peripheral pumps at different flow rates that dictate the hydraulic retention time (HRT) of the fresh medium into the anodic chamber.

Bacterial growth is of great importance within an MFC as it is directly related to the amount of fuel (substrate) that is being utilised which is reflected by the amount of current that is being generated (Ledezma, Greenman and Ieropoulos, 2012). Thus by controlling the bacterial growth, it is possible to keep the power performance at optimum levels. Bacterial growth is an element that this study attempted to optimise through the use of EvoBot by providing on-demand feeding to the MFCs, as presented in Chapter 5. In a closed system, planktonic bacteria grow in a well-defined lifecycle that is illustrated as a microbial growth curve with four different phases (**Figure 2.8**).

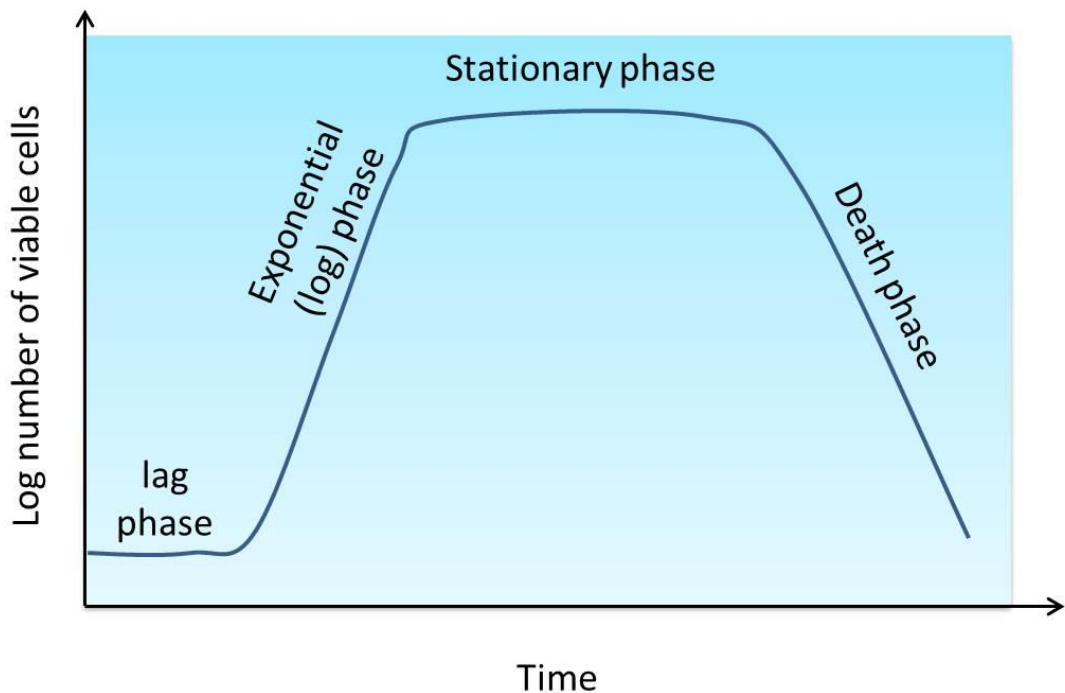


Figure 2.8 - Microbial growth curve in a batch (closed) system.

The initial phase is called the **lag phase** and reflects the initial response of bacteria to the introduction of fresh substrate. The duration of the lag phase depends on the complexity of the substrate, as new enzymes might need to be synthesised by bacteria in order to utilise different nutrients (Willey, Sherwood and Woolverton, 2009). Following that, the bacteria start to grow and divide at a constant rate which is called **exponential (log) phase**. The rate of growth depends upon the nutrient concentration until saturation reaches a sufficiently high nutrient levels. In a batch fed system, population growth eventually comes to an end and the growth curve becomes horizontal marking the **stationary phase** of microbial growth (Willey, Sherwood and Woolverton, 2009). However during that phase, the cells may remain metabolically active for some time but eventually, go into decline. Microbial cells may enter stationary phase because of nutrient limitation, and/or accumulation of toxic waste products. Eventually, after the stationary phase, microbial

cells enter the **death phase** where starving cells show an exponential decline in viability. Some cells lyse while others may remain viable for years. In the absence of fresh nutrients, death phase can last for a long time with the overall population size remaining constant (Willey, Sherwood and Woolverton, 2009). This occurs due to the “altruistic” nature of some microbial cells that die and disintegrate releasing sufficient nutrients to allow the survival of the rest of the microbial population. The surviving population constantly evolves and reproduces cells that are best able to consume the nutrients released from dead cells or can better cope in an environment with high accumulation of toxic waste. This altruistic behaviour is highly observed in biofilm bacteria too and this may allow the biofilm to survive starvation for years (Prakash, Veeregowda and Krishnappa, 2003). The fact that biofilms can withstand long term starvation adds an extra value to the MFC system as it can remain “hibernated” until fresh medium is available to be added and awaken the system (Winfield *et al.*, 2015a).

In open systems, the growth rate of planktonic bacterial cells can be determined using continuous culture systems such as chemostats. In a chemostat, fresh nutrient-limited medium is supplied to the cells at a constant rate while keeping all the other environmental conditions the same. Through this approach, the system can maintain a microbial population in “steady state” exponential growth for a prolonged period of time (Willey, Sherwood and Woolverton, 2009).

Similarly, in MFC open systems, continuous flow of fresh medium in the anode is important in order to achieve a steady-state which results in stable MFC power outputs (Ieropoulos, Winfield and Greenman, 2010b). A continuous feeding mode involves the constant inflow of fresh medium and the subsequent outflow of an equal volume of fluid. The outflow or effluent consists

of a mixture of old, and fresh medium and a proportion of biomass (daughter cells). Once a steady-state is achieved the concentration of biomass within the culture vessel (anode) remains constant (Singleton and Sainsbury, 2006). It has been reported in the literature that in continuously fed systems the growth rate of the anodic biofilm is directly correlated to the resulted current and hence the power output of the MFC (Greenman *et al.*, 2011). The latter can be maximised by controlling the biofilm's growth rate (Ledezma, Greenman and Ieropoulos, 2012).

A continuous flow system is beneficial for biofilm research as it allows the development of biofilms under different flow rates (substrate supply rate) that can determine their thickness. The development of a thick biofilm can limit the nutrient diffusion in all its layers whereas a thin biofilm can achieve higher metabolic growth rates due to greater diffusion of substrate to the anode surface-attached biofilm (Ieropoulos, Winfield and Greenman, 2010b; Greenman *et al.*, 2011). Regardless of the advantageous operation of an open system, continuously fed MFCs render a rarely reported issue of system blockage. Blockages can be caused in the inlet and/or outlet either due to the overgrowth of bacteria in the anode wall (You *et al.*, 2015) or the build-up of struvite in the case of urine-fed MFCs (You *et al.*, 2016). This can have a temporary negative effect on the MFC performance which can be resolved following the clean-up of the system (You *et al.*, 2015).

In laboratory scale studies the feeding mode depends on the experimental set-up and the purpose of the study. Investigations that are focused on wastewater treatment solutions are usually tested under continuous high flow rate feedings (Ahn and Logan, 2010; Min and Logan, 2004) whereas investigations of new MFC materials are most often tested in batch modes (Behera and Ghangrekar, 2011). However experiments that are aimed to be used in

field applications where only intermittent feeding will be available, are tested in semi-continuous/batch mode called pulse feeding (Walter *et al.*, 2016b).

2.1.2.2 Materials consisting an MFC system

Even though biofilms are the integral part of the MFC system, the efficiency of these to harvest the electrons and generate electricity is greatly affected by the design-components, structuring and environmental surroundings of the MFC units. The collective factors of integration are otherwise known as system configuration. Each and every one of the components within an MFC configuration is of great importance and needs to be identified or designed so that it interacts harmonically with the peripheral materials and does not hinder the power output and performance of the system. Another major challenge in designing MFCs is the associated cost that comes from each material. Ideally, this needs to be kept at a minimum in order to make MFCs an economical alternative method of energy production (cost per watt). An overview of the significance of these core MFC materials is presented below.

2.1.2.2.1 Anode Electrode

First and foremost, apart from its ability to conduct electricity, the choice of anodic electrode material needs to be made based on its ability to encourage biofilm formation on its surface. Equally, it needs to possess the following characteristics; high mechanical strength, large surface area, corrosion resistivity, biocompatibility, eco-friendliness and be cost-effective.

Materials that fulfill the criteria above include carbon-based (e.g. carbon veil, carbon cloth, carbon paper, carbon fibre, carbon and graphite nanotubes) (Wei, Liang and Huang, 2011) and non-corrosive metals (stainless-steel mesh) (Pocaznoi *et al.*, 2012) thus, they have been extensively used in la-

boratory (Zhou *et al.*, 2011) and field-based, MFC studies (Ieropoulos *et al.*, 2015). Each of these materials has been proven suitable for MFC purposes although there are some disadvantages associated with each of them, as summarised in **Table 1**, that make them unsuitable for universal usage. The selection of the anode material is highly dependent on the application that the MFC is intended to perform. For example, some materials are not ideal for scaled up MFC units (e.g. graphite plate) due to their low surface area and high cost, but are suitable for laboratory-based MFC applications such as microbial analysis of electroactive biofilms (Shewa, Chaganti and Lalman, 2014).

The porosity of the anode material is the main contribution to higher power per surface area, compared to smoother materials (Wei, Liang and Huang, 2011). This is attributed to the larger surface area for bacteria to attach, per unit of volume in the anodic chamber. Many studies showed that folded porous anode material in a three-dimensional (3D) pack shape have a great impact on the power performance as it is increasing the available surface area and are maximising bacterial colonisation (Ieropoulos, Greenman and Melhuish, 2008). In the same context some studies attempted to fill those packs with carbon-based granules to increase even greater the specific area (Rabaey *et al.*, 2005) however such a configuration can cause clogging in the long term as the porosity of the electrode is decreasing (Rabaey *et al.*, 2009).

In an effort to improve bacterial adhesion and maximise the electron transfer between bacteria and electrode surfaces, the focus of anodic electrode has been recently turned to surface modification (Fiset and Puig, 2015). This has been achieved using physical and/or chemical methods such as coating with nanomaterials (You *et al.*, 2014) or treatment with electrochemical oxidation

of electrolytes (Li *et al.*, 2014), this approach has been proven to be effective for laboratory scale experiments. A similar approach was used for an experiment presented in this thesis, where carbon nanoparticles were coated on anodic surface areas and their impact on the power output was assessed, more details on that experiment are presented in **Chapter 5.6**.

The bioelectrochemical processes that take place in the anodic compartment are important element of an MFC which in order to be optimised needs to be fully understood. Hence, there is a large body of knowledge invested in improving the understanding around electrochemical communication between biofilms and conductive surfaces (Pankratova and Gorton, 2017) as well as optimising anode electrode materials (Zhou *et al.*, 2011), electron transfer (Patil, Hägerhäll and Gorton, 2012) and anode inoculum for achieving maximum chemical to electrical energy conversion (Pandey *et al.*, 2016). Advancing the bio-electrochemical processes in the anode compartment was not the main focus of this thesis hence it is an element that this study only touched upon briefly. As mentioned above, in an effort to increase the anode surface area carbon veil was coated with carbon nanoparticles. Following the reviewing of the materials that are in the market and have been used for similar studies, all the MFC for this study contained carbon veil as their anode electrode of preference, due to the advantages presented in **Table 1**.

Anode Material	Advantage	Disadvantage	Reference
Carbon fibre veil	Low cost, Large surface area, high electrical conductivity, high porosity	Fragile (If not folded in a 3D shape)	Ieropoulos, Greenman and Melhuish, 2008
Carbon paper	Relatively porous, conductive, good for small scale MFCs	Thin, stiff, slightly brittle, high cost	Logan, 2008
Carbon cloth	Foldable, durable, porous, large surface area, high porosity, high electrical conductivity	Expensive	Guerrini <i>et al.</i> , 2014
Carbon brush	High surface area, high electrical conductivity	Expensive (due to titanium central rod)	Santoro <i>et al.</i> , 2013
Carbon mesh	Low cost, foldable	Low electrical conductivity, low durability	Wu <i>et al.</i> , 2017
Carbon felt	Low cost, Thick, fibrous - porous, loose texture, high electrical conductivity	It is restricting bacterial growth on the inner surface.	Chaudhuri and Lovley, 2003
Graphite plate	High strength	Low surface area, high cost, not suitable for scale-up MFCs	Taskan and Hasar, 2014
Stainless Steel plate	High mechanical strength, Relatively low cost, high electrical conductivity	Low surface area, biocompatibility issues, corrosion	Dumas <i>et al.</i> , 2007
Stainless Steel mesh	high conductivity, relatively low cost	biocompatibility issues, corrosion	Zheng <i>et al.</i> , 2015

Table 1 Advantages and disadvantages of the most commonly used anode electrode materials on MFCs.

2.1.2.2.2 Cathode Electrode

Imperfect cathode configurations and cathodic reactions (that are governed by the cathode electrode), can hinder the power output of the MFC systems (Logan, 2009). This study will work towards optimising the cathode electrode by using novel conductive materials that can increase the power output, as described in **Chapter 4**.

In smaller scale MFCs, similar to those used in this study, cathodes can work better than in large MFCs, due to an optimised surface area to volume ratio. In the most recent MFC configurations, the anodic electrode is coupled with a porous air-breathing cathode electrode which provides the system with the unending ability to use atmospheric oxygen as the electron acceptor (Papaharalabos *et al.*, 2013; Santoro *et al.*, 2015). Consequently, the MFCs used in this study will employ air-breathing cathodes as, up to date, it has been proven to be the most eco-friendly, cost effective and low maintenance. By having oxygen as the final electron acceptor it provides the cathode with a high redox potential (0.82V). The two processes underlying the cathodic oxygen reduction reaction (ORR) are:



with a) being the desired reaction for the production of water through a four-electron pathway and b) the alternative pathway which consists of two-electron reaction and leads to hydrogen peroxide formation. Incomplete reduction of oxygen can result in low energy conversion and production of destructive intermediates (Rismani-Yazdi *et al.*, 2008).

Subsequently, ideal cathode electrodes are the ones with high redox potential and the ability to readily capture protons. Materials that fulfill those re-

quirements are carboneous materials and non-corrosive metals, same as those mentioned above (**Table 1**) which were used as anode electrodes. Conversely, in the case of the cathode electrode, a catalyst is usually added to improve the ORR. The air-breathing cathode electrodes consist of three components:

- i. a gas diffusion layer (hydrophobic coating layer) exposed to the air which restricts water loss through the electrode while ensuring high oxygen fluxes from outside to inside.
- ii. a conductive supporting material which can double as the current collector (e.g. stainless steel mesh)
- iii. a catalyst-binder layer to speed up the ORR process

Current collectors are very important in securing high cathode performances too. Usually, they are of the same nature as the electrodes described in **Table 1** , with corrosion proof stainless steel meshes being the most popular due to their mechanical strength (Walter *et al.*, 2016b).

As briefly mentioned above, in this research study, alternative materials to those conventional ones have been explored in order to offer a degree of freedom in the design and material make-up of the next generation of MFCs which are envisaged to rise monolithically from 3D-printers in the near future. A literature overview on the development of 3D printable MFC parts as well as the experimental work carried in identifying novel alternatives is presented in **Chapter 4**.

Anodic and cathodic electrodes are physically separated by a semi-permeable membrane to avoid; short-circuiting and substrate crossover while allowing proton diffusion. The distance between the two electrodes needs to be kept at a minimum in order to avoid high Ohmic resistances. These re-

sistances are positively correlated with the distance that the ions (cations or anions) have to travel from the membrane to the cathode (Rismani-Yazdi *et al.*, 2008). Thus membrane selection, and the subsequent distance between the two electrodes is a vital parameter in minimising the internal resistance of the MFC system. For this reason, this study will explore alternative membrane materials that can improve the power output by decreasing internal resistance and overall MFC costs (**Chapter 4**).

2.1.2.2.3 Membrane

In electrochemical and bio-electrochemical systems, membranes act as a physical barrier between the anolyte and the catholyte. Membranes have been considered as the main contributor towards the high cost of the system and the bottleneck for its scale-up. Initially, as the MFC field emerged it was mainly influenced by the field of chemical fuel cells, thus the membrane material used were Nafion based (Bennetto, 1990; Allen and Bennetto, 1993). Nafion is a commercially available perfluorinated ion exchange membrane developed by Dupont in early 60s as part of their collaboration with General Electric (Parthasarathy, Martin and Srinivasan, 1990). Apart from Nafion, interpolymer cation exchange membranes (CEM) with added crosslinking agents, were then investigated as separators in mediator-less-MFCs (Grzebyk and Poźniak, 2005) which showed an increase in performance but were unstable for long term operation. Those two commonly used materials have been proven to be unsuitable for use in bio-electrochemical systems as their interaction with electro-active bacteria is non-favourable (e.g. oxygen flux to the anode). Apart from that, it has been also reported in the literature that even though membrane materials such as Hyflon can produce 1.5 times higher power output than standard CEM in individual MFCs, when connected

together (as a stack) the system can exhibit instability and cell reversal (Ieropoulos, Greenman and Melhuish, 2010).

In selecting membrane materials for practical implementation of MFCs; the cost, structure and physical properties need to be considered. Therefore a tremendous amount of studies have focused on finding alternative materials, either bespoke or readily available, that can be used as viable successors of the expensive and commercially available CEM (Li *et al.*, 2011; Yousefi, Mohebbi-Kalhari and Samimi, 2017; Winfield *et al.*, 2013a, 2016; Kondaveeti *et al.*, 2014). A short list of alternative materials that have been tested in MFC systems is shown below (**Table 2**). Among those mentioned, the most popular has proven to be ceramic based membranes which are; easily accessible, relatively cheap, structurally rigid and have beneficial porosity. Most importantly they have been proven to be ideal for scaled-up and scaled-down MFC systems that have been tested both in laboratory and field conditions (Ieropoulos *et al.*, 2016; Walter *et al.*, 2016b; Gajda *et al.*, 2016).

Ceramics is a versatile material and can have a double functionality within an MFC system, as due to its mechanical characteristics can serve both as a separator and as the structural component of the overall MFC housing, minimising even further the manufacturing costs. For this reason, ceramics were core materials in the context of this research study, however alternative clay based materials were investigated for their potential to be extruded and cure in the air without additional firing requirements, making them suitable for monolithically MFC printing. The experimental work on these materials is presented in **Chapter 4**.

Materials	References
Biodegradable shopping bags	Winfield, Chambers, <i>et al.</i> , 2013
Natural rubber	Winfield, Ieropoulos, <i>et al.</i> , 2013
Ceramics	Park and Zeikus, 2003; Behera and Ghangrekar, 2011
J-cloth	Fan, Hu and Liu, 2007
Laboratory gloves	Winfield <i>et al.</i> , 2014
3D-printed ion exchange membrane	Philamore <i>et al.</i> , 2015
Photocopy paper	Fraiwan and Choi, 2014, 2016; Winfield <i>et al.</i> , 2015

Table 2 Alternative materials tested as membranes for Microbial Fuel Cells.

2.1.2.2.4 MFC housing

MFC housing refers to the enclosure that houses the core MFC components explained above; microorganisms, anode electrode, membrane and cathode electrode. MFC housings need to be long lasting, structurally rigid and most importantly inert in order to avoid any electrical conflict with the system (i.e. avoidance of ionically conductive pathways (fluidic conductance) which can cause a short circuit).

Based on these characteristics there are numerous materials which qualify (i.e. glass, plastic, acrylic, ceramic). One can argue that the aspect of MFC housings can form the core of a review study on its own rights since there

have been a plethora of materials and configurations that have been examined so far. This is one of the beauties of this technology as it is versatile and can be adapted in any form and shape. One of the most traditional configurations used by many groups around the world is following Benetto's design (**Figure 2.3**) where cut-to-size acrylic sheets can be assembled together forming the MFC housing. The second most popular design is the universally known H-type MFC where two laboratory glass bottles are connected by a tube that houses the cation exchange membrane (**Figure 2.9A**). The latter is unable to be used for practical implementation due to its large footprint and design instability. MFC housings are designed and selected based on the intended use of the MFC system. Optimisation of those designs are still in development but many steps have been taken forward using the 3D printed custom made housings, which are described in this thesis, and reviewed in more detail in **Chapter 4**. For the purpose of this chapter a photographic overview of the different MFC housings and configurations that have been used so far in different laboratories including BBiC, is presented in **Figure 2.9**. This figure gives a visual idea of the versatility of the MFC design.

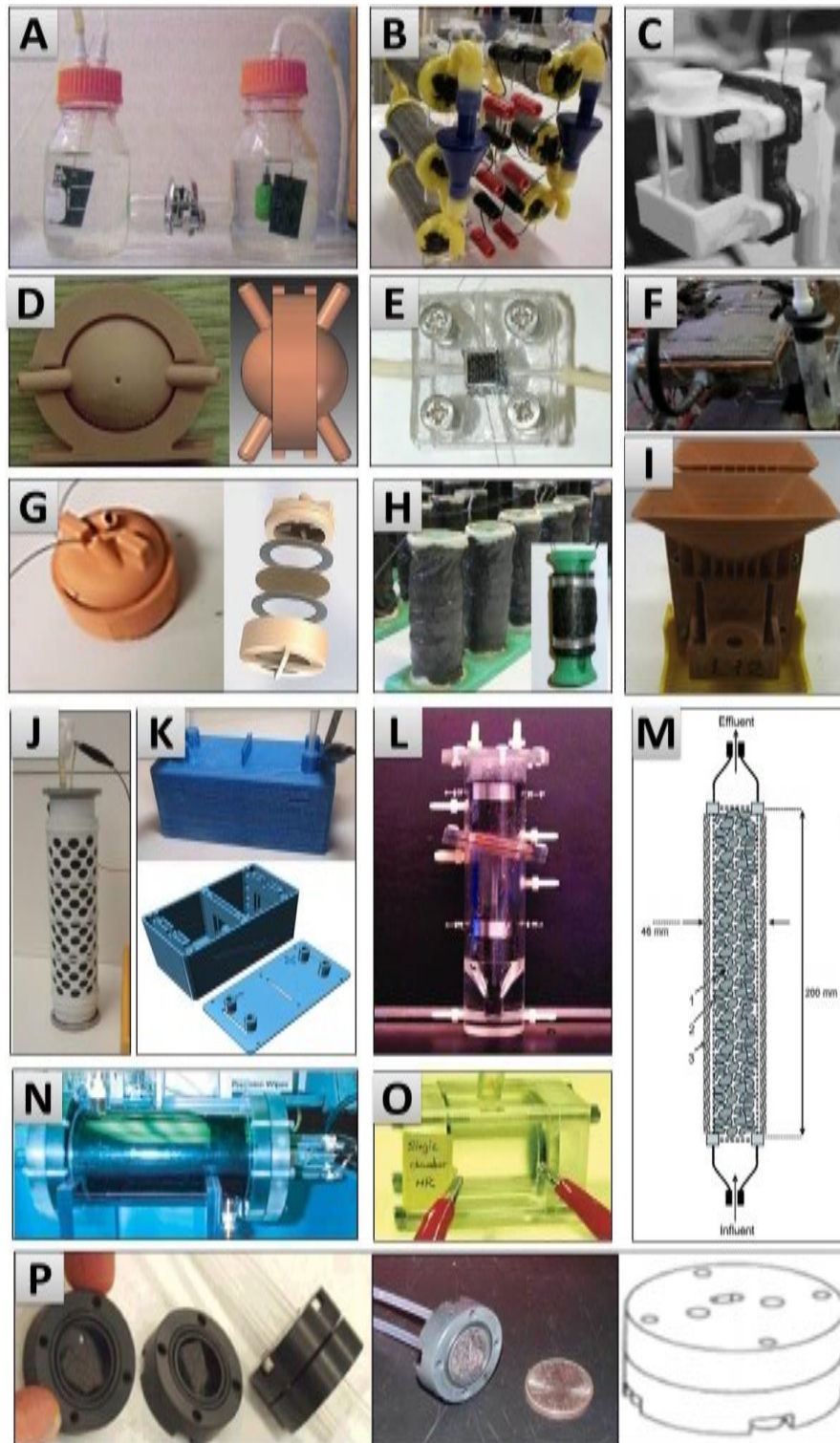


Figure 2.9 - Examples of different MFC designs with different housing materials.

A. H-type MFC using glass bottlesⁱⁱⁱ (Logan *et al.*, 2006) Copyright© American Chemical Society, **B.** Cylindrical MFCs in a stack assembly (Ieropoulos *et al.*, 2013a), **C.** Small scale MFCs out of ABS material^{iv} (Ieropoulos, Greenman and Melhuish, 2010) Copyright© Elsevier, **D.** Miniature (1.4 mL) MFC made out of Nanocure® material^v (Ieropoulos, Greenman and Melhuish, 2013) Copyright© Elsevier, **E.** Miniature MFC (64 µL) made out of Perspex material (Chouler *et al.*, 2016), **F.** Ceramic based flat MFC (Walter *et al.*, 2016a), **G.** Twist n' Play MFCs using Nanocure®^{vi} (Papaharalabos *et al.*, 2015a) Copyright© Elsevier, **H.** Finger size MFCs made out of PLA and natural rubber (Winfield *et al.*, 2015b)^{vii} Copyright© John Wiley and Sons, **I.** Nanocure® based MFCs for robotic applications^{viii} (Ieropoulos, Greenman and Melhuish, 2013) Copyright© Elsevier, **J.** Photograph of a tubular membrane electrode assembly MFC^{ix} (Kim *et al.*, 2009) Copyright© Elsevier, **K.** 3D-printed MFC designed by tomlslav available for download from PinShape (<https://bit.ly/2xOExSC>) **L.** Tubular type MFC with inclined membrane, anode below and cathode above^x (Logan *et al.*, 2006) Copyright© American Chemical Society, **M.** Schematic of a tubular shape - single chamber MFC^{xi} (Rabaey *et al.*, 2005) Copyright© American Chemical Society, **N.** Single chamber MFC containing eight graphite electrodes and a single air cathode^{xii} (Liu, Ramnarayanan and Logan, 2004) Copyright© American Chemical Society, **O.** Single chamber 25 mL MFC^{xiii} (Liu and Logan, 2004) Copyright© American Chemical Society, **P.** Coin size mini-MFC (1.2 mL) (Ringeisen *et al.*, 2006).

As mentioned above (section **2.1.2.2.3**), in the recent years ceramics have been proven a promising structural material and separator for MFCs (Winfield *et al.*, 2016). Clay materials such as terracotta and earthenware have been surrounding our everyday lives since 250 BC and have been used for various household purposes (structural, functional and decorative). This can be attributed to their versatility as their chemical composition, porosity, thickness, shape and geometry can be controlled based on specific applications (Yousefi, Mohebbi-Kalhari and Samimi, 2017). This kind of flexibility in design is very beneficial for an MFC system which is the reason ceramics have been dominating the MFC field since 2011 (Behera and Ghangrekar,

2011). These inexpensive materials made possible the practical implementation of MFC units in impactful field trial studies both nationally and internationally (Ieropoulos *et al.*, 2016). Clay based MFCs have the potential to make the technology widely affordable by achieving a low cost per MFC unit (£1 per single MFC). Minimising the costs of MFCs was the main challenge that influenced the experimental work presented in **Chapter 4**.

2.1.3 Applications

The pre-existing notion that MFC systems were just an invention for scientific curiosity that was deemed to be limited in the laboratory has been disproven in the last 10 years. Improved materials, configurations and reduction in material costs advanced the power output capabilities of MFCs and have made them capable of practical implementation, providing off-grid electricity and supplying power to autonomous robots. Biosensing is another noteworthy example of MFC application which has been successfully performing in laboratory conditions but is not deployed fully in the field yet; however, it will be mentioned in this chapter due to its significance on the rest of the thesis.

2.1.3.1 Wastewater treatment and renewable energy production

MFC's capabilities of converting complex biomass such as waste effluents, into electricity have made the technology popular lately. This enabled the technology to come a long way since its invention due to a substantial amount of research invested in improving every aspect of the MFC system. The ultimate aims were to increase the power density and reduce the associated manufacturing costs in order to make MFC a viable alternative energy source.

The massive turn into alternative and renewable energy sources has been fuelled by the global shortage of fossil fuels and climate change. Renewable energy production from waste using MFC technology is attracting growing attention as the ever-increasing worldwide energy demand is projected to increase 28% by 2040 (International Energy Agency, 2017). MFCs are not only proven to be a viable net electricity generating technology but also can be used as a technology for saving electricity especially in the case of waste water (WW) treatment plants (Du, Li and Gu, 2007). There is an undisputed global need for improved waste management systems and MFC cascades (multiple MFCs connected electrically and/or fluidically) can complement WW treatment processes by treating WW effluent and recovering energy simultaneously (Pandey *et al.*, 2016; Ahn and Logan, 2010; Pant *et al.*, 2012; Winfield, Ieropoulos and Greenman, 2012).

MFCs were first tested as WW treatment solutions in 1991 (Habermann and Pommer, 1991) due to the plethora of organics within WW that can fuel MFCs. Current WW treatment methods (i.e. pumping air to aerate the sludge) require high inputs of energy, therefore employing MFCs not only can save energy but can also facilitate the clean-up of waste streams (Holzman, 2005). MFCs treating WW could result in 50-90% less solids to be disposed of (Holzman, 2005) and MFC cascades fed with urine waste have been shown to reduce the chemical oxygen demand (COD) by up to 95% in real life field applications (Ieropoulos *et al.*, 2016), making it nearly suitable for discharge in the field (UK government threshold: 125 mg/L (GOV.UK, 2019) - PeePower™ effluent: 128 mg/L).

2.1.3.2 MFCs as biosensors

MFCs have the potential to be used as microbial biosensors for monitoring target contaminants (Su *et al.*, 2011). The production of electricity from an MFC reflects on the metabolic activity of the *in situ* microorganisms consuming the given organic compound. In cases where the supplied compound is toxic, the bacterial metabolic pathway(s) can be inhibited resulting in lower electricity production of the system. This capability allows MFCs to be used as *in situ* microbial biosensors for detecting toxic compounds in water (Chouler *et al.*, 2018). Apart from toxic waste, human waste (i.e. faeces and urine) is another large contaminant of water streams, especially in off-grid locations such as slums. It is critical to be able to evaluate polluted water streams (via a monitoring system) in order to provide those in remote areas better water quality that can benefit their health and livelihood prosperity. MFCs can be proven feasible biosensors of biological contaminants, such as faeces or urine, as these can enhance the metabolic activity and consequent power output of the system (Chang *et al.*, 2004; Kim, Chang and Moon, 2006). As such, it has been reported that a self-powered, floating MFC-based biosensor was able to detect urine presence in freshwater which stimulated both a visual and a sound cue, akin to an alarm system (Pasternak, Greenman and Ieropoulos, 2017). The literature evidence presented in this section can support the argument that MFC-based biosensors can provide easily manufactured, cheap and reliable water monitoring systems for toxic chemicals (Chouler *et al.*, 2018). Concomitantly, they can also work as online water quality monitoring systems for early warning of urine contamination in water streams at off-grid remote locations (Pasternak, Greenman and Ieropoulos, 2017).

2.1.3.3 Remote source of power

Being a versatile energy converter, MFC has the potential to be used as a power supplying system operating with microorganisms and organics sourced from the local environment. This capability makes it suitable for use in remote and resource-poor areas where discontinuous demand for power supply is needed and where solar panels cannot be used. Electricity generated from multiple units of MFC connected together (stacks) can be used directly to power small gadgets such as red LED lights (Gajda *et al.*, 2015a; Winfield *et al.*, 2015b) and DC-motor powered windmill toys (Gajda *et al.*, 2015b). MFCs can power larger appliances by amplifying the voltage through the implementation of energy harvesting modules. This voltage can then be used directly or stored intermittently in rechargeable devices such as capacitors and then distributed to the end-user (Ieropoulos, Greenman and Melhuish, 2003). Examples of MFC applications using energy harvester and/or capacitors include but are not restricted to wireless sensors (Shantaram *et al.*, 2005), digital wristwatch (Papaharalabos *et al.*, 2013), air-freshener (You *et al.*, 2016), an array of 40 white LED lights and smoke alarm detector (Ieropoulos *et al.*, 2015). Conventionally these gadgets are powered by rechargeable or alkaline batteries which contain toxic chemicals and have a limited life. The most notable example of them all is the charging up of a commercially available mobile phone (Ieropoulos *et al.*, 2013a) and a state-of-the-art smartphone (Walter *et al.*, 2017). This is of high importance as mobile phones are part and parcel of our everyday lives and are important in case of emergency or danger. Thus having the possibility of charging and powering up such smart devices -in remote locations- with MFCs, adds to the value of the technology. In the same line of work, wearable MFCs can be used to send wireless signals in case of danger (Taghavi *et al.*, 2015) or power up wearable electronics (Pang, Gao and Choi, 2017).

Even though all the aforementioned applications have been tested in laboratory conditions it is only a matter of time for their field deployment which is envisaged due to the rapid development of the technology. In the meantime, there have been other practical applications that have been successfully tested in the field. These include the PeePower™ urinals (Ieropoulos *et al.*, 2016) that have been tested in UK-based festivals such as Glastonbury and Camp Bestival and in developing countries such as Uganda and Kenya (UWE Bristol, 2018).

2.1.3.4 Autonomous robots and MFCs

The field of robotics is a modern technology that is following an increasing trend in interest (Iqbal and Khan, 2017). Robots have changed our everyday lives to a great extent. They are improving the automation in industrial applications (e.g. KUKA robots) and at the same time, they are even helping in household errands (e.g. iRobot vacuum cleaner). More importantly, robots are being deployed in dangerous and hazardous zones aiming to accomplish tasks that are too risky for humans to perform themselves (Saha, 2008). Such applications require robots to be mobile, this implies that robots need to be able to navigate themselves, avoid collisions and plan their path (Siegwart and Nourbakhsh, 2004). Most importantly though mobile robots need to exhibit energy autonomy that can free them from wire restrictions that limit their range of activity and limited operation time due to battery supply. Robots' power supply has been characterised as the bottleneck of their applications thus it is envisaged that green energy resources are the only way forward for powering the next generation of mobile autonomous robots (Wei and Yan, 2012).

MFCs have been contributing to the field of autonomous robotics since the early millennium with the development of “Gastronome” or otherwise called Chew-Chew train (Wilkinson, 2000). “Gastronome” employed an artificial stomach comprising of *Escherichia coli* inoculated MFCs that were metabolising sugars (dextrose). Artificial mediators were facilitating the electron transfer and the MFCs were powering the on-board rechargeable battery pack which ran the train’s motors and pumps (Wilkinson, 2000). Even though Wilkinson’s invention was not entirely autonomous, as the battery bank had to be conventionally fully charged before initiating the system, it inspired a whole new generation of food powered autonomous robots.

Concurrently to Wilkinson’s work, another bioinspired robot was created by Kelly *et al.* (Kelly, Holland and Melhuish, 2000) named “Slugbot”. Slugbot was intended to be the first robot which can gather its energy from the environment (in the form of organic food matter) and utilise it to power itself. Even though it achieved the former by collecting slugs from a muddy field, it never reached the latter. Nevertheless, it explored the potential of utilising naturally occurring organic sources from the environment to achieve energy autonomy in robotic systems.

Following Gastronome’s and Slugbot’s footsteps, a new series of biologically inspired robots called EcoBots made their appearance in 2002 and shook the world of autonomous robotics. EcoBot-I was the first of the series, it employed eight *E.coli* inoculated MFCs which with the aid of artificial mediators were oxidising sugars and charging the on-board capacitors. EcoBot-I was able to perform phototaxis and it was moved towards light every time the capacitor bank reached a certain threshold (Ieropoulos, Greenman and Melhuish, 2003; Ieropoulos, Melhuish and Greenman, 2004). Its’ successor was EcoBot-II which employed the same number of MFC units as its prede-

cessor but used air-breathing cathodes rather than chemical ones (Ieropoulos *et al.*, 2004, 2005). EcoBot-II was more advanced in functionality than EcoBot-I as on top of phototaxis it performed environmental monitoring (temperature sensing) and transmitted information through an on-board wireless transmitter. The other difference with its predecessor was the nutrient source, as EcoBot-II was the first of its kind to digest raw food such as rotten fruits, dead flies and prawn shells (Melhuish *et al.*, 2006). EcoBot-I and II were similar in appearance and MFC materials as shown in **Figure 2.10**.

In 2010 a more advanced robot was created; EcoBot-III (**Figure 2.10**) was the first to exhibit autonomous behaviour as it was able to collect food and water from its environment, digest the collected food and egest the waste (artificial digestion system) (Ieropoulos *et al.*, 2010a). EcoBot-III was able to perform temperature logging, moving towards food and water source and actuate its' pumps. The structure of the robot and the 48 MFCs on-board, were 3D-printed using rapid prototyping materials, the latter with Nanocure® resin and the former with ABS and polycarbonate. Three years later the team developed the last EcoBot of the series, so far. EcoBot-IV (**Figure 2.10**) was the worlds' first fully self-sustainable MFC powered robot. It had bio-inspired digestion and ingestion system and was able to power its electronics and transmit data about its performance to a computer (Papaharalabos *et al.*, 2015b).

The most recent bioinspired MFC powered autonomous robot is Row-Bot (**Figure 2.10**) (Rossiter *et al.*, 2015). This followed from the EcoBot example, but changed the environment from terrestrial to aquatic, since it was inspired by the water boatman beetle; an aquatic insect that feeds on algae and dead plants. The stomach of the robot was an MFC which digested the fluid and

algae and turned it to electricity that powered the robot to move forward and continue its operation (Rossiter *et al.*, 2015; Philamore *et al.*, 2016).

MFC powered robots have come a long way in the last 18 years and this is mainly attributed to the development of the MFC technology that brought improvements in materials, manufacturing techniques (e.g. 3D-printing), electronics and a better understanding of the underpinning science of the system. Nonetheless, more research is needed to improve the MFC systems that will be on-board autonomous robots providing uninterrupted power supply. Apart from power density and cost improvements, another critical factor is the reduction of the size of the MFC units so that it keeps the weight and footprint of the robot at a minimum. The body of work described in this thesis will tackle these issues and intents in improving MFC's power density and concomitantly reducing their costs. The resulted optimised MFCs are envisaged to power a new series of autonomous robots that can form a continuation of this thesis. This series of robots can have an advantage over the conventionally battery powered robots that need recharging every couple of hours or days. MFC powered robots can consume organic matter from their environment to gain their electrical energy making them able to forage freely.

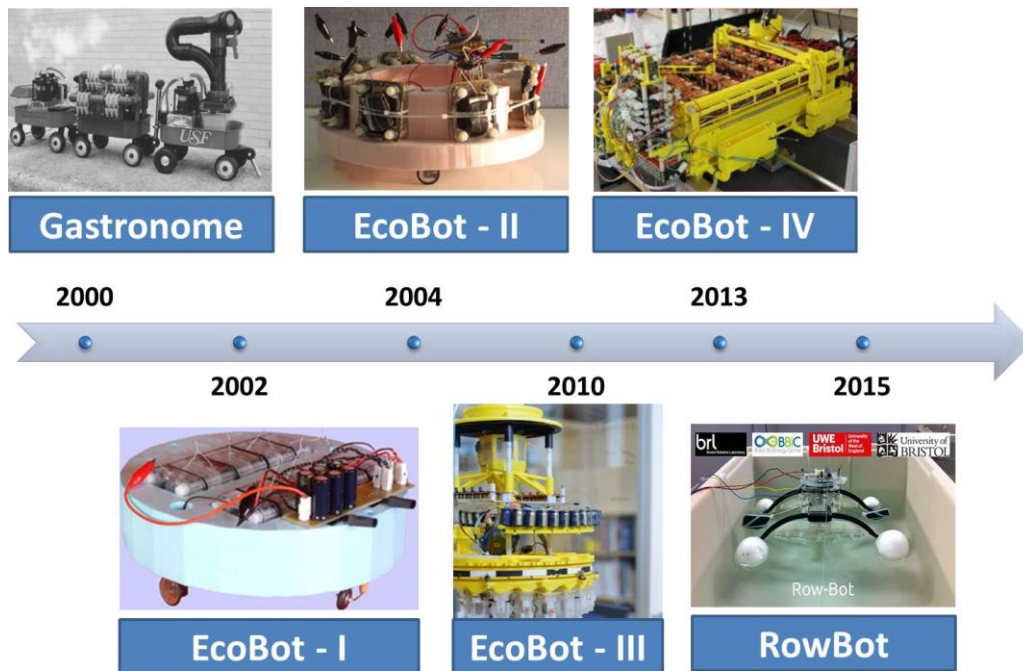


Figure 2.10 – MFC powered autonomous robots in chronological order until 2015.

2.2 MFC relevance to EVOBLISS project

The work described in this thesis falls under the overarching umbrella of the European Commission FP-7 funded project EVOBLISS (from 2014 to 2018, grant agreement 611640), an interdisciplinary project combining robotics, artificial intelligence, chemistry, and microbiology. The project aimed to create an open source expandable and customisable robotic workstation (called EvoBot), to develop new materials and applications based on a real-time feedback loop between the robot and the MFCs, in an attempt to enhance the MFC technology.

Through EvoBot (**Figure 2.11**) as its main apparatus, EVOBLISS took the 3D printing technology to the next level, by turning an open-source low-cost 3D printer to an interactive research tool that allowed the empirical study of adaptation and evolution of the MFC systems. The unique novelty of the project was that the adaptation and evolution occurred with energy abstraction as the main selective mechanism, which was used as the feedback signal triggering EvoBot's feeding mechanism. This was, in fact, the main scientific hypothesis of the overall EVOBLISS project, as written in the original proposal, and hence why it was tested as part of this study. As described above (**2.1.2.1**), MFCs usually are inoculated with WW which has a diverse population of bacteria, both electroactive and non-electroactive. Even though this is very beneficial compared to MFCs inoculated with pure strains of bacteria, this delays the maturation process as at least 3-4 weeks are needed for the electroactive organisms to colonise the electrode, and the non-electroactive to be washed out of the system. Thus only through temporal adaptation, the ecosystem is evolving to more suitable for electricity generation. This process can last from four weeks to three months (depending on the environment) delaying their installation in practical applications.

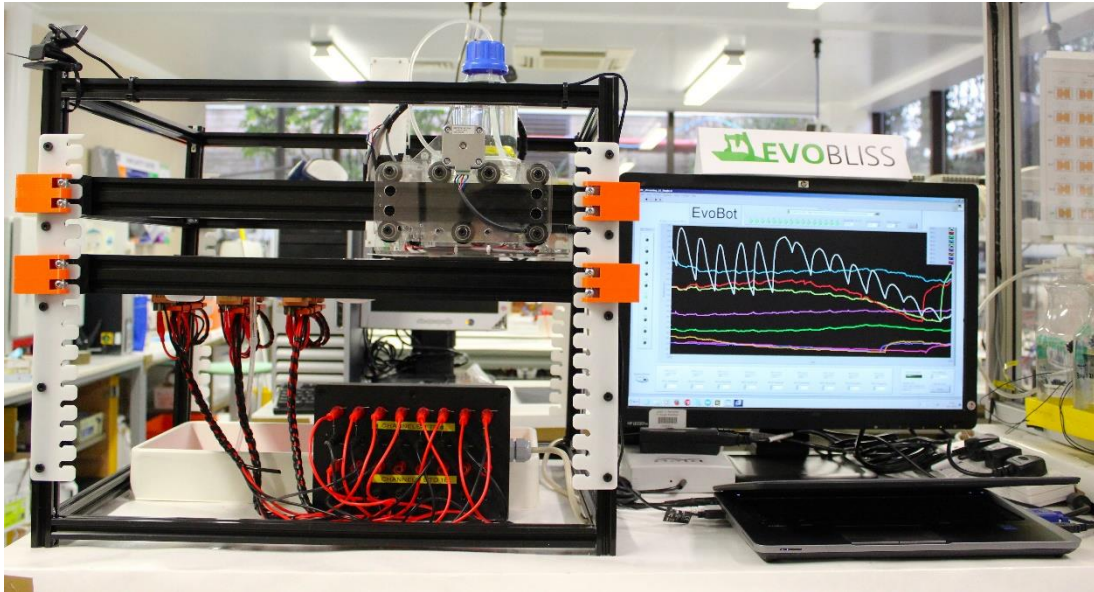


Figure 2.11 – EvoBot robotic workstation

EvoBot is a liquid handling robot which was the product of EvoBliss project. Here, EvoBot is connected with a laptop computer and runs experiment on MFCs, recording and displaying at the same time their voltage output.

EVOBLISS aimed to investigate the evolution and adaptability of the microcosm inside the MFCs in response to dynamic environments dictated by EvoBot, and decrease the time required from MFCs to achieve maximum power output. Such a project is perhaps the first pioneering attempt at adapting the 3D-printing technology to work like a chemostat, which is a standard microbiological procedure for controlling the environment of a growing culture. Similar to a chemostat, EvoBot will be controlling the development of the electroactive biofilms by

- i) inoculating the microorganisms in the MFC anodic vessels
- ii) accurately dosing them with the necessary organic substrate
- iii) adapting the frequency of feedstock supply based on the experimentation needs

- iv) monitoring their adaptation over time in response to feeding (e.g. voltage output) or change in feeding (e.g. types of fuel)
- v) reacting to the degradation of organic matter in real-time (e.g. by feeding the starving MFCs)

Hence EvoBot was aiming to reinforce, monitor and interact with the evolving microbial communities inside the MFCs, resulting in efficient energy generation. Complimentary it was aiming to accelerate the maturing process and produce MFCs with energy producing cultures at shorter periods of time than manually maintained MFCs. Further to this, through evolutionary algorithms EvoBot aimed to improve the existing MFC technology in terms of electricity generation by optimising the organic fuel that electroactive bacteria need to live and thrive.

Beyond the projects main aim another avenue of interest was explored and developed as part of EVOBLISS. EvoBot is a modified 3D printer, so naturally, the ability to also extrude material for MFC parts, such as membranes or electrodes was explored. The idea focused on exploring the possibility of using EvoBot both as a “maintenance machine” and a production tool which can 3D-print core MFC materials such as electrodes and membranes which can contribute to higher power output of MFCs and be potentially used in an EvoBot derived monolithically printed MFC.

The work package that this thesis is based on was the biggest and most critical of the EVOBLISS project since the successful evolution of the EvoBot nurtured MFCs were going to be empirically validated, in terms of accelerating the growth of microorganisms and improving energy output performance, on the EcoBot-II platform (2.1.3.4). This is where the EvoBot-matured MFCs were going to be assessed, in order to demonstrate the feasibility of the

EVOBLISS approach. The successful demonstration of such approach determined the project's success.

Overall, as explained above EVOBLISS aimed to interface the advantages of robotics and computation with the MFC living systems, and use the EvoBot robotic workstation to evolve the MFCs in order to address two important characteristics of living systems: **adaptability and stability**.

2.3 Aims and Objectives

The main purpose of this study was to increase the power output of MFCs and accelerate their maturing process by using EvoBot's interactive capabilities for their maintenance. Likewise, towards the same aim of improving the MFC power output the work focused on optimising the organic feedstock (fuel), supplied to the MFCs, through EvoBot evolutionary algorithms and optimising the core MFC materials (off-robot).

Specific objectives:

- a. To optimise critical MFC components such as electrodes and ion-exchange membranes using novel materials (potentially extrude-able)
- b. To establish a system of interface and interconnection whereby the real-time electrical output is monitored and fed back to the robot platform for control
- c. To investigate the selective pressure effects of substrate concentration and combination through interactive evolutionary experiments performed by the robot
- d. To evaluate the robotic approach on MFC biofilm maturing by comparing it against control MFCs (outside of the robotic platform)
- e. To evaluate the robotic approach on MFC biofilm maturing by employing the robot matured MFCs on EcoBot-II

Chapter 3 General Materials and Methods

This chapter aims to give an overview of the general materials employed for building the MFCs as well as the experimental methodology used throughout the study, and therefore act as a reference point for all the subsequent chapters. However, in the case where materials/methods are exclusive to a single experiment, the specific details will be described in that respective chapter.

3.1 Electrode Materials

The importance of both the anode and cathode electrode material on an MFC system were discussed in sections **2.1.2.2.1** and **2.1.2.2.2**. Next, the methods for fabricating the electrodes used throughout the study are described in detail.

3.1.1 Anode Electrode

The selection of anode material was based on its versatility, beneficial porosity and cost-effectiveness, thus the anode electrodes were constructed from untreated (catalyst-free) carbon veil fibre, with 30g/m² carbon loading (PMF Composites, Dorset, UK). The total surface area used for each experiment differs and this will be mentioned where it is pertinent.

Carbon veil is a foldable material which can be pleated to fit into different size anode compartments allowing the use of bigger surface area with smaller projected area. After folding, the carbon veil is pierced with a piece of nickel or stainless steel wire (approximately 10 cm in length) to secure the

electrode in place and provide the connection point for the data logger and external load crocodile clips.

3.1.2 Cathode Electrode

The cathode electrode is connected via an external load to the anode electrode. The size of both anode and cathode surface area electrodes is based on the literature, which teaches that the ideal ratio of solid cathode to anode is 1: 27 (Uría et al., 2012), which is the selected ratio used for every experiment in this study.

For the purposes of this study, two custom made electrodes for air-breathing cathodes were used as controls against alternative cathode electrodes under investigation. The two electrode types consisted of activated carbon paste with the only difference being the current collector material (carbon veil or stainless steel mesh). The composition and preparation of both electrodes is described next.

3.1.2.1 Activated carbon on Carbon Veil (AC/CV)

The cathode electrode was made of two layers; a gas diffusion layer (GDL) and a microporous layer (MPL). The GDL comprised a single sheet of the same carbon veil material used for the anode electrode but coated with 30% polytetrafluoroethylene (PTFE) (Sigma Aldrich, UK). The sheet was left to dry for 24 hours in room temperature, and once the GDL dried the activated carbon paste was applied on top to form a 2mm thick layer of MPL. The MPL was a mixture of activated carbon powder (G.Baldwin & Co., London, U.K.) blended with PTFE in a 4:1 ratio and deionised water (120 mL). The activated carbon paste was then hot pressed, using a household iron or heat press (Gajda et al., 2015a) and subsequently heated for 15 minutes at 200 °C to

allow MPL liquefaction. The resulted carbon loading on each cm^2 of the electrode was in total 90 ± 5 mg. Photographic image of the electrode is presented in **Figure 3.1A**.

3.1.2.2 Activated carbon on Stainless Steel (AC/SS)

This electrode was manufactured using the MPL activated carbon mixture described above and a stainless steel mesh (316SS, MeshDirect, UK) as the backbone and the current collector (Walter, Greenman and Ieropoulos, 2018). The carbon paste was hot pressed against the stainless steel mesh in both sides to produce a homogenous electrode assembly as shown in **Figure 3.1B**. The resulting carbon loading in each cm^2 was 186 ± 7 mg.

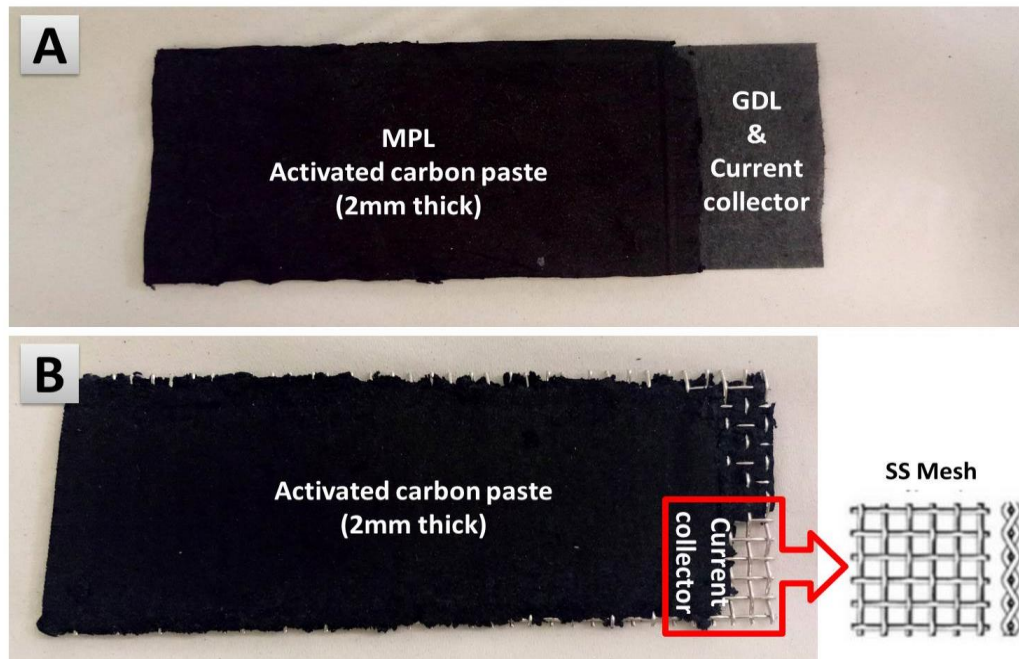


Figure 3.1 - Photos of the two mainly used types of air-breathing cathode electrodes in this study.

[A] AC/CV and [B] AC/SS.

3.2 Membranes and Preparation

The role of a semi-permeable membrane in an MFC system and the importance of selecting the material that makes up this membrane are described in section 2.1.2.2.3. The two main types of membranes that have been used as controls for this study are described below. These two types were selected for their applicability in small-scale MFCs.

3.2.1 Cation exchange membranes (CEM)

In all of the experiments where membrane materials were tested, the control membrane was CMI-7000S cation exchange membrane (Membranes Inter-

national, USA). The membranes were cut to shape based on the MFC requirements and then immersed in 5% NaCl solution for 12 hours at 40 °C to allow hydration and expansion.

3.2.2 Kilned Terracotta Clay membranes

Smooth red terracotta Valentine's clay (Bath Potters, UK) was used for the membrane fabrication in all the cases where "kilned clay" is mentioned in the following body of text. To fabricate flat ceramic membranes the terracotta clay was rolled with a rolling pin in order to remove air bubbles and until it reached 5 mm of thickness (**Figure 3.2**). Then, it was fed through a pasta making machine until it reached 2.5 mm thickness. The flat sheet was then cut to size (factoring 5.6% shrinkage loss due to firing) according to the MFC design and pierced through using a puncher at the four edges to make space for the screw to pass through during assembly. Then the shaped membrane was placed between two sheets of wood to absorb the moisture and dried for 12 hours. The membranes were then kilned at a temperature of 1070 °C for 7 hours, which cured the materials through structural bonding of the clay.

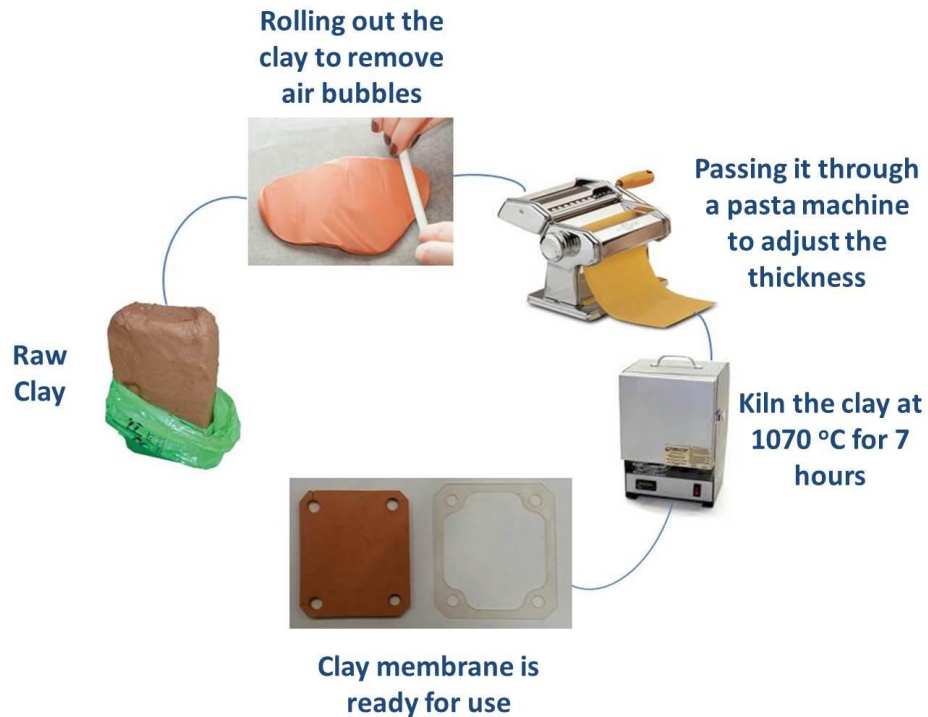


Figure 3.2 - In-house preparation technique for custom made clay membrane “kilned clay”.

3.3 MFC designs

As mentioned in section 2.1.2.2.4, MFCs come in different shapes and forms. During the period of this study three MFC designs were the most commonly used and are introduced below, however modifications to these systems were made in certain experiments, which will be pointed out later in their respective chapters.

3.3.1 Analytical type MFCs

The analytical square type MFCs were assembled using laser-cut polymethyl methacrylate, commonly known as acrylic or Perspex®, of different

thicknesses. These were used to construct the anodic and cathodic half-cells. To ensure leak-proofing, rubber gaskets were fitted between each Perspex piece and the whole assembly was tightened together using plastic studding and nuts. The capacity of the two chambers was 25 mL each. As shown in **Figure 3.3**, the two half-cells were separated by a CEM and had a chemical cathode consisting of liquid potassium hexacyanoferrate (ferricyanide-FeCn). Analytical type MFCs of that volumetric capacity employ folded carbon veil electrodes with 270 cm² total surface area. In most parts of the study analytical type MFCs were modified to accommodate open-to-air cathodes (for the reasons explained in 2.1.2.2.2), this is described in detail at the relevant sections.

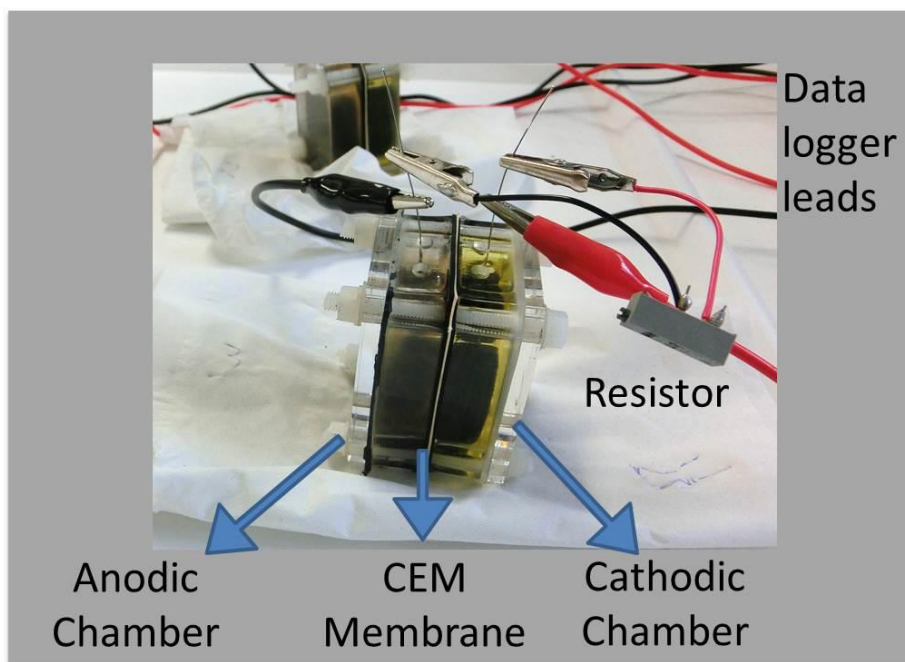


Figure 3.3 - Analytical type MFC with a liquid chemical cathode.

The different compartments are presented clearly along with the attached resistor which was employed in order to close the circuit and the data logger lead cables.

3.3.2 Small-scale MFCs

Small-scale MFCs were 3D printed using the EnvisionTec Perfactory printer at Bristol Robotics Laboratory (BRL) from Nanocure® photopolymer resin (RCP30) (Ieropoulos *et al.*, 2013c). Anodic and cathodic compartments were printed separately with the resulting parts shown in **Figure 3.4**. The small scale MFC design consists of a 6,25 mL anode chamber with a 67.5 cm² surface area electrode and an open-to-air cathode (with hydration capabilities). Both chambers have built-in inlet funnels and outflow mechanisms. In the case of anode, the incoming liquid fills up the chamber from the bottom up while the excess exits from the incorporated overflow exit. The cathode was designed to incorporate a built-in pocket that can hold 1mL of water while allowing any excess water, above that level, to escape through the outlet. As in the analytical type MFCs the anode and cathode are separated via a semi-permeable membrane that varies depending on the experiment. Two rubber gaskets, one for each half-cell, sandwich the membrane and ensure water-tight sealing. The final assembly is bolted together using stainless steel studs and nuts.

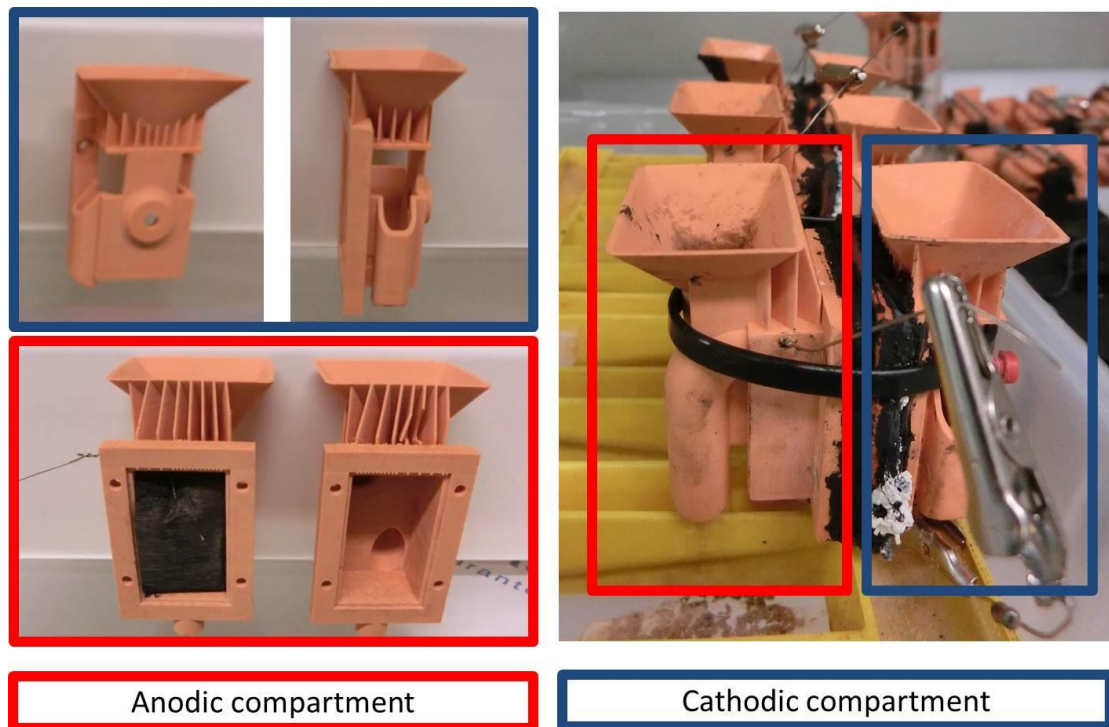


Figure 3.4 - 3D printed small-scale MFCs.

3.4 Inoculum and Feedstock

Inoculation process, as described in 2.1.2.1.1, is the required initiation process to kick start an MFC as it is the introduction of microorganism to the system. Selecting the type of microorganisms is important in establishing a strong electroactive biofilm that can contribute in the electron harvesting process. Following inoculation the bacteria need to be supplied with carbon energy rich feedstock to continue their metabolic processes that result in electron production. The type of bacteria and feedstock used in this study is described below.

3.4.1 Activated Sludge

Activated sewage sludge supplied from the Wessex Water Scientific Laboratory (Saltford, UK) was used as the mixed bacteria source for inoculating abiotic MFCs in all the experiments unless otherwise stated. To initiate the experiment, the MFCs were inoculated with activated sludge supplemented with nutrients as explained next (**3.4.2**), for the first four days. The anode chamber of the MFC was emptied and replenished with fresh sludge daily until the selected feedstock was introduced at the end of the inoculation period.

3.4.2 Tryptone Yeast Extract

Tryptone Yeast Extract (TYE) was used as a background solution in many experiments as a supplement of nutrients and amino acids. A strong stock solution of 1.5% TYE (1% Tryptone and 0.5% Yeast Extract) was prepared using 10g of Tryptone (Sigma Aldrich, UK) and 5g of Yeast Extract (Sigma Aldrich, UK) in a litre of deionised water before it was diluted in a stock of activated sludge. When TYE was used as a background solution, the final concentration of TYE in the mixture was 1:10 (0.15% TYE).

3.4.3 Urine

Urine was collected from healthy individuals, on a normal diet and without any medical conditions through a 125 L collection tank connected to an adapted male urinal at BRL. Urine was collected twice a day for experimental purposes and excess was stored in the fridge. On the time of collection from the tank, the pH of urine was on average pH 9.20(±), the conductivity was 29.1(±) mS and COD was 5.16(±) g/L.

3.5 Mode of feeding

Following the selection of feedstock, the feeding mode needs to be established in order to ensure the system receives the much needed carbon energy sources in frequent doses. The different modes of feeding used in MFC studies have been reviewed above (2.1.2.1.2) and the ones selected for this study are outlined in detail below.

3.5.1 Batch mode

MFCs that were maintained through a batch mode of feeding were completely emptied daily (weekdays) and refilled with the selected feedstock (100% refill). The emptying and refilling of the anode chamber occurred through extraction of the anolyte using a conventional syringe (Terumo®) followed by topping up with fresh media.

3.5.2 Continuous flow

Throughout the thesis, all the experiments that were fed in continuous flow mode were maintained using a 16-channel high accuracy peristaltic pump (205U, Watson Marlow, Falmouth, UK). This pump offers a high range of flow rates starting from 4.2 mL.h⁻¹ to 780 mL.h⁻¹, depending on the volume of the MFC anodic half cells each flow rate resulted in different hydraulic retention times (HRT).

MFCs that were operating under continuous flow mode were adapted accordingly in order to allow continuous movement of liquid in and out of the cell as well as percolation of liquid within the cell. The adaptations of these systems will be explained in their relevant sections.

3.6 Operational conditions

Unless otherwise stated all the experiments were performed at room temperature (22 ± 2 °C) within a temperature-controlled environment.

3.6.1 Practical challenges

Throughout the life span of this study, some inevitable challenges were encountered that caused temporary loss of data due to power cuts, computer failures, and laboratory shut-down. Other challenges included urine shortage, when water diluted urine had to be used instead and pump failures that interrupted the fuel supply. These occasions are mentioned and noted where appropriate.

3.7 Data capture

For the data collection, MFC output was recorded in millivolts (mV) against time using Agilent Keysight 34970A Data Acquisition / Data Logger Switch Unit (Keysight Technologies, UK) or PicoLog Datalogger ADC-24 (Pico Technologies, UK) with a 1, 3 or 5 min sample rate. Data were processed and analysed using MS Office Excel and GraphPad Prism® version 5.01 software package (GraphPad, San Diego, California, U.S.A).

3.8 Calculations

Current (I) in amperes (A) was calculated using Ohm's law, $I = V/R$, where V is the measured voltage and R is the known value of the external resistive

load in ohms (Ω) used in each experiment. Power (P) in watts (W) was calculated by multiplying voltage with current: $P = I \times V$.

In frequent cases throughout the text the power output is expressed as power density for comparison purposes. The power density in this thesis is calculated based on total anode surface area of the specific MFCs taking place in each experiment. This initially is expressed as μW per cm^2 of anode electrode with is calculated as shown below:

$$\text{Power density} = \frac{\text{Power Output } (\mu W)}{\text{Total anode surface area } (cm^2)}$$

However, to normalise the power density from $\mu W/cm^2$ to mW/m^2 , the total is multiplied by 10 (e.g. $1 \mu W/cm^2 = 10 mW/m^2$).

3.9 Polarisation experiment

Polarisation experiment is an electrochemical analysis performed on MFCs by sweeping the external resistance value in a gradual manner starting from open circuit (high resistance value) and finishing to a very low resistance value. This experiment provides information on the power output capabilities of the MFC system by identifying the maximum power transfer point (MPT) that an MFC can achieve. Specific information on each polarisation experiment will be described in the relevant chapters.

Polarisation experiments were carried out by connecting the MFCs to an 8-channel automated Resistorstat, developed by Degrenne et al. (2012). The external resistance (R_{ext}) values ranged from $30 k\Omega$ down to 3.74Ω with each resistance value held for 3 minutes. During polarisation, voltage output was recorded every 30 s (6 samples per resistance value) in order to monitor

and capture the dynamic response of MFCs to changes in R_{ext} . The MFCs were kept in open-circuit voltage for 2 hours prior to polarisation testing. Following the first polarisation experiment, the R_{ext} was changed to a value at which maximum power transfer was obtained.

3.10 Conductivity and pH measurements

All pH and conductivity measurements were taken using a benchtop pH meter (Hanna Instruments, HI2211 pH/ORP Meter) with a pH range of 0-14 and a handheld portable conductivity meter (Jenway, 470 Cond Meter) with a range from 0 – 199.9 mS.

3.11 Chemical Oxygen Demand (COD) analysis

Chemical oxygen demand (COD) analysis measures the amount of oxygen required to oxidise chemically the amount of oxidable components present in water samples and is expressed in mg/L of oxygen. This gives an indication of the oxygen demand characteristics of a sample (e.g. wastewater). The greater the COD value the harmful the sample is to the aquatic environment. Once this sample is discharged it can consume the available oxygen present in water depleting it and hence starving the aquatic life (e.g. fish).

COD removal analysis was carried out by analysing the influent sample and comparing it with the effluent sample after 24 hour retention time in the MFC systems under investigation. The analysis was conducted using the potassium dichromate oxidation method (CamLab, UK) with high range (HR) COD vials. Then 0.2 mL of sample (inlet and outlet) were taken from the MFC and filtered, using a 0.45 μm syringe filter (MILEX®HA, UK), before being added

into the vial. The sample was then heated up at 150°C for 2 hours and cooled down for another 2 hours. At last, the concentration was measured through a spectrophotometer (Lovibond Water testing).

3.12 Scanning electron microscopy (SEM)

To observe the surface morphology of the different abiotic materials under investigation, microscale images were acquired using FEI Quanta 650 field emission scanning electron microscopy (SEM) at difference magnifications. The samples were mounted on aluminium mounts using contact adhesive and were pre-treated using sputter coating in gold using Emscope SC500 sputter coating unit.

3.13 Energy-dispersive x-ray (EDX) spectroscopy

Following the SEM analysis, a qualitative chemical analysis took place. The present elements in the solid samples under investigation were determined using the Oxford Instruments Aztec energy dispersive X-ray (EDX) system and the main elemental content of each sample was identified.

3.14 Experimental data

The data obtained from the experiments, for statistical analysis, were in triplicates. Three identical MFCs were set up for each condition tested, including the controls. The mean voltage output of each triplicate was calculated in Excel for each time point and plotted against time to provide the temporal profile of the experiment. In some cases, in the text describing the experiment, the spread in data was reported to show how much variation there is in

the values of the data set. This was done by finding the mean of the set of data, then subtracting each number from the mean and expressing it in *mean±difference*. An example is presented below:

MFC 1	500 mV	Mean = $\frac{500+550+600}{3} = 550$ mV
MFC 2	550 mV	Difference 1 = $550 - 500 = 50$
MFC 3	600 mV	Difference 2 = $550 - 600 = -50$

Spread = 550 ± 50 mV

3.15 Conclusions

This methodology chapter aimed to provide the reader with the necessary understanding of the standard materials and methods used during the study. The subsequent chapters will guide the reader through the experimental journey that ultimately led to the novel findings highlighted in each chapter. To facilitate the flow of the thesis each chapter will include a succinct materials and methods section to describe the specifics of each experiment that have not been mentioned above, that where necessary, will cross-reference to this chapter.

Chapter 4 3D-Printable core materials for MFCs

As described in **Chapter 2**, the electrical performance of an MFC system relies on a number of factors including but not restricted to; the design of the system and its core structural (chassis) and functional (electrodes, connectors and membranes) materials. In the same chapter, the different designs of MFCs used so far were presented, showing that 3D printing can be an alternative method to manufacture bespoke and optimised MFCs. This chapter therefore aims to review the impact of 3D-printing on MFC research and then describe and discuss the series of experiments which were conducted as part of this study. The chapter is split into the three main sections focusing on the experiments conducted in the context of improving the three main MFC parts; separators, anode and cathode. Thus, following the literature review, the experiments on 3D-printable MEAs, extrude-able carbon energy sources and soft 3D-printed electrodes are presented individually. This set of experiments focused on investigating the 3D-printable core MFC materials that can result from EvoBot and can improve the performance of MFCs, bringing the field a step closer to monolithic MFC fabrication.

Parts of this chapter have been published in Journals and Conference Proceedings. Each relevant publication is mentioned at the start of each subchapter to provide better clarity.

4.1 3D-printing and its impact on MFC research

Additive manufacturing (AM) and three-dimensional (3D) printing are two interchangeably used terms to describe the process of producing layer-by-layer three-dimensional objects based on a virtual digital model of the object. The 3D printing technology made its first appearance in the 1980s in Japan when Hideo Kodama invented AM (Kodama, 1981). His method of automatically fabricating 3D plastic objects by exposing photo-hardening liquid to ultraviolet light and stacking the solidified successive cross-sectional layers together was the first pioneering attempt at 3D printing. Kodama's idea inspired the development of this technology and three years later Charles Hull patented the invention of stereolithography (SLA) (Hull, 1984). Hull's patent opened up a new avenue for manufacturing complex objects rapidly, reliably, accurately and economically. Since then, his groundbreaking development has driven major innovations in many sectors including food industry (Godoi, Prakash and Bhandari, 2016), cell biology (Mitchell, 2016) and pharmaceuticals (Jonathan and Karim, 2016).

MFC technology and 3D printing (rapid fabrication) were both employed in 2007 as part of the EcoBot-III project, where compartments of MFCs were fabricated and used on-board the entirely 3D-fabricated and uniquely designed body of the robot (Ieropoulos *et al.*, 2010a). In the years to follow more 3D printed polymer-based materials started to be investigated and tested against the conventional Perspex ones, showing the advantages of 3D printed compartments, not only in accelerating the assembly process but also in reducing the internal resistance of MFCs (Ledezma, Ieropoulos and Greenman, 2010). Several developments have been achieved in the field of MFCs due to 3D printing including the fabrication of Nanocure® housing (chassis) for small-scale MFCs. This development made it possible to scale-

up the technology by miniaturizing and multiplying the MFC units within a stack (Ieropoulos *et al.*, 2010b) and achieve their implementation in autonomous robots (Ieropoulos *et al.*, 2010a). This was just the beginning of a new era for the MFC research as the 3D printing technology gave unprecedented design freedom to the researchers, enabling them to explore novel materials with intricate geometry and complex features. This helped reduce the costs and assembly requirements for MFCs, such as the small-scale twist 'n' play MFCs (Papaharalabos *et al.*, 2013). Further to the advances in the area of MFC chassis, 3D printing opened new opportunities for using a vast array of printable materials to advance the inner functional system of the MFC such as using Tangoplus acrylate photopolymer resin for the rapid fabrication of ion exchange membranes (Philamore *et al.*, 2015), which is one of the most important components of the MFC (as detailed in **2.1.2.2.3**). A pocket of research focused on using AM techniques to fabricate both the outside housing and inner core system of the MFC. In a recent study, Calignano *et al.* (2015) managed to entirely print an MFC by combining three different AM techniques (selective laser melting - SLM, fused deposition modelling – FDM and spray coating technique). The bio-inspired lattice anode was rapidly fabricated using an aluminium alloy sprayed with marine inoculum and enclosed within a non-assembly mechanism MFC housing. The latest attempt towards monolithically printing MFCs reported the fabrication of the first 3D printable polymer anode using conductive PLA material combined with the use of Gel-Lay polymer as a viable alternative separator to the conventional cation exchange membrane (You *et al.*, 2017). The ease of bringing complex custom-made prototypes to life within a span of few days using 3D printing did not only help MFC research but it planted its roots into electrochemistry (Ambrosi and Pumera, 2016) exemplified by the production of conductive 3D printed electrodes for supercapacitors (Zhao *et al.*, 2014) and versatile microfluidic

flow cells for specific electrochemical experiments (Snowden *et al.*, 2010). Bioelectrochemistry and MFCs are a branch of electrochemistry, thus the notable developments mentioned above can also directly benefit MFC research where possible.

Adding to the above history of MFC advancements due to 3D printing techniques, in 2014 a novel line of work under the project name EVOBLISS was initiated. EVOBLISS aimed to turn a low-cost RepRap printer into a liquid handling robotic platform, named EvoBot, to maintain and improve the power output performance of MFCs while at the same time 3D print “evolved” parts for the next generation of MFCs. The ultimate aim of the project was the monolithic fabrication of MFC units that can be inoculated and maintained at high power output levels using the same exact platform that created them. The following chapter sections present the experimental work that led to identifying potentially 3D-printable materials suitable for MFC systems which can contribute to higher power output levels compared to conventional (control) materials. The first experimental work is presented directly below and it is focusing on identifying printable separators that can be part of a monolithically printed membrane electrode assembly.

4.2 Air-dry 3D-printable membrane electrode assembly

Part of this work has already been included in “Theodosiou, P., Greenman, J and Ieropoulos, I. Towards monolithically printed MFCs: Development of a 3D-printable membrane electrode assembly (MEA) *International Journal of Hydrogen Energy*” in press.

One of the main contributors affecting both cost and performance in MFCs is the commercially available membrane, which tends to be expensive. Polymeric separators based on Nafion or Nafion-derived fluorinated polymers are considered at the bottleneck of MFC progress and the main contributor to high cost and internal resistance (Harnisch and Schröder, 2009). Besides, those types of membrane are prone to biofouling after long term operation (more than 60 days) (Ghasemi *et al.*, 2013; Flimban *et al.*, 2018). The aforementioned is a result of microorganisms, microbial extracellular polymers and salts depositing on the membrane. This, along with possibly contact resistance, impacts negatively the MFC power performance (up to 37% decrease) due to the deterioration of the cation transfer which limits the charge transfer and increases the systems' internal resistance (up to 20%) (Xu *et al.*, 2012). In addition, in the open-to-air configuration, the cathode is often not well integrated within the membrane, therefore the contact resistance is even higher, and output is limited.

To overcome these issues, alternative MFC architectures and materials, such as ceramic based ones (Winfield *et al.*, 2016; Yousefi, Mohebbi-Kalhari and Samimi, 2017), need to be identified (or examined better) as well as ways to manufacture and integrate them. One possible design that can benefit the system is the integrated membrane electrode assembly (MEA) in which the cathode is built on the membrane itself. It was previously shown that the power output is improved by reducing the internal resistance (Nandy *et al.*, 2015).

MEA is the assembled system comprised of a membrane and electrode/s attached together as one through pressing with or without heat treatment in order to minimise the distance between them. This arrangement has been inherited from the traditional chemical abiotic fuel cell and showed higher

power densities compared to the conventional separated membrane and electrode configurations (Nandy *et al.*, 2015). However, only a few studies have focused on MEA influence on MFC systems and even fewer on 3D-fabrication techniques to manufacture these MEAs.

This investigation looks at 3D printing MFCs using novel extrude-able materials that can be produced from the EvoBot platform; a RepRap 3D printer turned to a robot which can inoculate, maintain and print parts for MFCs (Faíña *et al.*, 2016); more details of EvoBot are given in **Chapter 5**. The focus of this experimental study is on the development of cost-effective MEAs using extrude-able air-dry membranes coated with conductive paint. Different ceramic and polymeric based membranes were investigated and compared in terms of chemical composition and properties. The electrical conductivity, surface morphology and chemistry of the materials were also analysed and presented below along with the measured electrochemical performance in terms of power generation.

4.2.1 Specific Materials and Methods

4.2.1.1 Membrane Materials

For the scope of this experiment, three types of potentially extrude-able membranes were tested and compared against a conventional CEM. The materials tested were Fimo™ air-dry clay (Staedtler, German), terracotta air-dry clay (Hobbycraft, UK) and red terracotta clay. Even though all three membranes were prepared using the process described in **3.2**, only the terracotta clay was kilned. The other two membranes were dried overnight at room temperature. The thickness of the tested membranes was consistent for all the custom made membranes (2.5mm). The total surface area of the

membranes was 25 cm². The images of the different membranes utilised in this study are shown in **Figure 4.1**.

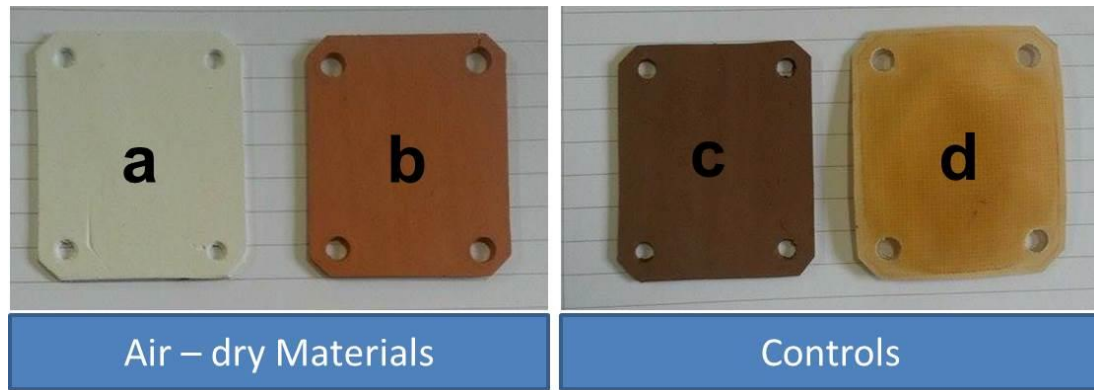


Figure 4.1 - Photographs of the four cut-to shape (25 cm²) membrane materials.

[A] Air-dry Fimo™, **[B]** Air-dry Clay, **[C]** Kilned Terracotta and **[D]** Cation exchange membrane.

4.2.1.2 Membrane electrode assembly

A conductive graphite coating was applied to each membrane and formed the cathode electrode. The coating was fabricated using polyurethane rubber coating (PlastiDip), white spirit and graphite powder as previously described (Winfield *et al.*, 2014). The membranes were coated uniformly with the conductive cathode mixture using a brush followed by the Dr. Blade technique using a spatula. Dr. Blade or otherwise known tape-casting is a well-known technique in the fabrication industry where a slurry (made out of conductive particles and binder additives) is applied onto a substrate using a blade in order to produce a thin layer of coating on the substrate. The surface resistance was measured during each coating as described in **4.2.1.4.2**. After the membrane electrode assembly had dried, a cable was attached to the cathode using conductive wire glue, to form the cathodic current collector.

4.2.1.3 MFC architecture

Twelve cubic analytical size MFCs (3.3.1) were modified for this experiment to accommodate an open-to-air cathode resulting in the use of the anodic half-cell only (Figure 4.2A). The cathode was integrated with the four different membranes (i.e. painted on one side) and directly glued to the anode chamber with an inert aquatic sealant (Aquabits, UK), with the cathode side facing open to air (Figure 4.2B). In order to maintain the moisture of the membrane electrode assemblies and maintain a liquid ‘bridge’ for proton transport, the MFCs were wrapped with Parafilm® which is a highly waterproof material but at the same time is permeable to oxygen (Figure 4.2C).

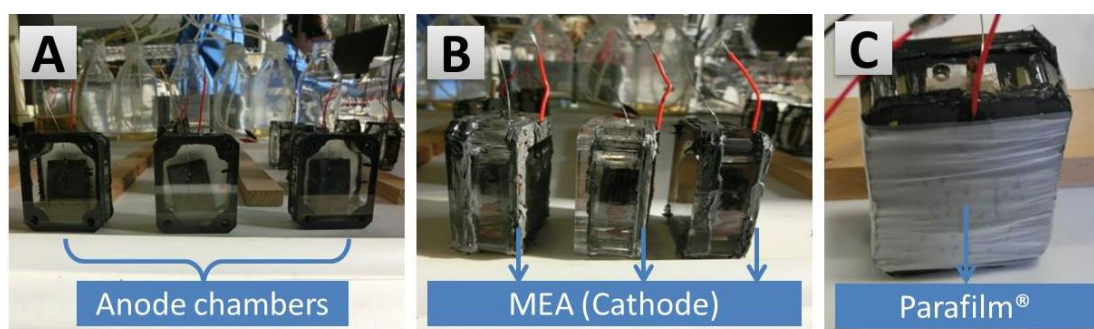


Figure 4.2 - Photographs of the MFC setup.

[A] Anode chambers with the anode electrodes, [B] side view showing the Membrane Electrode Assembly (MEA) glued on the anodic chamber and [C] the whole MFC assembly wrapped in Parafilm® to retain the moisture on the MEA.

4.2.1.4 Characterisation of membrane and electrode

The chemical composition of the membrane, as well as the morphology of the electrode, was conducted using the methods described in section 3.13 and 3.12 respectively. Additionally, two other tests were carried out; a hard-

ness test to evaluate the structural durability of the materials and an electrical conductivity test to observe the in-plane resistance of the MEA.

4.2.1.4.1 Hardness Test

The hardness of the membrane material was tested using the Vickers Hardness Testing equipment (Buehler, UK) (Clinton and Morrell, 1987). Particularly; the entire 25 cm² of the membrane was used for the hardness testing. Average values were obtained from five readings taken from five different locations on the membrane and located 5 cm apart.

4.2.1.4.2 Electrical conductivity of the multi-layer cathode

The surface conductivity of the cathode was measured through a handheld digital multimeter (TENMA, 72-7750). Particularly, crocodile clips were attached on the opposite sides of the membrane electrode assembly and the resistance was measured. This operation was repeated for each layer of graphite applied on the membrane. This method was only used to give an early indication of the in-plane resistance of each conductive coating addition.

4.2.1.5 Inoculation and feedstock

The twelve MFCs were inoculated with a mixture of 50% fresh human urine and 50% anolyte derived from another ongoing experiment operating on activated sludge and urine. The mixture was enriched with a background solution of 0.15 % TYE. The solution was left in a shaking incubator (Orbital Incubator S150) for 24 hours at a shaking speed of 130 rpm and at a temperature of 36.6°C. The solution was transferred to 15 mL centrifuge tubes (Corning, UK) and placed into the centrifuge (VWR Compact Star CS4) for 10

minutes at 5000rpm. Subsequently, the supernatant was removed and the pellet re-suspended into 5 mL of neat urine. The re-suspended medium was collected and formed the inoculum for the experiment. After the inoculation period during which the biofilm formed, the MFCs were fed manually in batch mode with urine.

4.2.1.6 External loading

The MFCs operated using a fixed load of 2.7 k Ω prior to polarisation experiment, which was conducted as described in section 3.9. Following the first polarisation experiment the R_{ext} was changed to 1 k Ω , a value at which maximum power was generated. This load was kept constant until the end of the experiment.

4.2.1.7 Breakdown of the experimental procedure

The experimental plan that was followed in this study has been summarised and presented at **Table 3**. The table, notes in detail the feeding regime followed, the operational conditions, urine replacements, timings and quantities of feedstock as well.

<i>Day 0</i>	Inoculation	100% inoculum	Full exchange (25 mL)
<i>Day 1-2</i>	Inoculation	50% inoculum – 50% urine	Full exchange (25 mL)
<i>Day 3-4</i>	-	No feeding	-
<i>Day 5-9</i>	Daily Feeding	100% urine	Full exchange (25 mL)
<i>Day 10-14</i>	Daily feeding	100% urine	5 mL top-up
<i>Day 15 onwards feeding regime: a complete exchange of anolyte early each week, followed by a daily top-up of 5 mL until the end of the week.</i>			
<i>Day 15-25</i>	Daily feeding	Water diluted urine	Feeding regime described above
<i>Day 26-30</i>	Daily feeding	100% urine	Feeding regime described above
<i>Day 30</i>	Polarization	Change of Rext. from 2.7 k Ω to 1 k Ω	
<i>Day 31-58</i>	Daily feeding	100% urine	Feeding regime described above
<i>Day 59-62</i>	Starvation period	No feeding	-
<i>Day 63-73</i>	Daily feeding	100% urine	Feeding regime described above

Table 3 Breakdown of the experimental scheme followed through the entire duration of the experiment.

4.2.2 Results and discussion

4.2.2.1 Material selection and analysis

Four different membranes (**Figure 4.1**) were selected and investigated as separators in MFCs fed with urine. Two of the membranes were based on air-dry techniques (Fimo™ air-dry clay and terracotta air-dry clay). Both are based on water, filling materials and cellulose derivatives. These two materials were selected due to the advantage of being malleable and extrude-able from an adapted 3D-printer nozzle, which can be incorporated in the EvoBot platform. Furthermore, the air-drying technique means that ceramics can be fabricated through normal atmospheric conditions without the utilisation of heat treatment. Red terracotta clay was another membrane used during the

experiment and acted as one of the controls to the investigation. However terracotta has to undergo high temperature treatment in controlled atmospheric conditions which allows the internal binding of the clay within the structure as needed (Ieropoulos *et al.*, 2017). The last membrane utilised was a commercial polymeric-based cation exchange membrane, which was used as the second control.

4.2.2.1.1 Chemical composition of the membranes

EDX system was employed for the qualitative chemical analysis of the elements composing each membrane tested during this investigation. C, O, Al, Si and F were the elements identified with percentages above 10% (**Figure 4.3.A**). Carbon and oxygen were detected in all four samples; however, it is notable that aluminium and silicon were detected only for the ceramic-based membranes. These elements are well known to be generally integrated within ceramic materials especially in their oxide form (Pasternak, Greenman and Ieropoulos, 2016) however their role in the cation transfer and overall MFC performance is yet to be identified.

As expected fluoride was only detected in the polymeric membranes confirming that it is not suitable for a sustainable technology as MFCs. Generally, polymeric membranes consist of a backbone of fluorinated polymer that gives mechanical strength and resistance to harsh and corrosive environments. Unfortunately, fluoride pollution can harm plants and wildlife and therefore the utilisation of fluorinated materials in MFCs might negatively impact the environment after long-term operation. In fact, if those MFCs are to be used on-board low-power robots that are programmed to perform a particular task and then degrade naturally in the environment (Rossiter, Winfield

and Ieropoulos, 2016) then the use of fluorinated membranes needs to be avoided.

Additionally, elements with a percentage lower than 5% were also reported (**Figure 4.3.B**). Traces of Na, Mg, K, Ca, Ti and Fe were detected within the ceramic-based samples. Only Na and N were detected on the polymeric membrane. Interestingly, a percentage of ~3.5% of Ca was measured in the air-dry clay and higher content (roughly 4%) of iron was detected in the terracotta sample. Overall, the two air-dry membranes had almost identical composition between each other and had similar composition to the terracotta, confirming that they might be by-products of the latter. The impact of their chemical composition in the overall power output of MFCs, requires further study.

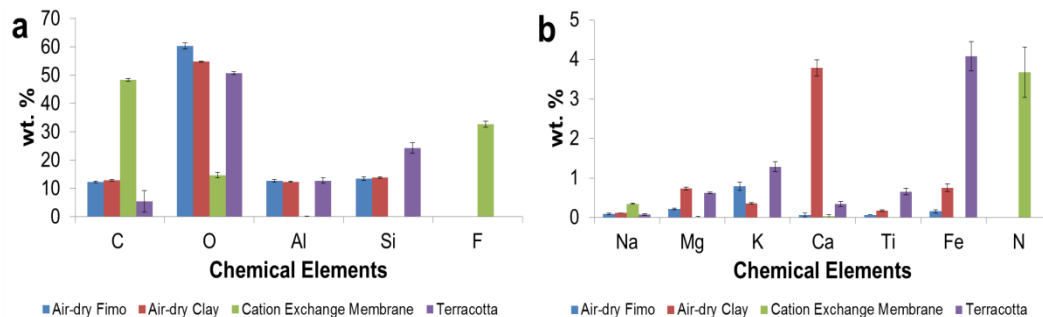


Figure 4.3 - ED-X analysis results data of the chemical elements between the four tested types of membranes.

[A] Major and minor components [B] trace elements

4.2.2.1.2 Morphology of the electrode

The morphology of the graphite-based coating was observed using SEM images at different magnifications (**Figure 4.4**). Increasing magnifications al-

lowed visualising the surface of the electrode in more detail. The surface of the electrode, in fact, seems to be fully covered by a quasi-uniform coating ensuring electrical continuity. At higher magnification, the graphite particles could be clearly detected with non-uniform shape and length within the micrometric shape in agreement with the manufacturer's specifications (Kaiyu Industrial LTD, 2018). This observation shows that the cathode electrode has an enhanced exposed area to atmospheric oxygen providing better oxygen reduction reaction. The importance of having high surface area in the cathode and its role in the oxygen reduction reaction has been reviewed above **(2.1.2.2.2)**.

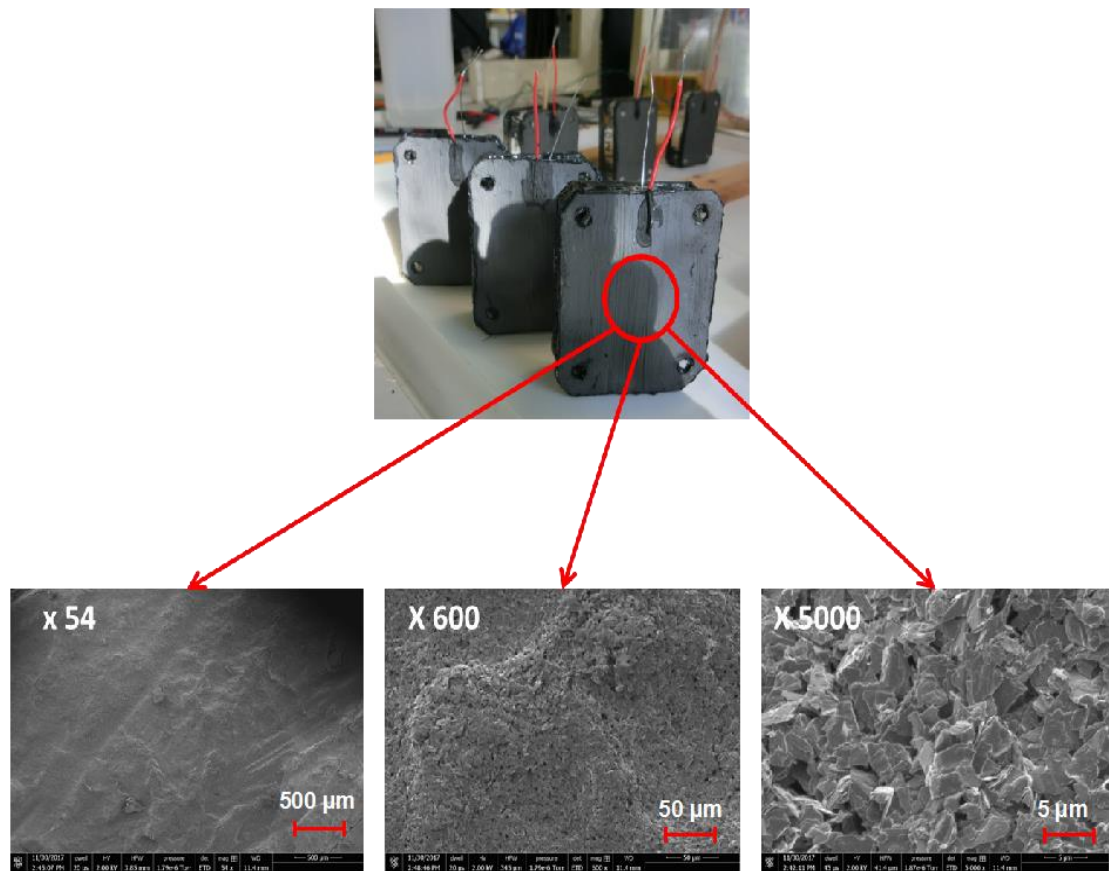


Figure 4.4 - SEM images at three different magnification of the MEA side surface coated with the graphite ink (cathode side).

4.2.2.1.3 Electrical conductivity of the multi-layer cathode

The MEAs were prepared by applying the conductive ink directly on to the already set membranes using a layer-by-layer technique. Each layer was left to air-dry before each in-plane resistance measurement was taken. **Figure 4.5A** shows the in-plane resistance of the air-dry clay and terracotta clay based MEAs after applying the first, second and third layer of conductive ink on their surfaces. These two materials were chosen for discussion because

their sets of data illustrate nicely the difference in resistance between the two differently made clays (air-dry and kilned). Initially the terracotta MEA had almost 2.5x higher resistance compared to air-dry clay. The difference was more exaggerated after applying the second layer of coating with terracotta being 5.0x higher than air-dry clay even though the overall resistance decreased for both by nearly 2.0x and 4.0x respectively. Despite the differences and high resistance values initially, by the time the third layer of conductive coating was applied and cured, both MEAs showed similar in-plane resistance values ($170 \pm 5 \Omega$). This suggested that by that time the conductive ink coating completely covered the surface of the membrane and bonded with the underlined layers of coating in a quasi-uniform manner, in agreement with the SEM micrographs. It is noteworthy that in an attempt to decrease the in-plane resistance even more, a fourth layer of coating was applied on the membranes. However, this had an adverse effect on the continuity of the electrode as it caused cracking of the upper layer of coating. Thus for the scope of this experiment, only three layers of coating were applied on each membrane to form the MEA, which was in accordance to what has been reported in the literature for similar conductive inks applied on paper-based MFCs (Winfield *et al.*, 2015a). Following the application of three consecutive layers of conductive ink on the MEAs the in-plane resistance values were measured and plotted on **Figure 4.5B**, showing that all MEAs had an overall resistance of $150 \pm 15 \Omega$. More specifically, Fimo™ had an in-plane resistance of 135Ω followed by CEM with a resistance of 143Ω , air-dry clay and terracotta as mentioned above had a similar resistance of 158Ω and 168Ω , respectively. These results have given an initial indication of the in-plane resistance after each layer of graphite coating, which can provide information on the current connecting losses of the MEA. In further investigation of MEA materials, through-plane resistance it is recommended to be measured in

order to provide more comprehensive results on the whole MEA resistance, preferably by employing the Wheatstone bridge method. This method uses an electrical circuit which measures an unknown electrical resistance by balancing two legs of a bridge circuit, one leg of which includes the unknown component (Ekelof, 2001). This technique can give more accurate measurement results than the in-plane resistance method, for further analysis.

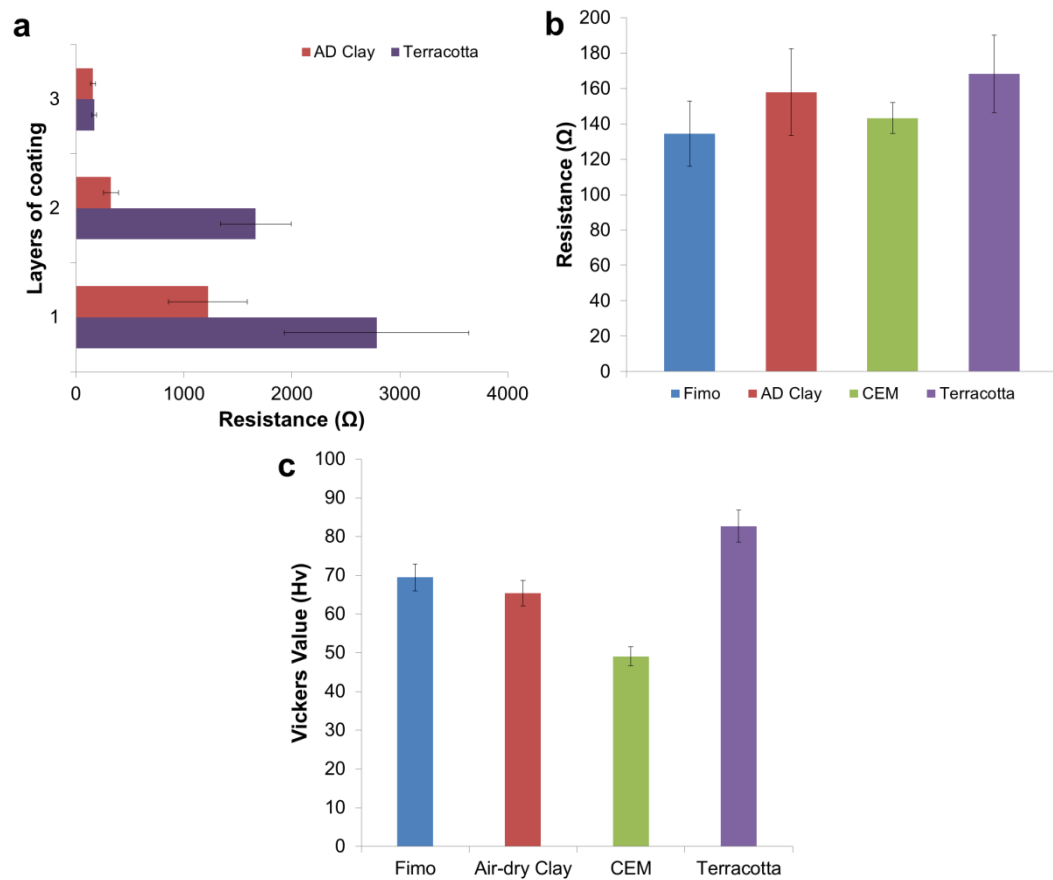


Figure 4.5 - Resistivity of the MEA and hardness of the membrane.

[A] Average resistance values after each coating on the membrane [B] Average surface resistance of the MEA electrode [C] hardness test based on Vickers value (Hv)

4.2.2.1.4 Structural rigidity of the membrane

It is well known from the literature that ceramics have many unique characteristics that make them suitable for use within MFC systems; one of these advantageous characteristics is their structural durability (Winfield *et al.*, 2016). In order to test the durability of the materials under investigation against terracotta, a Vickers hardness test was performed. Even though this technique is well used for testing metal materials, it has been reported in the

past that it can be used for ceramic materials (Clinton and Morrell, 1987) to give an indication of durability between different samples. The unit of hardness given by this test is the Vickers Pyramid Number (HV), the five values obtained from each ceramic testing were averaged and presented in **Figure 4.5C**. The results confirmed that terracotta was indeed the most durable/hardest (82.7 HV); however air-dry Fimo™ and air-dry clay were very comparable being only 13 and 17 HV units lower respectively. To put the results into perspective a window glass has a hardness value of 550 HV. Those data are early indications that even though air-dry clays are not as structurally robust as kilned terracotta; they can still be proven to be durable. The hardness of the materials was tested in order to observe the properties of the material in question, in terms of deformation from a standard source (the metal indenter), which would in turn provide an indication of the material's ability to resist wear, pressure, or damage, which is particularly relevant for shipping systems like these to other areas.

4.2.2.2 Power Output

4.2.2.2.1 Initial power output profile of the first fifteen days

For this experiment, MFCs using different membrane materials were tested with the ultimate aim to observe the feasibility of using air-dry clays that can be 3D-printed, as separators for MFCs. As previously mentioned (**4.2.1.5**), the MFCs were all inoculated with a mixture of activated sludge, tryptone-yeast extract and effluent from established urine fed MFC experiments. After inoculation, the MFCs were left in open circuit for three hours until the voltage plateaued. The observed potential difference between the anode and cathode from all the MFCs was roughly 600 ± 50 mV (data not shown). An external load of 2.7 k Ω was connected on all MFCs, closing the circuit and

initiating the power generation process by encouraging the formation of an electroactive biofilm on the anode electrode. The MFCs were maintained in a batch-fed mode as exemplified graphically by each increase (then decrease) in power output, accompanying each feed cycle. This is because the energy source availability within the anode chamber initially increases. That means, that bacterial growth rate and metabolism were limited by the supply rate of new carbon-energy substrates and therefore they respond to the new supply. The first two exchanges in anolyte consisted of replenishing fully the chamber with the aforementioned inoculum and urine in a 50%:50% ratio, which was sufficient to supply the bacteria with the much needed carbon energy sources to continue their metabolic activities during “periods of no feeding”, which were beyond the normal feeding cycle (**Figure 4.6**). During this period, the MFCs with air-dry clay membrane decreased in performance by 13.2%, which was similar with the air-dry Fimo™ (13.8% decrease). The MFCs with terracotta and CEM were the most affected showing a decrease of 18.6% and 40.0% respectively.

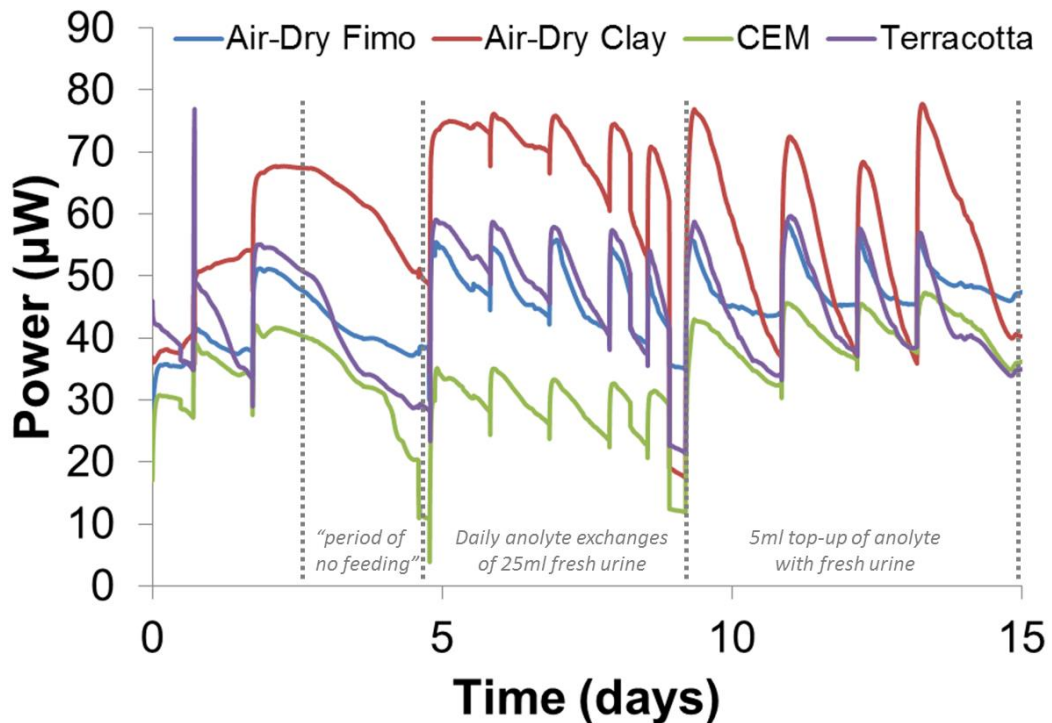


Figure 4.6 - Power generation recorded in the first 15 days of operations.

On the fifth day, the anode chamber of each MFC was replenished completely (25 mL) with fresh urine resulting in an increase in power output by 14.4% and 14.8% for the air-dry clay based MFCs, 29.7% for the CEM based MFCs and nearly 50% in the terracotta based MFCs (**Figure 4.6**). It is assumed that the terracotta based MEA had the greatest improvement in power following carbon-energy depletion, because of the higher porosity compared to the other materials, which has a direct impact on the cation rate of exchange. Higher porosity and non-selective materials will naturally allow a higher rate of cations to diffuse through – a process which is driven by electron-neutrality. This means that for selective or lower porosity materials even if the rate of electrons generated by the biofilm communities is at similar levels for all tested conditions, the power output will be lower, as a result of the

lower number of cations, diffusing through the membrane and reacting with the incoming electrons. This is also reflected by the fact that the terracotta based MEAs reached maximum power output just after 5 days of operation whereas the other materials needed more time to reach that. Such observation agrees with existing literature on ceramic-based MFCs (Pasternak, Greenman and Ieropoulos, 2016).

The following five days continued with daily anolyte exchanges of 25 mL fresh urine as indicated by the spikes on the graph. During this period, the MFCs showed a consistent increase in power output with a peak at 75 μW for air-dry clay followed by terracotta and air-dry Fimo™, which were almost on par at 58 μW and 54 μW , respectively; the CEM was the least performing with 37 μW . Nine days after the start of the experiment, following the empty/refill of the anode chambers with fresh organic matter, the mode of feeding was switched to 5 mL top-ups, after manually removing the same liquid volume from each anode. This resulted in an overall increase in power output of 11%-15%, however, this dropped quickly due to the lower amount of fresh carbon-energy available. Bacteria were presumably still consuming other by-products available in the suspension, within the 24 hour window between each feeding. However, the power output at the end of each feeding cycle was consistently around 40 μW each time. In order to compensate for the impact of each feeding approach on the power performance, it was decided to have a complete exchange of anolyte early each week, followed by a daily top-up of 5 mL until the end of the week. This strategy continued until the end of the experiment.

4.2.2.2.2 Long term power output profile of the entire experiment duration

As explained earlier, the experiment was maintained at a constant external load of 2.7 k Ω for the initial 30 days of operation, during which it was clearly observed that the air-dry clay was the best performing, while the air-dry Fimo™ and terracotta were on a par; in most cases, CEM was the least performing. Although a steady-state was achieved within the first fifteen days of operation for all the MFCs, this was lost due to urine shortage and having to use diluted urine (50:50) (3.6.1) between the fifteenth and twenty-fifth day of the experiment (Figure 4.7). It is envisaged that the steady state would have continued at the same levels if neat urine had been supplied to the bacteria. This hypothesis is confirmed by the data of the twenty-fifth day where the output of the MFCs recovered to the previous levels once un-diluted neat urine was supplied. Following a month of operation at a constant load, the MFCs were subjected to polarisation using an automated Resistorstat in order to identify the optimum resistance value based on each system that can give the maximum power output. Although the polarisation results are discussed in detail below (4.2.2.2.3), the impact of identifying and applying the optimum external load on the MFCs will be discussed here. The results of the polarisation experiment showed that those particular MFC systems were optimal when subjected to an external loading of 1 k Ω resistance. Once the external resistance switched to 1 k Ω , Fimo™ outperformed the rest and the overall power output of all others also increased by 25%-50%. The performance of the MFCs was maintained at the same levels for the following month until complete starvation of four consecutive days brought all the systems to nearly zero (from day 58 to day 62). During this period, all the anode MFC chambers completely dried out from evaporation (Figure 4.7). Howev-

er, once the MFCs were fed again, the bacterial communities of the already established anode biofilm switched from inactive mode (carbon limited) to active mode. Therefore, the power performance recovered immediately back to similar levels as those from the last feeding. More specifically, Fimo™ separated MFCs reached 91.25% recovery, air-dry clay and CEM reached full recovery (100%), while interestingly terracotta separated MFCs had an increase of 13.4%. However, compared to the highest levels of performance recorded during days 30-45, the percentage of recovery was 63.5%, 64%, 40.5% and 91% for Fimo™, air-dry clay, CEM and terracotta respectively. The recovery profile of the previously dried and inactive MFCs adds an extra value to the feasibility of those systems. MFCs are biological entities that not only have long-term power production capabilities -for as long as organic matter is supplied- but more importantly, can survive elongated periods of starvation with demonstrable fast response/recovery. Besides, inexpensive materials such as air-dry clays and terracotta can be used to fabricate these MFCs, which is an economic advantage over traditional commercially available ion exchange membranes.

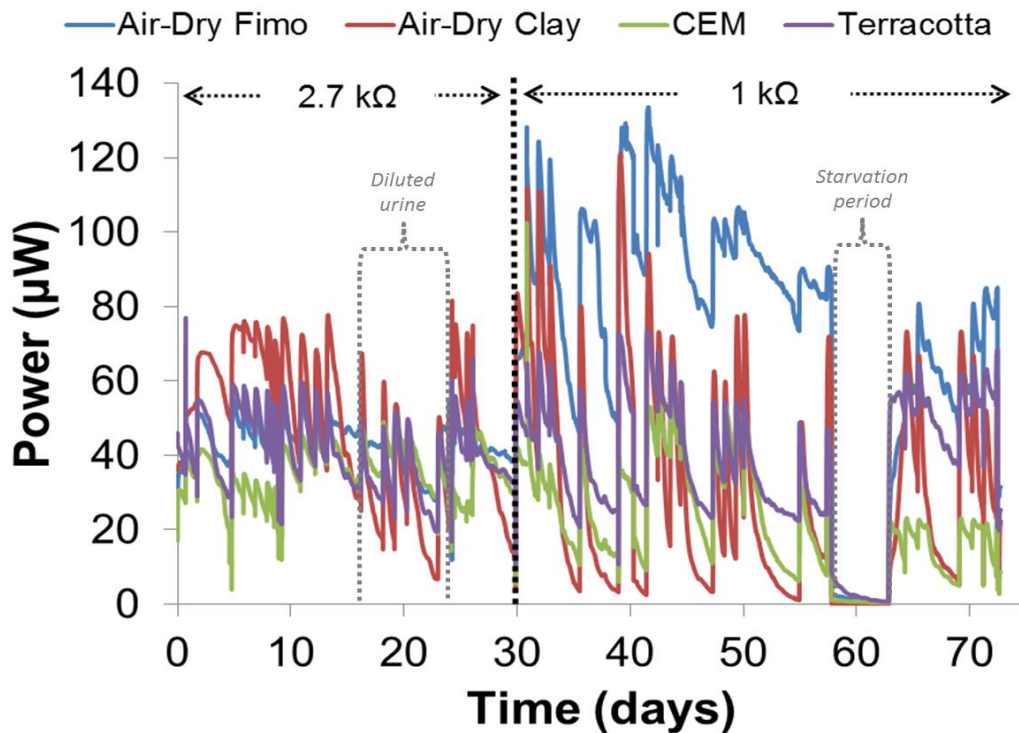


Figure 4.7 - Power generation over 70 days operations (n=3)

4.2.2.2.3 Polarisation results

After a whole month of operation under a constant load (2.7 kΩ), all the MFCs were subjected to polarisation analysis by sweeping the external resistance value in a gradual manner starting from infinite resistance (open circuit) and finishing at a very low resistance value (heavy load). Throughout the polarisation experiment, the voltage output of the cells was recorded as a function of resistance, making it possible for the automated system to calculate the current and subsequently the power output. Using the aforementioned data, polarisation curve was generated (**Figure 4.8A**), by plotting the voltage versus current. The recordings from each triplicate of MFCs were

averaged and plotted including standard deviation. The initial values at 1M Ω resistance (no current) show the open circuit voltage (OCV) of all the cells at around 600 \pm 50 mV. The OCV of the tested MFCs was around 500 mV below the theoretical OCV value (1.1 V) for open-to-air cathode MFCs. Primarily this is due to activation overpotentials, which is a characteristic of MFCs with air-breathing cathodes operating on the ORR in neutral media (Santoro *et al.*, 2017). These OCV values are in agreement with other open-to-air MFC devices under similar operating conditions (You *et al.*, 2014; Papaharalabos *et al.*, 2013). Although in the literature there are also higher OCV values reported (0.7-1.0 V), the cathode electrodes of those MFCs were either supplemented with ferricyanide, during the polarisation experiment, or were moistened continuously with tap water (Logan, 2008; Ieropoulos, Greenman and Melhuish, 2010; Ieropoulos, Melhuish and Greenman, 2007).

The purpose of the polarisation experiment is to understand better the specific characteristics of the systems under examination in order to measure their power outputs. **Figure 4.8B** shows the power curves generated, this graph gives us the possibility to assess the maximum power transfer (MPT) point, which is the maximum peak of each power curve and corresponds to the optimum resistance value that can give this output. Based on the results, it is evident that air-dry clay had the highest power output at 130 μ W followed by air-dry FimoTM with 111 μ W. These results were in accordance with the real-time data shown above, proving that the air-dry membranes generated the highest amount of power output. The two underperforming MFCs were the controls; terracotta (73 μ W) and CEM giving around 50% less than the air-dry clay (66 μ W).

Comparing the power density of the MFCs reported herein with other MEA-based MFCs in the literature, the 3D-printable ones are showing promising

results. In particular, a study on tubular MFCs with air-breathing cathodes based on CEM-MEA had a power density of 5 W m^{-3} (based on the anodic liquid volume of 200 mL) (Kim *et al.*, 2009). This output is 0.2 W m^{-3} less than the air-dry clay-MEA of this study, calculated based on a reactor volume of 25 mL. Besides, apart from the advantage over the power density, the MEA used in the aforementioned study (Kim *et al.*, 2009) was fabricated using carbon cloth coated with a mixture of Pt powder and carbon black bonded together with Nafion resin, which inherently increases the cost.

Following the polarisation analysis and based on the MPT point, the optimal external resistance was identified ($1\text{ k}\Omega$). Once the MFCs were connected to this lower resistance value, the performance levels began to diverge and Fimo™ produced the highest power output (**Figure 4.7**). Although after the change in external resistance, the results of the polarisation differed from the real-time data (day 30 onwards) and Fimo™ ended up outperforming the air-dry, in all cases, the soft materials were operating better than the conventional cation exchange membrane.

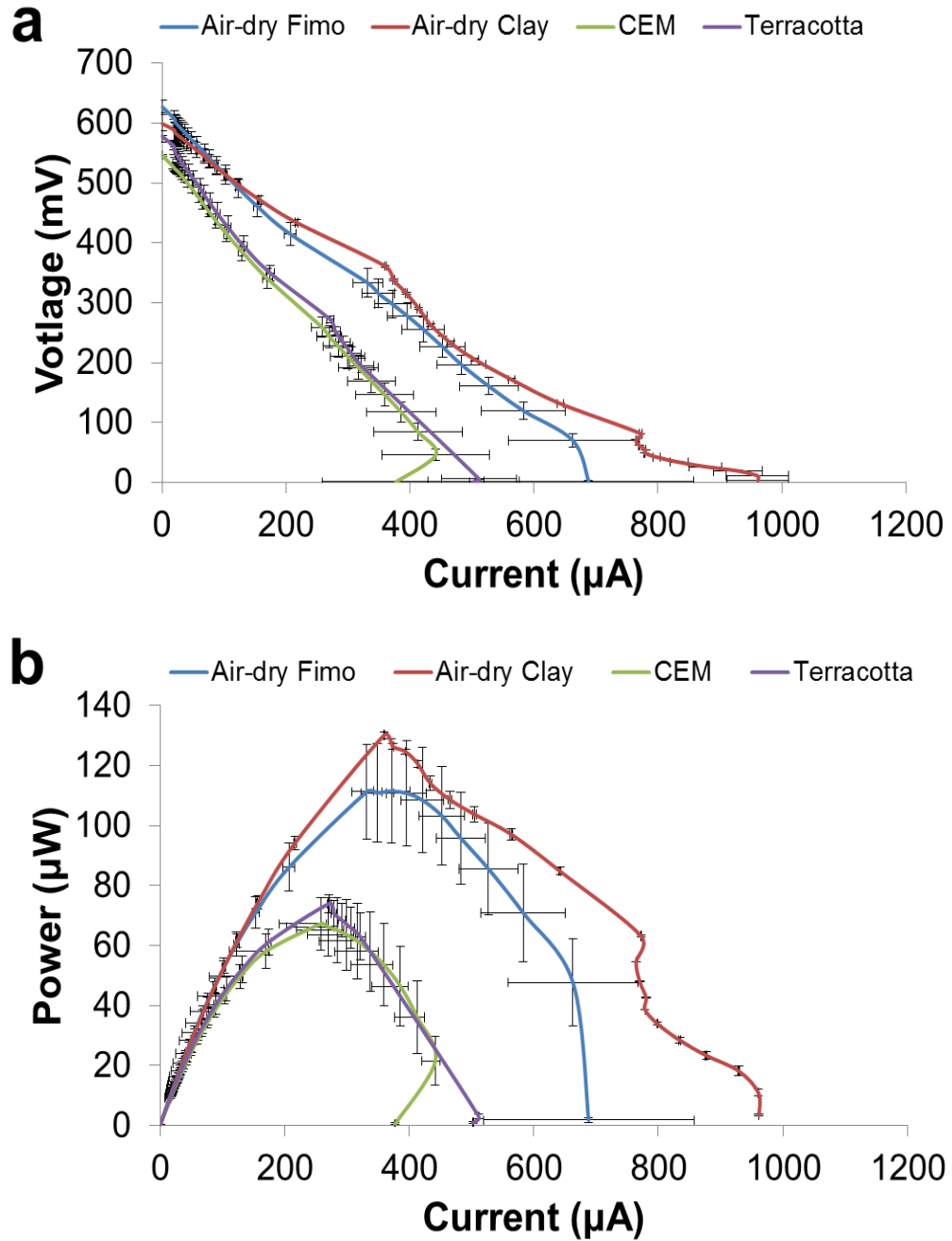


Figure 4.8 - Polarisation results [A] voltage vs current curve and [B] power curve. (n=3)

4.2.2.3 Chemical Oxygen Demand Analysis

Following the increase in performance due to the external loading shift, a COD analysis was conducted to observe the rate of COD decrease within a 24 hour period. On the eleventh day following the switch in external resistance (forty-second day of the entire experiment), prior to replenishing the anode chamber with the 25 mL of urine, a sample of that was taken for COD analysis. In parallel to that, a sample from that urine (25 mL) was kept in a closed container on the bench to observe the decrease in COD without being treated in MFC. The following day, a sample of the effluent of all the MFCs was taken and analysed. The results of this analysis are presented in **Figure 4.9A.**, which shows that MFCs with air-dry Fimo™ MEA had a decrease of almost $82\pm 1\%$ in COD which was 4% higher than air-dry clay and terracotta. CEM based MFCs resulted in $63\pm 1\%$ COD decrease. The control COD reduction occurring in the closed glass bottle after 24 hours was 4.7%; this value was deducted from the overall percentage decreases of all MFCs. This was in order to demonstrate the decrease in COD, which was induced due to the bioelectrocatalytic activity of the electroactive microorganisms presented in the anode and also by fermentative floating microorganisms.

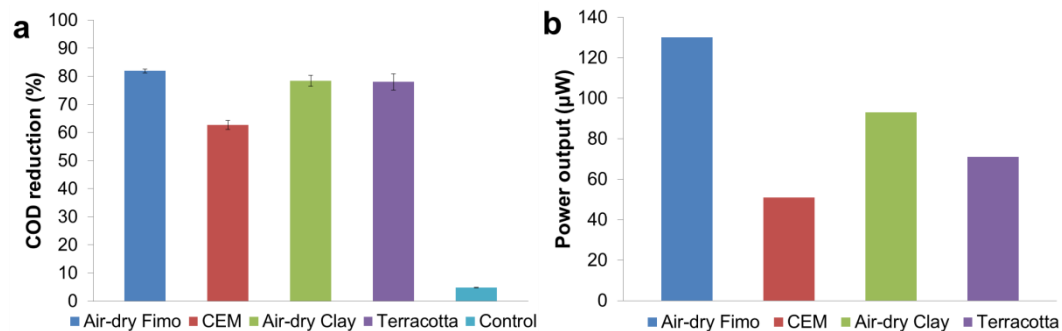


Figure 4.9 - COD reduction results and power output at the time of sampling.

[A] Percentage of COD reduction of fresh urine within 24 hours in an MFC and in a closed glass bottle (control). **[B]** Power Output of the MFCs at the moment that the samples for COD analysis were taken.

The results of the COD analysis are in agreement with the real-time data of that period (day 42), which confirm and support the literature which reports that MFCs operating at higher power densities have higher COD removal rates due to the enhanced abstraction of electrons (Ledezma, Greenman and Ieropoulos, 2013; Zhang *et al.*, 2015). For the sake of clarity, **Figure 4.9B** shows the power output of the MFCs at the time that the samples were taken. Based on that in terms of power output Fimo™ was at 130 µW, air-dry clay and terracotta performed 29% and 45% lower than Fimo™ whereas CEM had a 60% less power output than the aforementioned (51 µW). **Figure 4.9** demonstrates clearly the correlation of power output to COD reduction and adds an extra value to the feasibility of those MEAs as alternative conductive separators of MFCs.

4.2.2.4 Cost Analysis

As microbial fuel cell is a technology producing low quantity of electricity, particular attention needs to be given towards maximizing the performance

while minimizing the costs. In this section, the cost of membranes is illustrated and discussed (**Figure 4.10**). The cost of the ceramic membranes was calculated considering 1 kilo of raw materials. More specifically, at the moment of purchase air-dry Fimo™ cost 4.94 £ kg⁻¹, air-dry clay cost 3.75 £ kg⁻¹ while terracotta was the least expensive of all as it was 33% cheaper than air-dry clay and roughly 50% cheaper than air-dry Fimo™. The cost of the latter was in fact 2.52 £ kg⁻¹. The CEM cost was considered to be 188 £ m⁻¹ (250\$ m⁻¹) according to the supplier. Each membrane was weighed during fabrication and therefore the composition was known. In the case of CEM, a total area of 25 cm² was used. In order to fabricate the ceramic membranes, 6 g, 8 g and 10 g of air-dry Fimo™, air-dry clay and terracotta respectively were used. Consequently, the overall cost for each membrane (with an area of 25 cm²) was similar for air-dry Fimo™ and air-dry clay at £0.030 per membrane and terracotta being slightly lower at £0.025 per membrane mainly due to the lower cost of the raw material. CEM was the most expensive costing £0.78 per membrane (**Figure 4.10A**). This means that it is possible to fabricate 26 air-dry Fimo™/air-dry clay membranes or 31 terracotta membranes for every CEM membrane at the same cost. As mentioned in the introduction of this thesis, to make MFCs affordable and accessible everywhere in the world the price per unit need to be as low as possible. The ultimate aim is to achieve a cost per unit around £1. Membranes such as the ones tested here which can cost only as little as £0.025 can be proven an economic alternative minimising the overall costs of MFCs and achieving that aim.

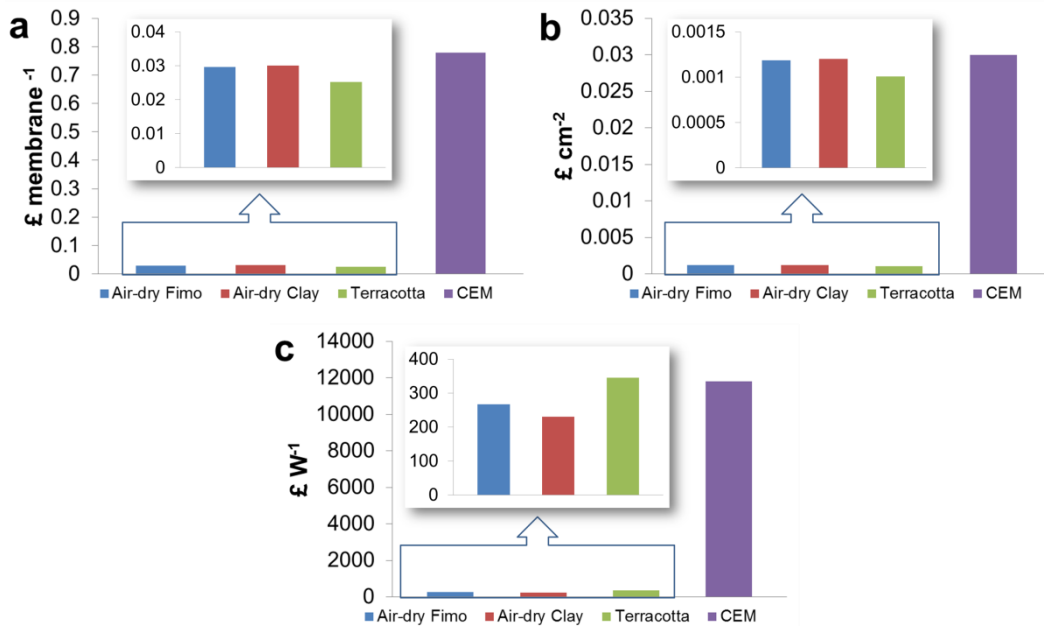


Figure 4.10 - Cost analysis of the membranes.

[A] Overall cost of the membranes, **[B]** Cost of the membrane for unit of area and **[C]** Cost of the membrane for unit of power produced.

Another important aspect to consider is the cost of the membrane density meaning the cost of the membrane per cm^2 . The results are shown in **Figure 4.10B**. The trend reflects the cost of the raw materials with terracotta having the lowest cost per surface area and CEM the highest. Particularly, the cost for terracotta was roughly 0.1 pence per cm^2 (10£ m^{-2}) followed by air-dry Fimo™ and air-dry clay which amounted to roughly 0.12 pence per cm^2 (12£ m^{-2}) and CEM thirty times higher than that ($\approx 300\text{£ m}^{-2}$).

Finally, the cost of the membrane for each Watt produced was also calculated (**Figure 4.10C**). The power from the peak of power curves (**Figure 4.8B**) was considered in $130\text{ }\mu\text{W}$, $111\text{ }\mu\text{W}$, $73\text{ }\mu\text{W}$ and $60\text{ }\mu\text{W}$ for air-dry clay, air-dry Fimo™, terracotta and CEM respectively. Due to the higher performance, air-dry clay had the higher value of cost per power produced, among the ma-

materials investigated, that was quantified in 230 £ W⁻¹ (**Figure 4.10C**). Slightly higher value was achieved by air-dry Fimo™ with 267 £ W⁻¹. Terracotta had a cost per W produced of 345 £ W⁻¹ and CEM had an astonishing value of 11818 £ W⁻¹. The cost per W produced of CEM was 34, 44, 51 times higher compared to terracotta, air-dry Fimo™ and air-dry clay respectively. Among the three clay-based membranes, the most cost-effective material tested was air-dry clay. The cost per W produced was 14% and 33% better compared to air-dry Fimo™ and terracotta respectively. Air-dry Fimo™, air-dry clay and terracotta seem to be very promising cost-effective membranes materials that can replace the more expensive and not environmentally-friendly polymeric membranes. It must be noted that the cost of kilning or shipping from abroad was not taken into account for these economic calculations.

4.2.3 Connection with EvoBot

EvoBot (**Figure 4.11A**) is a RepRap open-source customisable 3D-printer modified successfully to operate as a liquid handling robot for culturing and maintaining MFCs based on an established feedback loop between the MFC systems and the python controlled platform (Theodosiou *et al.*, 2017). The feedback loop between the MFC output and the EvoBot controller, allowing the robot to respond to changes in MFC electrical output, is a novel contribution from the overall EVOBLISS project, as it allows the robot to operate as an automated chemostat and has greatly benefited this thesis. Since EvoBot is a 3D-printer turned into a robot it still holds its 3D-printing capabilities and so it can be employed to extrude (3D-print) parts for MFCs with the ultimate aim to monolithically print and nurture those already made MFCs. EvoBot's hardware and software were designed and developed as part of EVOBLISS from the consortium partners in IT University (ITU), Copenhagen.

The process of manufacturing terracotta ceramic based membranes usually takes 2-3 days from start to finish as described in Ieropoulos et al. (2017), including initially making the membranes, cutting them to size, drying between two pieces of wood by applying pressure, and finally firing for 8 hours in the kiln. Based on the results in the previous section, Fimo™ demonstrated that it could act as a promising membrane and so the focus turned to 3D printing such membranes using the EvoBot platform, an automated process that would speed up manufacturing. Fimo™ is a malleable and easy to process material that does not require firing at a high temperature to cure as opposed to terracotta ceramic. It only needs to be exposed to air at normal room temperature and hardens within a few hours. These attributes highlighted that the material would be suitable for extrusion from the EvoBot platform (**Figure 4.11.B**) and immediate use.

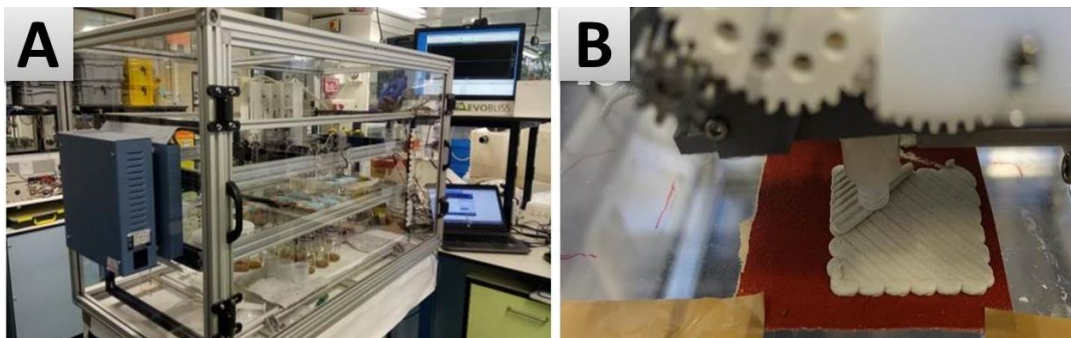


Figure 4.11 - EvoBot RepRap 3D-printer.

[A] Extended EvoBot within its Evo-world enclosure performing experiments on MFCs under controlled conditions **[B]** EvoBot with an adapted extruder 3D-prints Fimo™ membranes. (Source: www.evobliss-project.eu.)

However, since the modelling clay is thick, it cannot be extruded from the EvoBot syringes directly as it requires more force than liquids or semi-viscous materials. To combat this, one of the robot syringes was adapted (by the ITU partners) using an existing open-source paste extruder developed by

the 3D printing community and made available to the public via Thingiverse (<https://www.thingiverse.com/thing:20733>). The adapted extruder is presented in **Figure 4.12**. This work (i.e. developing EvoBot) was completed by the EVOBLISS partners from IT University, Copenhagen. The extruder was mounted in a heavy payload module, and the extruder motor connected directly to the stepper driver on the RAMPS board of the EvoBot (**Figure 4.12**). As most of the EvoBot's design is shared with existing 3D printing technology, the integration to control the extrusion was straightforward. In order to 3D print a desired shape, a design was created in a computer-aided design (CAD) program and exported as an STL file, the standard format in 3D printing. Then this file was imported into a slicer program, which generates the paths of the nozzle for EvoBot (**Figure 4.13**). Different paths can be generated by tuning the settings of the slicer. As an example, parameters such as number of contours, infill percentage, overlapping between the passes or the layer height can influence the curing properties of the 3D printed membranes. These paths are a sequence of G-code commands that the EvoBot can interpret. However, EvoBot has special G codes for the vertical movements of the modules, as each module can be moved in the Z-axis independently. In order to adapt the output of the slicer to something that can be executed by EvoBot, a post-processing algorithm was implemented by the ITU partners. This post process, changes standard vertical movements (G1 Zx.xx commands) with custom commands (M290 ly Sx.xx) and comments out the last G92 E0 which flips the X and Z axis. The modified file with G-codes can then be sent to EvoBot for printing.

Initially, the printing trial started using only one layer of clay however the monolayer was prone to cracking. To combat this, overlapping between each printing path was introduced as well as a second layer of clay, which improved the final outcome. The direction of the extrusion between the top and

bottom deposit was perpendicular and the second layer compressed with the first layer, creating a continuous membrane, even after drying.

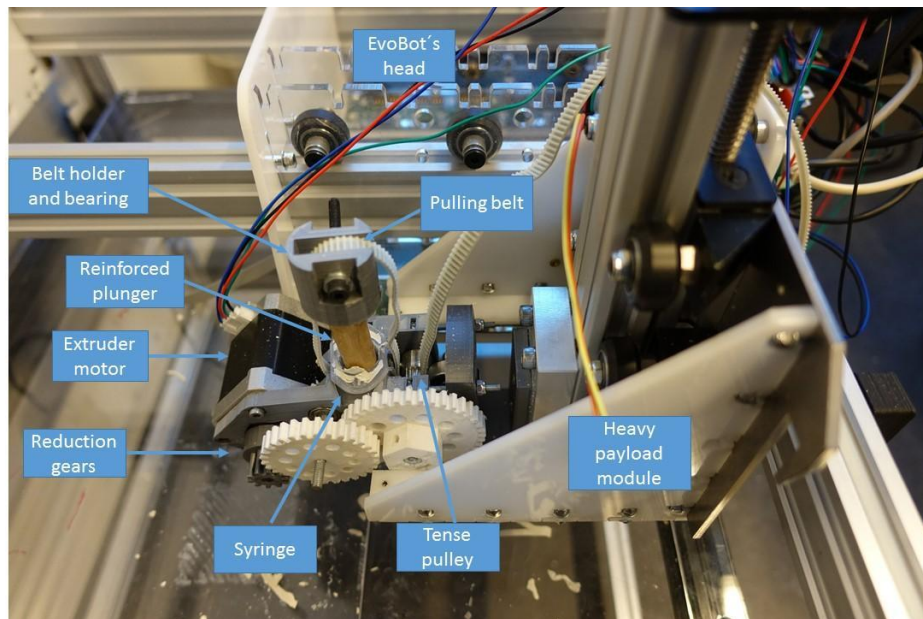


Figure 4.12 - Universal paste extruder mounted on a heavy payload module on the EvoBot robotic head.

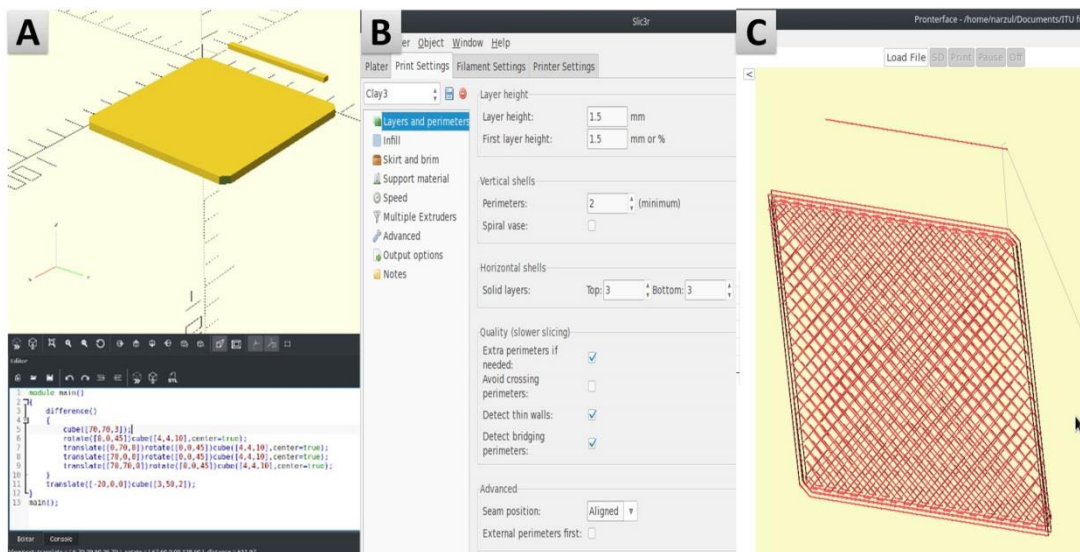


Figure 4.13 - The process of 3D printing membranes.

[A] The model created in OpenScad and exported to an STL file and introduced into **[B]** Slic3r, where the user selects the right parameters to create the path for the nozzle. **[C]** The paths are post-processed and imported into Pronterface, which sends the G-codes to the robot.

The experimental evidence presented above pushes forward the idea of monolithically 3D-printed MFCs as it shows the feasibility of creating core MFC materials that can potentially emerge from platforms such as EvoBot and help realise mass manufacturing. However, monolithically printed MFCs will require an extrude-able (preferably viscous) carbon energy source that can act as both a substrate and a substratum for the electroactive biofilm. The experimental rationale and procedure towards identifying those nutritionally rich extrude-able materials is presented in the next section (4.3).

4.3 Printable substrate/ carbon energy source

Based on the work published in “Ieropoulos, I., Theodosiou, P., Taylor, B., Greenman, J. and Melhuish, C. (2017) ‘Gelatin as a promising printable feedstock for microbial fuel cells (MFC)’, *International Journal of Hydrogen Energy*, 42(3), pp. 1783–1790”.

Having discussed how to construct printable MEAs using EvoBot, the following section presents the results from MFCs’ fed for the first time with soft materials (gelatine and alginate) as a nutrient feedstock and Nafion® as a negative control. The aim of the study was to identify soft materials that could be used as feedstock for MFCs and that were extrude-able via the EvoBot platform and can form biodegrade-able MFCs. This was evaluated based on the power output response, and the behaviour of the MFCs after feeding them with these different soft materials. Biodegrade-able MFCs are useful in sustainable robotic applications for creating robots that can perform certain tasks (e.g. environmental monitoring) for a certain period of time (i.e. a month) and then naturally decompose. This approach eliminates the need for decommissioning robots from hard to reach or polluted areas as they can degrade naturally.

The materials tested were selected based on their physicochemical properties, as these are critical in ensuring that maximum growth conditions are maintained within the MFCs, which is reflected by the power output performance levels. To fulfil those requirements the ideal substratum has to have:

- a) the appropriate porosity, which will facilitate both access to the electrode surface for the microbes and free percolation of the liquid medium to reach all the colonised parts
- b) the appropriate conductivity, in order to encourage optimum surface reactions, between the microbial cells and the electrode surface.

These are the key mechanisms that maintain a fixed thickness biofilm on a given surface area of electrode material, since the direct conductance of electrons (charge transfer) is the primary mechanism of bacterial survival, under anaerobic conditions. Metabolically, the electrode surface acts as the end-terminal electron acceptor for anaerobic microbes in the MFC. The material must also be biocompatible, chemically inert, long-life and with good structural integrity.

4.3.1 Specific Materials and Methods

4.3.1.1 MFC design

The twelve modified analytical cells employed in this study had open-to-air cathodes with AC/CV electrode **Figure 4.14A**. The custom-made AC/CV was used due to its potentially extrude-able ability and a single layer of terracotta clay (~2 mm) was used as a semi-permeable membrane for the same reason **Figure 4.14B-C**. To assemble (bolt) the cell together without fracturing the ceramic membrane, a thick layer of silicone was placed between the anode

chamber and the cathode framework, acting as a ‘cushion’ for the ceramic membrane.

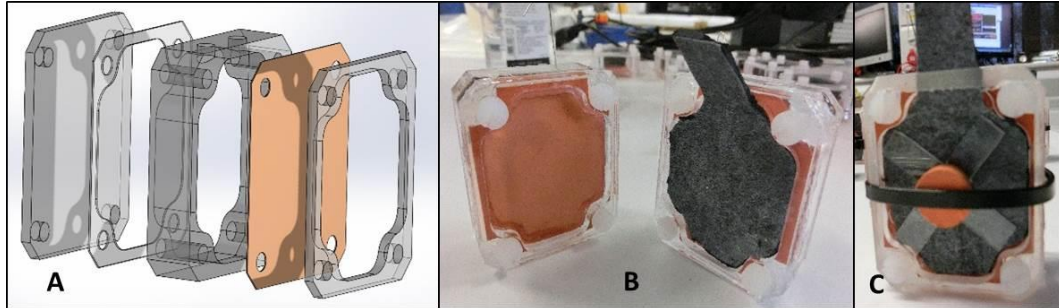


Figure 4.14 - MFC design and set-up.

[A] Computer aided design (CAD) of the modified MFCs. **[B]** Clay membrane and the attached AC/CV electrode. **[C]** Open to air cathode construction. The cathode electrode sheet was directly attached onto the exposed membrane but in order to ensure the electrode-membrane contact, a thin (0.5 mm) Perspex cross was pressed against the electrode using a cut-to-shape cork that was tightened with a cable tie.

4.3.1.2 Inoculation process and $R_{ext.}$ conditions

Activated sludge was injected manually into the sterile chamber and the experiment initially started in batch mode before becoming continuous flow. Three sludge exchanges occurred in the first three days of the experiment by emptying the chamber and re-filling it with fresh inoculum. For the next three batch mode feedings the inoculum used was sludge enriched with TYE (0.15%). Due to inherent absorption/evaporation processes, the experiments turned into continuous flow on the 18th day of the experiment. The flow rate of the constant pumping was $4.2 \text{ mL}\cdot\text{h}^{-1}$ resulting in a hydraulic retention time (HRT) of 5.92 hrs. The feedstock used was full strength (1.5%) TYE. One hour after the first inoculation, once the open circuit cells reached a plateau, an $R_{ext.}$ of $2.7 \text{ k}\Omega$ was connected and this remained unchanged until the end of the experiment.

4.3.1.3 Feeding regime and process

After 18 days of being fed 1.5% TYE, the MFC triplicates were fed with water-soluble pork-derived gelatine powder (240 Bloom Type A, MM ingredients, UK), sodium alginate (pure powder, Minerals Water, UK) and as a negative control, liquid Nafion® perfluorinated resin solution (Sigma Aldrich, UK). TYE (0.15%) was also used as a background solution in all experiments. To ensure that the same weight of nutrients was added, the final concentration of the target material in solution was 2%. This concentration was selected after testing different ratios in order to obtain a liquid state with sufficient viscosity that will enable it to be pumped through the tubes without causing blockages. The positive control triplicate was fed with neat human urine and 0.15% TYE background solution. The cells were fed in continuous flow and this was maintained at a 4.2 mL.h⁻¹ flow rate.

4.3.2 Results and Discussion

4.3.2.1 Rationale of selecting the target materials

In this experiment gelatine, alginate and Nafion were tested as substrates with the prospect of being used in the future as bacterial substrata or jelly-like membranes for the 3D printed MFCs. Each of these materials was selected because of its distinct properties. Gelatine and alginate are biodegradable and all the materials tested are biocompatible. It is quite evident that gelatine is a material that can be employed as both a substratum (3D extrude-able) and as a substrate (microbially utilise-able), and this forms part of future work.

Nafion was only used as a negative control, due to its excellent ion-exchange properties, and the data showed that if Nafion should be employed in a mon-

olithically printed MFC, in a jellified state, it will be detrimental to the system. Thus printable membranes such as the ones described above (4.2) are more favourable alternatives.

4.3.2.1.1 Alginate and gelatine

Alginate or gelatine, as well as pectin, can be mixed with food proteins to be incorporated into the 3D printing process (Godoi, Prakash and Bhandari, 2016). For these reasons, alginate and gelatine were tested as possible printable feedstock for the MFCs' bacterial community. This was due to their ability to be 3D printed and blended with carbon energy sources, as well as used as immobilising agents for bacterial cells on electrode surfaces allowing their accumulation as a digesting biofilm.

Alginate is a polysaccharide and the second most abundant biopolymer in the world next to cellulose (Melvik and Dornish, 2004). It is composed of mannuronic and glucuronic acid residues which are cross-linked by calcium acids and form the ionotropic gel (Godoi, Prakash and Bhandari, 2016). Alginate is derived from seaweed and has been used as a useful cell-immobilising (entrapment) technique in biotechnology due to its biocompatible properties as well as its ability to form heat-stable gels that can be developed and set in room temperature (Melvik and Dornish, 2004). Some species of bacteria can hydrolyse alginate into cell transportable sugars with subsequent fermentation into short-chain fatty acids (Michel *et al.*, 1996).

Gelatine is an animal derived protein which has been known to be used as gelling agent in early bacteriological media as a source of growth promoting substance (Koser, Chinn and Saunders, 1938). However over the years, agar based media proved more suitable for bacterial cultivation than gelatine based media as gelatine cannot remain solid in temperatures above 37 °C

(optimal condition for pathogen growth) and it can be digested by many bacteria. Bacteria possessing the enzyme gelatinase can break down gelatine into amino acids by hydrolyzing it (Levine and Carpenter, 1922). Apart from their biochemical and physiological characteristics, both gelatine and alginate powders are considerably inexpensive substances (approximately £4-5/kg).

4.3.2.1.2 Nafion (control)

Nafion is the main component of the commercially available PEM for MFCs as it offers excellent thermal and mechanical stability as well as conductivity. Nafion's high cost (liquid: £100/ 25 mL) though means it is not a sustainable option for MFC scale-up and practical applications. On another note, Nafion membranes require activation/hydration prior to use and cannot be 3D printed, however, the Nafion liquid mixed with polymers, can be deposited from the EvoBot platform into a solid layer and form a thin layer of membrane. Even though, it is well known that Nafion is not a carbon energy source, in this experiment it was used as feedstock for the purpose to identify if a jelly form Nafion membrane will cause biofouling (Chae *et al.*, 2008) which is a common effect observed in Nafion membranes (anode side) or have a detrimental effect on the bacterial community.

4.3.2.2 Batch mode inoculation and continuous flow operation

The power output obtained during the microorganisms' inoculation with neat sludge, is highlighted in **Figure 4.15A**. The loaded cells were able to develop a visibly dense biofilm over the electrode, which gave approximately 20µW of power output. After the inoculation and colonisation phase, the electrode biofilm was exposed to sludge in TYE (1:10) and the power output increased by

three-fold (**Figure 4.15B**). Although the performance of the cells was consistent and repeatable, a high evaporation loss caused the anode chamber to dry within 96 hours, leaving behind semi-solid sediment at the bottom of the chamber, and having a deteriorating effect on the performance of the cells. An almost zero power performance was recorded after the anode chamber was left to dry out completely (**Figure 4.15C**). As can be seen from **Figure 4.15D**, once the cells turned to continuous flow operation, the power output increased by 0.4-fold. This shows the consistency of the twelve cells' behaviour when all of them were fed with the same feedstock at the same flow rate. Near the end of the experiment, MFC 7-9 due to pump failure resulted in declining power outputs (690-700 hour).

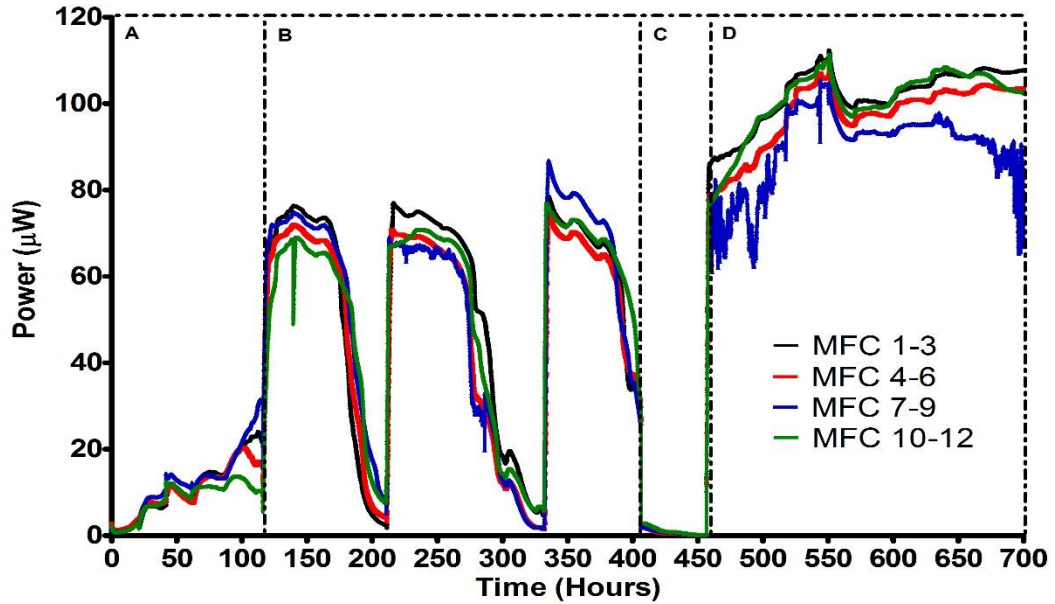


Figure 4.15 - Power profile of the inoculation process and initial feeding of the twelve MFCs.

[A] Batch mode inoculation period of the fuel cells with neat sludge, **[B]** TYE and sludge (1:10). The power decrease was related to the absorption loss of anolyte liquid, due to the clay membrane, **[C]** Total dry period of the cells, **[D]** Continuous flow. Data represented as mean ($n=3$)

On the one hand, as the early results showed, the use of a ceramic membrane in an open to the air batch mode fed MFC allow a significant percentage of water to be absorbed leaving the anode chamber almost dry having a detrimental effect on the performance (**Figure 4.15B**). On the other hand, the always hydrated clay membrane in continuous flow offers a higher rate of proton/cation transfer (Ghadge *et al.*, 2014) reflected by the higher output. Clay membranes possess a great advantage over the conventional polymeric PEM (e.g. Nafion), due to their beneficial porosity, low cost, durability, as well as their ability to be 3D printed (Herpt, 2016); as discussed earlier (**4.2**).

4.3.2.3 Initial response of cells fed with soft materials

After continuously feeding the 12 MFCs with TYE for ~10 days, the two triplicate groups, namely MFCs 4-6, and MFCs 7-9, were fed with the target polymeric feedstock substrates gelatine and alginate, respectively, whereas MFCs 10-12 were fed with the negative control, Nafion. MFCs 1-3 were fed with the positive control urine medium. Even though the feedstock switching had a slight decreasing effect on the MFC power output for the first 10 hours, after this period the performance levels began to diverge (**Figure 4.16B**). The power output from the first 5 days showed that the urine fed MFCs' performance improved, compared with that from the soft material fed MFCs whose performance decreased. Similar power decreasing levels were recorded from alginate and gelatine, with the only difference being that gelatine was more than two-fold higher in power performance than alginate. A possible explanation for the superiority of gelatine over alginate is the difference in the calorific value of the two substances (gelatine: 329 kCal/100g – alginate: 248 kCal/100g). As stated in section **4.3.1.3**, the dilution of the compounds was standardised based on their viscosity and not their calorific value. As shown in **Figure 4.16**, the performance from the Nafion fed MFCs deteriorated rapidly over time.

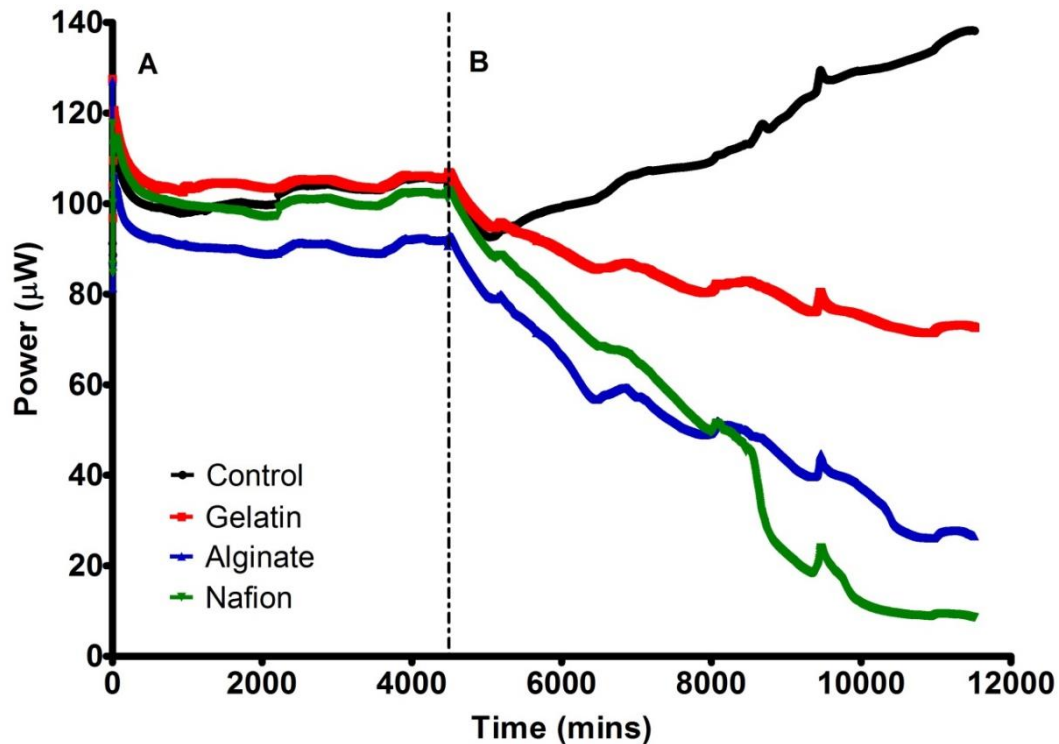


Figure 4.16 - Time profile of MFC's after feeding with soft materials for the first time.

[A] The last three days of the 18-day period followed by [B] the response once the feed-stock changed. The fuel cells were fed with 1.5% TYE for the first 18 days, and then target soft materials added. Gelatine outperformed the other soft materials ($p < 0.0001$).

4.3.2.4 Overall performance and starvation period of the cells

The average power production of the MFCs fed with different soft materials is shown below (Figure 4.17). The data were consistent with the initial response to the change of feedstock. The urine fed control MFCs remained the highest in power output with the maximum being 149.23 μW ; gelatine followed as the second best with a maximum power at 111.26 μW . The average power production over the period of the whole duration of the experiment for control, gelatine, alginate and Nafion was 105.28 μW (SD=32.52), 79.54

μW (SD=22.67), 39.27 μW (SD=25.04) and 19.79 μW (SD=26.19) respectively. The performance is represented also as the area under curve, shown in the graph of **Figure 4.18A**.

While constant pumping was supplied to the MFCs the output was stable over time, however, when the feeding paused for ten days and cells left to starve, a different behaviour was observed. The pausing of feeding was done in order to observe the behaviour of the cells under starvation conditions and assess the longevity of each feedstock. Gelatine fed cells appeared to have better longevity as their performance gradually declined, and even for the first four days they had stable performance (**Figure 4.17- inset**). The rate of decrease of the positive control (urine) cells was the fastest among all the others with a decreasing trend of $0.73 \mu\text{W}\cdot\text{h}^{-1}$. In all cases, Nafion was consistently close to zero. The mean power output during the starvation period for the four feedstocks was 42.92 μW (SD=30.43) for control, 75.64 μW (SD=29.53) for gelatine, 38.25 μW (SD=27.14) for alginate and 1.80 μW (SD=2.0) for Nafion. The area under curve of the starvation period is presented in **Figure 4.18B**.

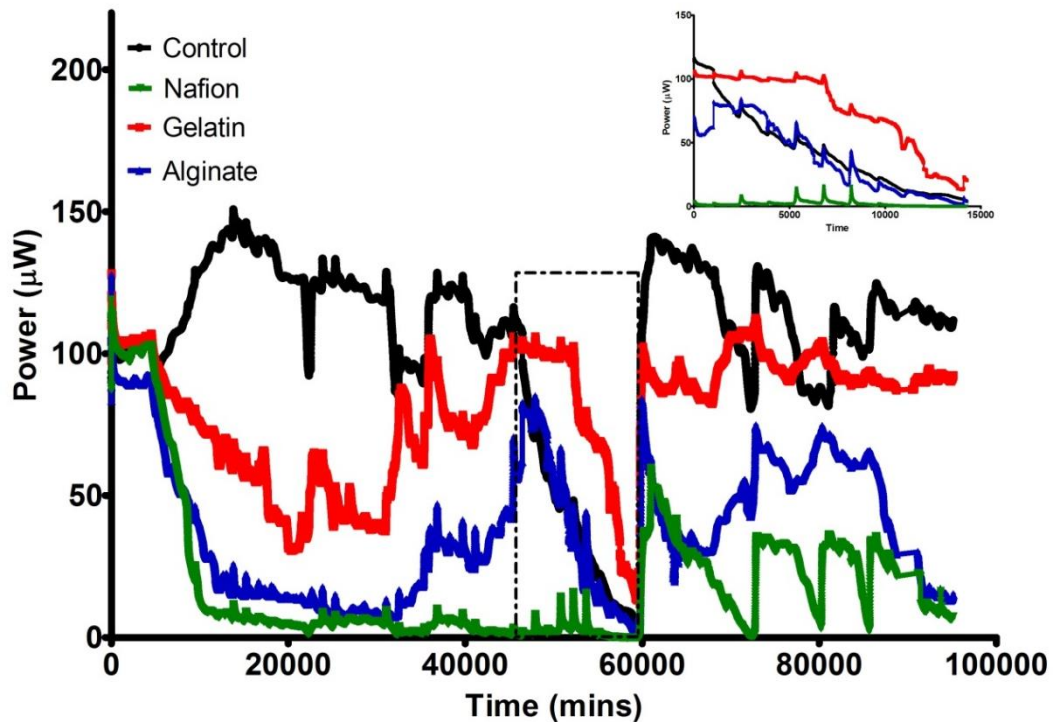


Figure 4.17 - Average power production of MFCs after feeding with different soft materials.

Starvation period (total 10 days) is highlighted in the dotted box, a magnification of which is shown as the inset graph. Gelatine fed MFCs decreased at the slowest rate, which was the reason for its higher power output.

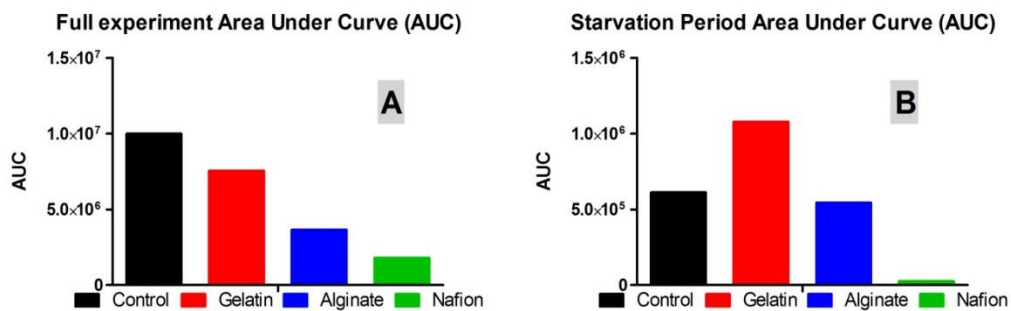


Figure 4.18 - Area under curve (AUC) of the full experiment [A] and the starvation period [B].

4.3.2.5 Polarisation experiment

The polarisation experiment was conducted two months after the start of the experiment. By this time the biofilm community was already well established and developed based on the 2.7 k Ω load. Polarisation power curves (**Figure 4.19**) are consistent with the temporal power output data (**Figure 4.17**).

Some studies suggest that early and regular polarisation experiments can determine the ideal resistance for maximum power production and by switching to that ideal load value the best power performance is achieved (Lovley, 2008). Other studies indicated that changing the external resistance does not improve the power output, as different combinations of microbial communities are developed based on each load that leads to comparable power outputs, showing the flexibility and resilience of MFC systems (Lyon *et al.*, 2010). Thus, despite that in this study the polarisation experiment occurred at the latter stage when the cells had already operated under a stable resistance load, it is believed that the unchanged load did not have a limiting effect on the MFCs' performance.

Nevertheless, an overshoot phenomenon was observed in the polarisation curves (Winfield *et al.*, 2011). The overshoot phenomenon occurs when there is either a delay in or prevention of charged molecules (ions and electrons) transfer, which results in decreasing the current at the same time as the voltage. Power overshoot can be caused by a number of factors, some of which have been previously described in detail, such as sample rate, flow rate, inoculum, feeding mode, anolyte and catholyte composition as well as anode and cathode redox potential levels (Zhu *et al.*, 2013; Watson and Logan, 2011; Ieropoulos, Winfield and Greenman, 2010a). In this case, it is suspected that this was due to the complex nature of the substrates used (as well as the molecular weight/size) in conjunction with the flow rate (resultant

HRT), which appear to have resulted in high mass-transfer (kinetic) losses. The power output recorded during the polarisation experiments was much higher (>3-fold) compared to the levels recorded in the real-time temporal curves. This might be due to the short time of sampling (3 mins) during the polarisation experiment, suggesting that the period was not sufficiently long to reach steady-state conditions for identifying the optimum resistance value for long-term experiments with a fixed load (Winfield *et al.*, 2011).

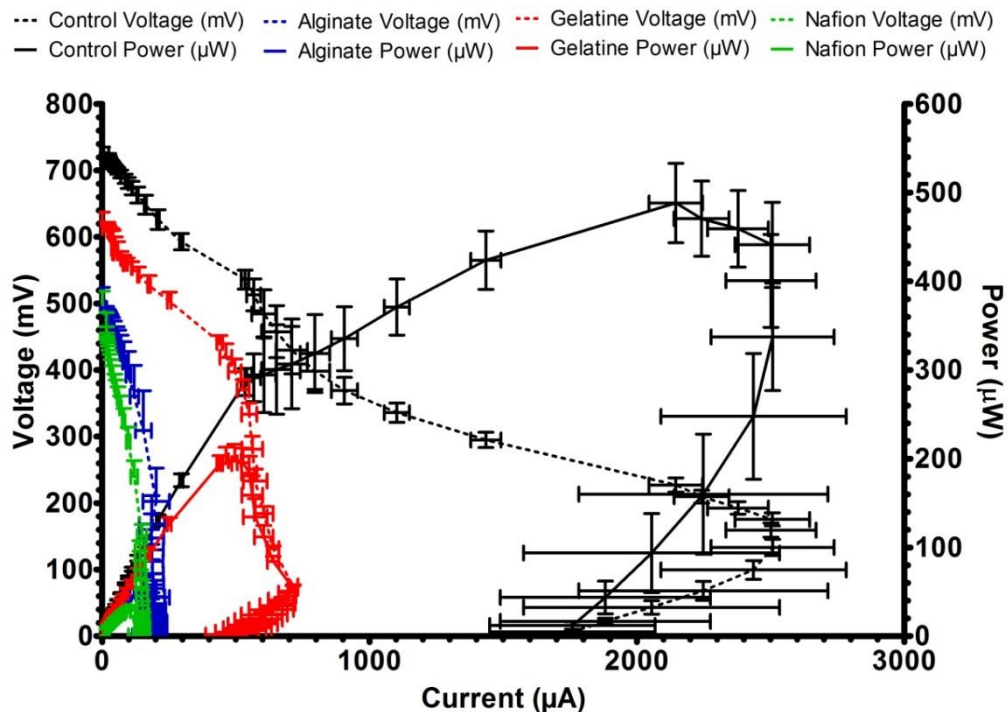


Figure 4.19 - Power curves produced after two months operation on a fixed load of 2.7 kΩ

4.3.3 Connection with EvoBot

The long-chain polymer composition of gelatine and chitin renders the feed-stock to be longer lasting than monomeric substrates, which wash through the system or are quickly utilised. Whereas proteolytic enzymes (such as

gelatinease) are commonly encountered amongst many different species of microorganism, the enzyme to hydrolyse chitin is thought to be relatively rare and is encountered more in marine species. Gelatine's outperformance over the other soft materials and its viscous characteristics make it a suitable material to be employed in the 3D process. With the aim of monolithically fabricated MFCs gelatine can provide nutrients during a starving period or act as an endogenous store of fuel. For a material to be employed in the 3D process it should be soft and easily extruded using a RepRap EvoBot machine and can also be used as a structural material. The gelatine, as a feedstock and activated carbon paste as an electrode, serves the aim of the experiment as a suitable alternative printable substratum and an electron acceptor.

This work is a continuation of the work presented in the previous section (4.2), outlining the line of research towards identifying printable MFC materials that can act as; physical separators of anode and cathode, or organic substrata. However further investigation is needed in discovering different material combinations which could make up an entirely 3D printed fuel cell including the electrodes. To do so the electrode material of choice needs to be in a malleable state to allow its extrusion as well as being able to become rigid without further treatment (i.e. air drying). This will provide structural robustness to the electrode and subsequently to the fuel cell as a whole. Having the above rationale in mind an experiment was designed to investigate the feasibility of developing a custom made alginate based carbon mixture as a 3-D printable cathode electrode for MFCs. This work is described in detail in the following section (4.4).

4.4 3D-Printable Cathode Electrode

Based on the work presented in "Theodosiou, P., Greenman, J. and Ieropoulos, I. (2018) '3D-Printable Cathode Electrode for Monolithically Printed Microbial Fuel Cells (MFCs), *Electrochemical Society Transactions*, Seattle (US), May 2018".

At the beginning of this chapter (4.1) a historical overview was presented based on the impact that additive manufacturing (AM) and 3D-printing have had on MFC research. AM and 3D-printing are playing an increasing role in advancing the MFC technology, by substituting essential structural components i.e. chassis and separators, with 3D-printed parts. That has helped overcome many time-consuming MFC assembly steps however to date there have been no studies to the author's knowledge that have focused on identifying electrodes that can be 3D-printed and used directly on MFCs. This would be a big step towards advancing the technology for mass manufacturing of MFCs using only 3D-printers. Thus the experiment presented here builds on the previously discussed experiments (4.2 and 4.3) and it follows the same line of work focusing on identifying electrode materials that can contribute within a monolithically 3D-printed MFC. This chapter section aims to; describe the development of an inexpensive, conductive and printable alginate-based electrode, which can be extruded from the EvoBot platform, and report on the advances of this material as a cathode electrode on air-breathing cathodes.

4.4.1 Specific Materials and Methods

4.4.1.1 MFC architecture

Three triplicates of single chamber analytical size MFCs were assembled for this experiment as described in 3.3.1. The cathodic half-cell was removed

completely and the cathode electrodes in examination were directly attached to the CEM membrane forming open-to-air cathodes. The anode electrode used in all the MFCs was a catalyst-free carbon veil (3.1.1).

4.4.1.2 Cathode electrode materials

Two types of cathode electrode materials were tested against the control AC/CV PTFE-based cathode electrode named PTFE_AC (3.1.2.1) (Figure 4.20). The materials trialed were a) a solid commercially available coconut shell derived sintered carbon block filter cartridge (Water Filter Man LTD, UK) named AC_BLOCK and b) a custom made PTFE-free/alginate based electrode (PTFE_FREE_AC) which was made using activated carbon (80g) and alginate (Minerals Water Ltd, 20 g). These two were mixed with distilled water into a thick paste. Prior to mixing, carbon and alginate were homogenized using an electric coffee grinder (Andrew James 150W, UK). The paste was then transferred to a syringe from where it was extruded directly onto the membrane (10 mL) (Figure 4.21) and dried/solidified on the bench in 24 hours (Figure 4.22). This mixture was enough for 10 electrodes (e.g. 2g of alginate/electrode). The final weight of all the dried electrodes was 3.8 ± 0.2 g.

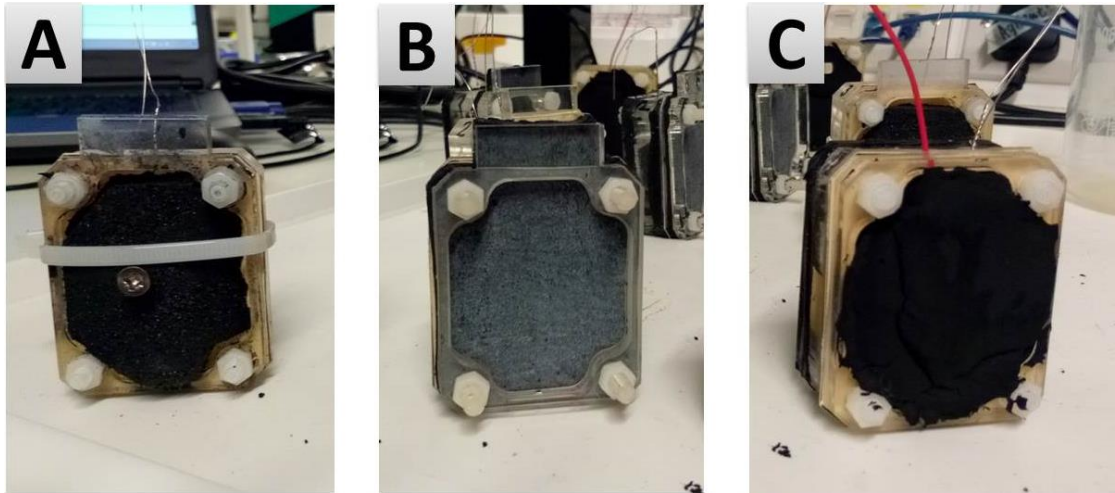


Figure 4.20 – Photographs of the three different cathode electrodes used in this study.

[A] AC_BLOCK: Activated carbon block as the commercial option, pierced through with a SS screw as the current collector **[B] PTFE_AC (AC/CV):** Activated carbon on carbon veil (AC/CV) PTFE-based electrode as the control and **[C] PTFE_FREE_AC:** PTFE-free alginate based electrode as the extrude-able electrode.

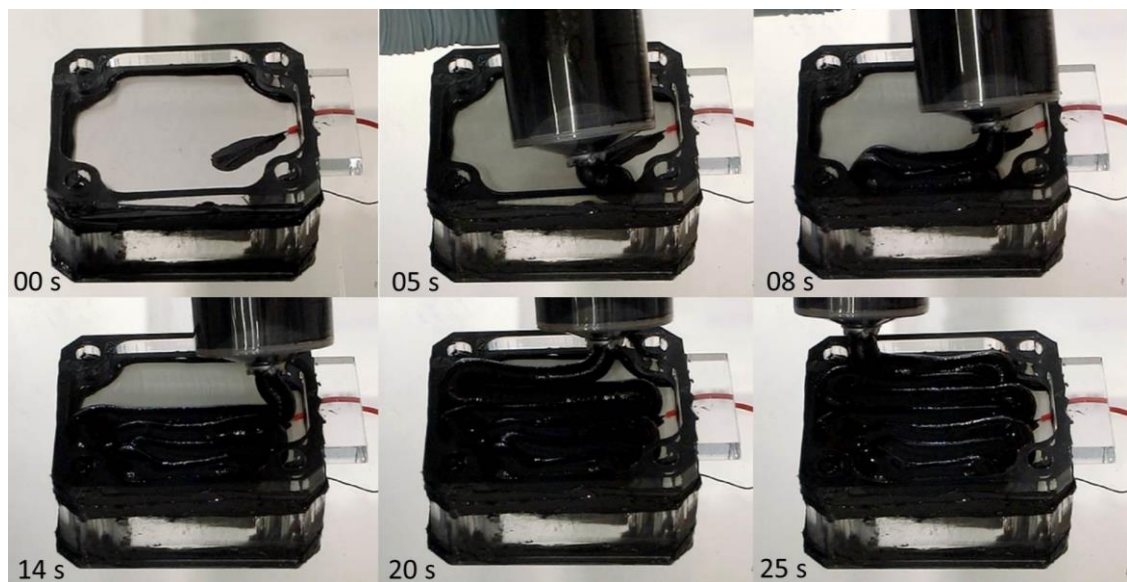


Figure 4.21 – Time-lapse photography of the manual extrusion of the PTFE-free/alginate based cathode electrode on the membrane of an assembled MFC.



Figure 4.22 - Manually extruded PTFE-free alginate electrode 0, 2 and 24 hours after extrusion, showing the electrode settling and solidifying (air-drying).

4.4.1.3 Inoculation, feedstock and R_{ext} conditions

The cells were inoculated with acclimated activated sludge supplemented (1:10) with full strength TYE (1.5% w/v) for the initial five days which consisted of daily full exchanges (four in total). Then the MFCs were fed daily (batch mode) with neat human urine and they were operating under a 2.7 k Ω load for the whole duration of the experiment.

4.4.1.4 Electrochemical analysis of the cathode electrode

Linear sweep voltammetry (LSV) was performed in order to examine the electrocatalytic activities of the cathode electrodes under investigation. Be-

fore the electrochemical analysis took place, MFCs were left to stabilise overnight with neat urine as their anolyte solution. This allowed the membrane to be fully hydrated and guarantee liquid continuity. Cathode polarisation curves were run from open circuit voltage (OCV) to -250 mV (vs Ag/AgCl) with a scan rate of 0.25 mV s^{-1} . LSV was performed using an SP-50 potentiostat/galvanostat from Biologic, France. For this analysis, a three-electrode configuration was used with a reference electrode (Ag/AgCl) inserted near the anode electrode according to the literature (Zhang *et al.*, 2014). The anode was used as the counter electrode, the cathode as the working electrode and the reference channel was connected to the reference electrode placed in the anodic solution. For statistical significance, every electrochemical experiment was run in triplicates.

4.4.2 Results and discussion

4.4.2.1 Material selection rationale

4.4.2.1.1 Activated carbon (AC)

AC is a porous, solid surface material which can merge with different molecular structures (Chambre, 2014). It derives from a wide range of carbon-rich raw materials such as coconut shells and wood and it is activated using chemical or steam activation. The latter is the common technique for the activation of coal and coconut shell raw materials. Activated carbon exhibits an extended interparticulate surface area which offers to the material a high degree of porosity and excellent adsorbent characteristics (Chambre, 2014). This, is attributed to its unique properties such as; large surface area (500-2000 m^2 aggregated surface area per gram of AC), high degree of surface reactivity, universal adsorption and pore size (micro- and macro-pores) which

allows adsorbents to easily attach to the inner surface of the AC. AC carbon is the conductive element of choice when it comes to electrode materials throughout this thesis study due to its availability, cost effectiveness and eco-friendliness.

4.4.2.1.2 Sodium alginate

Sodium alginate is a versatile, economical and high-modulus polysaccharide extracted from brown algae which has recently attracted a lot of interest as an eco-friendly binder for both anodic and cathodic electrodes in the lithium ion (Li-ion) battery industry (Bigoni *et al.*, 2017; Xu *et al.*, 2013; Kovalenko *et al.*, 2011). The properties of alginate have been discussed previously **4.3.2.1.1** in relation to using alginate as a printable carbon energy feedstock for MFCs. In this experiment, the focus was to investigate whether it could be used as a biodegradable binder in MFC electrodes in an attempt to move away from employing the toxic PTFE binder. Similarly to preparing a Li-ion battery electrode, the PTFE_FREE alginate based electrode was formed into a slurry by mixing the conductive carbon powder (PAC) with alginate as the polymeric binder and de-ionised water as a solvent. However, instead of casting the slurry into a metal foil current collector (as in Li-ion) it was deposited on the membrane directly using a syringe. Although binders are electrochemically inactive, they still play an important part in the stability and integrity of the electrodes (Kovalenko *et al.*, 2011) as well as the performance of the cell (Bigoni *et al.*, 2017). Also, water-processed binders such as alginate can cure in the air and don't require further treatment. Besides, they are an economical and eco-friendly alternative to toxic electrode components and costly manufacturing processes.

4.4.2.1.3 Carbon Block

Bonded activated carbon (AC) filters are used in a wide variety of purification techniques including water purification, gas purification, and air filters. For such applications, GAC is the common choice because it has the flexibility to be incorporated as loose-fill within filter housing or into carbon blocks (Jefferies, 1995). The industrial manufacturing of bonded carbon filters requires the incorporation of various chemical processes in order to bond the carbon particles into a rigid matrix.

Gas molecules are adsorbed into the carbon block by diffusing into the pores of AC where they get trapped into the walls. Since the surface area of the block is extremely large the number of pores within the block is equally large. With these properties in mind, this type of filter was selected as the commercially available product to be trialled as the of-the-shelf air-breathing cathode electrode for the MFCs. In this study, the AC block was made out of coconut-based AC which is considered effective as it offers high porosity and surface area facilitating quick adsorption, which is why is preferred for use in gas and water filters. Further, coconut shells are found freely in nature making the manufacturing process more sustainable.

The manufacturing process of bonded carbon filters from loose GAC proved to be disadvantageous for their use as air-breathing cathode electrodes in this study. This is because the chemical bonding process alters the carbon particles having a detrimental effect on their ability to bond with gas compounds (Chambre, 2014). The bonding process initially requires the AC to be soaked in water for 24-hours, which can cause leaching of useful impregnated chemicals, followed by a soaking in bonding agents such as polystyrene which can impact the adsorption capacity of the granules. It is hypothesised that these factors influenced the underperformance of this type of electrodes

in this MFC setup as presented below. Similar observations were published in a recent study where sintered AC blocks were employed in self-stratifying MFCs treating urine (Walter, Greenman and Ieropoulos, 2018). Among the different cathodes tested in that study AC block was the least performing but was the most economical.

4.4.2.2 Power output and polarisation

4.4.2.2.1 Continuous power output

At the initial stages of the experiment, the MFCs were inoculated with TYE-supplemented activated sludge. The power output was increasing incrementally after each inoculation as shown in the **Figure 4.23A and B**. In all cases the MFCs almost doubled in power output from their initial sludge exchange until their fourth and last exchange that occurred on day 7 (instead of day 5 due to power cut - **3.6.1**). Initially PTFE_FREE_AC was performing at 21 μW , PTFE_AC at 14 μW and AC_BLOCK at 7 μW whereas on day 7 they were performing at 42, 23 and 15 μW respectively.

The end of the inoculation period signalled the beginning of the urine feeding cycle when initially 50% of the anolyte was removed and exchanged with neat urine (day 8), as shown in **Figure 4.23C**. At the beginning this had a positive impact on the PTFE_FREE_AC MFCs, which saw an increase of 68.75% in power output, however it did not have the same effect on the other two MFCs that remained almost unaffected. To investigate this further on day 11 all the MFC anodes were emptied completely, anolyte was sucked through the carbon veil electrode, and then replenished with 100% neat urine. The MFCs responded unanimously to this feeding and instantly the power output reached 67 μW for the PTFE_FREE_AC, 24 μW for the PTFE_AC and 10 μW for the AC_BLOCK. During the next 13 days the MFCs

steadily increased in power output despite a 79 hour shut down of the experiment when they were left unmaintained. This shows the resilience of the system, which even after being left unattended, without daily feedings, can still continue to thrive as long as carbon energy source is added to the system. This is visualised more clearly from day 23 to day 25 when the MFCs steadily degraded their organic fuel but were reinvigorated when fed (**Figure 4.23D**).

Looking at the temporal behaviour, the MFCs with the 3D-printed alginate based cathode electrode (PTFE_FREE_AC) performed better than the control (PTFE_AC) and the commercially bought sintered carbon block (AC_BLOCK), which in fact was the least performing. The area under the curve was calculated for the whole experiment and is presented in **Figure 4.24**.

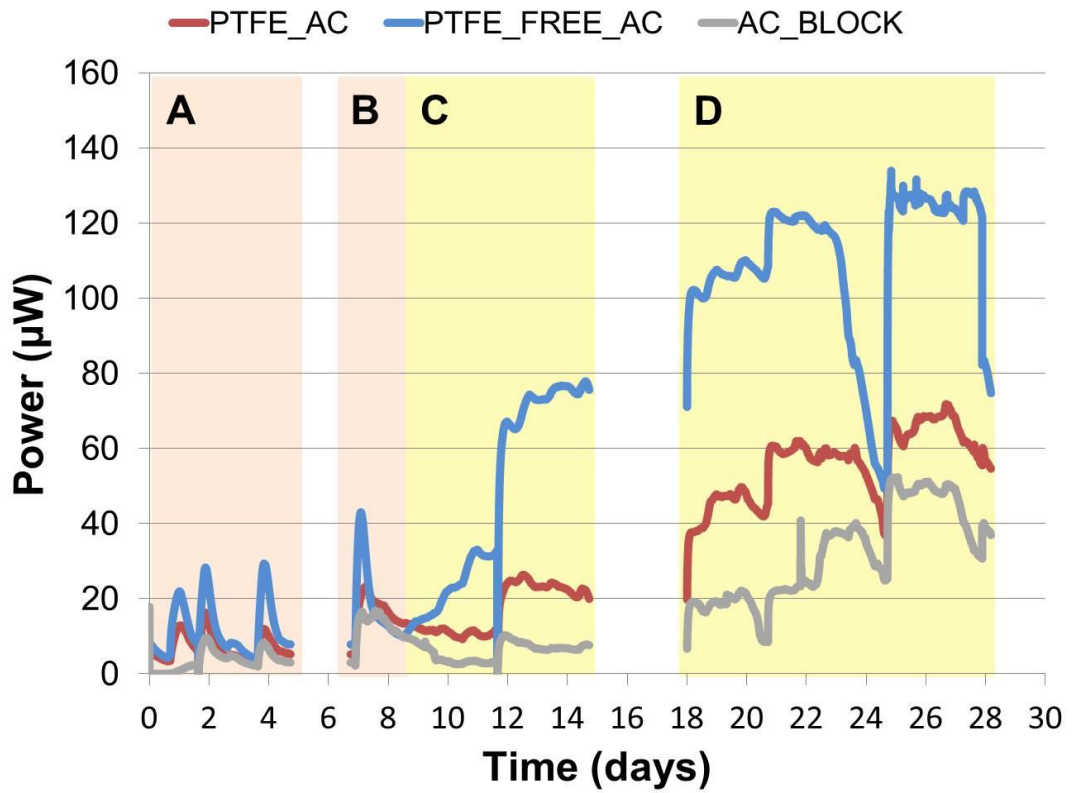


Figure 4.23 – Temporal power output of the MFCs employing different cathode electrodes.

[A] Inoculation phase consisting of three sludge exchanges as indicated from the spikes in the graph, **[B]** Single re-inoculation following a 48 hour of power cut and loss of data, **[C]** Initiation of urine feeding cycle and **[D]** Continuation of urine feeding cycle following a 79 hours experiment shut-down (as explained in 3.6.1).

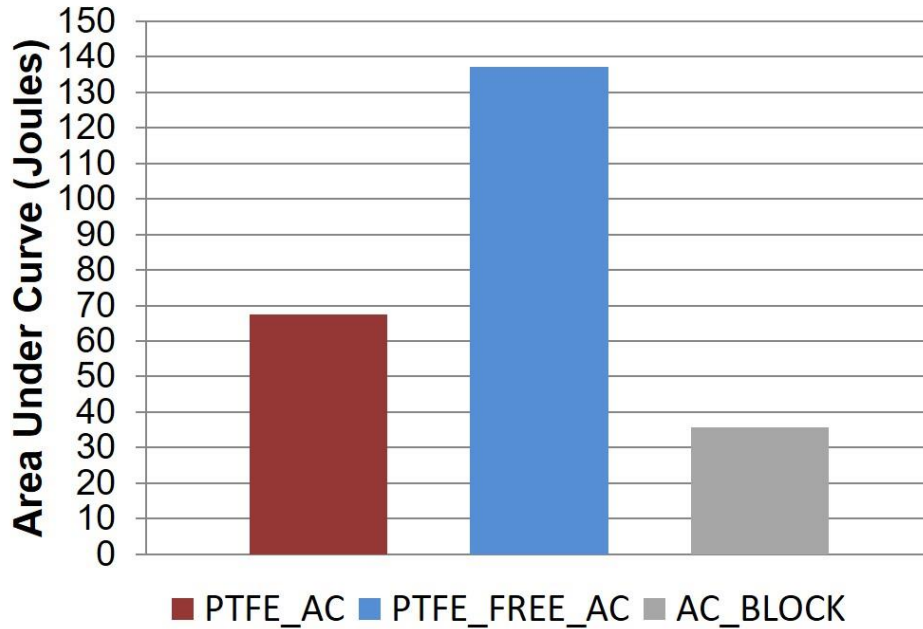


Figure 4.24 - Overall calculated area under the curve, presented in Joules, based on the temporal power output data.

4.4.2.2.2 Polarisation results operating MFCs

Following the temporal power output of the systems (discussed above) a polarisation experiment was conducted to identify the maximum power output capabilities of the three whole MFC systems. The results of this experiment are presented in **Figure 4.25** and are in agreement in terms of the order of performance with the real-time (temporal) data. The MPT for the MFC employing the alginate based PTFE_FREE electrode was $285.5 \mu\text{W}$, which was $190.45 \mu\text{W}$ higher than the control PTFE_AC and $200.27 \mu\text{W}$ more than the sintered carbon block. The difference in the magnitude of power output between the real-time data and the polarisation data are due to R_{ext} , which was not optimal during the duration of the experiment.

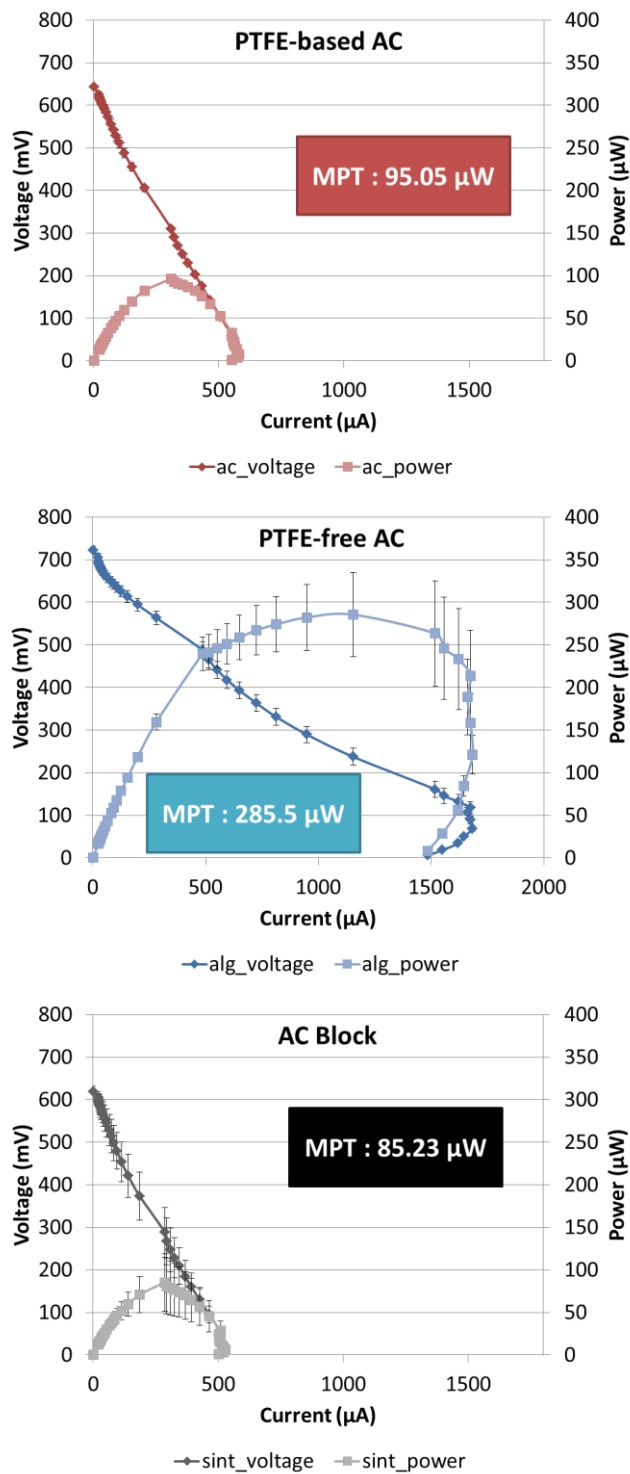


Figure 4.25 – Polarisation results of the three types of MFCs examined. (n=3)

4.4.2.2.3 Cathode electrode LSVs

To investigate the electrocatalytic activity of the air-breathing cathodes, LSV was carried out under clean conditions, using neat urine (pH=9.2) as the electrolyte solution. Prior to running the LSV, the cells were left to soak overnight in the urine solution, ensuring liquid continuity between the membrane and the electrodes as well as achieving a stable open circuit potential (OCP) for all the cathodes tested. The resulting OCP of the two custom made electrodes, PTFE_AC and PTFE_FREE_AC was 85 ± 18 mV (vs Ag/AgCl) and 108 ± 8 mV (vs Ag/AgCl) respectively whilst the commercially available AC_BLOCK had an OCP of around 163 ± 15 mV (vs Ag/AgCl), which was the highest of all (**Figure 4.26**). This can be attributed to two factors; firstly the AC carbon base employs granular activated carbon (GAC) instead of powdered activated carbon (PAC) and GAC has higher reactivity with gases than PAC. Secondly, during the manufacturing process, GAC is sintered into rigid blocks which increases the number of pores within the block leaving a higher surface area for oxygen reduction compared to the other two tested electrodes which were made manually with PAC. However all the electrodes were below the theoretical value of ORR vs Ag/Ag Cl at pH=9 which is 580 mV, mostly because these values are based on platinum electrodes and not carbon-based electrodes. Furthermore, OCP only shows the thermodynamic difference in potentials between the anode and the cathode electrode (against a reference electrode) which is not a determining factor of the performance of the MFC once it is closed circuited, as reflected from the power curves (**Figure 4.25**). The LSV data (**Figure 4.26**) show that, PTFE_AC and AC_BLOCK had low current outputs and also underwent higher activation losses than PTFE_FREE_AC. Overall the LSV data confirmed that the 3D-printed ones (PTFE_FREE_AC) produced notably higher current output than the rest (6 ± 1.5 mA at -250mV vs Ag/AgCl).

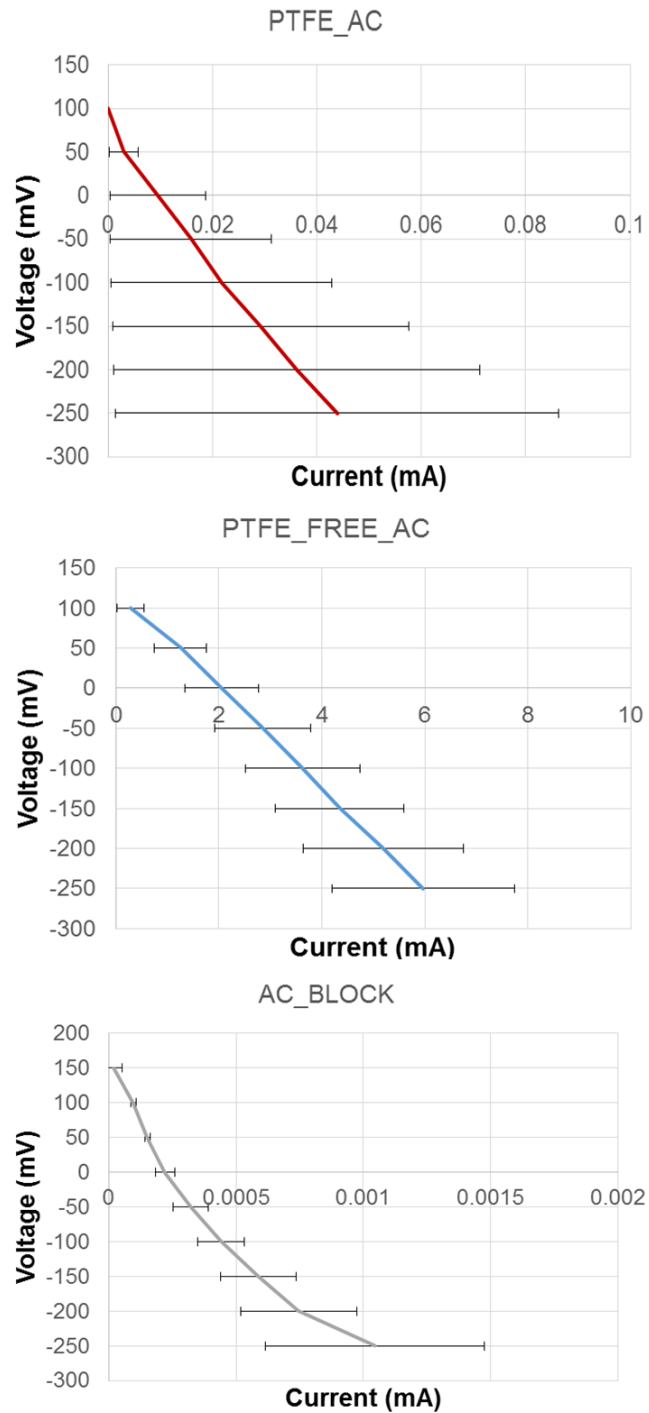


Figure 4.26 – Linear sweep voltammetry results of the three cathode electrodes (250 mV/S) (n=3).

4.4.2.3 Cost analysis

An important factor to consider in the effort to improve the MFC performance is not only the power output but also the cost effectiveness of the materials, especially when using alginate. In perspective with the aim of £1 per MFC, the alginate electrode is the most suitable one in reducing the overall costs. PTFE_AC cathode electrode requires PTFE coated carbon veil sheet as well as a mixture of PTFE and AC. PTFE is a highly toxic and expensive material (£138/500mL, Sigma Aldrich, 2017) compared to food grade alginate which only costs £8.76 per 500g. Moreover, the 3D-printed alginate based electrode (PTFE_FREE) was the cheapest. That is because it does not require a supporting material or heat treatment to set, thus the assembly and manufacturing cost is even less than the conventional electrode (PTFE_AC). Hence, by removing the extra costs regarding materials and assembly for cathode electrode using the 3D-printed ones, the cost per electrode can cost £0.035 (not factoring 3D-printing energy costs).

4.4.3 Connection with EvoBot

Following the successful implementation of PTFE_FREE alginate based electrode on MFC membranes using manual syringe extrusion, the next step was to test the same extrusion using syringes on the EvoBot platform. For this test, the syringe was preloaded with conductive paste and attached to the robotic head without any modifications (i.e. implementing an extruder) because the viscosity of the paste was sufficient for the syringe motors to push the paste through. Similarly to printing the Fimo™ membrane as described above (4.2.3), to extrude the conductive paste the desired shape was created in CAD. This dictated the path that the syringe nozzle of EvoBot

needed to follow. A time-lapse figure of the EvoBot extruding the cathode electrode is shown below (**Figure 4.27**).

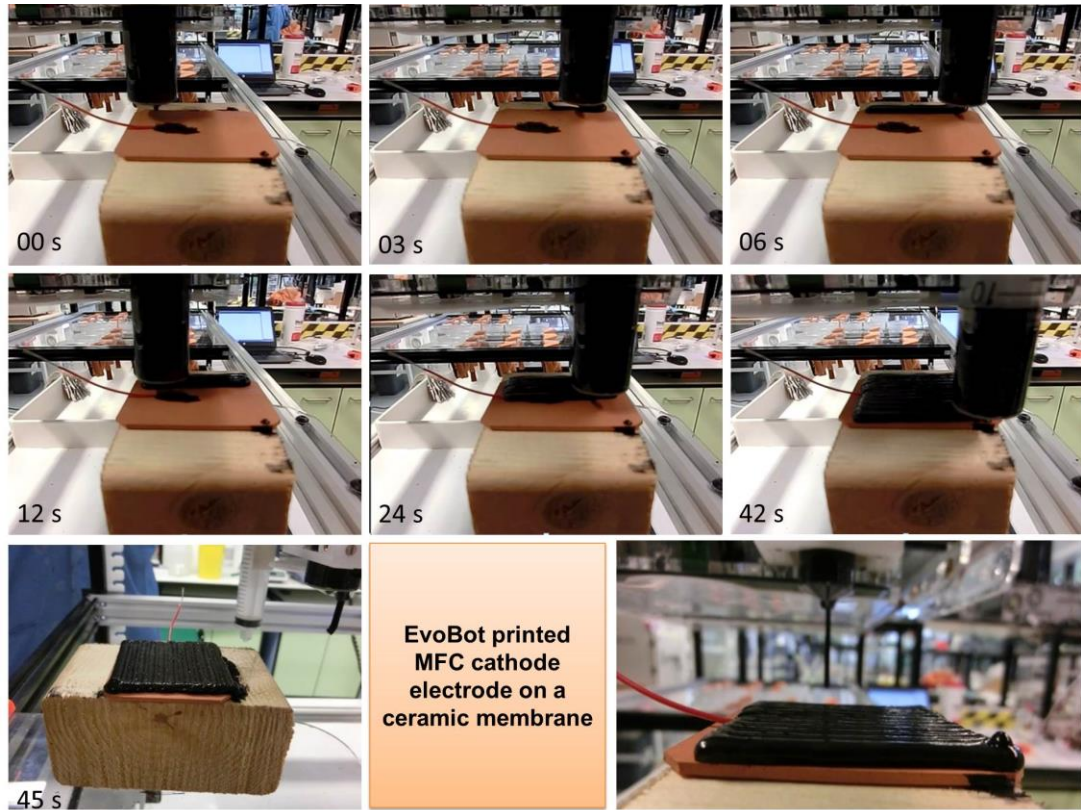


Figure 4.27 - Time-lapse photographs of the EvoBot extrusion of the PTFE-free/alginate based cathode electrode on a ceramic MFC membrane.

4.5 Conclusions and future work

The key to advance the MFC design is to optimise the construction and design of units through the use of 3D fabrication techniques. The 3D printed/extruded MFCs will not only speed up the manufacturing process of individual units, but can also help in automating the production process of multiple units for scale-up. This will benefit the electrical power output as rapidly

fabricated multiple units can be stacked together to increase voltage or current output (Ieropoulos, Greenman and Melhuish, 2008). Another important advantage of 3D-printing MFCs will be the standardisation of the technology. At the moment, a standard MFC archetype does not exist, making the comparison of MFCs between groups around the world difficult. The possibility of 3D-printing MFCs can standardise the design making it easily accessible and exchangeable with different research groups globally that have access to a 3D-printer.

A series of three experiments were presented in this chapter. Firstly it was demonstrated that; alternative, extrude-able, EvoBot printed, membrane materials and MEAs which do not require firing, can be employed in MFCs and provide higher power outputs at lower costs than conventional CEM. This is a novelty in the MFC research, as in fact, the MFCs with air-dry clay based MEAs produced up to 50% more power than the controls. Since the MFC technology relies on low-cost materials, due to the small amount of electricity generated per MFC unit, the fact that terracotta, air-dry Fimo™ and air-dry clay were 40 ± 10 times cheaper than CEM (per Watt produced), adds an extra advantage in using these materials. In addition those MFCs had a COD reduction of nearly 80% which was 20% more than what the CEM based MFCs achieved. At last, the capabilities of those air-cured materials open another novel and promising avenue to the MFC research as they can be fabricated using 3D printing and/or extrusion techniques on the EvoBot platform. Apart from extrusion, EvoBot can be customised and a brush/roller can be incorporated into its robotic head. This could apply a uniform conductive coating onto the dried extruded membranes, akin to a robotic painting machine (Grosser, 2011), achieving the complete MEA fabrication.

Secondly, it was shown that carbon-energy supplemented printable materials such as gelatine and alginate can potentially act as printable feedstock in a monolithically printed MFC. These were proven to be able to sustain bacterial cells with carbon energy for longer periods (under starvation conditions) compared to urine. This experiment can be investigated further by optimising the feeding regimes with feedstock that has been standardised based on calorific value (even urine), rather than based on utilisable-energy concentration which was the methods used in this study. This may provide a clearer picture between alginate and gelatine as carbon energy sources in further studies. Such experiment can be used to explore the breakdown-utilisation rates, within an MFC, of different substrata when mixed with small molecular weight compounds that can be degraded easily (i.e. acetate). This approach can result in “evolving” and adapting microbial communities to degrade a diverse range of CE sources based on the media availability and experimental purposes. Such experiments can investigate further the “switch on” mechanisms of different bacterial cells (Magasanik, 1961).

The third and final experiment of this investigation demonstrated the development of a cost effective, eco-friendly, air-dried, extrude-able, 3D-printed electrode (PTFE_FREE_AC) which could successfully act as a cathode electrode in an MFC system. The conductive element was initially manually deposited, to evaluate the effectiveness of the material as a cathode and the experiment showed its superiority over the other two tested electrodes, PTFE_AC and AC_BLOCK. Finally the electrode was successfully extruded from the on-board EvoBot syringe without the need for any hardware modifications to the unit. Hence it was shown that replacing the conventional PTFE-based AC carbon electrodes with the alginate based conductive paste, is a valuable development towards printable MFCs since both the membrane and the cathode electrodes can emerge from the same platform.

The overall work described in this chapter has contributed to a bigger picture on 3D fabricating MFCs and the experiments above can be considered as steps towards entirely printable MFC units. Moreover, based on these findings it is envisaged that in the future EvoBot-like machines will be able to fabricate MFC. This chapter has addressed the improvement of MFC performance through material optimisation and configuration modification. However, work still needs to be carried out to improve the performance of the MFCs using automatic laboratory techniques which is an element that is still in hibernation in the sector of MFC research. EvoBot as an automated liquid handling robot has the ability to experiment on MFCs with the ultimate goal to increase their power performance. The work towards this goal is presented and discussed in detail in **Chapter 5**.

Chapter 5 EvoBot and MFCs

The previous chapter (**Chapter 4**) gave an overview of the bench experiments leading to the optimisation of core MFC materials. The focus was on 3D-printable ones that can be extruded from the EvoBot platform. However as EvoBot is modular and multifunctional, apart from its 3D-printing capabilities, it can also operate as a laboratory assistant for performing interactive experiments with MFCs. The ultimate aim of this interaction is to improve the power output levels of MFCs that can be then used for practical applications. Thus this chapter, through a series of experiments stated as Phases I-V, aims to cover the range of EvoBot-performed MFC experiments, leading to the final step of this study which was the running of the original EcoBot-II, using the EvoBot-matured MFCs.

Parts of this chapter have been included in the following publications:

Theodosiou, P., Faina, A., Nejatimoharrami, F., Stoy, K., Greenman, J., Melhuish, C. and Ieropoulos, I. (2017) EvoBot: Towards a Robot-Chemostat for Culturing and Maintaining Microbial Fuel Cells (MFCs). In: *Biomimetic and Biohybrid Systems* [online]. Springer, Cham. pp. 453–464.

Faíña, A., Nejatimoharrami, F., Stoy, K., **Theodosiou, P.**, Taylor, B. and Ieropoulos, I. (2016) EvoBot: An Open-Source , Modular Liquid Handling Robot for Nurturing Microbial Fuel Cells. In: *Proceedings of the Artificial Life Conference 2016*. 2016 pp. 626–633.

EvoBot has been developed by Prof. Kasper Stoy, Assistant Prof. Andres Faina and Dr. Farzad Nejatimoharrami from the IT University of Copenhagen, as part of EVOBLISS project.

5.1 The making of EvoBot

The term robot has been defined by the International Organization for Standardization (ISO) as:

“a programmable actuated mechanism with a degree of autonomy, which is able to move within its environment in order to perform intended tasks”.

Historically, the first commercially available laboratory robot, the Robot Chemist, was marketed in 1959 with the aim to automate wet-chemical analytical procedures (Rosenfeld, 2000). This was the first step towards laboratory automation practices. Twenty years later, laboratory robots were introduced into the pharmaceutical industry for drug analysis (Bogue, 2011). After a long period of adoption, robots are today playing a significant role in all aspects of laboratory procedures; from routine chemical analysis to drug development and DNA analysis. Autonomous laboratory robotics have generally advanced laboratory procedures since they offer: accuracy, speed, convenience and they are cost effective compared to labour cost. One research area that can directly benefit from such advances in laboratory robotics is MFCs.

As it has been mentioned earlier (2.1.3), MFCs have been closely associated with autonomous robots due to their capabilities of providing energy autonomy to biologically inspired robots; Gastrobot (Wilkinson, 2000), EcoBot I, II, III (Ieropoulos, 2003; Ieropoulos *et al.*, 2005, 2010a) and Row-bot (Rossiter *et al.*, 2015; Philamore *et al.*, 2016). These examples are proof-positive that energy autonomy is both plausible and feasible through the use of MFCs, however research is still needed to reach full MFC potential and increase the capabilities of these artefacts, which are known as Symbots (Melhuish *et al.*, 2006).

Due to the increasing demand for alternative - renewable methods of powering robots (Iqbal and Khan, 2017), MFC research emphasis is on the development of the next generation of improved and optimised MFCs offering maximum power production. In this line of thought, EvoBot attempts to implement the 3D RepRap technology as a mechanism for printing organic and inorganic substrata as well as accurately dosing the biofilm (microbial community adhered to the anode electrode) of the fuel cell with organic matter in the same manner as a chemostat. The idea of a laboratory robot that can inoculate and maintain MFCs, in a similar manner to the maintenance of bacterial cultures within a chemostat, was first captured in the original EVOBLISS project proposal that predates this thesis.

The chemostat is a widely-used apparatus for culturing cells (Monod, 1950) enabling the experimental control of cell growth rate, in order to study the adaptive evolution of microbes and to achieve dynamic steady-states (Ziv, Brandt and Gresham, 2013). The cell culture grows and evolves within the chemostat in the presence of a continuous flow of nutrients. The vessel retains a constant volume, as an overflow system is in place (**Figure 5.1**). These principles were transferred on the EvoBot platform. The MFC bioreactors acted as the biofilm culture vessels and the continuous flow of nutrients was replaced by an on-demand fuel supply triggered by the MFC electrical output. This correlation and experimental line of work has never been explored before and contributes to the novelty of this thesis.

EvoBot aims to act as a Robot-Chemostat for monitoring and interacting with evolving systems and eventually producing optimally evolved/adapted MFCs with improved energy generation capabilities, which is a pioneering step for the MFC technology. Hence, this thesis investigated if such a machine can

accelerate the maturing process of the MFCs resulting in an optimum microbial consortium, for energy production, at a shorter period of time.

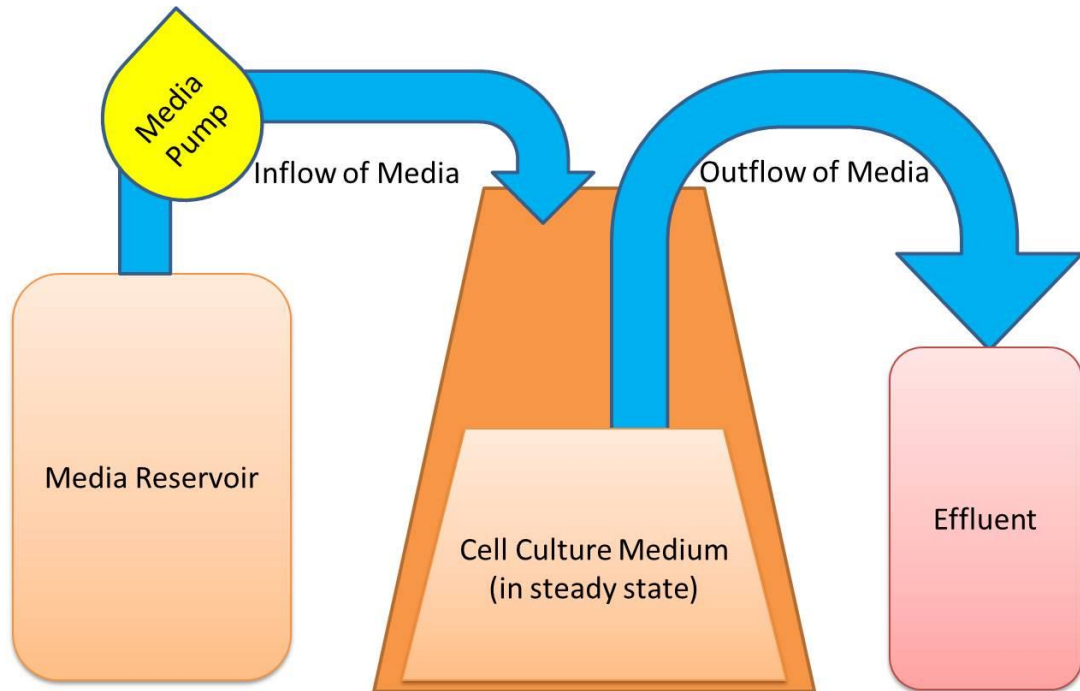


Figure 5.1 - Graphical representation of the chemostat method/biofilm continuous culture reactor for culturing bacterial cells.

5.1.1 Characteristics

EvoBot is a modular, open source, versatile, and affordable robotic platform, which has been developed to perform liquid handling experiments; in the context of the EVOBLISS EU project (FP7-ICT). EvoBot has been used in seven different laboratories around the world for diverse applications, such as interaction with MFCs (Faíña *et al.*, 2016), moving droplets, improving the quality of artificial life experiments (Nejatimoharrami *et al.*, 2016) and performing OCT scans on biofilms (Blauert, Horn and Wagner, 2015).

EvoBot consists of an upper actuation layer, an experimental layer in the middle, and a sensing layer (with a camera) at the bottom (**Figure 5.2**). The actuation layer comprises the robot head and modules mounted on it. The modules are plugged into the head and are usually designed to perform an action on the experiment. However, they may also have sensor functionality e.g. optical coherence tomography (OCT) scanning, an imaging technique which allows for optical sectioning of the sample. Such a sample can be the electroactive anodic biofilm of an active MFC with transparent anode chamber. The head, which holds the modules, can be moved in the horizontal plane. EvoBot's modularity allows for support of modules of different kinds for various applications. The experiment-dependent modules could entail syringe modules for liquid dispensing or aspirating, grippers to move the containers over the experimental layer or dispose dirty containers, an OCT scanner module to perform OCT scans, an extruder module to 3D print MFC parts (as shown in **4.2.3**), and other potential experiment-specific tools.

The experimental layer consists of a transparent Poly methyl methacrylate (PMMA) sheet on which reaction vessels (e.g. Petri dishes, well plates, beakers etc.) and/or MFCs are positioned. The actuation layer interacts with the experimental layer by filling or emptying a specific volume to/from a syringe, washing a syringe, or/and disposing dirty containers.

The robot frame is built from Aluminium profiles, which, the experimental layer and actuation layer are mounted on. The layers can easily be moved up or down on the robot frame with a cam lever mechanism.

Configuring EvoBot for different experiments is easy, as modules can be simply removed or plugged at the appropriate position. The head is responsible for moving the modules in the x-y plane, while the modules have motors to move vertically. The robot head can accommodate syringe modules to as-

pirate or dispense liquid at 17 potential positions, and up to 11 syringes can be used simultaneously as the socket positions overlap with adjacent ones.

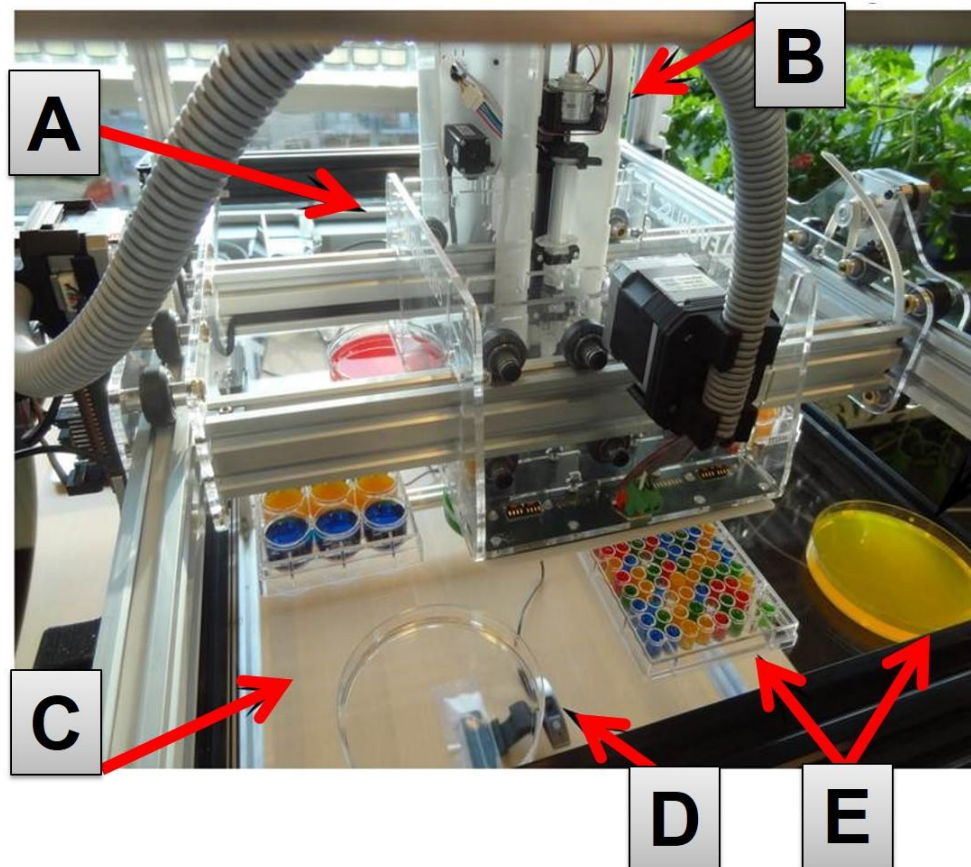


Figure 5.2 - Overview of the actuation and experimental layer of the robot.

[A] EvoBot's actuation layer consists of a moving head on which various modules, such as [B] syringe modules can be mounted. In this figure the [C] experimental layer accommodates [E] different vessels, and the [D] camera at the bottom acts as the sensing layer by collecting experiment data.

EvoBot's design is based on open-source 3D printers using an Arduino board and a RAMPS shield. This electronics design allows building on existing software for open-source 3D printers. A computer controls the robot by communicating with the Arduino through serial communication. The Arduino

is connected to the RAMPS shield. The RAMPS shield controls the three stepper motors to move the robot head, the modules mounted on the robot head, as well as the two direct-current (DC) pumps.

5.1.2 Scope

As described earlier (5.1), EvoBot was developed to operate in the same manner as the chemostat and the work has been broken down into five different phases. These phases (experiments) were performed by the author of this thesis at UWE, Bristol. During Phase I, EvoBot demonstrated interface and interconnection with an MFC. Shortly after, during Phase II a long-term experiment with 9 MFCs was performed. Using a feedback loop, EvoBot maintained the MFCs by controlling the nutrient supply rate when the power dropped below a pre-set threshold. On Phase III the experiment was optimised further and was able to take twice as many MFCs on the platform (than Phase II) and through the use of two DC pumps and two syringes, it supplied media to the on-board vessels that redistributed to the fuel cells. This work focused on demonstrating the development of EvoBot as a modern-day, robotic, biofilm bioreactor for continuously culturing the biofilm of the MFCs (based on the “chemostat” approach). The main aim of phases I to III was to examine whether MFCs could be optimised through EvoBot interaction in order to produce higher power outputs.

Phase IV gave the opportunity to experiment on the established MFCs by implementing an evolutionary algorithm (CMA-ES) in order to identify and develop a feedstock more suited for high power performing MFCs. The unique novelty of these experiments presented in Phase I-IV is the fact that adaptation and evolution occurred with energy abstraction as the main selec-

tive mechanism, which is used as the feedback signal to interact with the EvoBot feeding mechanism.

Based on the knowledge gathered during the four previous experimental phases, a final experiment was set-up for Phase V. This investigated the impact of the EvoBot automated feeding process against the conventional manual batch feeding process, on the length of the maturing period as well as on the power output levels of the MFCs. The optimised MFCs were then empirically evaluated to explore whether they could power another robot using the EcoBot-II as the testing platform. In the following sections the five phases that showcase EvoBot's versatility will be described in detail.

5.2 Phase I - Interface and interconnection

This section describes the infrastructure and execution of the interconnection experiment between an MFC and EvoBot, which was pursued and established for real-time output capture, recording and control. The electrical interface was set-up using a data-logger connected to the EvoBot computer which allowed both individual and collective (i.e. stack – when applicable) MFC readings to be recorded. The electrical connections on the platform allowed for the MFCs to be connected using “plug & play” interfaces to allow easy access to the MFCs once they are ready for detachment and use in practical applications. These electrical connections aimed to interface with the EvoBot controller, for real-time feedback control. In particular the experiment investigated if the electrical signal of the MFCs can effect a behaviour change in the robotic head which will react either with the microcosms inside the MFCs (by supplying the anodes with fuel) or/and the abiotic open-to-air side (by hydrating the cathodes with water).

Initially during the Phase I experiment, threshold readings from the electrical output of the MFC were used to control the pumping mechanism mounted on the robotic head in order to actuate and deliver fuel (when starved). Hence the overall aim of this experiment was the proof-of-principle that a robotic system such as EvoBot can interface and interact with living systems (MFCs) by monitoring the real-time electrical output and feeding it back to EvoBot to control the MFC's electrical behaviour.

5.2.1 Specific Materials and Methods

5.2.1.1 Hardware

The first version of EvoBot was used for this experiment. It had a length of 600 cm and the MFC was placed on the arena (**Figure 5.3A**). A detailed report of the robots design, mechanics and electronics is presented in Faíña et al. (2016) and for this purpose it will not be included in detail here. The liquid was delivered to the MFC via a DC pump attached to the robotic head as described in section 0 (**Figure 5.3C**).

5.2.1.2 Software

Laboratory Virtual Instrument Engineering Workbench (LabVIEW) from National Instruments, Texas, US was used to create the applications that interacted with the real-time data produced from MFCs. Using LabVIEW a multi-layer program was compiled in which a function was written that collected the data from the Picolog data logger and output that data as a string of values. LabVIEW sampled the Picolog file every 1 minute for the MFC voltage reading. The feeding scripts were written in Python language (Python 3.6.0). In the case where the MFC voltage dropped below the preset threshold limit that was set in LabView, the python script was activating the robotic head

(actuation layer) to move above the MFC anode and deposit by pump 12.5 mL of inoculum. After the disposing of the liquid, the head of the robot homed itself.

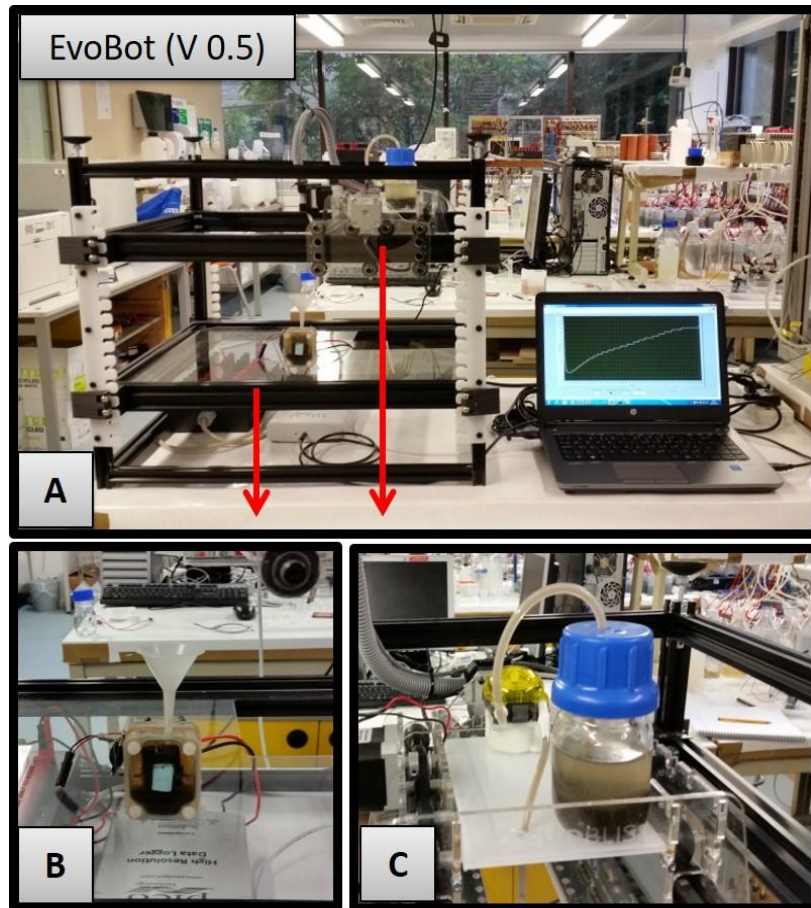


Figure 5.3 - Experimental set-up of Phase I: Interface and Interconnection experiment.

[A] The robot and data-logger are connected with the laptop computer which acts as a real-time voltage display. **[B]** The photo shows the anode of the MFC, pressed against the membrane using a rectangular piece of inert styrene material and **[C]** the DC pump connected to the bottle containing the sludge.

5.2.1.3 MFCs

A standard analytical size two-chamber cubic MFC (**3.3.1**) was placed on the EvoBot experimental arena (**Figure 5.3B**). The anode and cathode electrode were connected with a 3 k Ω load.

The MFC was inoculated with activated sludge supplemented with 5mM sodium acetate as the CE source. Connected to the robot board, the DC pump was used for pumping the enriched sludge into the anode chamber. The DC pump was calibrated and the length of time it was allowed to pump (activation time) dictated how much liquid volume should be dispensed. For this experiment, in order to dispense 12.5 mL of sludge the pump was activated for 37 seconds.

Electrical output (voltage) was measured in real-time using a PicoLog ADC-24 interface, both the EvoBot and the data-logger were connected in the same HP laptop computer.

5.2.2 Results and discussion

As explained in a previous chapter (**2.1.2**) the microbial metabolism, utilises the carbon energy source within the anode chamber of the MFC which eventually depletes the carbon content resulting in a drop in voltage; in other words, as the fuel runs out, the voltage decreases. This was the foundation of this initial and critical experiment, which focussed on identifying whether the change in voltage would trigger the robotic arm of the EvoBot platform. The triggering could cause the robotic hand to move and feed the MFC with more organic material when the voltage drops below a threshold. As a result of the interaction, the MFCs could be maintained at higher output levels and the experiment could be prolonged.

To test this theory, the experiment started using an abiotic MFC as described earlier (**0**). At the outset, the MFC was dry and contained no bacteria (therefore zero voltage was recorded). The null voltage actuated the arm to move and deliver approximately 12.5 mL of activated sludge into the anode chamber (**Figure 5.3B**). The 12.5 mL was fed into the anode chamber of the MFC using a DC pump that was connected to a 50 mL bottle of activated sludge (**Figure 5.3C**).

After the robot had deposited the 12.5 mL of activated sludge (**Figure 5.4A**), the MFC voltage increased and stabilised at approximately 27 mV. Next, the command “Feeding Threshold” was set to 20 mV with the original intention being to let the voltage naturally decrease as the microbes consumed the food in the sludge. However, since the time period for a freshly inoculated MFC, to fall under 20mV, can take up to 24 hours, 10 mL of sludge was manually removed to simulate food consumption (**Figure 5.4B**); due to the disturbance when removing the anolyte a spike in voltage was observed. However, once the voltage decreased below the pre-set feeding threshold the robot arm was activated to move to the position above the MFC anode inlet and initiated the DC pump for 37 seconds, thus introducing 12.5 mL of new sludge medium into the MFC.

This short but significant experiment showed that the feedback loop between the MFC output (the voltage and power to maintain that voltage) produced by the microorganism living inside an MFC communicated with the robotic controller, which was then able to activate a python script that initiated a set of given tasks. This chain reaction resulted in the supply of fresh fuel to replace the depleted feedstock leading to increasing the MFC voltage above the minimum threshold. This robotic interactive approach can be of a direct benefit

to the MFC research community because it gives control and automation to the complex process of MFC inoculation, cultivation and maintenance.

Conventionally, MFCs that are tested in laboratory conditions need reliable feeding and maintenance provided by the researcher responsible for that experiment. As discussed earlier in **2.1.2.1** this can either be in the form of periodical feeding usually occurring daily (batch-fed) or in the form of a constant feeding supplied by a pump (continuous flow). Both methods have their respective advantages and disadvantages. However none of these methods can provide the MFCs with the much needed fuel on-demand (e.g. when the microbes in the biofilm need it the most). Besides, continuously fed systems that need constant pumping of fresh media may result in an excess supply of fuel when it is not necessary resulting in the over-consumption (efficiency waste) of the specific fuel.

Thus with software such as LabView and background Python scripts it is possible to change that and set threshold limit voltages – either a higher or a lower threshold – with a specific command that activates the EvoBot robotic arm to perform a given task based on the users' needs. When low voltage is detected (below threshold) these types of commands can include but are not restricted to the robotic arm selecting a specific substrate (nutrient, pH buffer, mediator) and depositing to an underperforming MFC. On the flipside, if a higher voltage is detected (above threshold) then a recommended action could be to extract a portion of that “strong” microbial community and transfer it into an abiotic MFC. This would ensure that colonisation is initiated using a healthy electroactive community.

In summary this experimental trial showed that the robot is able to maintain the MFCs by reacting to the carbon energy source depletion within the anode as reflected by the power output. Additionally, these findings demonstrate for

the first time that an MFC's real-time electrical output can establish a feedback loop with the EvoBot. Hence, this novel use of the EvoBot can advance the inoculation and maturation process of MFCs using the robot as the automated reactive laboratory assistant, rather than relying on fed-batch or continuous flow systems.

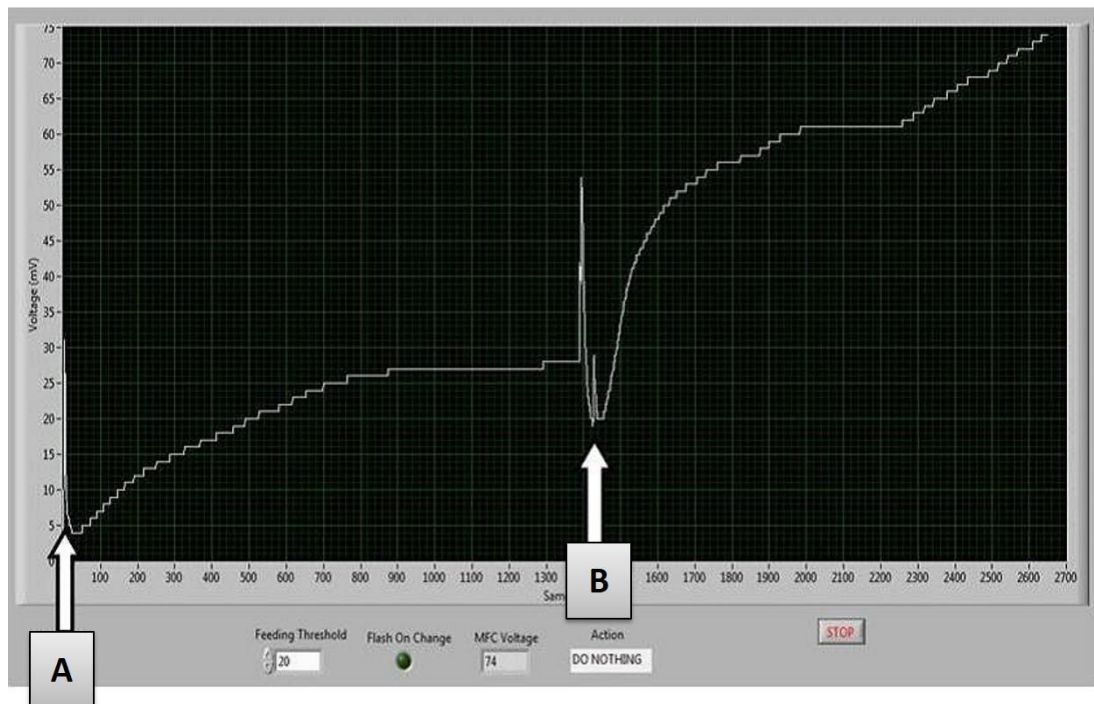


Figure 5.4 - Screen capture of the voltage increase.

[A] Initially the MFC output was zero as the MFC was abiotic, this triggered the robotic arm to move to the fuel cell and activate the pump to feed the pre-set amount of inoculum (12.5 mL) to the anode. **[B]** At point B, 10 mL of the analyte were manually removed to rapidly simulate food consumption and as a consequence, the voltage dropped. Since the MFC output fell below the pre-set threshold of 20mV the robotic arm was activated and another 12.5 mL of inoculum were deposited to the anode; as a result, the voltage of the MFC continued to increase.

5.3 Phase II – Optimisation of substrate parameters

During Phase-I, EvoBot responded to the lower voltage threshold resulting from CE depletion. However, the signal output of the MFC is dependent on both a large number of physicochemical conditions as well as a large number of metabolic processes occurring within the microbial community. Apart from CE depletion these can include but are not restricted to feedstock concentration, pH shifts, and temperature fluctuations (that can interfere with the speed of the bacterial metabolic processes). These processes can be positively or negatively affected by other pressures occurring within the MFC. For example, the pH within the anode chamber will be optimal for some microorganisms and sub-optimal for others, including electroactive organisms, therefore pH will be an important parameter for the EvoBot to control. Other selective pressures affecting the MFC anode include the type and concentration of food substrates. Currently the use of a standard 1.5% TYE as a microbial medium is commonly preferred in the experimental studies although more precise data relating to the specific needs of the microbial community could be attained by using a defined medium mix. Having this in mind the following experiment was conducted as part of Phase II, which focused on optimising the substrate parameters in order to maintain a healthy biofilm and to improve the MFC power performance. The substrate parameters that this experiment tried to optimise were the source of fuel (acetate, lactate, cellulose) and the concentration of each fuel (0.25% w/v, 0.5% w/v, 1.0% w/v). Initial investigation was conducted using the EvoBot platform to test the aforementioned feed substrates at the three different concentrations and observe the behaviour of both EvoBot and the MFCs..

As part of this experiment, EvoBot was set the task of maintaining nine individually connected MFCs and testing their behaviour using either acetate, lactate or cellulose as feedstock at 0.25% w/v, 0.5% w/v and 1.0% w/v. Concomitantly, in order to analyse the advantages of using the EvoBot over the conventional batch-fed mode, another set of MFCs were prepared using identical materials and methods and operated as controls. The only difference between the two MFC sets was the mode of operation and maintenance. One was carried out manually and the other one was carried out by the EvoBot platform (**Figure 5.6**). The manually operated experiment was used as the control of the study and was named “replica” since it was identical to the MFC set on the robotic platform. In the case of the robot experiment, the voltage was sampled every minute, the MFCs were hydrated every four hours and only fed if the voltage was below the specified threshold. In contrast, the voltage of the “replica” (on the bench) was sampled every three minutes, and the MFCs were hydrated twice a day - morning and afternoon - and fed once every morning, reflecting the conventional manual mode of maintaining MFCs.

5.3.1 Specific Materials and Methods

5.3.1.1 Hardware

The same hardware was used here as described in **5.2.1.1**, with minor modifications. These included the alteration of the experimental arena layout and addition of a syringe module. Taking advantage of the built-in flow-through mechanism that the small-scale MFCs (**3.3.2**) have, the sterile MFCs were embedded (resting on the pre-laser-cut gap) in the arena, thus allowing the effluent to drip into a container placed underneath the robot. The layout of

the arena included the feedstock beakers, the ethanol and water beakers (for the 'wash cycle') as well as the waste funnel. A schematic representation of the layout and a photograph of the actual set-up is shown in **Figure 5.5** and **Figure 5.6** respectively. Additionally for this experiment a 10 mL syringe module was added on the robot's head to enable the delivery of media in the anode reactors.

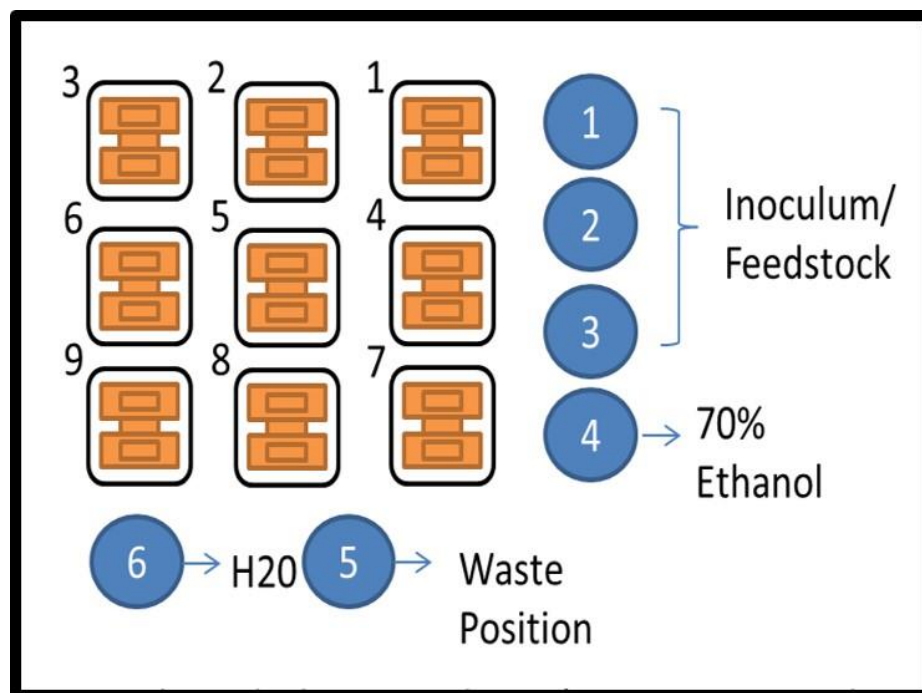


Figure 5.5 – Layout of Phase II experiment on EvoBot platform.

Schematic representation of the experimental layer. Initially beakers 1, 2, 3 contained the activated sludge (inoculum) which was replaced at the end of the inoculation period with acetate, lactate and cellulose media respectively.

5.3.1.2 Software

Each MFC was individually connected to a separate channel on the Picolog data acquisition unit, which was connected to a PC, so that the voltage output of each unit could be continuously recorded. A set of MFC feed functions was created in LabView, which sampled the Picolog DLL file every 60 seconds for the MFC voltage reading. A threshold limit for each MFC was set in LabView so that when the voltage dropped below the threshold, a Python script would activate to move the head of the robot over the food source, draw 3 mL of substrate (carbon fuel) and then inject this into the MFC.

After the feed substrate has been deposited into the anode, the syringe module would go through a wash cycle where 3.5 mL of 70% ethanol was drawn into the syringe and disposed of, down a waste tube on the Evobot platform, followed by the taking of 3.5 mL of sterile distilled H₂O into the syringe, before disposing this down a waste tube and then returning the robot head to the home position. At the home position, the feed function paused for 60 minutes to allow stabilisation of the MFC and for the voltage to increase above the threshold.

A cathode hydration cycle was also incorporated in a separate function in LabView, which activated a Python script every 4 hours. This script moved the robot head over the position of each MFC and deposited 3.12 mL of deionised water into the cathode chamber before returning to the home position.

For the Evobot experiments, the 'wash cycle' with ethanol and deionised water was deemed necessary in order to avoid cross-contamination between the different carbon-energy sources (acetate, lactate and cellulose). Howev-

er, it was not necessary for the replica bench experiment, which was carried out manually and used separate syringes for each feedstock.

5.3.1.3 MFCs

Small-scale MFCs (3.3.2) were employed with CEM separators. The anode electrode was as described earlier (3.1.1). This had a total surface area of 168 cm² and a projected (exposed) surface area of 5.25 cm² housed in an 18 mm x 28 mm anodic chamber. The cathode used was the AC/CV created as explained in 3.1.2.1.

For the MFC experiment on the EvoBot platform, the inoculation (i.e. introduction of live microorganisms in a sterile MFC) was carried out using the anolyte from already established MFCs. This was activated sludge fed with carbon sources such as TYE over a period of months. In order to prevent blockages of the syringe needle it had been sieved to remove large particles (>1 mm). For the replica bench experiment, neat activated sludge was used as the initial inoculum.

To inoculate the MFCs and test the activation of the EvoBot head, the feedstock beakers initially contained the activated sludge inoculum; the EvoBot syringe then picked up 6 mL (in two doses of 3 mL) and deposited into each of the MFCs to begin colonisation. All the nutrient beakers contained activated sludge during the inoculation phase. As soon as the MFCs had been inoculated the beakers were replaced with clean ones containing feed substrate. Over the course of the experiment three different feed concentrations were used at 0.25%, 0.5% and 1% w/v for each of the feed sources; acetate, lactate and cellulose. The target media were supplemented with a weak solu-

tion of TYE (0.15%). All MFCs in both experiments were kept under a fixed load of 3.9 k Ω , for the whole duration.

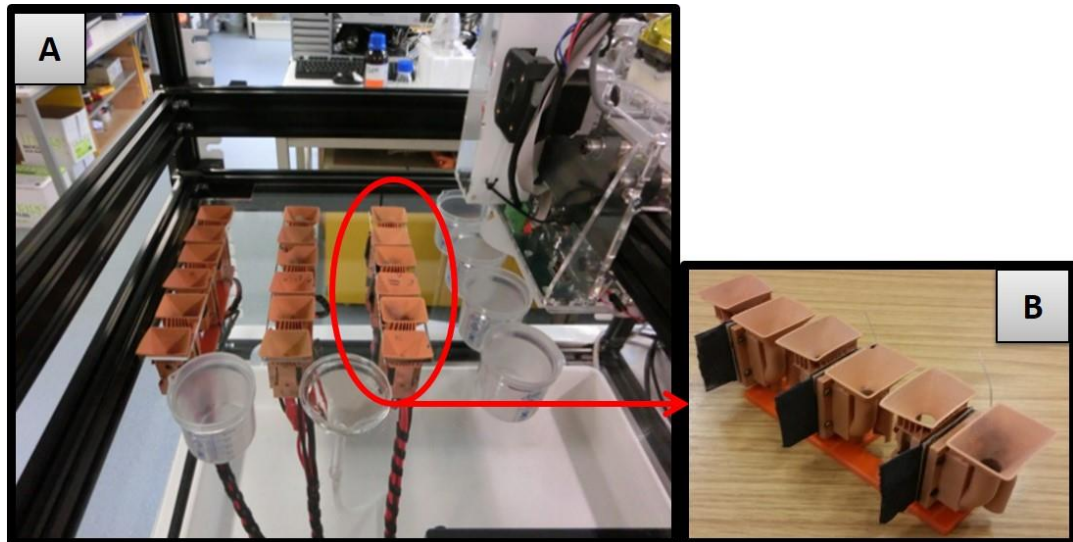


Figure 5.6 – Phase II experimental set up on EvoBot.

[A] Nine individually connected MFCs were operated with Evobot platform. The experiment took place on the experiment layer (arena) of the robot. The replica bench experiment was setup in exactly the same manner (photo not shown). The MFCs as well as the beakers and waste funnel were embedded in the already pre-cut acrylic sheet of the experimental arena. Underneath that, a drip tray was positioned to collect the effluent and waste liquids. **[B]** A triplicate of the 3D- printed small scale MFCs as used on the experiment sitting on their 3D- printed base.

5.3.2 Results and discussions

This experiment focused on using the EvoBot platform to inoculate empty MFCs and monitor how the power profiles develop over time with only EvoBot supporting the cells. Since the experiment focussed on monitoring the individual performances of MFCs, they were arranged electrically as individual units (instead of connected as a stack). In this way, the performance of

individual MFCs could be identified and compared to other identical units. Subsequently the EvoBot platform was able to focus on the parameters that might have contributed to factors causing performance variation and begin to replicate these in other MFCs.

5.3.2.1 EvoBot automated feeding VS manual feeding

The experiment lasted approximately 8 weeks for the EvoBot experiment and 2 weeks for the “replica” (manual feeding) and the comparisons between the experiments were made for the same period. To show the automated feeding profile of EvoBot maintained MFCs, the power output of one MFC fed by EvoBot and the feeding events are shown in **Figure 5.7**.

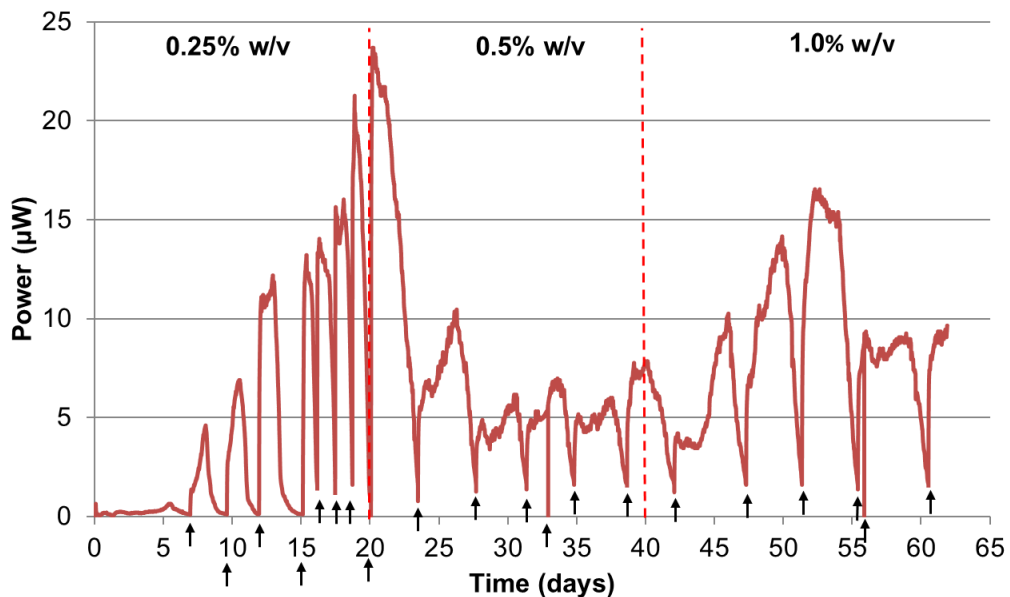


Figure 5.7 – Indicative power output from one of the MFCs (MFC2) fed by the EvoBot with sodium acetate.

The arrows indicate the points where the voltage output of the MFC dropped below the 80mV threshold, which was the trigger for feeding the MFC. The dotted lines indicate the periods during which three different concentrations of sodium acetate were tested.

As explained above during the “replica” experiment, MFCs were fed daily regardless of their power output and hydrated twice as oppose to the EvoBot maintained MFCs which were hydrated every 3 hours. During the two week testing period a significant performance difference was found between the replica experiment and the EvoBot experiment (**Figure 5.8**). The replica experiment (**Figure 5.8B**) achieved higher power levels compared to those on the robot. The difference was almost ten times higher for cellulose fed MFCs, and four times higher for lactate and acetate fed MFCs. This difference could have been due to the wash cycle with ethanol, which would have inevitably left residual ethanol in the syringe during the course of the experiment - the replica experiment did not require a cleaning cycle. Also, the sieving of sludge for the inoculation of the MFCs may have well resulted in a less enriched inoculum, and this was done to prevent the syringe needle from blocking - again, this was not an issue for the parallel bench experiment.

Nevertheless, having automated feeding pulses which were dictated by the voltage threshold, the behaviour of a MFC could more closely be monitored continuously in a way that would otherwise require an operator to be continuously present. In addition, the automated hydration cycle was advantageous, since it helped us identify empirically the aqueous O_2 saturation levels for the ORR that is necessary for the open-to-air cathodes. In other words, beyond this ‘performance saturation’ point, the addition of more water did not result in an increased MFC performance. This can be illustrated on the acetate fed MFC (inset of **Figure 5.8A**). The fluctuating electrical output is the response to the cathode hydration, however as can be seen, the overall performance during that feeding cycle, remains the same (on average).

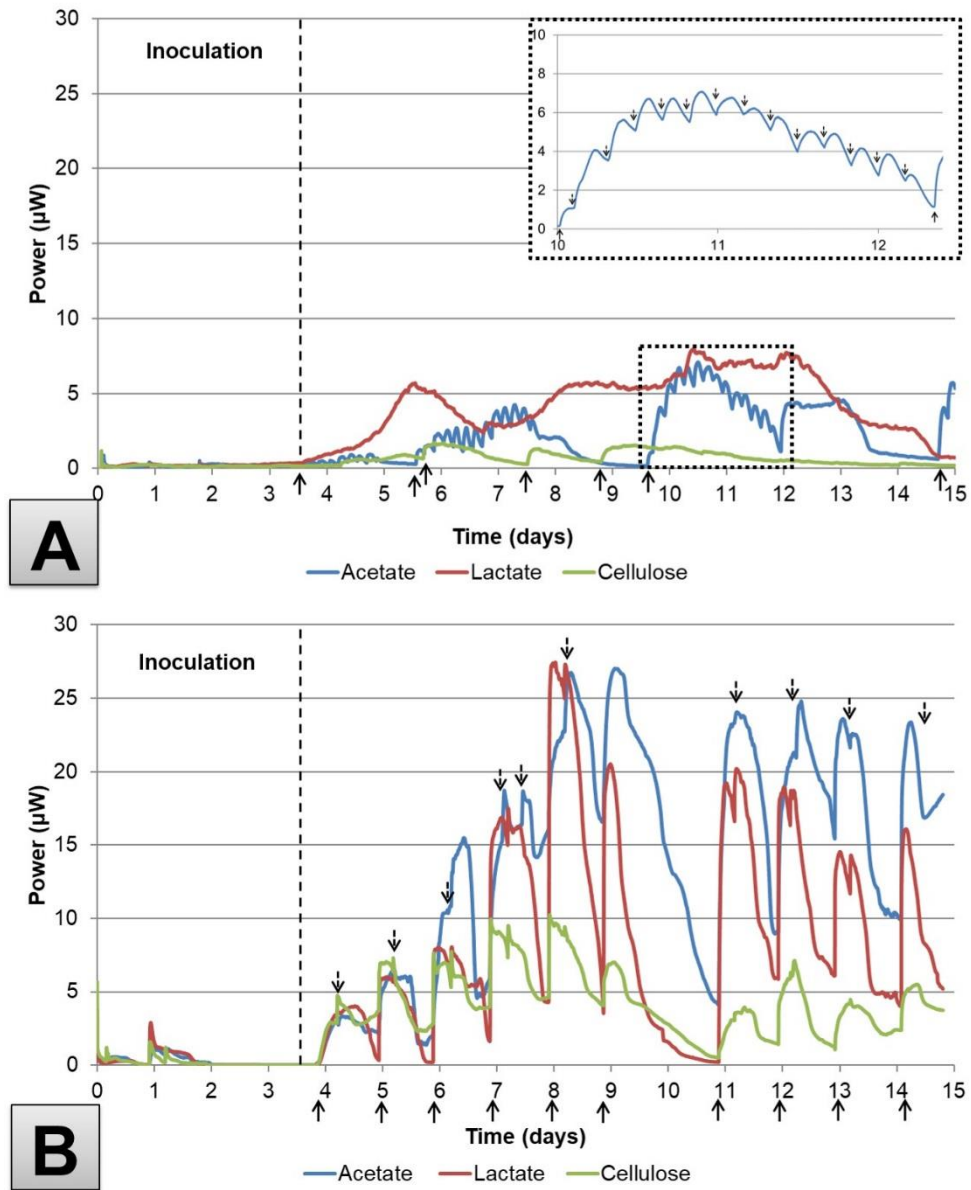


Figure 5.8 – Power output profile of the [A] EvoBot maintained and [B] manually maintained MFCs for a time period of two weeks.

On both graphs solid arrows indicate time of feeding and on graph B, dotted arrows indicate hydration of the cathode. On graph A hydrations are not pointed out for better clarity as EvoBot induced hydrations every 3 hours as can be seen on the inset in the graph (small frequent spikes).

5.3.2.2 Substrate concentration impact on MFCs

Despite the underperforming MFCs on the robot, the experiment continued for a total of 8 weeks as it was crucial to test both the durability of the robot and the interaction of the MFCs with it. This was the first automated EvoBot experiment and the lessons learned proved invaluable for its' future improvement. Furthermore the overall aim of the experiment was to identify, using the robotic feedback loop, the optimal substrate concentration of three given substrates that can yield the highest power output out of the MFCs. The experiment successfully optimised the substrate parameters and using its feedback loop showed that acetate was the best fuel among the rest especially at a concentration of 1.0% w/v.

The average power output of acetate, lactate and cellulose fed MFC triplicates at three different feedstock concentrations is displayed in **Figure 5.9A**, **B** and **C** respectively. Each concentration was tested for a period of 20 days each. At the end of that period the feedstock was manually prepared (on the bench) and loaded into the vessels on the platform. It was picked up by the syringe and distributed to the corresponding MFCs. Based on **Figure 5.9A** acetate fed MFCs were performing best when fed with the 1.0% acetate solution and they reached a steady state at $13 \pm 1 \mu\text{W}$. The MFCs fed on 0.25% lactate solution reached a similar power output however this was sustained only for a day (day 15-16) (**Figure 5.9B**). After the lactate concentration was increased to 0.5% on day 20, the MFCs declined at first before recovering and steadily increasing to reach $\sim 10 \mu\text{W}$ on the 28th day. Overall, the cellulose fed MFCs were the least performing with a maximum output of only $1.5 \pm 0.25 \mu\text{W}$ at 0.25% concentration (**Figure 5.9C**). Increasing the concentration of the cellulose solution had a negative impact on the MFCs' perfor-

mance which can be attributed to the inability of the microbial community to metabolise cellulose and transfer electrons to the anode electrode.

As explained in **2.1.2.1**, MFCs have tremendous electron donor versatility, unlike chemical fuel cells which can only oxidise specific electron donors. This versatility means they can oxidise both simple (e.g. acetate, lactate) and complex substrates. This experiment demonstrated that the oxidation of lactate caused the second highest electric power production. Moreover it showed that compared to lactate, acetate is a more preferable electron donor and a more effective fuel in terms of electricity generation, similar results were observed by Vasylyv et al. (2013). Cellulose on the other hand was not suitable for high power production due to the lack of cellulolytic activity from electrochemically active bacteria found in municipal wastewater. For the efficient conversion of cellulose to electricity a syntrophic microbial community such as *Clostridium cellulolyticum* and *Geobacter sulfurreducens* that uses an insoluble electron donor (cellulose) and electron acceptor (anode) is required (Ren, Ward and Regan, 2007).

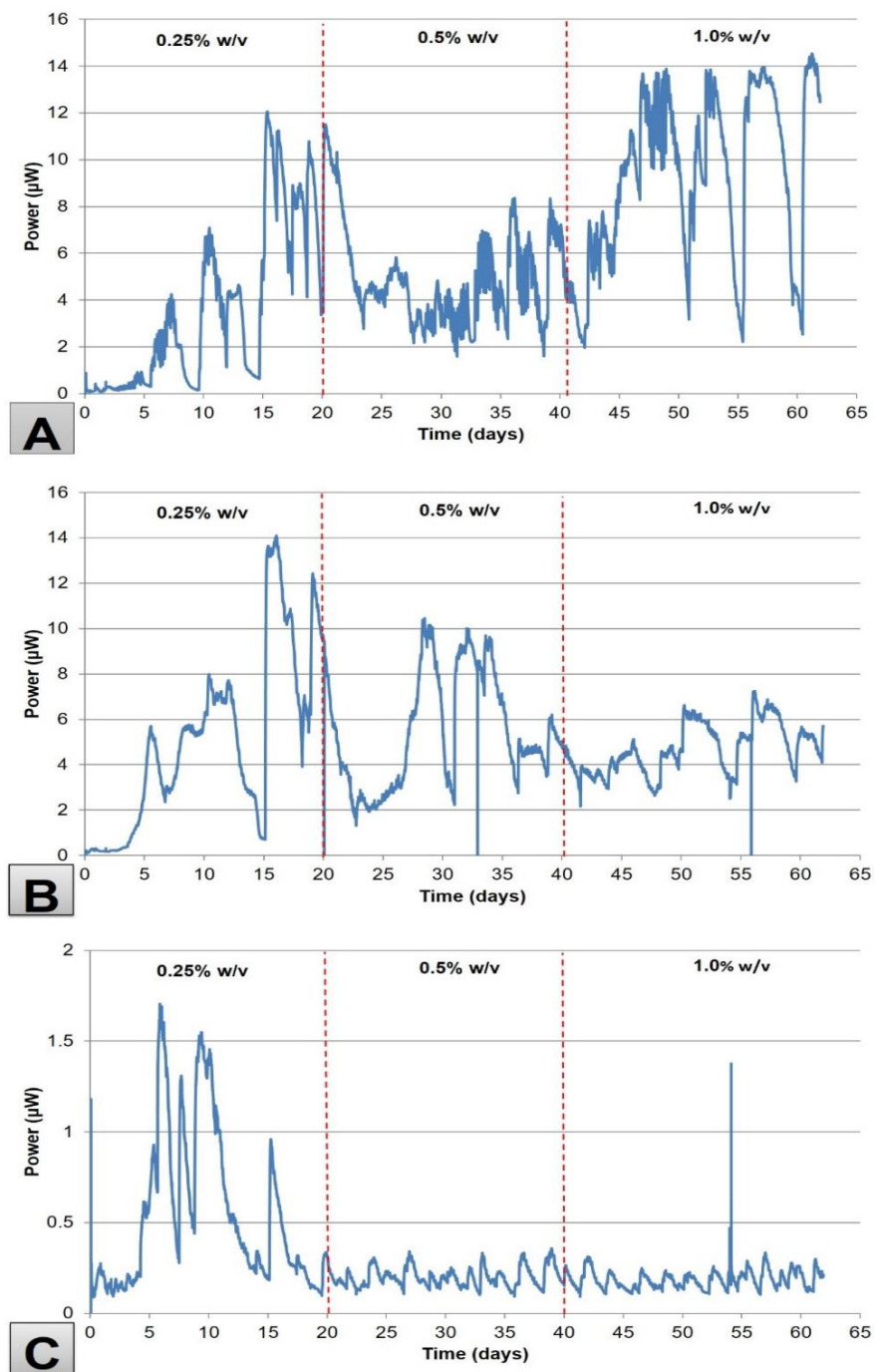


Figure 5.9 – Temporal power output of [A] acetate, [B] lactate and [C] cellulose fed MFCs, at different concentrations, via the EvoBot.

Spikes on the graph are indicative of the occurred feedings.

5.3.2.3 Robot improvements

The intention of EvoBot is to perform new interactive experiments which will allow the user to pose different scientific questions, possess novel data never recorded before and develop better MFCs. To accomplish that, initial experiments (detailed in the previous section) were needed to identify areas needing improvement. Such features include the incorporation of more syringe modules onto the robotic head in order to avoid cross contamination issues of media. This will eliminate the need of a 'wash cycle' and its associated issues such as lower performance caused by the ethanol residues. Furthermore a wider bore needle or tubing could be added to the module allowing the syringe to draw thicker viscosity liquids without causing blockage and subsequent hardware failures. Moreover, a dispensing module could be developed for deployment on the robot, which could be connected to external pumps to provide pure reagents or solutions. This approach allows different organic materials to be used to feed the MFCs without having to draw on the same syringe. Finally, the enlargement of EvoBot's experimental arena can provide the space for a larger number of MFCs and/or allow the parallel operation of more experiments.

This was the first demonstration using the EvoBot platform to feed live-operating MFCs over a significant period of time (8 weeks). Having EvoBot driven experiments provides the fuel cells with automated feeding and hydration pulses, which are dictated by the voltage threshold, as well as continuously monitoring and maintaining the MFCs, eliminating human intervention. This initial experiment was significant in getting a better understanding of what is needed in order to improve/adapt the robot, based on the experimental needs.

5.4 Phase III – Adaptation / Chemostat-like operation

During Phase II critical issues and areas of improvement were identified. These were addressed and resolved before performing the Phase III: Adaptation and chemostat mimicking experiment. In this experiment EvoBot was primarily used for MFC inoculation and maintenance as well as a characterisation tool akin to chemostat. The improved robot made it possible to perform two different experiments using continuous feeding cycles/pulses (called the “chemostat” approach). The experimental set-up is presented in **Figure 5.11**.

In microbiology, the chemostat is the most common type of continuous culture device. It is an open system where a culture vessel maintains a constant volume. As fresh medium is added at a constant rate, an equal volume of spent culture is removed at the same rate and as a result, the growth rate is equal to the dilution rate ($\mu = D$) and the system reaches dynamic equilibrium. In the natural world, a plethora of biofilms are formed in continuous or periodic nutrient replenishing conditions and can be regarded as open systems as well (Greenman, Ieropoulos and Melhuish, 2011). Because the anodic biofilm electrodes are made from perfusable carbon veil the MFC falls within the general category of matrix perfusion systems. In the literature, it has been reported that such systems have similarities to a chemostat model (Greenman, Ieropoulos and Melhuish, 2011). Thus in this experiment the anode compartment of the fuel cell is referred to as the culture vessel (chemostat analogy).

5.4.1 Specific Materials and Methods

The robot as well as the MFCs were improved based on the needs identified during the Phase II experiment. The hardware, software and MFC alterations are described below.

5.4.1.1 Hardware

The robot syringe module was adapted to host 20 mL syringe rather than 5 mL syringe (as in Phase II). Two pumps were placed on the external profile of the robot rather than on the robot head and these were connected to a dispensing module which was added on board. This allowed the creation of fresh media on-board eliminating the need for the media to be manually prepared on the bench. The camera was placed on the side of the robot, to record the feeding/maintenance of the MFCs. Lastly, the robot was elongated from 600 cm to 1000 cm which gave enough space for hosting twice the number of MFCs compared to Phase II.

5.4.1.2 Software

Python script activated the pumps for a certain time frame to allow all the liquid to move from the end of the media tube to the tip of the dispensing module nozzle. Every 24 hours the robot initiated the pumps to fill the pre-specified beakers with the media and when full, the syringe module drew the liquid (5 mL) from the beakers and dispensed it to the anode compartment of the MFCs. The coordinates of each item on the experimental layer were stored into Python dictionaries.

5.4.1.3 MFCs

A set of 18 small-scale MFCs were adapted for this experiment (**Figure 5.10**). A 3 mm custom-made terracotta flat sheet (prepared as previously reported in **3.2.2**), was used as the membrane. For cathode electrode, 5 mL of alginate based electrode (**4.4**) was deposited manually using a syringe directly onto the membrane and solidified after 24 hours (**Figure 5.10**). After the inoculation period, the MFCs were loaded with 1 k Ω . The MFCs for this experiment were fed with casein (1 g/L) dissolved in 4mL of 1M NaOH buffered using 3 mM PIPES buffer and deionized water. This feedstock was trialled to observe if it is suitable for MFCs given that it is a protein, and it informed the Phase IV experiment.

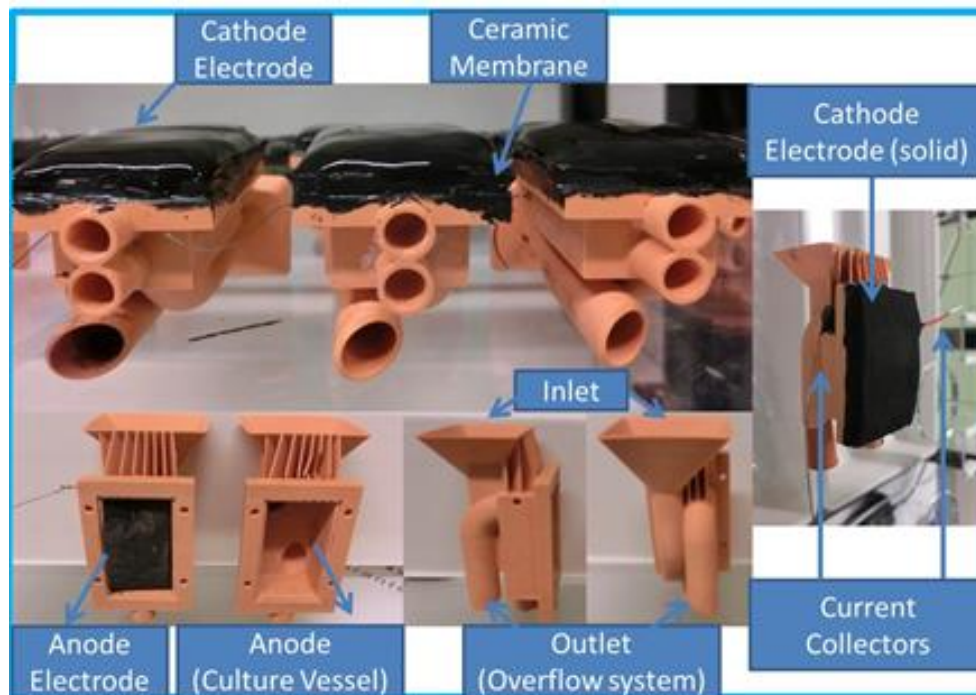


Figure 5.10 – Modified Nanocure® printed MFCs for Phase III.

The anode compartment of the MFC acted like the culture vessel of a biofilm reactor/chemostat. Fresh medium entered through the inlet, whilst effluent was overflowing through the outlet.

Initially the fuel cells were inoculated with activated sludge and then with effluent from active urine fed MFCs. After a total of two weeks inoculation, the cells left to starve for a week to ensure that no traces of urine were left in the anode. The experiment started with the introduction of sterile sodium acetate medium to the 9 MFCs and with sterile casein medium to the other 9 MFCs. The pH of the media was buffered to 7. The media were contained within two bottles; each bottle was connected to a DC pump and had an air filter (**Figure 5.11B**). The tubing of the pump led to the dispensing module of the robot (**Figure 5.11A and D**). For each experimental cycle the pump was set

to deposit and distribute the required amount of feedstock (overall volume 50 mL) to the specified beakers around the arena and then the syringe collected the liquid from the beaker and distributed it to the anode chambers of the fuel cells.

5.4.2 Results and discussion

Even though the system in the current study was a batch-fed culture system, i.e. not a continuous flow system like a conventional chemostat, the results show that slow transitional repeat states can be maintained following further CE source supply and subsequent depletion (**Figure 5.12**). These promising findings and this continuing line of work could provide useful insights into; repeat batch fed microbial fuel cell systems, their behaviour as well provide understanding on how to increase or optimise their power production capabilities. The results are a stepping stone for the next phase of experiments which focuses on combining the chemostatic abilities of the robot with evolutionary algorithms for the creation of optimised feedstock.

Based on the data of **Figure 5.12** it can be observed that even though all the MFCs were fed exactly with the same feedstock at the same time, the output differs. This can be attributed to the fact that the inoculation period was not optimised for these MFCs. Bacteria need to synthesise special enzymes in order to hydrolyse proteins. In order to be able to do that, the inoculation process should induce this synthesising process by slowly adding protein into the feedstock mixture. This is an approach that has been adopted for the Phase IV experiment in order to “train” the bacteria in consuming casein more efficiently.

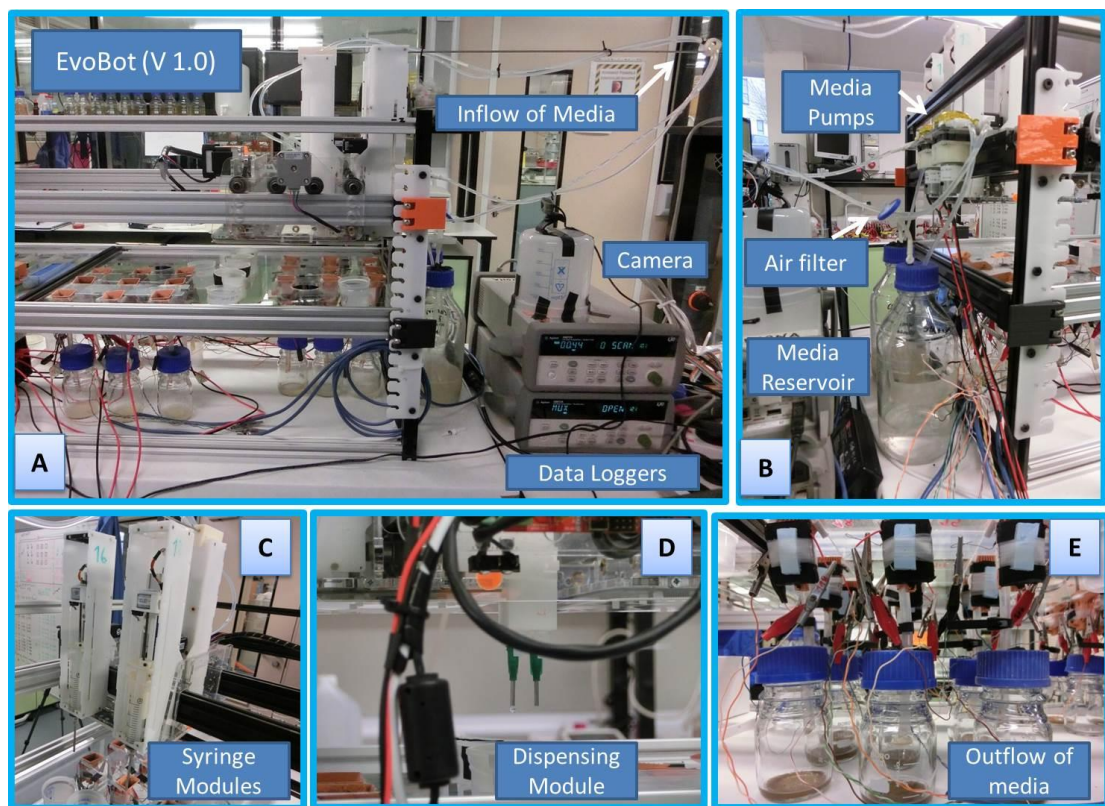


Figure 5.11 – Improved EvoBot based on the Chemostat approach for Phase III experiments.

[A] EvoBot was able to host two experiments that count in total 18 MFCs. The data loggers were connected to the MFCs and the computer, and a camera monitored the experiment 24/7. **[B]** Similar to the chemostat the media reservoir was connected to the DC pumps and the tubes were connected to the **[D]** dispensing module. **[C]** The syringes were set to draw the liquid and dispense it to the culture vessel. **[E]** The waste perfusate was collected from the bottom into bottles (outflow stream) for further analysis.

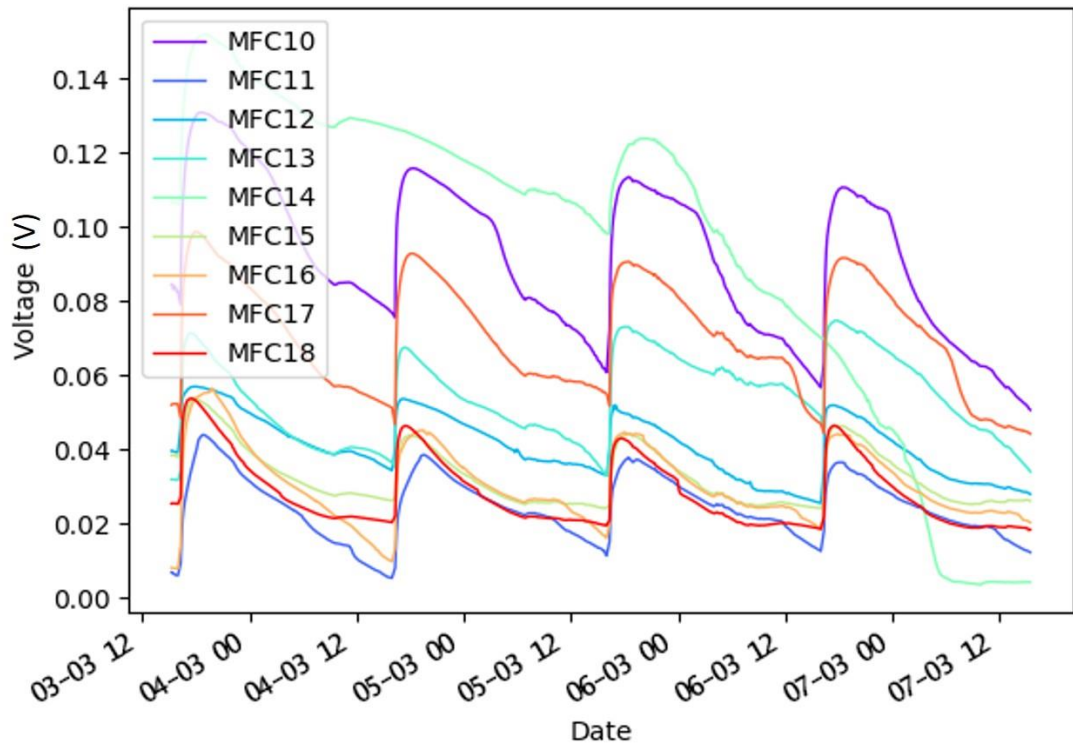


Figure 5.12 – Python generated graph based on the power output of the MFCs fed with casein.

The graph shows the data produced within five days of EvoBot feeding nine MFCs. The data show the reproducibility and stability of these cells when the fresh medium is fed to the bio-film daily. The non-periodic feeding of MFC 14, and consequent deterioration of performance was due to the liquid level of feedstock being below the lowest reach of the syringe needle; resulting in abnormal dispensing of volume (less frequent feeding). Undesired as this was, it demonstrates how depletion of the CE source affects bacterial metabolism, and therefore power output. In other words, it demonstrates the value of the automated maintenance, provided by EvoBot.

5.5 Phase IV - Evolutionary experiment

Substrate combination is one of the most important biological factors affecting MFC performance (Pant *et al.*, 2010). Microbes by nature are incredibly diverse in their metabolism - as they can produce enzymes, synthesise vitamins and amino acids based on the carbon energy source availability which allows a great variety of substrates to be used as carbon energy sources for electricity generation. This has resulted in the investigation of an exhaustive list of refined and unrefined substrates which have been reported in the literature throughout the years (Melhuish *et al.*, 2006; Pant *et al.*, 2010; Pandey *et al.*, 2016). However the effect that a combination of vastly different substrates can have in the MFC performance is yet to be explored fully (You *et al.*, 2015).

Taking this into account an experiment using 24 MFCs, the EvoBot robot and evolutionary algorithm (CMA-ES; covariance matrix adaptation evolution strategy) was used to identify the ideal proportionate combination of acetate, casein and urine using voltage readings as the main parameter for the algorithm to evolve the recipe. Acetate (carbohydrate) and casein (protein) are examples of two completely different chemically composed organic compounds with different molecular structures. The first derives from bacterial fermentation products while the latter from dairy products. Thus they were used as exemplars since acetate represents an accessible short-chain-sugar-based carbohydrate whereas casein represents a more complex long-chain-sugar-based protein. Urine on the other hand is chemically rich in substances favourable to the MFC microcosms as described below, thus was selected as a “control” for this study.

5.5.1 Specific Materials and Methods

Phase IV is a continuation of Phase III thus the same hardware, software and MFCs are used here as well. Below a more detailed description is given to the inoculation and carbon energy sources used as these are the crucial parameters of the experiment.

5.5.1.1 Inoculation and carbon energy sources

Activated sludge was used as the inoculum and the inoculation period lasted for four consecutive days after that the three different substrates were introduced to their respective MFCs.

5.5.1.1.1 Sodium Acetate

Sodium acetate anhydrous (1.3g/L) (Sigma Aldrich, UK) dissolved in deionized water was used for this experiment. Sodium acetate is the anhydrous, sodium salt form of acetic acid. The fact that sodium acetate only partially ionises when dissolved in water provides the solution with buffering properties, thus for this experiment the solution was buffered to pH 7 using 3mM PIPES buffer and sterilised using an autoclave. The experiment was conducted at room temperature (20 °C) where acetate is not subject to any other microbial conversions (i.e. methanogenesis) (Aelterman, 2009).

Acetate is a monomer, non-fermentable carboxylic acid and due to its molecular structure (short-chain carbohydrate) is easily utilisable. For this reason acetate has been widely used in MFC research since 2002 (Bond & Lovley, 2003). In their study Bond and Lovley found that current production by *Geobacter sulfurreducens* biofilms is directly related to the consumption of

acetate in batch mode fed systems and concluded that acetate can be used to induce electroactive bacteria.

5.5.1.1.2 Casein

Casein powder (1 g/L) was dissolved in 4mL of 1M NaOH before being mixed with the sterile prepared media of 3 mM PIPES buffer and deionized water. Casein is a complex polymer protein which is hydrolysed into monomers by bacteria. Casein usually is found in dairy wastewater effluents. Acetate and casein were standardised based on their COD values 1.5 ± 0.3 g/L.

A study using acetate and casein media for continuous flow MFC systems (You *et al.*, 2015) used a multivitamin and multi-mineral media for cultivating the MFCs. For the purpose of this study the media were not enriched with any other nutrients or vitamins as the purpose was to investigate solely the impact of the EvoBot “training” on the performance of the MFCs using a mixture of casein, acetate and urine as the only carbon sources.

5.5.1.1.3 Urine

Untreated human urine was used as the third carbon energy source for this experiment. Urine remained unbuffered throughout the experiment. Urine is the by-product of human and animal metabolism with an average daily excretion of 1.5-2.5 L per human (Ieropoulos *et al.*, 2013b). As a liquid mixture, urine is rich in different nutrients for bacterial utilisation, its normal chemical composition consists of organic and inorganic compounds (proteins, hormones, metabolites) as well as urea (9.3 g/L), uric acid (1.8 g/L) chloride (1.87 g/L), sodium (1.17 g/L), potassium (0.750 g/L) and creatine (0.670 g/L). A more extensive list of urine non-mineral composition can be found in Ieropoulos *et al.*, 2012. The direct conversion of urine into electricity was firstly

reported in 2012 (Ieropoulos, Greenman and Melhuish, 2012) and since then it has been used widely around the world in MFC research.

5.5.2 Results and discussion

5.5.2.1 Inoculation and adaptation period

On the first day of inoculation once the MFCs OCV stabilised, $R_{ext.}$ of 1 k Ω was applied to all 24 cells, initiating the power output generation. In less than two hours the recorded OCV was around 400 \pm 50 mV as shown in **Figure 5.13**. This figure shows the open circuit voltage of all the 24 MFCs used for this experiment. Once the inoculum was added to the cells, voltage (potential difference) was observed, and all the cell's voltage followed the same trajectory.

After the inoculation, the adaptation period took place. During the adaptation period, Group A (MFC 1-9) were slowly switched from acetate to casein, and Group B (MFC 10-18) from casein to acetate, as shown in the table below (**Table 4**). Group C (MFC 19-24) on the other hand were fed throughout with fresh neat urine. The results of the adaptation period are presented below in **Figure 5.14**. As voltage was the dictating factor for the algorithm to evolve, the results in this section, unlike before, are reported in voltage rather than power.

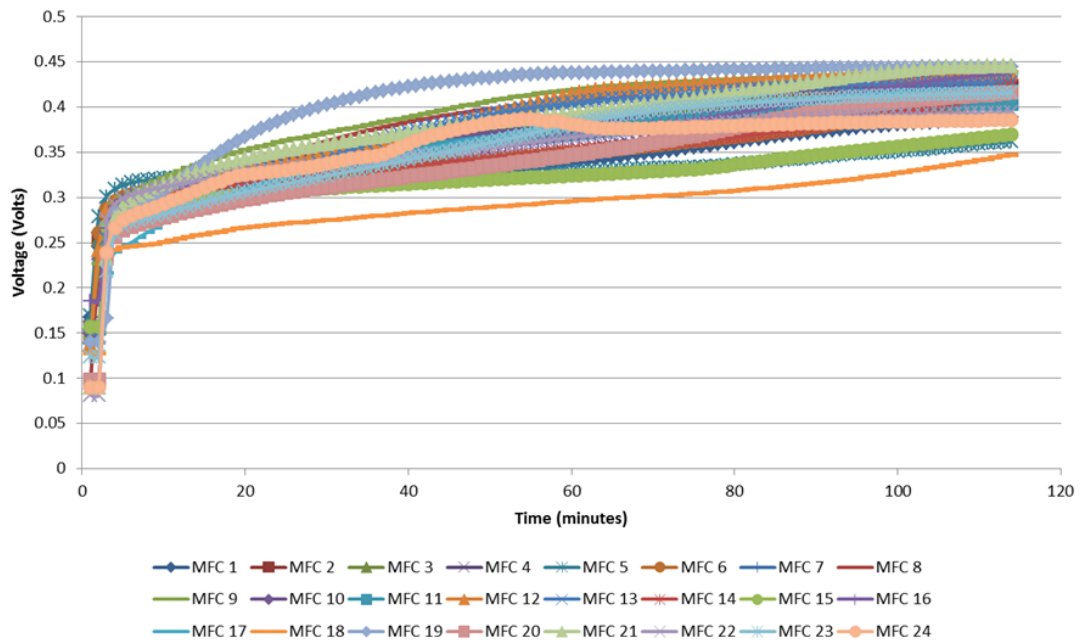


Figure 5.13 – OCV of 24 individually fed MFCs inoculated by EvoBot with activated sludge.

Group A – Acetate Matured MFCs	Group B – Casein Matured MFCs
100% Acetate	100% Casein
90% Acetate - 10% Casein	90% Casein – 10% Acetate
80% Acetate - 20% Casein	80% Casein – 20% Acetate
70% Acetate - 30% Casein	70% Casein – 30% Acetate
60% Acetate - 40% Casein	60% Casein – 40% Acetate
50% Acetate - 50% Casein	50% Casein – 50% Acetate
40% Acetate - 60% Casein	40% Casein – 60% Acetate
30% Acetate - 70% Casein	30% Casein – 70% Acetate
20% Acetate - 80% Casein	20% Casein – 80% Acetate
10% Acetate - 90% Casein	10% Casein – 90% Acetate
100% Casein	100% Acetate

Table 4 Adaptation period feeding schedule for MFCs on Group A and B.

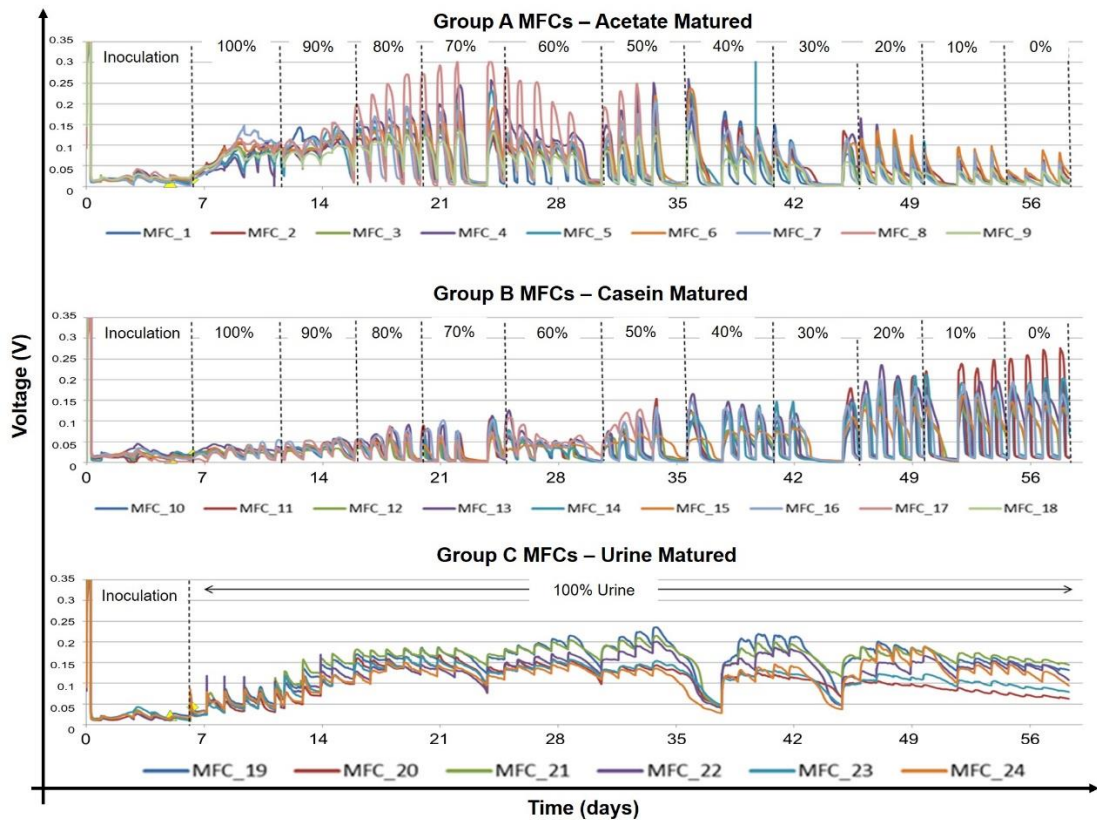


Figure 5.14 – Temporal voltage output of the three groups of MFCs during the adaptation period.

The performance is displayed in voltage under $1\text{k}\Omega$ resistance. Each region is annotated with the recipe fed at that time. HRT for each feeding was 24hrs.

These data demonstrate that the acetate group, which gradually switched to casein, performed best when fed with a substrate combination of 70% acetate and 30% casein. Based on the trend of the graph (Group A) it is apparent that when more casein is added to the system the voltage drops. This is the same when looking at the casein-maturing group (Group B) as when more acetate is added to the system the voltage increases, reaching a peak when fed with 100% acetate. At the same time the urine matured group

(Group C) shows an overall steady voltage output. The adaptation period lasted 60 days and after that the MFCs were left to starve and dropped to 0 ± 5 mV before the next experiment (evolutionary algorithm) was initiated.

5.5.2.2 Evolutionary algorithm

The evolutionary algorithm selected different amounts of the three previously used media and tested them in triplicate MFCs. As the voltage levels of the MFCs vary, it is not possible to use the voltage of the MFCs as a direct fitness. In order to address this issue, the evolutionary algorithm tested all the MFCs with a recipe of 1/3 casein, 1/3 acetate and 1/3 urine at start-up. This base voltage level was stored during the whole experiment and used to normalise the voltages of the MFCs. Therefore, the effects of the different recipes can be compared even if they were tested in MFCs with different power output levels.

The evaluation of the whole population was carried out in parallel. For each generation, 8 different recipes were prepared in each of the beakers located on the EvoBot arena. The dispensing module prepared the recipes and then the syringe module picked up the liquid mixture and dispensed it in each triplicate. The routine was as follows:

- MFCs 1-9 were fed from beakers A, B and C.
- MFCs 10-18 were fed from beakers D, E and F.
- MFCs 19-24 were fed from beakers G and H.

Then, the evaluation phase started and the voltages for all the MFCs were sampled every minute for 4 hours. After this time, the fitness of each recipe was calculated and a new population of recipes was created. The details of this evolution are specified in **Appendix A.1**.

The evolutionary algorithm ran for two consecutive days and 12 generations were created and tested on the MFCs. The graph of the evolution is shown in **Figure 5.15**. The best fitness improves until generation four, and after that decreases, while the median improves slightly. From the recipe combinations tested in this experiment, it is evident that there is not a strong effect on the voltage output caused by the evolutionary generated recipe. However, this can be attributed to the fact that individual slight changes in the recipe produced only minor variations in the voltage output. From the data, it is suggested that more dramatic changes in the recipes would have resulted in bigger response changes to the MFC output, and improved fitness.

In addition to the recipe effect, it appeared that the MFCs themselves (where each recipe was tested) had more influence than the actual recipes, in the overall fitness evolution. As can be seen in the evolution graph (**Figure 5.15**), the MFCs 16-18 and MFCs 1-3 perform best most of the time, while MFCs 7-9 and 19-21 are suboptimal across most generations. While the MFCs matured using three different organic materials, triplicates of each group are more powerful than others. This can be explained by the fact that before the final genetic algorithm (GA) experiment other small duration GA experiments took place with the same MFCs (data not shown). These small experiments helped solve some system glitches and optimise the algorithm at the same time. An example of a prior GA experiment is one that used the power output as the determining factor for improving the algorithm, however the fact that each triplicate had different outputs resulted in false data and an incorrectly evolved algorithm. Even though all these previous algorithm trials gave us all the necessary understanding of how the MFC systems react to the evolutionary experiments and help to develop the final one, the feedings had an effect on the MFC outputs resulting in some triplicates performing better than the others.

Finally, it is worth noting that all the MFCs got fitness higher than one in the Generation 0. This could be explained because the base voltage did not reach a steady state before the start of the experiment. If time had been permitting the MFCs would have been fed a few times with the 33% media before the evolutionary algorithm started, in order to provide a more stable starting point.

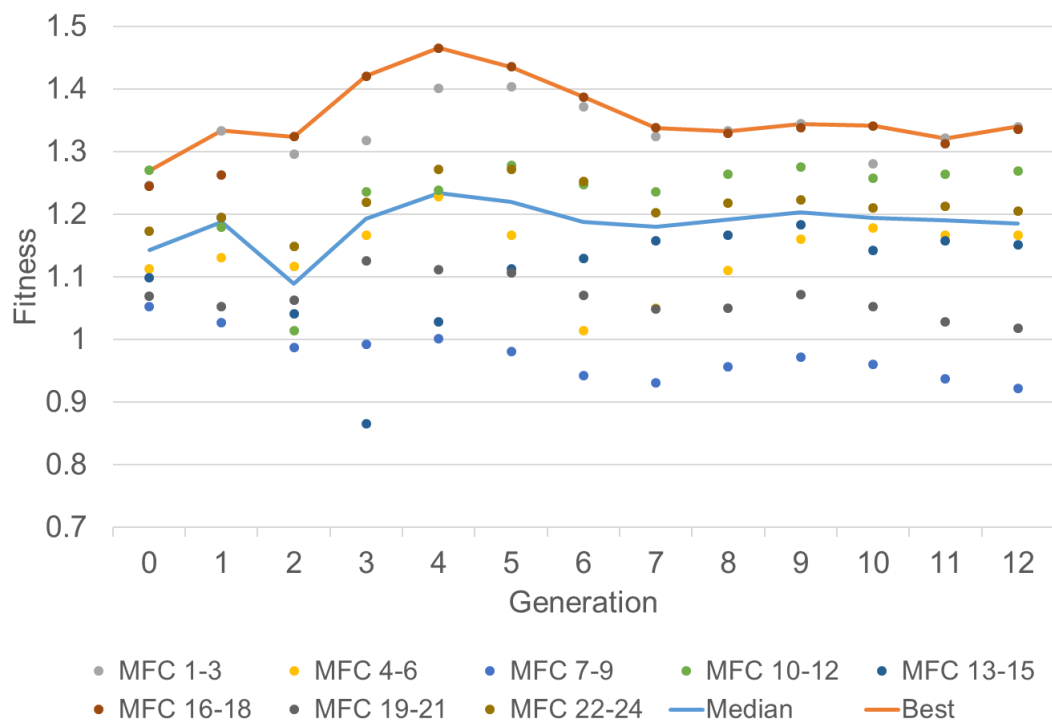


Figure 5.15 – Fitness evolution over each generation

As previously mentioned, initially the algorithm started by feeding all the cells with 1/3 (33%) of each media to set a reference point for calculating the change in voltage that each new recipe caused. Then the algorithm started to generate random combinations. However after Generation 4 it is observed (**Figure 5.16**) that the algorithm started using higher amounts of urine (as

expected) but also unexpectedly it used higher amounts of casein than acetate in the mixtures. From Generation 4 until Generation 7 the amounts of acetate fluctuated from 0-20% however after G7 the algorithm increased to 10-30%. This shows that by the end of the experimental period the algorithm, as anticipated, became more specific in the choice of substrates and the ratios between urine, acetate and casein.

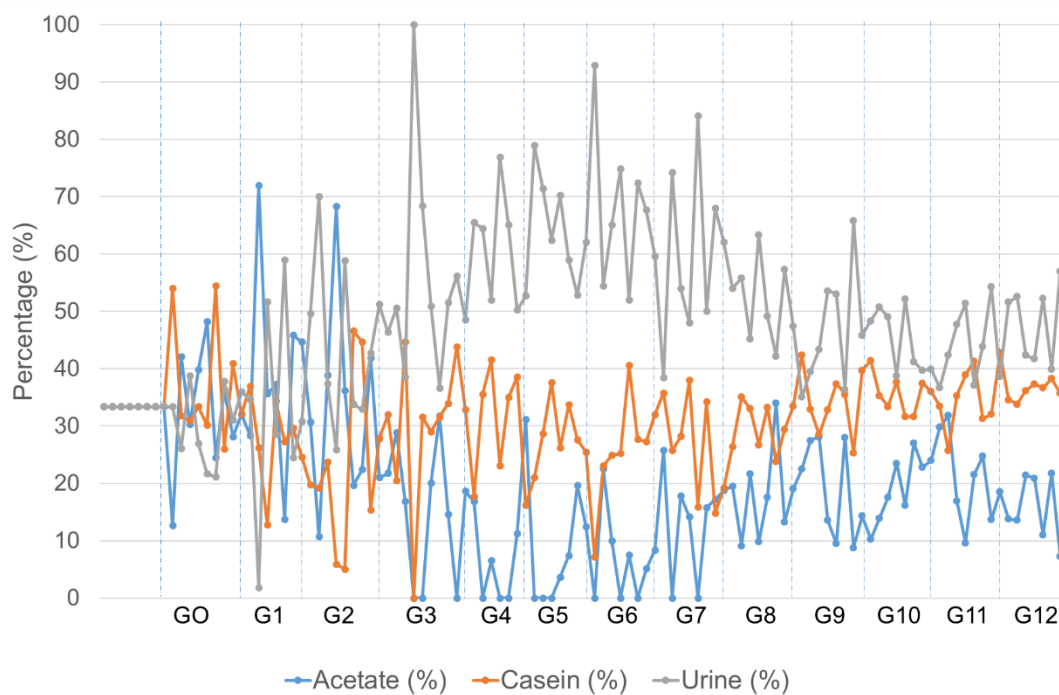


Figure 5.16 – Percentages of each feedstock per generation based on the algorithm recipes.

For each generation there were 8 different recipes (recipe per beaker) which then was tested on 8 different triplicates.

The resulted voltage output of each triplicate from Group A, B and C, to the tested recipes is clearly presented in **Figure 5.17**, **Figure 5.18** and **Figure 5.19** respectively. From Group A the MFCs that had consistent voltage out-

put throughout the two week period were MFC 1-3. Overall however all the MFCs of Group A had on average a voltage output of 60-80 mV. Based on the graph (**Figure 5.17**) it is concluded that none of the evolutionary produced recipes caused a noticeable improvement in output. Apart from the reasons discussed above, this can be attributed to the short testing period between each generation (24 hours). It is hypothesised that a longer intermit period between each generation could have allowed all the carbon energy available in the anode to be metabolised resulting in a clearer output profile once the new recipes were introduced. The results presented below provide a closer look at the voltage output in alignment with the feeding composition during each generation.

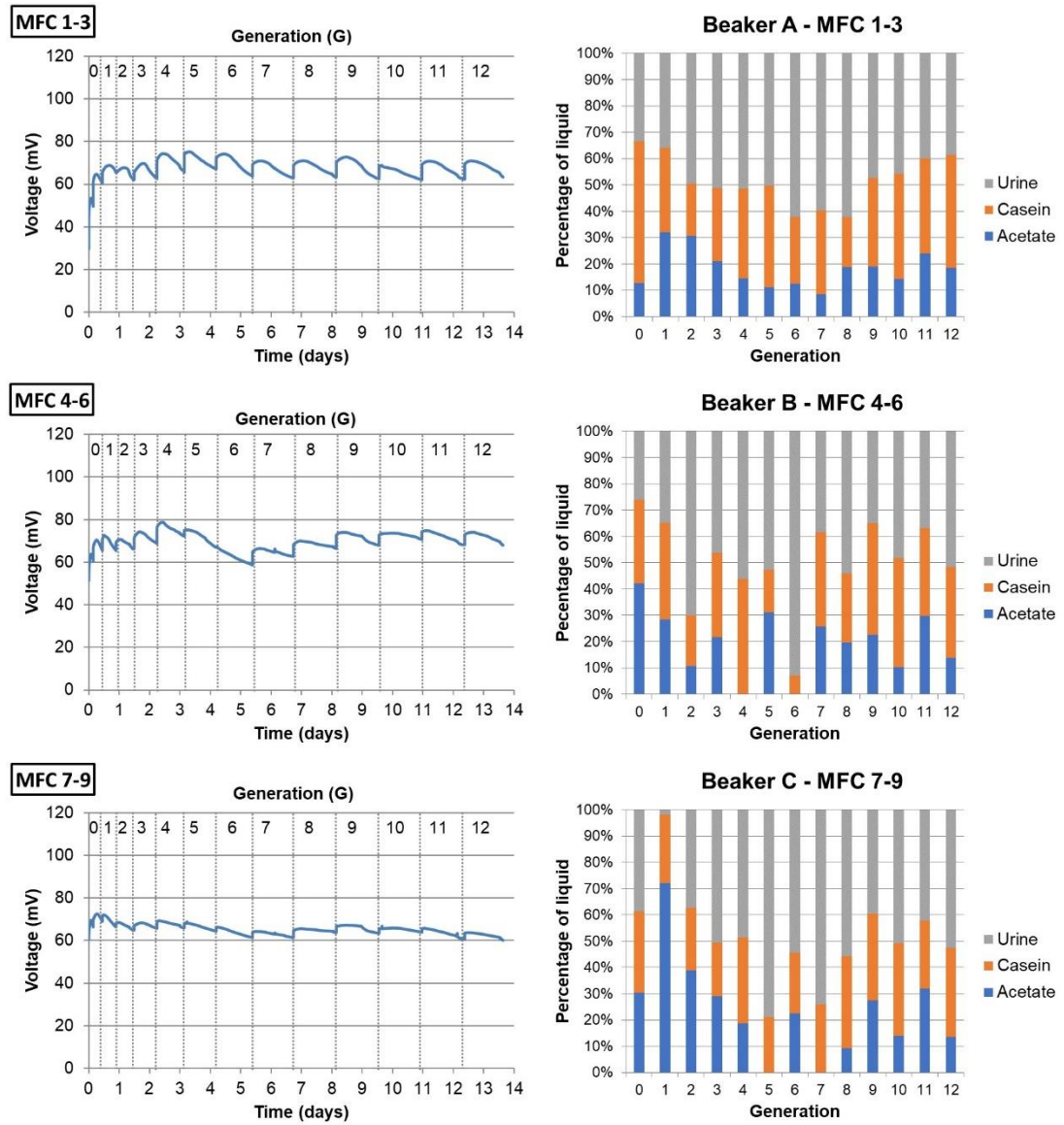


Figure 5.17 – Average (n=3) temporal voltage output of Group A MFCs as they responded to each generation recipe.

Compared to Group A, Group B MFCs had in overall a slightly higher output (75±5 mV) which can be attributed to the fact that since they were matured on casein they were able to oxidise casein easier than Group A.

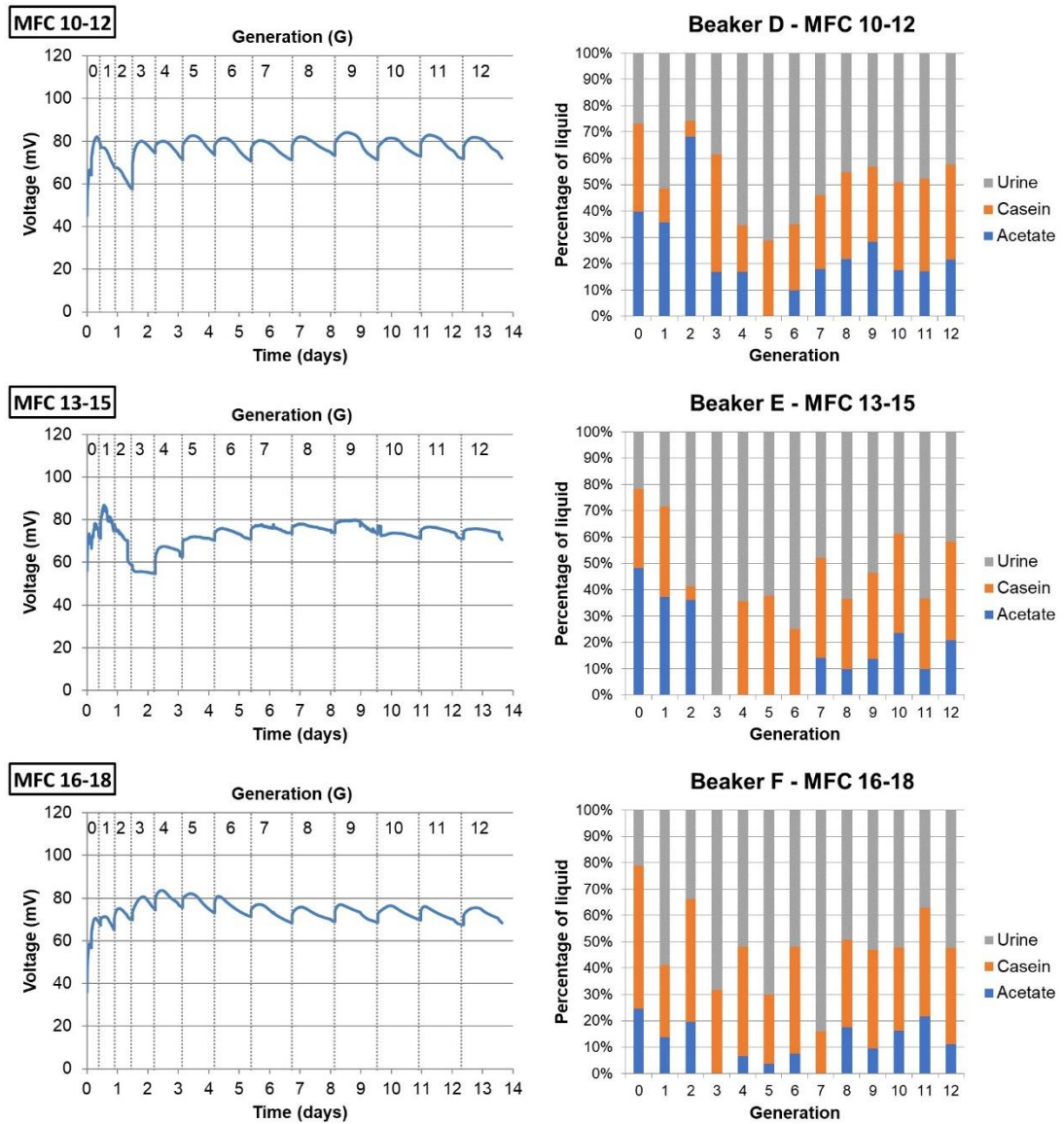


Figure 5.18 – Average (n=3) temporal voltage output of Group B MFCs as they responded to each generation recipe.

The above hypothesis can be confirmed based on the results of Group C. The urine matured MFCs were the least performing since they were only “trained” on that specific substrate; as the microbes were unable to oxidise

casein in that short timeframe. For MFCs 22-24, higher voltage outputs were observed (~60 mV) when higher percentages of urine and acetate were used in each recipe,

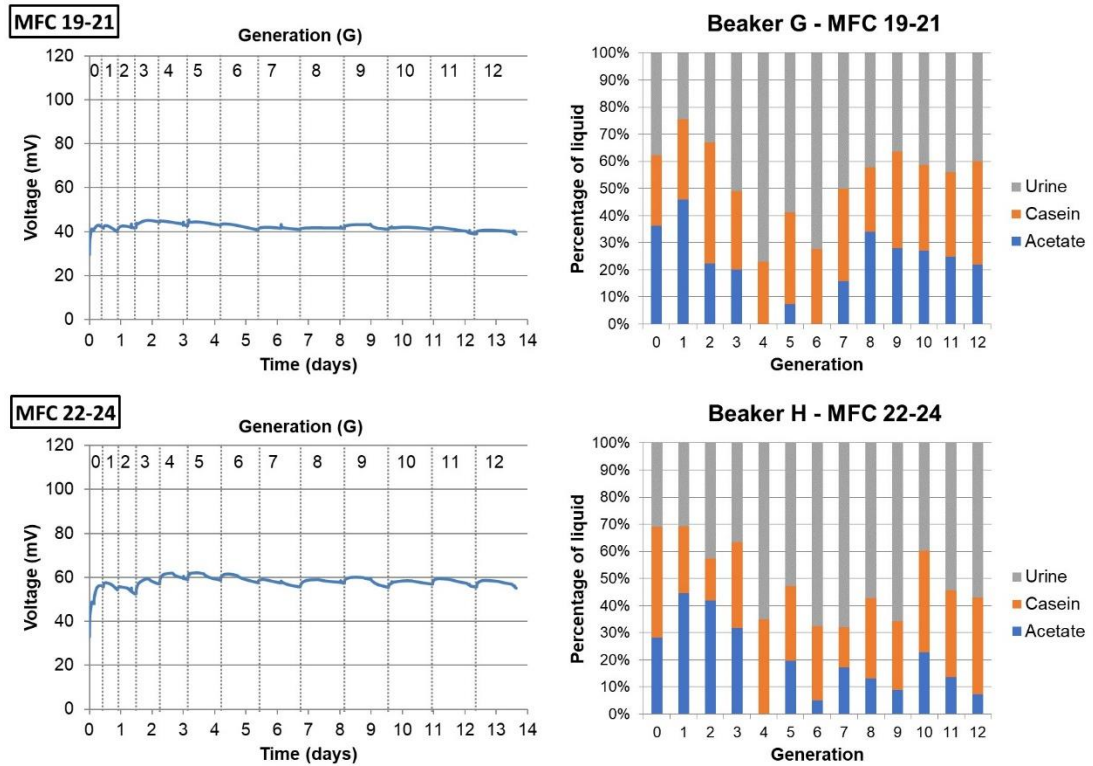


Figure 5.19 – Average (n=3) temporal voltage output of Group C MFCs as they responded to each generation recipe.

This experiment used evolutionary algorithm to try and identify the best available combination of acetate (carbohydrate), protein (casein) and urine in improving the MFC performance. This experiment did not succeed in optimising the feedstock and ultimately producing a fuel consisting that gives high voltage output. Nevertheless, it showed for the first time the interaction between evolutionary algorithms and robotic system in assisting MFCs resulting in novel observations about automated feeding regimes and power output

responses. Also the evolutionary process itself provides an excellent stepping stone for future research, as now, through this experiment it has been proven possible to combine microbiological evolution/adaptation to computational evolution using genetic algorithms and MFCs.

Moreover the results obtained by this experiment are interesting and novel as it demonstrated that although casein alone is not a good substrate for MFCs due to its complex structure, in the majority of cases, the algorithm chose casein over acetate. These results showed that using a combination of carbon energy sources created via evolutionary algorithms can be a viable way to create alternative complex media for bacterial growth (i.e supplemented with minerals and vitamins). This experiment has the potential to be developed further by including more parameters in terms of substrates and allow the algorithm to run for longer periods of time, if the hardware allows.

5.6 Phase V - EcoBot-II behavioural experiments powered by the EvoBot-matured MFCs

One of the main aims of this PhD study, as defined earlier (2.3) was to improve the MFC performance through the interaction with the robot via the feedback loop, so that the optimised MFCs can be trialled on-board low power robots to provide autonomy. By establishing this interaction in the previous Phases (I-IV), Phase V moved into applying this to practice and testing the EvoBot derived MFCs on the EcoBot-II robot.

To demonstrate this, two parallel experiments were performed; on the one hand a group of MFCs was inoculated and maintained using the EvoBot, while on the other hand, another group was inoculated and maintained man-

ually. These two experiments were set-up using 8 MFCs, which were intended to provide power on-board EcoBot-II. Behavioural experiments (i.e. using MFCs on robots to perform tasks) were then performed comparable to the original EcoBot-II experiments undertaken in 2004-2006 (Ieropoulos *et al.*, 2005; Melhuish *et al.*, 2006; Ieropoulos *et al.*, 2009).

To provide adequate information on EcoBot-II and the small-scale MFCs, existing data from the literature will be compared against the robot maintained MFCs. The original EcoBot-II (2006 ed.) used the analytical type MFCs (25mL), carbon veil as the anode electrode and hydrated carbon veil as the cathode. The average peak power outputs of these type of MFCs reported in the literature using acetate as the carbon energy source produced 24.9 μW and 42.8 μW when fed 0.1% prawn exoskeleton (Melhuish *et al.*, 2006). In the same publication, fly-fed MFCs with open-to-air cathode produced a current output of 70 μA . The periodically hydrated MFCs had an open circuit potential of 450 mV and an average current of 45 μA (Ieropoulos *et al.*, 2007). Small-scale MFCs have been used in the past also, using three different types of membranes, cation exchange membrane and Hyflon® ion membranes in two different thicknesses 3 and 10 μm (Ieropoulos *et al.* 2010). The average results are presented below (**Table 5**). Similar small scale architecture MFCs with carbon black micro-porous layer (MPL) cathode electrodes have also been reported in the literature (Papaharalabos *et al.* 2013). The temporal profile of these MFCs showed a voltage output of 325 mV under 2.7 k Ω (4.3 mW/m²). The power and polarisation curves of these improved MFCs showed maximum power transfer (MPT) point at 95 μW (10.6 mW/m²) and starting open circuit voltage at around 550 mV (Papaharalabos *et al.* 2013).

Ion selective membrane	Mean Voltage (mV)	Mean Current (μ A)	Mean Power (μ W)
Cation Exchange Membrane	61,24	61,27	3,77
E87-03 Hyflon (3 μ m)	93,55	93,64	8,76
E87-10 Hyflon (10 μ m)	74,35	74,42	5,53

Table 5 Average (n=3) comparative data from the membrane investigations on small-scale (6,25 mL) MFCs as presented in Ieropoulos *et al.*, 2010.

5.6.1 Specific Materials and Methods

For this line of experiments the MFCs were slightly modified as shown in **Figure 5.20**. For the anode a carbon fibre veil with an initial carbon loading of 20 g/m² was used for all 16 MFCs with a surface area of 67.5 cm². However unlike in previous experiments the active area of the carbon veil was coated with a mixture of nano-sized carbon black particles (Vulcan XC-72R) (Cabot Corporation, Stanlow, UK) and isopropanol. This resulted in decreasing the electrode's resistance as shown in **Figure 5.21**. Coating was carried out using the dipping/drying technique using ethanol dispersion as described in the literature (Zheng *et al.*, 2015b), with this technique an average carbon loading of 5.5 \pm 0.5 mg/cm² was achieved. The binder used was 5% polyvinyl alcohol (7 μ l per mg of mixture) (Cheng, Liu and Logan, 2006) which was mixed with the suspension. Following the coating, the electrodes were heat treated at 190 °C for 1 hour, and then were folded down and placed inside the anode chamber. As a separator custom made ceramic membranes were produced using the same technique described in **3.2.2**. The membrane surface area was 12 cm² and the thickness averaged 3 mm. The cathodes used in this experiment were the AC/SS (**3.1.2.2**).

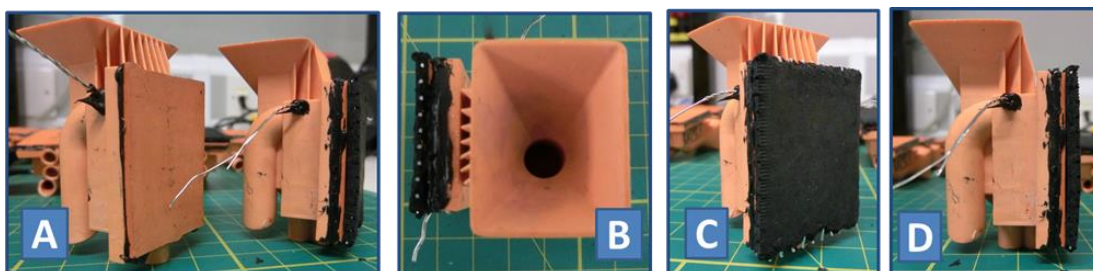


Figure 5.20 – Modified small-scale MFCs (2018 ed.)

[A] Anode and cathode compartment was separated by a custom made ceramic membrane connected directly to the cathode electrode. **[B]** Anode funnel shaped inlet **[C]** The cathode electrode was supported by a SS-mesh which formed the current collector as well **[D]** Side view of the MFC showing the anode and cathode part as well as the anode outlet.

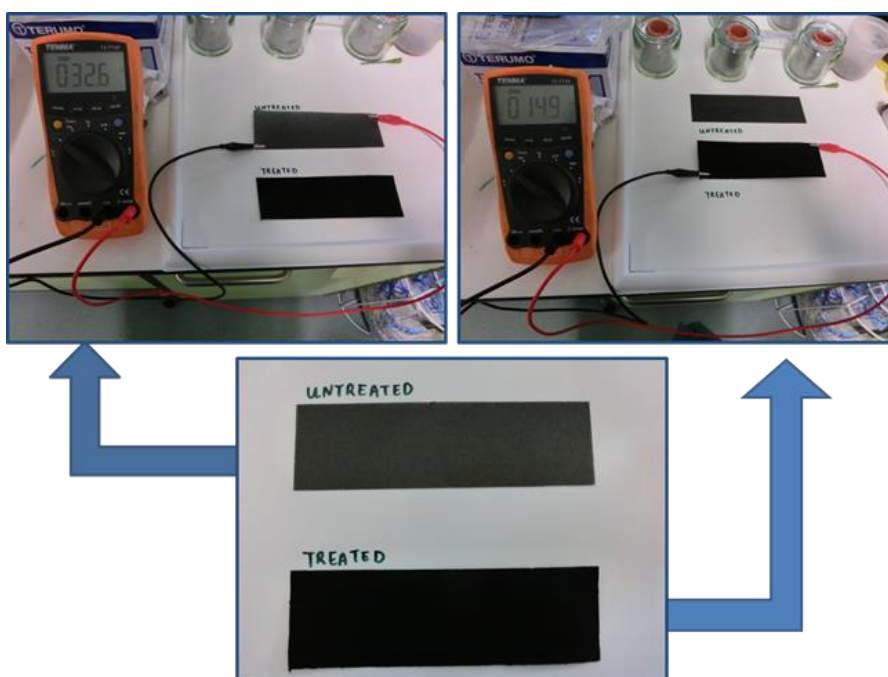


Figure 5.21 – Treated and untreated carbon veil electrode and their resistance.

The treated electrode with the carbon nanoparticles was more conductive than the untreated one, resulting in lower resistance (half compared to the untreated) as the surface area has increased dramatically. The resistance of the folded electrode was on average 1.5 – 1.8 Ω compared to 3.8 Ω for the untreated electrode (picture not shown).

5.6.2 Results and discussion

5.6.2.1 Inoculation period

For the sake of comparison the 16 MFCs on EvoBot arena and bench experiment were inoculated using activated sludge enriched with 25 g/L of nutrient broth as previously reported in the original EcoBot-II publication (Melhuish *et al.*, 2006). As the feedback loop is triggered by the MFC voltage reading, the threshold was set to 400 mV to initiate the inoculation process. Since all the abiotic MFCs were below the specified threshold (below 0 mV) the robot fed all the MFCs in the first run. The feedback loop was running every hour checking for underperforming MFCs that were subsequently fed if they were below the threshold. Once the MFCs stabilised above 400 mV the threshold was increased to 500mV which triggered another round of inoculation and the voltage output of the MFCs increased accordingly as is shown in **Figure 5.22**. To have comparable conditions for the bench experiment the MFCs on the bench were re-inoculated as well, as indicated by the arrow on the same graph. The voltage results demonstrate nicely the value of changing the voltage threshold using the EVOBLISS software in improving the voltage output of the MFCs, even at open circuit conditions. As indicated from the results the MFCs inoculated by the robot had open circuit potentials around 550-600 mV whereas the MFCs maintained manually had an average OCV of 450-500 mV.

For unexpected reasons during the process of the experiment the Arduino board short-circuited and was not functioning which meant the experiment had to pause for repairing purposes, during the offline period a third re-inoculation took place manually (data not shown).

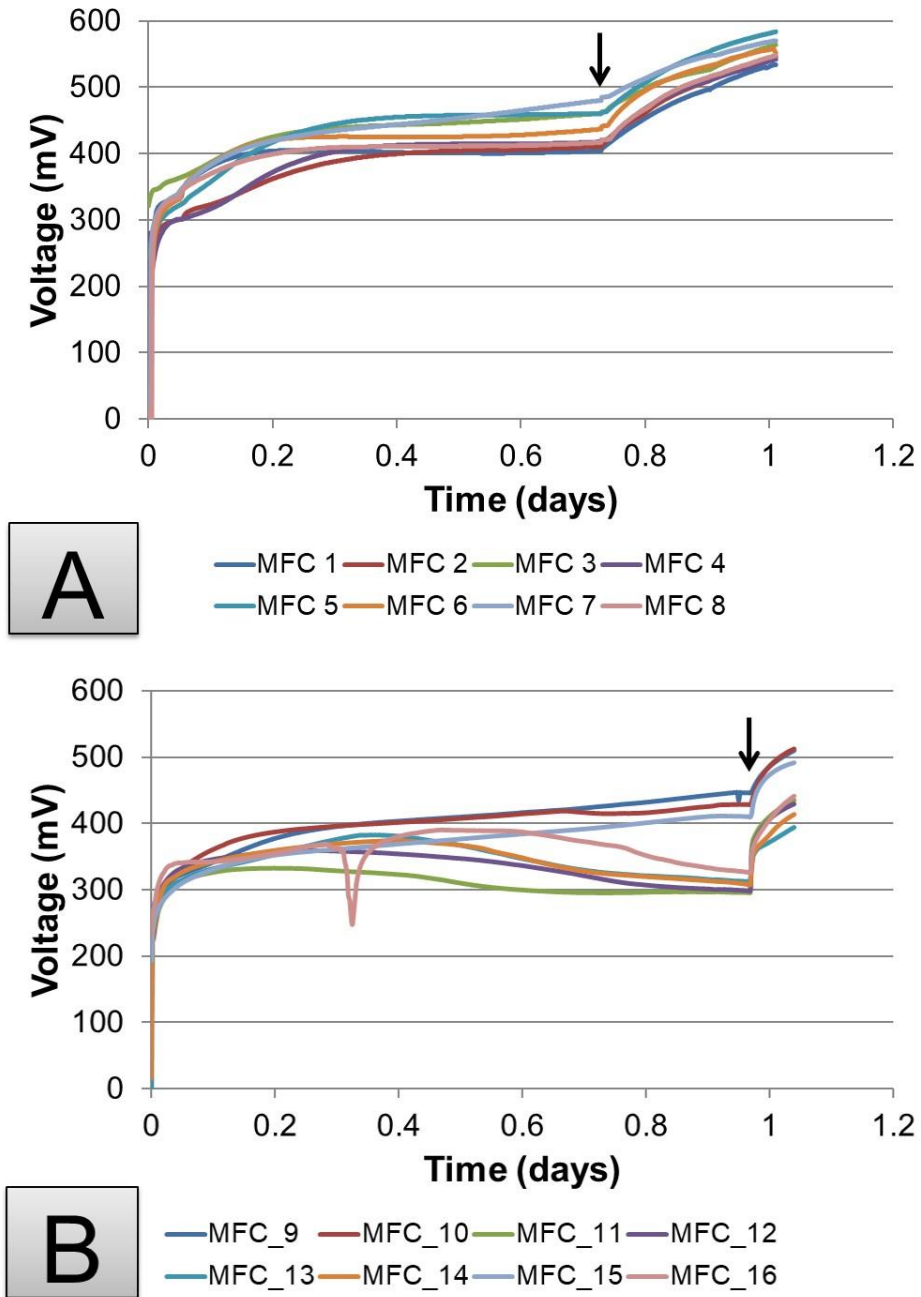


Figure 5.22 – OCV voltage from [A] the 8 MFCs plugged on EvoBot compared to [B] the ones on the bench.

Once all the MFCs stabilised above 400mV the threshold changed to 500 mV as it is indicated by the arrow.

5.6.2.2 Continuous voltage output and polarisation

As described previously the EvoBot was maintaining the MFCs by using the voltage output as the threshold triggering the feeding mechanisms. Thus unlike previous chapters, here the data on the graphs will be presented in voltage rather than power, to aid the discussion. **Figure 5.24** illustrates the benefit of EvoBot threshold reaction as a mean of improving the MFC output. In the sections D, E and F it is demonstrated that by sweeping the threshold value in the software and forcing the robot to feed the MFCs until that threshold is reached, the MFC performance increases incrementally. In section D the threshold was set to 400 mV and subsequently the MFCs were maintained at an average voltage level of 480 mV. Increasing the threshold by 50 mV resulted in an average performance of 500mV (**Figure 5.24E**) and by increasing that again by 50 mV the MFCs reached an average output of 535 mV. This is the exact novelty of such an apparatus as the EvoBot platform via the feedback loop is inoculating and maintaining the MFCs until maturity that in a sense is evolving (i.e. optimising) them based on energy abstraction as the main selective pressure. It is noteworthy that such MFCs usually take between two weeks to couple of months, to reach that level of maturity using batch or continuous feeding modes. However, in this case the MFCs were able to reach maturity within 5 days of operation and on the 6th day they were connected onboard EcoBot-II to power the robot. When first plugged into EcoBot-II the MFCs were able to charge the capacitors every 1.04 minutes. This is a considerable improvement compared to the old EcoBot-II (2006 ed.) which were 4 times bigger in volume and electrode surface area and were using chemical cathodes (FeCn). In this study they were fed with flies and were able to charge the capacitors every 14 minutes (Ieropoulos *et al.*, 2009). For an empirical comparison the 2006 ed. EcoBot-II

was able to move 20 cm in 40 mins compared to the 2018 ed. EcoBot-II which covered the same region in less than 14 minutes. Photographs of EcoBot-II 2018 ed., can be found in **Appendix A.2** of this thesis.

In terms of current output (data not shown) the MFCs had an average initial current output of 125 μA which increased to 200 μA within just 6 days. This is 2.5 times higher output than the average current reported in Melhuish *et al.* (2006) after 4 weeks of experimentation. The presented data confirm that by increasing the voltage threshold on the EvoBot program it improves the power performance of the MFCs in a fraction of the time that they would have otherwise taken. To validate further these findings the data of the manually fed parallel experiment are presented below **Figure 5.23**.

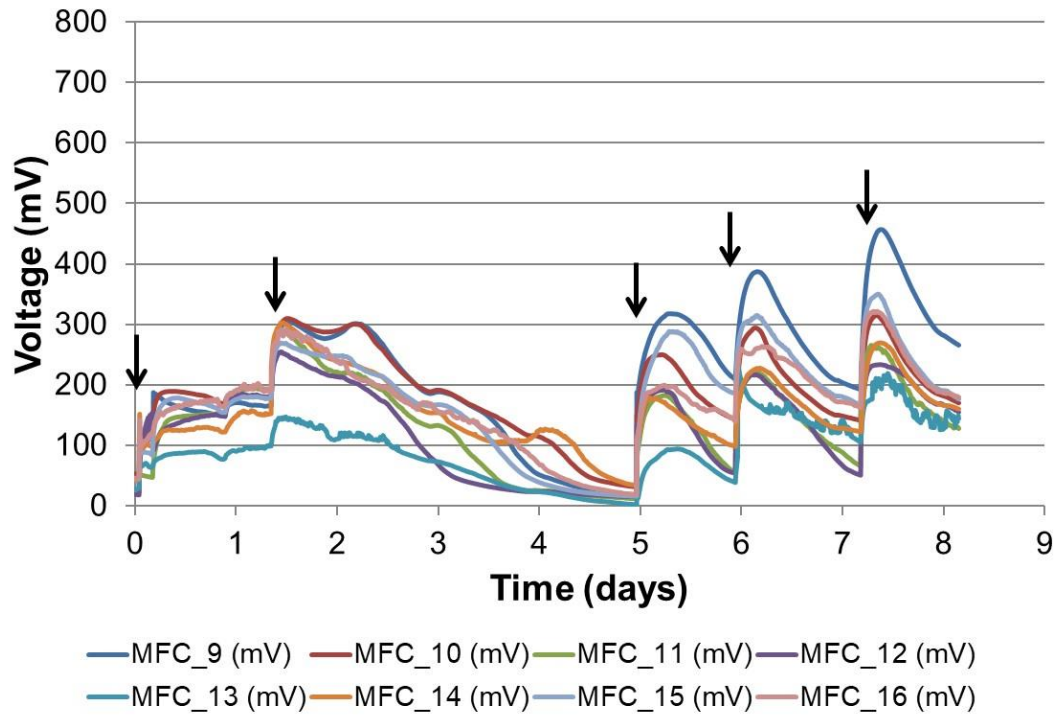


Figure 5.23 - Temporal voltage behaviour of the MFCs maintained manually and fed once a day (batch-mode feeding).

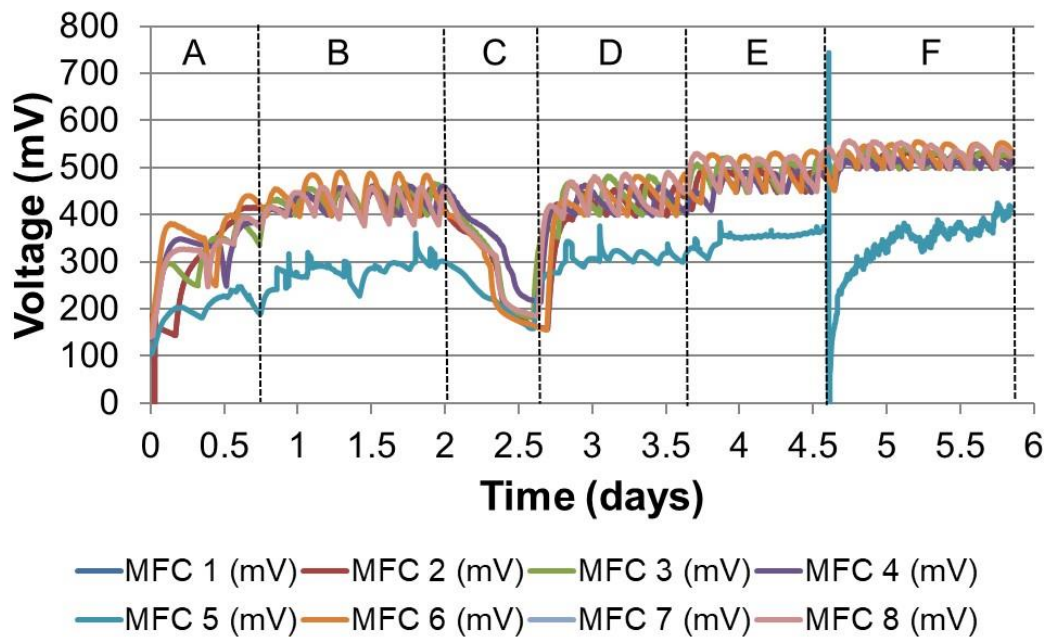


Figure 5.24 – Temporal voltage behaviour of the MFCs maintained by the EvoBot robot and based on different threshold values under 2.7 k Ω load.

[A] Feedback loop running every 4 hrs – Threshold 250 mV **[B]** Feedback loop running every 4 hrs – Threshold 400 mV **[C]** Loop was running but urine bottle was empty during weekend **[D]** Urine bottle replaced – Threshold 400 mV. **[E]** Feedback loop running every 4 hrs – Threshold 450 mV **[F]** Feedback loop running every 1 hr – Threshold 500 mV.

Out of the 8 MFCs one was underperforming and did not follow the same trend as the others (MFC 5), the MFC was removed, examined and reattached. Even though the robot managed to improve its performance and recover it, it was still not up to the standards of the others.

The manually maintained MFCs against the EvoBot maintained MFCs, differ not only in terms of output but also in terms of consistency. The data on **Figure 5.24** show an almost identical voltage output from the tested MFCs, which is not present on the manually batch-fed MFCs. This shows the superiority of an automatic maintenance system in producing MFCs that can have reproducible results and high power output levels.

The power output levels of each group of MFCs can be seen more clearly from the polarisation analysis results presented in **Figure 5.26**. EvoBot matured MFCs had an overall higher MPT point reaching on average $\sim 180 \mu\text{W}$ whereas the batch-fed MFCs had a MPT that was $50 \mu\text{W}$ lower. Additionally the robot maintained MFCs had almost double the current output compared to their bench controls and almost 200 mV higher OCV.

As mentioned earlier (**5.1.2**), this experiment aimed to investigate the impact of the EvoBot automated feeding process against the conventional manual batch feeding process not in terms of output levels of the MFCs but also in terms of the length of the maturing period. For the sake of empirical comparison the manually fed MFCs kept running for more than a month in order to observe if they would achieve the same levels of performance ($500\text{-}525 \text{ mV}$) as the EvoBot-matured ones achieve, in just 6 days. This, as can be seen in **Figure 5.25**, was not able to be achieved from the manually maintained MFCs even after a month of operation. This shows the superiority of the EvoBot-maturing process against the widely used batch feeding process for cultivating optimised MFCs for higher power production at a fraction of the time.

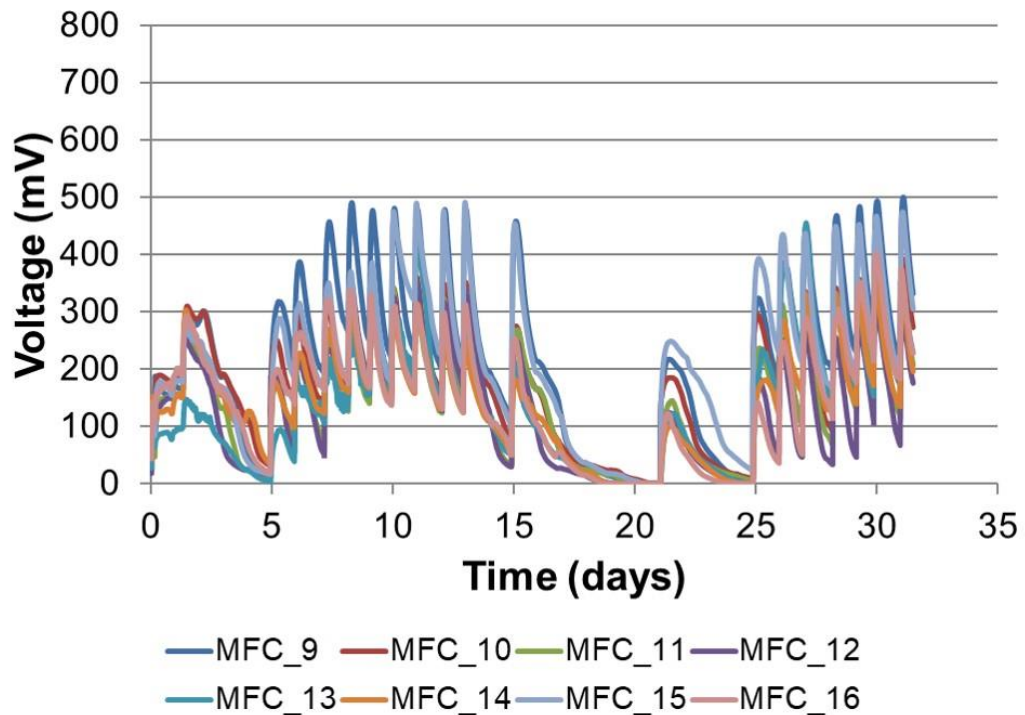


Figure 5.25 – Long-term temporal voltage behaviour of the manually maintained MFCs.

To bring the data into context with the existing literature mentioned above, a summarised graph was created (**Figure 5.27**). Based on the 2006 data the batch-fed MFCs that powered EcoBot-II had a power output of 0.09 mW/m^2 which is 220 times lower than the batch-fed MFCs used for this comparative experiment (2018 edition). This demonstrates that the advancement in materials over the 12 years is the sole factor attributed to this improvement in performance. This highlights the progress made in MFC research in terms of materials and their crucial impact in MFC performance. Lastly, since all 16 MFCs created for this comparative study between EvoBot and control (bench) were identical, having only the way of maintenance/feeding differing, their difference in performance (7.4 mW/m^2) can only be attributed to Evo-

Bot's feedback loop feeding system. Hence this experiment demonstrated the equal importance of core MFC materials and automated feeding pulses dictated by the voltage output, in maximising the overall power output of MFCs.

Microbial fuel cell technology provides a sustainable alternative to chemical batteries. However, in order to make this technology as stable as possible, all of its core components need to be optimised in order to minimise any unnecessary energy losses that will lower even further its power capabilities. This thesis through the experimentation presented in **Chapter 4**, tackled this issue. This off-robot investigation proved that electrode materials based on alginate and carbon as well as membrane materials based on clay improved the power output of MFCs. These advancements were then applied on MFCs that were trialled on the EvoBot workstation. Hence, the experiments presented above (**Chapter 5**) tie together the two main lines of work described in this thesis. The MFCs with improved materials were fed on-demand by the robot showing that automated feeding pulses improves the power output even further (**Chapter 5**). MFC research at the moment focuses only on improving one element of MFC at a time. The work presented in **Chapter 4 and 5** shows that this thesis took a rounded approach in optimising the technology using a robotic workstation as its main tool. This is something that was never tried before and forms the novelty of this thesis.

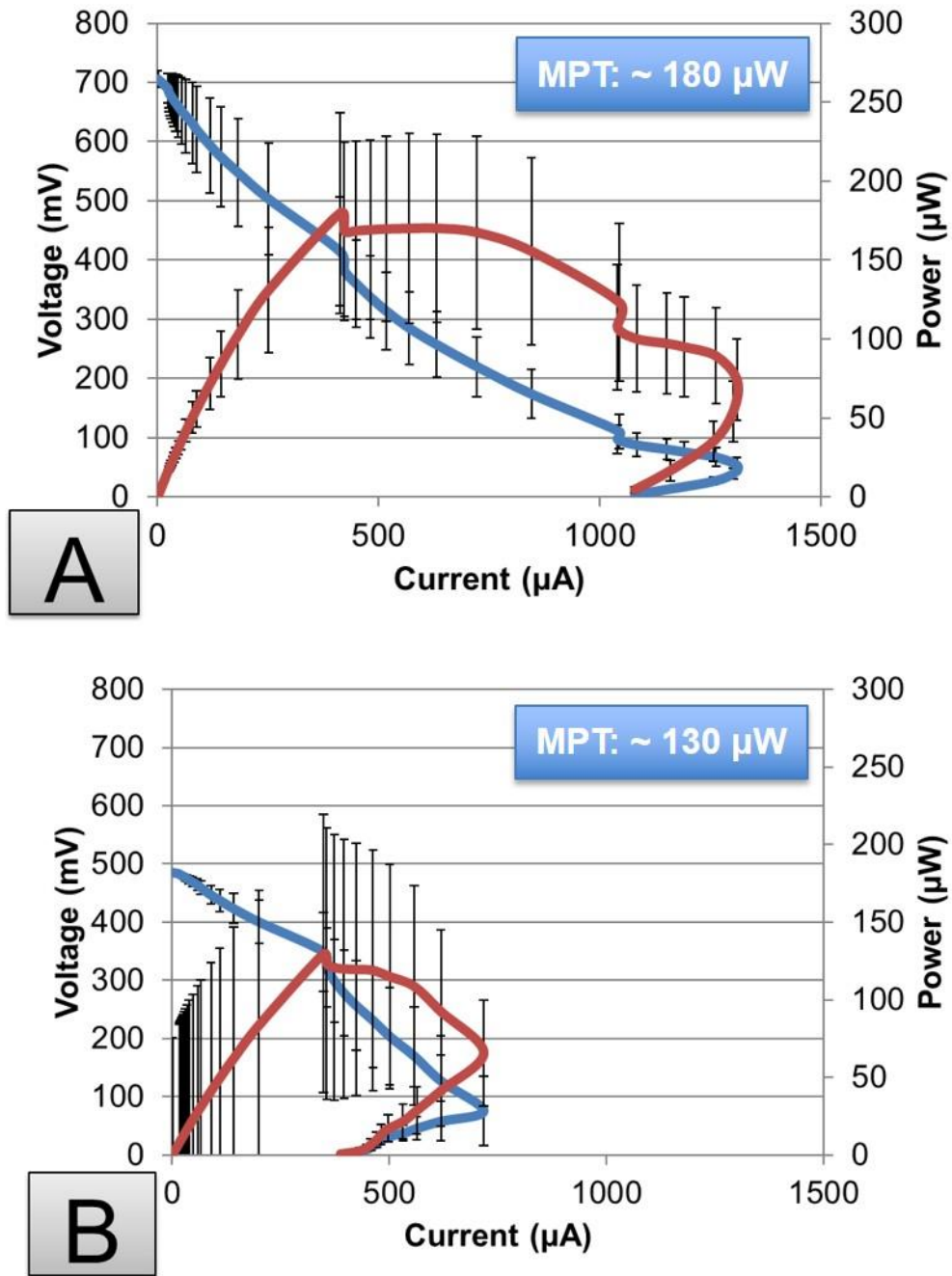
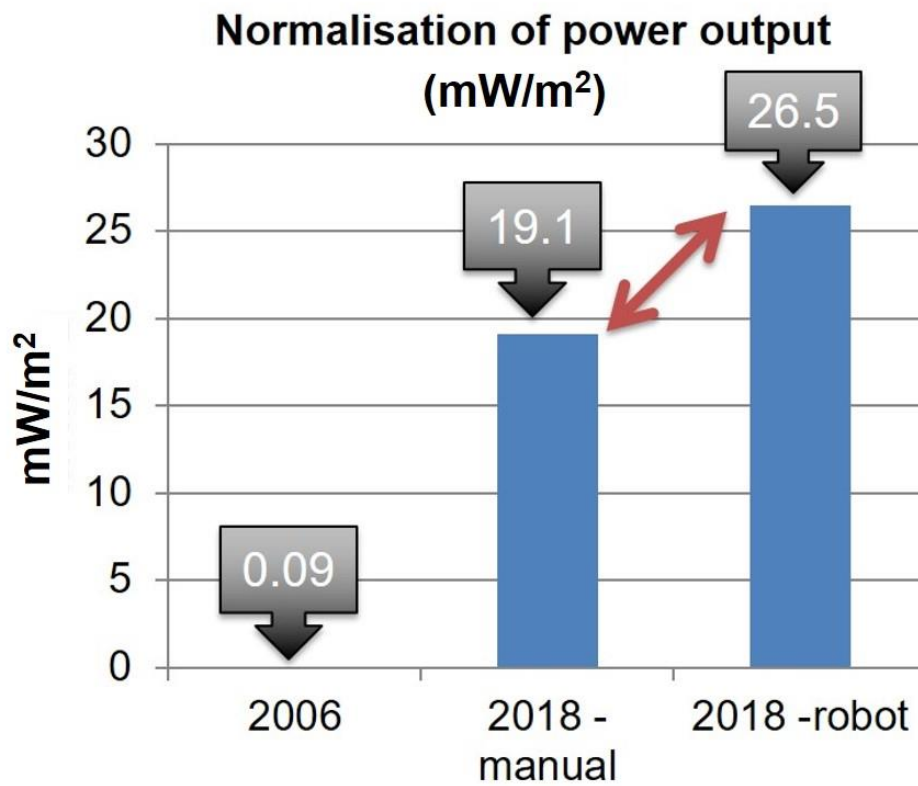


Figure 5.26 – Mean ($n=8$) polarisation results gathered on the 6th day of operation.

[A] EvoBot matured MFCs [B] Manually/ Bench matured MFCs



EcoBot-II MFCs	P Output (μW)	mW/m²
2006 – manual	2.54	0.094074
2018 – manual	129	19.1
2018 – robot	179	26.5

Figure 5.27 – Summary graph comparing existing literature data from EcoBot-II 2006 edition MFCs to EcoBot-II 2018 edition MFCs.

5.7 Conclusions

The work presented in this chapter demonstrates the potential of using the EvoBot, an open-source modified RepRap 3D-printer, for the inoculation, maintenance and study of MFC systems. Furthermore, it presents the possibilities that this type of robot can be developed along the lines of robotically controlled environments integrated with MFC-based bioreactors with similarities as well as important differences to the well characterised planktonic chemostat. These experiments can be considered as the precursors to the development of a new class of living robots (Symbots), which can enforce, monitor and interact with evolving systems, such as MFCs. As a result, such a platform would not only benefit the MFC field but the robotics field as well. EvoBot could potentially be used in the future as a maturing/optimising factory for MFCs that can be used to power small robots. Indeed, it may even be that EvoBot itself is powered by the very same MFCs that it had built, inoculated and maintained.

Chapter 6 Conclusions and Further work

6.1 Executive summary

Microbial Fuel Cells (MFCs) are energy converters that use the bio-catalytic activity of microorganisms to generate electricity through the oxidation of organic matter. This work has demonstrated a new way of experimenting with MFCs via a liquid handling robot called EvoBot that through a feedback loop mechanism can interact, influence and optimise MFC units leading to improved power output levels. The work presented in this thesis, through a series of five chapters, explores the five main project research objectives. In Chapter 1 the outline of this work and the contention of this study is described. Chapter 2 elaborates on the theoretical underpinnings for these research questions through a literature review, followed by three empirical chapters. Chapter 3 gives a detailed overview of the experimental methods and the materials used in this study. Chapter 4 describes the identification of 3D-printable materials that can make up all the components of an MFC. Notably, these materials improved the MFC performance compared to conventional materials. Chapter 5 presents the series of interactive experiments between EvoBot robot and MFCs and how these improved the power output of the latter by 7.4 mW/m^2 (up to 26.5 mW/m^2) compared to the manually maintained MFCs. Finally Chapter 6 summarises the findings of the study, outlines the novelty of the project and identifies directions for future research.

This PhD work started in 2014 as part of the EvoBliss project. The state-of-art MFC during that time was the small scale (6.25 mL) MFC employed in

EcoBot-IV (Papaharalabos *et al.*, 2013, 2015b). The maximum power density of these MFC were 10.6 mW/m². This formed the benchmark for this study and the advancements made in this thesis aimed at improving this output. Following the improvements of core MFC materials and the automatic experimentation of MFCs using EvoBot, the power density of the same structure MFCs had more than doubled (26.5 mW/m²) (**Chapter 5**).

Apart from the power density another critical factor in making this technology more affordable and accessible is the cost of its core materials. In this thesis different clay based membrane materials were investigated against the expensive, widely-used CEM. Clay membranes were proven feasible substitutes of the CEM as they improved the power output by 2.1 mW/m² (CEM: 2.7 mW/m² – Terracotta: 4.8 mW/m²) and reduced the costs by almost 30-times (CEM: £0.78/membrane – Terracotta: £0.025/membrane). Furthermore, as part of the investigation on alternative economical cathode electrodes, this thesis substituted toxic and expensive PTFE with alginate as the electrode binder. Alginate based electrodes almost tripled the power output of the MFCs (PTFE: 3.55 mW/m² – Alginate: 10.57 mW/m²) and reduced the costs by 16-times (PTFE: £0.55/electrode – Alginate: £0.035/electrode). The additional benefit of alginate based electrodes and clay based membranes is their ability to be 3D-printed by the EvoBot as shown in **Chapter 4**. The advancement made in during this PhD push a bit further the boundaries of MFC research and open a new direction for the systematic experimentation and optimisation of MFCs, using interactive robotic workstations such as EvoBot.

6.2 General discussion and conclusions

Microbial fuel cells is a promising sustainable technology that can generate electricity whilst treating wastewater effluents. In comparison with conven-

tional chemical batteries, MFCs can generate electricity for as long as fuel (organic matter) is supplied to them however, they are generating low power (from μWatts to mWatts). As a technology MFCs are inherently interdisciplinary and versatile systems, hence a holistic approach is needed to improve their performance.

This study investigated both MFC systems on-board the robotic workstation (EvoBot) and MFCs on the bench (off-robot). The former focused on improving the MFC power performance through MFC – robot interaction, by influencing the feeding patterns and regimes. The bench experiments focused on developing 3D-printable core MFC materials that can be extruded from the EvoBot platform. Once incorporated into working MFCs, these novel materials influenced positively the overall performance of the system. Considering that the EvoBot robot is an open-source, modular robotic workstation designed to be easily reconfigurable and extendable, it provides a versatile and low cost tool to carry out MFC research. This thesis has documented the suite of exclusive experiments demonstrating the unique interaction between the automated robotic platform and the MFCs.

For example, when EvoBot's automated feeding was dictated in real-time by the MFCs voltage, the absolute power over time significantly improved (by $50 \mu\text{W}$ or 7.4 mW/m^2) when compared to conventionally maintained MFCs. This highlighted the benefit of using EvoBot to inoculate and maintain abiotic MFCs in order to improve their performance so that can be used on board autonomous robots such as EcoBot-II. During the final evaluation of the EvoBot-matured MFCs, the feedback loop system improved MFC power output by 3-fold within just 6 days, as opposed to the average four weeks which is the standard time in manually maintained experiments. These EvoBot-matured MFCs were able to charge the EcoBot-II capacitors within just 1 mi-

nute and 4 seconds enabling phototaxis, a task that took the 2006 edition EcoBot-II 14 minutes to achieve using a month's matured MFCs. These results can certainly be considered a success because one of the main aims of the EVOBLISS project was to create a robot that acts as an MFC factory to produce a new generation of MFCs to be plugged into and power autonomous robots. The applications of these MFC are not restricted only to robots since as mentioned in **Chapter 2**, MFCs can power; smart gadgets such as digital thermometers and mobile phones, remote sensors for environmental monitoring, pumps and wireless sensors.

Even though it is beyond the scope of this thesis, at this stage the power requirements of the EvoBot itself will be discussed in order to put it into perspective with the MFC power capabilities. Taking into account that EvoBot actuates only every hour, and this lasts for 20 minutes (i.e. feeding cycle), it means that it is only active for 30% of the time. The rest 70% of the time EvoBot is in idle mode and only records the MFC voltage. During idle mode the average current consumption is 137 mA. However once the feeding experiment is ongoing the system draws an average current of 930 mA and a peak current of 1.35A at 12 V. Peak time is when all the larger components of the robot are active i.e. pumps and motors. Since the EvoBot was never intended to be powered by MFCs, its' hardware was not optimised for this purpose. EvoBot could be adapted to be powered by MFCs only when its motors and pumps are substituted with low consumption counterparts. This can form a new project in the future, where collectives of MFCs can power their own maintenance machine. At the current moment is not feasible to power EvoBot directly from MFCs, however as the technology progresses this might be a reality in the future.

Nevertheless, EvoBot achieved its aim and monitored important parameters such as the response of MFCs to different feedstock concentrations and regimes. Subsequently, it reacted on these parameters in real-time and performed necessary functions to keep the living cells alive and to thrive for a prolonged periods of time. This was achieved by supplying the biofilm cultures in MFCs with fuel when needed while concomitantly monitoring their behaviour and reacting to voltage drops with new feeding injections. This approach would benefit those working in the MFC field because it offers a new way of maintaining and studying these living cells. Furthermore, this approach bridges the gap between the batch and continuous modes of feeding that have been used extensively in laboratory research to date. Furthermore, robotic systems can rapidly distinguish MFCs between different intrinsic factors (e.g. species of colonising microbes and their ecological proportions; size/shape/design of MFC) as well as extrinsic physicochemical factors such as temperature, pH, pO_2 , redox, osmotic pressure, type and concentration of nutrients. Biofilm reactors may offer many advantages compared to conventional chemostats so the two approaches (robot and biofilm bioreactor) can advance the biofilm and MFC research respectively.

Concomitantly to the MFC-robot interaction work, this thesis reported on the discovery and use of novel materials for critical MFC components. For instance the study on 3D-printable MEA revealed for the first time that MFCs with air-dry clay produced up to 50% more power than the controls (fluorinated-based). Additionally this line of work showed for the first time that gelatine is a promising soft material that can be 3D printed (in higher viscosities) and can also be used as a feedstock for MFC operation. These novel findings contribute towards developing fully monolithically printed MFCs. This can help standardise the MFC design which at the moment varies widely be-

tween research groups, resulting in non-uniform or transferable material improvements, which delay the overall advancement of the technology.

6.3 Novelty of the project

This study is the first pioneering attempt to employ a liquid handling robot (EvoBot), to inoculate, sustain and maintain living MFC systems. This was achieved using an automated reactive feeding system based on an established feedback communication loop with the MFC. EvoBot opens a new avenue for systematic experimentation with living, bio-hybrid system, allowing the study of evolution and adaptation through this interactive and synergistic relationship. The ability of EvoBot to interact with the MFCs in real-time, both improving and stabilising their output via a feedback loop mechanism is a novel approach that to the knowledge of the authors covers virgin ground in the MFC technology research. In addition for the first-time to the author's knowledge an extended research study on MFC systems was conducted using a robotic platform such as EvoBot which investigated the adaptability and stability of those systems at the same time. Thus, the overall interaction of the biochemical systems (MFCs) with the 3D printing technology which led to a Robot-Chemostat behavioural experiments can be described as the main novelty of this thesis.

An additional novelty is the use of evolutionary algorithms on-board EvoBot to optimise the feedstock regimes for the living cells. Although, this was just a preliminary line of work it does offer an intriguing avenue for future MFC research. Evolutionary algorithms that evolve based on the response of MFCs to new fuel combinations can be an efficient technique for reinventing new MFC substrates. Such an automated system could test and optimise the MFC feedstock resulting in increased power output capabilities. Concomi-

tantly, it can contribute to the development of personalised feedstock for MFCs that are indicative of each working environments.

Based on the results presented in this thesis it is evident that EvoBot can be used as an invaluable research tool for MFC research. This can help standardise the MFC experimental processes between different groups around the world. Moreover, since the platform itself is derived from a RepRap 3D printer, it still holds an inherent ability to print three-dimensional structures. Novel results from this study showed that 3D printable air-dry materials can improve the MFC performance and act as membranes or electrodes in monolithically printed MFCs. The possibility of using one platform both for 3D printing MFC objects and performing live MFC experiments, is another novelty of the project as the same research tool can be turned into a production tool and vice versa.

6.4 Future work

The sets of experiments performed throughout this project are the precursors for further investigation and possible avenues as detailed next.

Initially, EvoBot's abilities can be extended further via a set of hardware modifications giving it a broader realm of 3D-printing capabilities. For example, in addition to extrusion, EvoBot can be customised to incorporate a brush/roller into its robotic head. This could apply a uniform conductive coating onto the dried extruded membranes akin to a robotic painting machine (Grosser, 2011) achieving a complete and automated MEA fabrication.

Apart from that, a pH module can be incorporated into the robotic head to add another element of interaction with the MFCs. Such an apparatus can automatically test the inlet pH as well as the outlet pH of the anodic chamber

in real-time, and can control the pH to help understand the relationship between power output and analyte pH. Also, it can give insight into the chemical and microbial transformations that take place within each chamber. This idea inspired the development of a research project that took place at IT University of Copenhagen, Denmark (EVOBLISS project collaborators) where a prototype was developed as part of an MSc study.

An experiment that has the potential to be explored further and result in important findings is the evolutionary algorithm experiment that was introduced for the first time in this thesis. The ability to automatically test a wide range of feedstock recipes and improve the combinations by assessing the resulting performance of MFCs, opens a whole new avenue of interdisciplinary study between bioelectrochemistry, evolutionary biology and artificial intelligence.

EvoBot as a standalone open-source platform can continue to be used to perform interactive experiments all over the world. These will have the ability to produce high quality reproducible data from multiple comparisons of conditions across a wide range of the physicochemical realm; data that would be difficult to achieve through conventional manual experimentation on MFCs and electroactive biofilms. This in the future can result in laboratory scale EvoBot-based MFC farms (akin to hydroponic farms), that can maintain multiple small MFCs simultaneously and preparing them for practical uses (e.g. powering remote sensors, degrading pollutants in the wastewater etc.).

Following the work carried out in this PhD project and by continuing the development of this robot it is believed that valuable results can emerge that can shape further the future of MFCs and fully address the physicochemical parameters that influence their electrical behaviour.

6.5 List of publications from this thesis

Theodosiou, P., Ieropoulos, I., Taylor, B., Greenman, J., and Melhuish, C. (2015) Gelatin as a Promising Printable Nutrient Feedstock for Microbial Fuel Cells (MFC) In: *Proceedings of EFC2015 European Fuel Cell Technology & Applications Conference - Piero Lunghi*, 16-18 December, 2015, Naples, Italy., pp. 307-308.

Faíña, A., Nejatimoharrami, F., Stoy, K., **Theodosiou, P.**, Taylor, B., & Ieropoulos, I. (2016). EvoBot: An Open-Source, Modular Liquid Handling Robot for Nurturing Microbial Fuel Cells. In: *Proceedings of the Artificial Life Conference 2016*. pp. 626–633.

Ieropoulos, I., **Theodosiou, P.**, Taylor, B., Greenman, J. and Melhuish, C. (2016) Gelatin as a promising printable feedstock for microbial fuel cells (MFC). *International Journal of Hydrogen Energy*, 42 (3). pp. 1783-1790. ISSN 0360-3199

Theodosiou, P., Faina, A., Nejatimoharrami, F., Stoy, K., Greenman, J., Melhuish, C. and Ieropoulos, I. (2017) EvoBot: Towards a robot-chemostat for culturing and maintaining Microbial Fuel Cells (MFCs). In: Mangan, M., Cutkosky, M., Mura, A., Verschure, P. F., Prescott, T. and Lepora, N., eds. (2017) *Biomimetic and Biohybrid Systems*. Springer. ISBN 9783642398018

Theodosiou, P., Ieropoulos, I. Greenman, J., and Melhuish, C. (2017) 3D-Printable Membrane Electrode Assembly (MEA) for 3D-Printable Microbial

Fuel Cells (MFCs). *231st ECS Meeting, May 28 – June 1, 2017 – New Orleans, LA, USA, Abstract no. 2078*, © The Electrochemical Society.

Theodosiou, P., Greenman, J., Melhuish, C., and Ieropoulos, I. (2017) Towards Monolithically Printed MFCs: A Report on the Development of a 3D-Printable Membrane Electrode Assembly (MEA) In: *Proceedings of EFC2017 European Fuel Cell Technology & Applications Conference - Piero Lunghi*, 12-15 December, 2017, Naples, Italy. EFC 17166.

Theodosiou, P., Greenman, J., and Ieropoulos, I. (2018) 3D-Printable Cathode Electrode for Monolithically Printed Microbial Fuel Cells (MFCs) *233rd ECS Meeting, May 13 – 17, 2018 – Seattle, WA, USA, Abstract no. 2255*, © The Electrochemical Society.

Theodosiou, P., Greenman, J., and Ieropoulos, I. (2019). Towards monolithically printed Mfcs: Development of a 3d-printable membrane electrode assembly (mea). *International Journal of Hydrogen Energy*. In press DOI:10.1016/j.ijhydene.2018.12.163.

References

- Ahn, Y. and Logan, B.E. (2010) Effectiveness of domestic wastewater treatment using microbial fuel cells at ambient and mesophilic temperatures. *Bioresource Technology*. 101 (2), pp. 469–475. doi:10.1016/j.biortech.2009.07.039.
- Alivisatos, A.P., Blaser, M.J., Brodie, E.L., Chun, M., Dangl, J.L., Donohue, T.J., Dorrestein, P.C., Gilbert, J.A., Green, J.L., Jansson, J.K., Knight, R., Maxon, M.E., McFall-Ngai, M.J., Miller, J.F., et al. (2015) A unified initiative to harness Earth's microbiomes. *Science* [online]. 350 (6260), pp. 507–508.
- Allen, R.M. and Bennetto, H.P. (1993) Microbial fuel-cells: Electricity Production from Carbohydrates. *Applied Biochemistry and Biotechnology*. 39 (40), pp. 27–40.
- Ambrosi, A. and Pumera, M. (2016) 3D-printing technologies for electrochemical applications. *Chemical Society Reviews* [online]. 45 (10), pp. 2740–2755. doi:10.1039/C5CS00714C.
- Behera, M. and Ghangrekar, M.M. (2011) Electricity generation in low cost microbial fuel cell made up of earthenware of different thickness. *Water Science and Technology*. 64 (12), pp. 2468–2473. doi:10.2166/wst.2011.822.
- Bennetto, H.P. (1990) Electricity generation by microorganisms. *Biotechnology Education*. 1 (4), pp. 163–168.

- Beveridge, T.J., Chang, I.S., Kim, B.H., Kim, S., Culley, D.E., Reed, S.B., Margaret, F., Saffarini, D.A., Hill, E.A., Shi, L., Dwayne, A., Gorby, Y.A., Yanina, S., Mclean, J.S., et al. (2009) Electrically conductive bacterial nanowires produced by *Shewanella oneidensis* strain MR-1 and other microorganisms. *Proceedings of the National Academy of Sciences* [online]. 106 (23), pp. 9535–9535.
- Bigoni, F., Giorgio, F. De, Soavi, F. and Arbizzani, C. (2017) Sodium Alginate : A Water-Processable Binder in High-Voltage Cathode Formulations. *Journal of the Electrochemical Society*. 164 (1), pp. 6171–6177. doi:10.1149/2.0281701jes.
- Blauert, F., Horn, H. and Wagner, M. (2015) Time-resolved biofilm deformation measurements using optical coherence tomography. *Biotechnology and Bioengineering*. 112 (9), pp. 1893–1905. doi:10.1002/bit.25590.
- Bogue, R. (2011) Robots in the laboratory: a review of applications. *Industrial Robot: An International Journal*. 39 (2), pp. 113–119. doi:10.1108/01439911111106327.
- Bond, D.R. and Lovley, D.R. (2003) Electricity Production by *Geobacter sulfurreducens* Attached to Electrodes. *Applied and environmental microbiology*. 69 (3), pp. 1548–1555. doi:10.1128/AEM.69.3.1548.
- Calignano, F., Tommasi, T., Manfredi, D. and Chiolerio, A. (2015) Additive Manufacturing of a Microbial Fuel Cell — A detailed study. *Nature Publishing Group* [online]. pp. 1–10. doi:10.1038/srep17373.
- Canfield, J.H., Goldner, B.H. and Lutwack, R. (1963) *NASA Technical Report, Magna Corporation, Anaheim, California, USA.*

- Chae, K., Choi, M., Ajayi, F. and Park, W. (2008) Mass transport through a proton exchange membrane (nafion) in microbial fuel cells†. *Energy & Fuels* [online]. 22 (11), pp. 169–176. doi:10.1021/ef700308u.
- Chambre, A. (2014) Effects of Carbon Filtration Type on Filter Efficiency and Efficacy : Granular Loose-Fill vs . Bonded Filters. *Air science*. 1 (March), pp. 1–5.
- Chang, I.S., Jang, J.K., Gil, G.C., Kim, M., Kim, H.J., Cho, B.W. and Kim, B.H. (2004) Continuous determination of biochemical oxygen demand using microbial fuel cell type biosensor. *Biosensors and Bioelectronics*. 19 (6), pp. 607–613. doi:10.1016/S0956-5663(03)00272-0.
- Chaudhuri, S.K. and Lovley, D.R. (2003) Electricity generation by direct oxidation of glucose in mediatorless microbial fuel cells. *Nature biotechnology* [online]. 21 (10), pp. 1229–1232. doi:10.1038/nbt867
- Cheng, S., Liu, H. and Logan, B.E. (2006) Power densities using different cathode catalysts (Pt and CoTMPP) and polymer binders (Nafion and PTFE) in single chamber microbial fuel cells. *Environmental Science and Technology*. 40 (1), pp. 364–369. doi:10.1021/es0512071.
- Chouler, J., Cruz-Izquierdo, Á., Rengaraj, S., Scott, J.L. and Di Lorenzo, M. (2018) A screen-printed paper microbial fuel cell biosensor for detection of toxic compounds in water. *Biosensors and Bioelectronics* [online]. 102 (September 2017), pp. 49–56. doi:10.1016/j.bios.2017.11.018.
- Chouler, J., Padgett, G.A., Cameron, P.J., Preuss, K., Titirici, M.M., Ieropoulos, I. and Di Lorenzo, M. (2016) Towards effective small scale microbial fuel cells for energy generation from urine. *Electrochimica Acta* [online]. 192 pp. 89–98. doi:10.1016/j.electacta.2016.01.112.

- Clinton, D.J. and Morrell, R. (1987) Hardness testing of ceramic materials. *Materials Chemistry and Physics*. 17 (5), pp. 461–473.
doi:10.1016/0254-0584(87)90096-4.
- Cohen, B. (1931) The Bacterial Culture as an Electrical Half-Cell. *Journal of Bacteriology*. 21 (1), pp. 18–19.
- Comeau, Y. (2008) Microbial metabolism. In: *Biological Wastewater Treatment - Principles, Modelling and Design*. pp. 9–32.
doi:10.1016/0307-4412(75)90033-3.
- Costerton, J.W., Stewart, P.S. and Greenberg, E.P. (1999) Bacterial biofilms: a common cause of persistent infections. *Science* [online]. 284 (5418), pp. 1318–1322.
- Degrenne, N., Buret, F., Allard, B. and Bevilacqua, P. (2012) Electrical energy generation from a large number of microbial fuel cells operating at maximum power point electrical load. *Journal of Power Sources*. 205 pp. 188–193. doi:10.1016/j.jpowsour.2012.01.082.
- Du, Z., Li, H. and Gu, T. (2007) A state of the art review on microbial fuel cells: A promising technology for wastewater treatment and bioenergy. *Biotechnology Advances*. 25 (5), pp. 464–482.
doi:10.1016/j.biotechadv.2007.05.004.
- Dulon, S., Parot, S., Delia, M. and Bergel, A. (2007) Electroactive biofilms : new means for electrochemistry. *Journal of Applied Electrochemistry* [online]. 37 (1), pp. 173–179.
- Dumas, C., Mollica, A., Féron, D., Basséguy, R., Etcheverry, L. and Bergel, A. (2007) *Marine microbial fuel cell: Use of stainless steel electrodes as*

anode and cathode materials. doi:10.1016/j.electacta.2007.06.069.

Ekelof, S. (2001) The genesis of the Wheatstone bridge. *Engineering Science and Education Journal*. 10 (1), pp. 37–40.
doi:10.1049/esej:20010106.

Faiña, A., Nejatimoharrami, F., Stoy, K., Theodosiou, P., Taylor, B. and Ieropoulos, I. (2016) EvoBot : An Open-Source , Modular Liquid Handling Robot for Nurturing Microbial Fuel Cells. In: *Proceedings of the Artificial Life Conference 2016*. 2016 pp. 626–633.

Fan, Y., Hu, H. and Liu, H. (2007) Enhanced Coulombic efficiency and power density of air-cathode microbial fuel cells with an improved cell configuration. *Journal of Power Sources* [online]. 171 (2), pp. 348–354.
doi:10.1016/J.JPOWSOUR.2007.06.220

Feng, Y., Lee, H., Wang, X. and Liu, Y. (2009) Electricity Generation in Microbial Fuel Cells at different temperature and Isolation of Electrogenic Bacteria. *2009 Asia-Pacific Power and Energy Engineering Conference (Appeec), Vols 1-7*. pp. 530–534.

Fernandez, A., Huang, S., Seston, S., Xing, J., Hickey, R., Criddle, C. and Tiedje, J. (1999) How Stable Is Stable? Function versus Community Composition. *APPLIED AND ENVIRONMENTAL MICROBIOLOGY* [online]. 65 (8), pp. 3697–3704.

Fiset, E. and Puig, S. (2015) Modified Carbon Electrodes : A New Approach for Bioelectrochemical Systems. *Journal of Bioremediation & Biodegradation*. 6 (1), pp. 1–2. doi:10.4172/2155-6199.1000e16.

Flimban, S.G.A., Hassan, S.H.A., Rahman, M.M. and Oh, S.E. (2018) The

effect of Nafion membrane fouling on the power generation of a microbial fuel cell. *International Journal of Hydrogen Energy* [online]. pp. 1–9. doi:10.1016/j.ijhydene.2018.02.097.

Fraiwan, A. and Choi, S. (2016) A stackable, two-chambered, paper-based microbial fuel cell. *Biosensors and Bioelectronics* [online]. 83 pp. 27–32. doi:10.1016/j.bios.2016.04.025.

Fraiwan, A. and Choi, S. (2014) Bacteria-powered battery on paper. *Phys. Chem. Chem. Phys.* [online]. 16 (47), pp. 26288–26293. doi:10.1039/C4CP04804K.

Gajda, I., Greenman, J., Melhuish, C. and Ieropoulos, I. (2015a) Simultaneous electricity generation and microbially-assisted electrosynthesis in ceramic MFCs. In: *Bioelectrochemistry*. 2015 pp. 58–64. doi:10.1016/j.bioelechem.2015.03.001.

Gajda, I., Greenman, J., Melhuish, C. and Ieropoulos, I.A. (2016) Electricity and disinfectant production from wastewater: Microbial Fuel Cell as a self-powered electrolyser. *Scientific Reports* [online]. 6 (1), pp. 25571. doi:10.1038/srep25571.

Gajda, I., Stinchcombe, A., Greenman, J., Melhuish, C. and Ieropoulos, I. (2015b) Ceramic MFCs with internal cathode producing sufficient power for practical applications. *International Journal of Hydrogen Energy* [online]. 40 (42), pp. 14627–14631. doi:10.1016/j.ijhydene.2015.06.039.

Ghadge, A.N., Sreemannarayana, M., Duteanu, N. and Ghangrekar, M.. (2014) Influence of ceramic separator's characteristics on microbial fuel cell performance. *Journal of Electrochemical Science and Engineering*. 4 (4), pp. 315–326. doi:10.5599/jese.2014.

Ghasemi, M., Wan Daud, W.R., Ismail, M., Rahimnejad, M., Ismail, A.F., Leong, J.X., Miskan, M. and Ben Liew, K. (2013) Effect of pre-treatment and biofouling of proton exchange membrane on microbial fuel cell performance. *International Journal of Hydrogen Energy* [online]. 38 (13), pp. 5480–5484. doi:10.1016/j.ijhydene.2012.09.148.

Godoi, F.C., Prakash, S. and Bhandari, B.R. (2016) 3d printing technologies applied for food design: Status and prospects. *Journal of Food Engineering* [online]. 179 pp. 44–54. doi:10.1016/j.jfoodeng.2016.01.025.

GOV.UK (2019) *Waste water treatment works: treatment monitoring and compliance limits*. Available from: <https://www.gov.uk/government/publications/waste-water-treatment-works-treatment-monitoring-and-compliance-limits/waste-water-treatment-works-treatment-monitoring-and-compliance-limits>.

Gralnick, J.A. and Newman, D.K. (2007) MicroReview: Extracellular respiration. *Molecular Microbiology*. 65 (1), pp. 1–11. doi:10.1111/j.1365-2958.2007.05778.x.

Greenman, J., Ieropoulos, I. and Melhuish, C. (2011) Microbial Fuel Cells – Scalability and their Use in Robotics. In: *Applications of Electrochemistry and Nanotechnology in Biology and Medicine I*,. pp. pp.239-290. doi:DOI: 10.1007/978-1-4614-0347-0_3.

Greenman, J., Ledezma, P., Pereira-Medrano, A., Wright, P. and Ieropoulos, I. (2011) The importance of specific growth rate of biofilms for electricity production in microbial fuel cell systems. In: *IWA Biofilm 2011: Processes in Biofilms*. 2011 pp. 2–4.

Grosser, B. (2011) *Interactive Robotic Painting Machine*. Available from: <https://bengrosser.com/projects/interactive-robotic-painting->

machine/#related [Accessed 6 September 2018].

Grzebyk, M. and Poźniak, G. (2005) Microbial fuel cells (MFCs) with interpolymer cation exchange membranes. *Separation and Purification Technology* [online]. 41 (3), pp. 321–328. doi:10.1016/j.seppur.2004.04.009

Guerrini, E., Grattieri, M., Trasatti, S.P., Bestetti, M. and Cristiani, P. (2014) Performance explorations of single chamber microbial fuel cells by using various microelectrodes applied to biocathodes. *International Journal of Hydrogen Energy* [online]. 39 (36), pp. 21837–21846. doi:10.1016/J.IJHYDENE.2014.06.132

Habermann, W. and Pommer, E.W. (1991) Biological fuel cells with sulphide storage capacity. *Applied Microbiology and Biotechnology*. 35 pp. 128–133.

Haluk, B. and Jerome, B. (2015) *Biofilms in Bioelectrochemical Systems: From Laboratory Practise to Data Interpretation*. (no place) John Wiley & Sons.

Harnisch, F. and Schröder, U. (2009) Selectivity versus mobility: Separation of anode and cathode in microbial bioelectrochemical systems. *ChemSusChem*. 2 (10), pp. 921–926. doi:10.1002/cssc.200900111.

Herpt, O. (2016) *Functional 3D Printed Ceramics - Olivier van Herpt*.

Holzman, D.C. (2005) Microbe Power! *Environmental Health Perspectives* [online]. 113 (11), pp. 754–757. Available from: <https://www.ncbi.nlm.nih.gov/pmc/articles/PMC1310948/pdf/ehp0113-a00754.pdf> [Accessed 20 August 2018].

Hull, C. (1984) *Apparatus for production of three-dimensional objects by stereolithography* p.pp. US4575330.

Ieropoulos, I. (2003) Imitating Metabolism : Energy Autonomy in Biologically Inspired Robots. *Animals*. (January 2003), pp. 1–4.

Ieropoulos, I. a., Greenman, J. and Melhuish, C. (2013) Miniature microbial fuel cells and stacks for urine utilisation. *International Journal of Hydrogen Energy* [online]. 38 (1), pp. 492–496.
doi:10.1016/j.ijhydene.2012.09.062

Ieropoulos, I. a, Ledezma, P., Stinchcombe, A., Papaharalabos, G., Melhuish, C. and Greenman, J. (2013a) Waste to real energy: the first MFC powered mobile phone. *Physical chemistry chemical physics : PCCP* [online]. 15 (37), pp. 15312–15316. doi:10.1039/c3cp52889h

Ieropoulos, I., Gajda, I., You, J. and Greenman, J. (2013b) Urine—waste or resource? The economic and social aspects. *Reviews in Advanced Sciences and Engineering* [online]. 2 (3), pp. 192–199.
doi:10.1166/rase.2013.1033.

Ieropoulos, I., Greenman, J., Lewis, D. and Knoop, O. (2013c) Energy production and sanitation improvement using microbial fuel cells. *Journal of Water, Sanitation and Hygiene for Development*. pp. 383–391. doi:10.2166/washdev.2013.117.

Ieropoulos, I., Greenman, J. and Melhuish, C. (2003) Imitating Metabolism : Energy Autonomy in Biologically Inspired Robots. In: *Proceeding of AISB'03, Second International Symposium on Imitation in Animals and Artifacts*. 2003 pp. 191–194.

- Ieropoulos, I., Greenman, J. and Melhuish, C. (2010) Improved energy output levels from small-scale Microbial Fuel Cells. *Bioelectrochemistry (Amsterdam, Netherlands)* [online]. 78 (1), pp. 44–50. doi:10.1016/j.bioelechem.2009.05.009
- Ieropoulos, I., Greenman, J. and Melhuish, C. (2008) Microbial fuel cells based on carbon veil electrodes: Stack configuration and scalability. *International Journal of Energy Research*. 32 (13), pp. 1228–1240. doi:10.1002/er.1419.
- Ieropoulos, I., Greenman, J. and Melhuish, C. (2012) Urine utilisation by microbial fuel cells; energy fuel for the future. *Physical chemistry chemical physics: PCCP* [online]. 14 (1), pp. 94–98. doi:10.1039/c1cp23213d
- Ieropoulos, I., Greenman, J., Melhuish, C. and Horsfield, I. (2009) Artificial symbiosis in EcoBots. In: *Artificial Life Models in Hardware*. pp. 185–211. doi:10.1007/978-1-84882-530-7_9.
- Ieropoulos, I., Greenman, J., Melhuish, C. and Horsfield, I. (2010a) EcoBot-III: a robot with guts. *The 12th International Conference on the Synthesis and Simulation of Living Systems* [online]. pp. 733–740. Available from: <http://mitpress.mit.edu/catalog/item/default.asp?ttype=2&tid=12433>.
- Ieropoulos, I., Melhuish, C. and Greenman, J. (2007) Artificial gills for robots: MFC behaviour in water. *Bioinspiration & biomimetics*. 2 pp. S83–S93. doi:10.1088/1748-3182/2/3/S02.
- Ieropoulos, I., Melhuish, C. and Greenman, J. (2004) Energetically Autonomous Robots. *8th Intelligent Autonomous Systems Conference*. (July), pp. 128–135.

Ieropoulos, I., Melhuish, C., Greenman, J. and Horsfield, I. (2005) EcoBot-II: An artificial agent with a natural metabolism. *International Journal of Advanced Robotic Systems*. 2 (4), pp. 295–300. doi:10.5772/5777.

Ieropoulos, I., Melhuish, C., Greenman, J., Horsfield, I. and Hart, J. (2004) *Energy autonomy in robots through Microbial Fuel Cells*.

Ieropoulos, I., Theodosiou, P., Taylor, B., Greenman, J. and Melhuish, C. (2017) Gelatin as a promising printable feedstock for microbial fuel cells (MFC). *International Journal of Hydrogen Energy*. 42 (3), pp. 1783–1790. doi:10.1016/j.ijhydene.2016.11.083.

Ieropoulos, I., Winfield, J., Gajda, I., Walter, A., Papaharalabos, G., Jimenez, I.M., Pasternak, G., You, J., Tremouli, A., Stinchcombe, A., Forbes, S. and Greenman, J. (2015) *The Practical Implementation of Microbial Fuel Cell Technology* [online]. (no place) Elsevier Ltd.

Ieropoulos, I., Winfield, J. and Greenman, J. (2010a) Effects of flow-rate, inoculum and time on the internal resistance of microbial fuel cells. *Bioresource Technology* [online]. 101 (10), pp. 3520–3525. doi:10.1016/j.biortech.2009.12.108

Ieropoulos, I., Winfield, J. and Greenman, J. (2010b) Effects of flow-rate, inoculum and time on the internal resistance of microbial fuel cells. *Bioresource Technology*. 101 (10), pp. 3520–3525. doi:10.1016/j.biortech.2009.12.108.

Ieropoulos, I., Winfield, J., Greenman, J. and Melhuish, C. (2010b) Small Scale Microbial Fuel Cells and Different Ways of Reporting Output. In: *ECS Transactions*. 2010 pp. 1–9.

Ieropoulos, I.A., Stinchcombe, A., Gajda, I., Forbes, S., Merino-Jimenez, I., Pasternak, G., Sanchez-Herranz, D. and Greenman, J. (2016) Pee power urinal – microbial fuel cell technology field trials in the context of sanitation. *Environmental Science: Water Research & Technology* [online]. 2 (2), pp. 336–343. doi:10.1039/C5EW00270B.

International Energy Agency (2017) *World Energy Outlook 2017* [online]. (no place) OECD. [Accessed 4 July 2018].

Iqbal, J. and Khan, Z.H. (2017) The potential role of renewable energy sources in robot's power system: A case study of Pakistan. *Renewable and Sustainable Energy Reviews* [online]. 75 pp. 106–122. doi:10.1016/J.RSER.2016.10.055

Jefferies, D. (1995) Activated Carbon Filters: Comparing loose-fill with bonded carbon filters. *Filtration & Separation*. 32 (5), pp. 385–387.

Jonathan, G. and Karim, A. (2016) 3D printing in pharmaceuticals: A new tool for designing customized drug delivery systems. *International Journal of Pharmaceutics* [online]. 499 (1), pp. 376–394. doi:10.1016/j.ijpharm.2015.12.071

Kaiyu Industrial LTD (2018) *Micronized Graphite*. Available from: <http://www.kyugraphite.com/micronized-graphite-3276941.html>.

Katuri, K.P., Kavanagh, P., Rengaraj, S. and Leech, D. (2010) *Geobacter sulfurreducens* biofilms developed under different growth conditions on glassy carbon electrodes: insights using cyclic voltammetry. *Chemical communications (Cambridge, England)* [online]. 46 (26), pp. 4758–4760. doi:10.1039/c003342a.

Kelly, I., Holland, O. and Melhuish, C. (2000) SlugBot: A Robotic Predator in the Natural World. In: M. Sugisaka & H. Tanaka (ed.). *Proceedings of the international symposium on artificial life and robotics for human welfare and artificial life robotics* [online]. 2000 pp. 470–475.

Kim, B.H., Chang, I.S. and Moon, H. (2006) Microbial Fuel Cell-Type Biochemical Oxygen Demand Sensor. *Encyclopedia of Sensors*. X pp. 1–12.

Kim, J.R., Premier, G.C., Hawkes, F.R., Dinsdale, R.M. and Guwy, A.J. (2009) Development of a tubular microbial fuel cell (MFC) employing a membrane electrode assembly cathode. *Journal of Power Sources* [online]. 187 (2), pp. 393–399. doi:10.1016/j.jpowsour.2008.11.020

Kodama, H. (1981) Automatic method for fabricating a three-dimensional plastic model with photo-hardening polymer. *Review of Scientific Instruments*. 52 (11), pp. 1770–1773. doi:10.1063/1.1136492.

Kondaveeti, S., Lee, J., Kakarla, R., Kim, H.S. and Min, B. (2014) Low-cost separators for enhanced power production and field application of microbial fuel cells (MFCs). *Electrochimica Acta* [online]. 132 pp. 434–440. doi:10.1016/J.ELECTACTA.2014.03.046

Koser, S.A., Chinn, B.E.N.D. and Saunders, F. (1938) Gelatin as a source of growth-promoting substances for bacteria. *Journal of Bacteriology*. 36 (1), pp. 57–65.

Kovalenko, I., Zdyrko, B., Magasinski, A., Hertzberg, B., Milicev, Z., Burtovyy, R., Luzinov, I. and Yushin, G. (2011) A Major Constituent of Brown Algae for Use in High-Capacity Li-Ion Batteries. *Science* [online]. 334 (6052), pp. 75–79. doi:10.1126/science.1209150.

- Kumar, R., Singh, L., Wahid, Z.A. and Din, M.F.M. (2015) Exoelectrogens in microbial fuel cells toward bioelectricity generation: a review. *International Journal of Energy Research* [online]. 39 (8), pp. 1048–1067. doi:10.1002/er.3305
- Ledezma, P., Greenman, J. and Ieropoulos, I. (2012) Maximising electricity production by controlling the biofilm specific growth rate in microbial fuel cells. *Bioresource Technology* [online]. 118 pp. 615–618. doi:10.1016/j.biortech.2012.05.054
- Ledezma, P., Greenman, J. and Ieropoulos, I. (2013) MFC-cascade stacks maximise COD reduction and avoid voltage reversal under adverse conditions. *Bioresource Technology* [online]. 134 pp. 158–165. doi:10.1016/j.biortech.2013.01.119
- Ledezma, P., Ieropoulos, I. and Greenman, J. (2010) Comparative analysis of different polymer materials for the construction of microbial fuel cell stacks. *Journal of Biotechnology* [online]. 150 (NOVEMBER), pp. 143–143. doi:10.1016/j.jbiotec.2010.08.373.
- Levine, M. and Carpenter, D. (1922) Gelatin liquefaction by bacteria. *Journal of Bacteriology*. 8 (4), pp. 297–306.
- Li, B., Zhou, J., Zhou, X., Wang, X., Li, B., Santoro, C., Grattieri, M., Babanova, S., Artyushkova, K., Atanassov, P. and Schuler, A.J. (2014) Surface modification of microbial fuel cells anodes: Approaches to practical design. *Electrochimica Acta* [online]. 134 pp. 116–126. doi:10.1016/j.electacta.2014.04.136.
- Li, W.-W., Sheng, G.-P., Liu, X.-W. and Yu, H.-Q. (2011) Recent advances in the separators for microbial fuel cells. *Special Issue: Biofuels - II: Algal Biofuels and Microbial Fuel Cells* [online]. 102 (1), pp. 244–252. doi:10.1016/j.biortech.2010.03.090.

- Liu, H. and Logan, B.E. (2004) Electricity Generation Using an Air-Cathode Single Chamber Microbial Fuel Cell in the Presence and Absence of a Proton Exchange Membrane. *Environmental Science & Technology* [online]. 38 (14), pp. 4040–4046. doi:10.1021/es0499344
- Liu, H., Ramnarayanan, R. and Logan, E.B. (2004) Production of Electricity during Wastewater Treatment Using a Single Chamber Microbial Fuel Cell. *Environmental Science & Technology* [online]. 38 (7), pp. 2281–2285. doi:10.1021/es034923g
- Logan, B. (2008) *Microbial Fuel Cells* [online]. Hoboken, New Jersey: John Wiley & Sons.
- Logan, B.E. (2009) Exoelectrogenic bacteria that power microbial fuel cells. *Nature Reviews Microbiology* [online]. 7 (5), pp. 375–381. doi:10.1038/nrmicro2113.
- Logan, B.E., Hamelers, B., Rozendal, R., Schröder, U., Keller, J., Freguia, S., Aelterman, P., Verstraete, W. and Rabaey, K. (2006) Microbial fuel cells: Methodology and technology. *Environmental Science and Technology*. 40 (17), pp. 5181–5192. doi:10.1021/es0605016.
- Lovley, D.R. (2008) The microbe electric: conversion of organic matter to electricity. *Current opinion in biotechnology* [online]. 19 (6), pp. 564–571. doi:10.1016/j.copbio.2008.10.005.
- Lyon, D.Y., Buret, F., Vogel, T.M. and Monier, J.-M. (2010) Is resistance futile? Changing external resistance does not improve microbial fuel cell performance. *Bioelectrochemistry (Amsterdam, Netherlands)* [online]. 78 (1), pp. 2–7. doi:10.1016/j.bioelechem.2009.09.001

- Magasanik, B. (1961) Catabolite Repression. *Cold Spring Harbor Symposia of Quantitative Biology*. 26 pp. 249–256.
doi:10.1101/SQB.1961.026.01.031.
- Melhuish, C., Ieropoulos, I., Greenman, J. and Horsfield, I. (2006) Energetically autonomous robots: Food for thought. *Autonomous Robots* [online]. 21 (3), pp. 187–198. doi:10.1007/s10514-006-6574-5
- Melvik, J.E. and Dornish, M. (2004) Alginate as a Carrier for Cell Immobilisation. In: *Fundamentals of Cell Immobilisation Biotechnology*. pp. 33–51.
- Michel, C., Lahaye, M., Bonnet, C., Mabeau, S. and Barry, J.L. (1996) In vitro fermentation by human faecal bacteria of total and purified dietary fibres from brown seaweeds. *The British journal of nutrition*. pp. 263–280.
doi:10.1079/BJN19960129.
- Min, B. and Logan, B.E. (2004) Continuous electricity generation from domestic wastewater and organic substrates in a flat plate microbial fuel cell. *Environmental Science and Technology*. 38 (21), pp. 5809–5814.
doi:Doi 10.1021/Es0491026.
- Mitchell, M.G. (2016) Applications of 3D Printing in Cell Biology. In: *Cell Biology* [online]. (no place) Academic Press, Elsevier. pp. 121–162.
doi:10.1016/B978-0-12-801853-8.00002-8
- Monod J (1950) La technique de culture continue. Theorie et applications. *Annales de l'Institut Pasteur*. 79 (4), pp. 390–410.
- Nandy, A., Kumar, V., Mondal, S., Dutta, K., Salah, M. and Kundu, P.P. (2015) Performance evaluation of microbial fuel cells: Effect of varying

electrode configuration and presence of a membrane electrode assembly. *New Biotechnology* [online]. 32 (2), pp. 272–281. doi:10.1016/j.nbt.2014.11.003.

Nejatimoharrami, F., Faiña, A., Cejkova, J., Hanczyc, M.M. and Stoy, K. (2016) Robotic Automation to Augment Quality of Artificial Chemical Life Experiments. In: *Proceedings of the Artificial Life Conference 2016*. 2016 pp. 634–635.

Nevin, K.P., Richter, H., Covalla, S.F., Johnson, J.P., Woodard, T.L., Orloff, A.L., Jia, H., Zhang, M. and Lovley, D.R. (2008) Power output and coulombic efficiencies from biofilms of *Geobacter sulfurreducens* comparable to mixed community microbial fuel cells. *Environmental Microbiology*. 10 (10), pp. 2505–2514. doi:10.1111/j.1462-2920.2008.01675.x.

Pandey, P., Shinde, V.N., Deopurkar, R.L., Kale, S.P., Patil, S.A. and Pant, D. (2016) Recent advances in the use of different substrates in microbial fuel cells toward wastewater treatment and simultaneous energy recovery. *Applied Energy* [online]. 168 pp. 706–723. doi:10.1016/j.apenergy.2016.01.056

Pang, S., Gao, Y. and Choi, S. (2017) Flexible and Stretchable Biobatteries: Monolithic Integration of Membrane-Free Microbial Fuel Cells in a Single Textile Layer. *Advanced Energy Materials*. 1702261 pp. 1–8. doi:10.1002/aenm.201702261.

Pankratova, G. and Gorton, L. (2017) Electrochemical communication between living cells and conductive surfaces. *Current Opinion in Electrochemistry* [online]. doi:10.1016/j.coelec.2017.09.013.

Pant, D., Van Bogaert, G., Diels, L. and Vanbroekhoven, K. (2010) A review of the substrates used in microbial fuel cells (MFCs) for sustainable

energy production. *Bioresource Technology* [online]. 101 (6), pp. 1533–1543. doi:10.1016/j.biortech.2009.10.017

Pant, D., Singh, A., Van Bogaert, G., Irving Olsen, S., Singh Nigam, P., Diels, L. and Vanbroekhoven, K. (2012) Bioelectrochemical systems (BES) for sustainable energy production and product recovery from organic wastes and industrial wastewaters. *RSC Advances* [online]. 2 (4), pp. 1248–1263. doi:10.1039/C1RA00839K.

Papaharalabos, G., Greenman, J., Melhuish, C. and Ieropoulos, I. (2015a) A novel small scale Microbial Fuel Cell design for increased electricity generation and waste water treatment. *International Journal of Hydrogen Energy* [online]. 40 (11), pp. 4263–4268. doi:10.1016/j.ijhydene.2015.01.117

Papaharalabos, G., Greenman, J., Melhuish, C., Santoro, C., Cristiani, P., Li, B. and Ieropoulos, I. (2013) Increased power output from micro porous layer (MPL) cathode microbial fuel cells (MFC). *International Journal of Hydrogen Energy* [online]. 38 (26), pp. 11552–11558. doi:10.1016/j.ijhydene.2013.05.138

Papaharalabos, G., Stinchcombe, A., Greenman, J., Melhuish, C. and Ieropoulos, I. (2015b) EcoBot IV : A Robotic Energy Harvester. In: *Hydrogen and Fuel Cell Research Hub H2FCSUPERGEN*. 2015

Park, D.H. and Zeikus, J.G. (2000) Electricity Generation in Microbial Fuel Cells Using Neutral Red as an Electronophore. *APPLIED AND ENVIRONMENTAL MICROBIOLOGY* [online]. 66 (4), pp. 1292–1297.

Park, D.H. and Zeikus, J.G. (2003) Improved fuel cell and electrode designs for producing electricity from microbial degradation. *Biotechnology and Bioengineering* [online]. 81 (3), pp. 348–355. doi:10.1002/bit.10501

Parthasarathy, A., Martin, C.R. and Srinivasan, S. (1990) *Investigations of the Oxygen Reduction Reaction at the Platinum/Nafion Interface Using a Solid State Electrochemical Cell* [online]. Available from: <http://www.dtic.mil/dtic/tr/fulltext/u2/a227674.pdf> [Accessed 14 August 2018].

Pasternak, G., Greenman, J. and Ieropoulos, I. (2016) Comprehensive Study on Ceramic Membranes for Low-Cost Microbial Fuel Cells. *ChemSusChem*. 9 (1), pp. 88–96. doi:10.1002/cssc.201501320.

Pasternak, G., Greenman, J. and Ieropoulos, I. (2017) Self-powered, autonomous Biological Oxygen Demand biosensor for online water quality monitoring. *Sensors and Actuators, B: Chemical* [online]. 244 (January), pp. 815–822. doi:10.1016/j.snb.2017.01.019.

Patil, S.A., Hägerhäll, C. and Gorton, L. (2012) Electron transfer mechanisms between microorganisms and electrodes in bioelectrochemical systems. *Bioanalytical Reviews*. 4 (2–4), pp. 159–192. doi:10.1007/s12566-012-0033-x.

Pham, T.H., Boon, N., Aelterman, P., Clauwaert, P., De Schamphelaire, L., Vanhaecke, L., De Maeyer, K., Höfte, M., Verstraete, W. and Rabaey, K. (2008) Metabolites produced by *Pseudomonas* sp. enable a Gram-positive bacterium to achieve extracellular electron transfer. *Applied Microbiology and Biotechnology*. 77 (5), pp. 1119–1129. doi:10.1007/s00253-007-1248-6.

Philamore, H., Ieropoulos, I., Stinchcombe, A. and Rossiter, J. (2016) Toward Energetically Autonomous Foraging Soft Robots. *Soft Robotics* [online]. 3 (4), pp. 186–197. doi:10.1089/soro.2016.0020.

Philamore, H., Rossiter, J., Walters, P., Winfield, J. and Ieropoulos, I. (2015) Cast and 3D printed ion exchange membranes for monolithic microbial

fuel cell fabrication. *Journal of Power Sources* [online]. 289 pp. 91–99. doi:10.1016/j.jpowsour.2015.04.113

Pocaznoi, D., Calmet, A., Etcheverry, L., Erable, B. and Bergel, A. (2012) Stainless steel is a promising electrode material for anodes of microbial fuel cells. *Energy & Environmental Science* [online]. 5 (11), pp. 9645–9652. doi:10.1039/C2EE22429A

Potter, M. (1911) Electrical Effects Accompanying the Decomposition of Organic Compounds Published by : The Royal Society Electrical Effects accompanying the Decomposition of Organic. *Proceedings of the Royal Society of London. Series B, Containing Papers of a Biological Character*,. 84 (571), pp. 260–276.

Prakash, B., Veeregowda, B.M. and Krishnappa, G. (2003) Biofilms: A survival strategy of bacteria. *Current Science* [online]. 85 (19), pp. 1299–1307. doi:10.2307/24108133

Rabaey, K., Angenent, L., Schroder, U. and Keller, J. (2009) *Bioelectrochemical Systems: From Extracellular Electron Transfer to Biotechnological Application*.

Rabaey, K., Clauwaert, P., Aelterman, P. and Verstraete, W. (2005) Tubular Microbial Fuel Cells for Efficient Electricity Generation. *Environmental Science and Technology* [online]. 39 (20), pp. 8077–8082. doi:10.1021/ES050986l

Reguera, G., McCarthy, K.D., Mehta, T., Nicoll, J.S., Tuominen, M.T. and Lovley, D.R. (2005) Extracellular electron transfer via microbial nanowires. *Nature* [online]. 435 (7045), pp. 1098–1101. doi:10.1038/nature03661

Reguera, G., Nevin, K.P., Nicoll, J.S., Covalla, S.F., Woodard, T.L. and Lovley, D.R. (2006) Biofilm and nanowire production leads to increased current in *Geobacter sulfurreducens* fuel cells. *Applied and environmental microbiology* [online]. 72 (11), pp. 7345–7348.
doi:10.1128/AEM.01444-06

Ren, Z., Ward, T.E. and Regan, J.M. (2007) Electricity production from cellulose in a microbial fuel cell using a defined binary culture. *Environmental Science and Technology*. 41 (13), pp. 4781–4786.
doi:10.1021/es070577h.

Ringeisen, B.R., Henderson, E., Wu, P.K., Pietron, J., Ray, R., Little, B., Biffinger, J.C. and Jones-Meehan, J.M. (2006) High power density from a miniature microbial fuel cell using *Shewanella oneidensis* DSP10. *Environmental Science and Technology* [online]. 40 (8), pp. 2629–2634.

Rismani-Yazdi, H., Carver, S.M., Christy, A.D. and Tuovinen, O.H. (2008) Cathodic limitations in microbial fuel cells: An overview. *Journal of Power Sources* [online]. 180 (2), pp. 683–694.
doi:10.1016/J.JPOWSOUR.2008.02.074

Rosenfeld, L. (2000) A Golden Age of Clinical Chemistry : 1948 – 1960. *Clinical Chemistry*. 46 (10), pp. 1705–1714.

Rossiter, J., Philamore, H., Stinchcombe, A. and Ieropoulos, I. (2015) Row-bot: An energetically autonomous artificial water boatman. In: *Proceedings of 2015 IEEE/RSJ International Conference on Intelligent Robots and Systems (IROS)*. pp. 3888–3893.

Rossiter, J., Winfield, J. and Ieropoulos, I. (2016) *Here today, gone tomorrow: biodegradable soft robots*. 9798 pp. 97981S.
doi:10.1117/12.2220611.

- Rulkens, W. (2008) Sewage Sludge as a Biomass Resource for the Production of Energy: Overview and Assessment of the Various Options. *Energy & Fuels* [online]. 22 (1), pp. 9–15. doi:10.1021/ef700267m
- Saha, S.K. (2008) Introduction to robotics. *McGraw-Hill Education (India)* [online]. pp. 1–21. doi:10.1111/j.1464-410X.2011.10513.x.
- Santoro, C., Arbizzani, C., Erable, B. and Ieropoulos, I. (2017) Microbial fuel cells: From fundamentals to applications. A review. *Journal of Power Sources* [online]. 356 pp. 225–244. doi:10.1016/j.jpowsour.2017.03.109.
- Santoro, C., Artyushkova, K., Gajda, I., Babanova, S., Serov, A., Atanassov, P., Greenman, J., Colombo, A., Trasatti, S., Ieropoulos, I. and Cristiani, P. (2015) Cathode materials for ceramic based microbial fuel cells (MFCs). *International Journal of Hydrogen Energy* [online]. 40 (42), pp. 14706–14715. doi:10.1016/j.ijhydene.2015.07.054.
- Santoro, C., Ieropoulos, I., Greenman, J., Cristiani, P., Vadas, T., Mackay, A. and Li, B. (2013) Current generation in membraneless single chamber microbial fuel cells (MFCs) treating urine. *Journal of Power Sources* [online]. 238 pp. 190–196. doi:10.1016/j.jpowsour.2013.03.095
- Shantaram, A., Beyenal, H., Raajan, R., Veluchamy, A. and Lewandowski, Z. (2005) Wireless Sensors Powered by Microbial Fuel Cells. *Environmental Science and Technology* [online]. 39 (13), pp. 5037–5042. doi:10.1021/es0480668
- Shewa, W.A., Chaganti, S.R. and Lalman, J.A. (2014) Electricity Generation and Biofilm Formation in Microbial Fuel Cells Using Plate Anodes Constructed from Various Grades of Graphite. *Journal of Green Engineering* [online]. 4 pp. 13–32. doi:10.13052/jge1904-4720.412

Siegwart, R. and Nourbakhsh, I.R. (2004) *Introduction to Autonomous Mobile Robots*.

Singleton, P. and Sainsbury, D. (2006) Continuous culture (continuous-flow culture ; continuous cultivation ; open culture ; open-system culture) *Dicitionary of Microbiology & Molecular Biology*.

Snaidr, J., Amann, R., Huber, I., Ludwig, W. and Schleifer, K.-H. (1997) Phylogenetic Analysis and In Situ Identification of Bacteria in Activated Sludge *APPLIED AND ENVIRONMENTAL MICROBIOLOGY* [online] 63 (7).

Snowden, M.E., King, P.H., Covington, J.A., MacPherson, J. V. and Unwin, P.R. (2010) Fabrication of versatile channel flow cells for quantitative electroanalysis using prototyping. *Analytical Chemistry*. 82 (8), pp. 3124–3131. doi:10.1021/ac100345v.

Su, L., Jia, W., Hou, C. and Lei, Y. (2011) Microbial biosensors: A review. *Biosensors and Bioelectronics* [online]. 26 (5), pp. 1788–1799. doi:10.1016/j.bios.2010.09.005.

Taghavi, M., Stinchcombe, A., Greenman, J., Mattoli, V., Beccai, L., Mazzolai, B., Melhuish, C. and Ieropoulos, I.A. (2015) Self sufficient wireless transmitter powered by foot-pumped urine operating wearable MFC. *Bioinspiration & Biomimetics* [online]. 11 (1), pp. 016001. doi:10.1088/1748-3190/11/1/016001

Taskan, E. and Hasar, H. (2014) Comprehensive Comparison of a New Tin-Coated Copper Mesh and a Graphite Plate Electrode as an Anode Material in Microbial Fuel Cell. *Applied Biochemistry and Biotechnology*. 175 (4), pp. 2300–2308. doi:10.1007/s12010-014-1439-4.

Theodosiou, P., Faina, A., Nejatimoharrami, F., Stoy, K., Greenman, J., Melhuish, C. and Ieropoulos, I. (2017) EvoBot: Towards a Robot-Chemostat for Culturing and Maintaining Microbial Fuel Cells (MFCs). In: *Biomimetic and Biohybrid Systems* [online]. (no place) Springer, Cham. pp. 453–464. doi:10.1007/978-3-319-63537-8_38

Torres, C.I., Kato Marcus, A. and Rittmann, B.E. (2007) Kinetics of consumption of fermentation products by anode-respiring bacteria. *APPLIED MICROBIAL AND CELL PHYSIOLOGY* [online]. 77 pp. 689–697. doi:10.1007/s00253-007-1198-z

Uría, N., Sánchez, D., Mas, R., Sánchez, O., Muñoz, F.X. and Mas, J. (2012) Effect of the cathode/anode ratio and the choice of cathode catalyst on the performance of microbial fuel cell transducers for the determination of microbial activity. *Sensors and Actuators, B: Chemical*. 170 pp. 88–94. doi:10.1016/j.snb.2011.02.030.

Vasylyv, O.M., Bilyy, O.I., Ferensovych, Y.P. and Hnatush, S.O. (2013) *Application of acetate, lactate, and fumarate as electron donors in microbial fuel cell*. 8825 pp. 88250Q. doi=10.1117/12.2021381doi:10.1117/12.2021381.

Walter, X.A., Forbes, S., Greenman, J. and Ieropoulos, I.A. (2016a) From single MFC to cascade configuration: The relationship between size, hydraulic retention time and power density. *Sustainable Energy Technologies and Assessments* [online]. 14 pp. 74–79. doi:10.1016/j.seta.2016.01.006.

Walter, X.A., Gajda, I., Forbes, S., Winfield, J., Greenman, J. and Ieropoulos, I. (2016b) Scaling-up of a novel, simplified MFC stack based on a self-stratifying urine column. *Biotechnology for Biofuels* [online]. 9 (1), pp. 93. doi:10.1186/s13068-016-0504-3.

Walter, X.A., Greenman, J. and Ieropoulos, I. (2018) Binder materials for the cathodes applied to self-stratifying membraneless microbial fuel cell. *Bioelectrochemistry* [online]. 123 (April), pp. 119–124. doi:10.1016/j.bioelechem.2018.04.011.

Walter, X.A., Stinchcombe, A., Greenman, J. and Ieropoulos, I. (2017) Urine transduction to usable energy: A modular MFC approach for smartphone and remote system charging. *Applied Energy* [online]. 192 pp. 575–581. doi:10.1016/j.apenergy.2016.06.006.

Watanabe, K., Teramoto, M., Futamata, H. and Harayama, S. (1998) Molecular Detection, Isolation, and Physiological Characterization of Functionally Dominant Phenol-Degrading Bacteria in Activated Sludge *APPLIED AND ENVIRONMENTAL MICROBIOLOGY* [online] 64 (11).

Watson, V.J. and Logan, B.E. (2011) Analysis of polarization methods for elimination of power overshoot in microbial fuel cells. *Electrochemistry Communications* [online]. 13 (1), pp. 54–56. doi:10.1016/j.elecom.2010.11.011.

Wei, J., Liang, P. and Huang, X. (2011) Recent progress in electrodes for microbial fuel cells. *Bioresour. Technol.* [online]. 102 (20), pp. 9335–9344. doi:10.1016/j.biortech.2011.07.019.

Wei, Y. and Yan, Z. (2012) Applications of Renewable Energy for Robots. In: *Proceedings of the world automation congress*. 2012 pp. 1–3.

Wells, D.A. (1859) *The Science of Common Things: A Familiar Explanation of the First Principles of Physical Science*. (no place) Ivison, Blakeman, Taylor & Company.

Whittaker, E.T. (1910) *A History of the Theories of Aether and Electricity: From the Age of Descartes to the Close of the Nineteenth Century*.

Wilkinson, S. (2000) 'Gastrobots'- Benefits and Challenges of Microbial Fuel Cells in Food Powered Robot Applications. *Autonomous Robots* [online]. 9 (2), pp. 99–111. doi:10.1023/A:1008984516499.

Willey, J.M., Sherwood, L.M. and Woolverton, C.J. (2009) *Prescott's Principles of Microbiology*. (no place) McGraw-Hill.

Winfield, J., Chambers, L.D., Rossiter, J., Greenman, J. and Ieropoulos, I. (2015a) Urine-activated origami microbial fuel cells to signal proof of life. *Journal of Materials Chemistry A* [online]. 3 (13), pp. 7058–7065. doi:10.1039/C5TA00687B.

Winfield, J., Chambers, L.D., Rossiter, J. and Ieropoulos, I. (2013a) Comparing the short and long term stability of biodegradable, ceramic and cation exchange membranes in microbial fuel cells. *Bioresource Technology* [online]. 148 pp. 480–486. doi:10.1016/j.biortech.2013.08.163

Winfield, J., Chambers, L.D., Rossiter, J., Stinchcombe, A., Walter, X.A., Greenman, J. and Ieropoulos, I. (2015b) Fade to Green: A Biodegradable Stack of Microbial Fuel Cells. *ChemSusChem*. 8 (16), pp. 2705–2712. doi:10.1002/cssc.201500431.

Winfield, J., Chambers, L.D., Stinchcombe, A., Rossiter, J. and Ieropoulos, I. (2014) The power of glove: Soft microbial fuel cell for low-power electronics. *Journal of Power Sources* [online]. 249 pp. 327–332. doi:10.1016/j.jpowsour.2013.10.096

- Winfield, J., Gajda, I., Greenman, J. and Ieropoulos, I. (2016) A review into the use of ceramics in microbial fuel cells. *Bioresource Technology* [online]. 215 pp. 296–303. doi:10.1016/j.biortech.2016.03.135.
- Winfield, J., Ieropoulos, I. and Greenman, J. (2012) Investigating a cascade of seven hydraulically connected microbial fuel cells. *Bioresource Technology* [online]. 110 pp. 245–250. doi:10.1016/j.biortech.2012.01.095.
- Winfield, J., Ieropoulos, I., Greenman, J. and Dennis, J. (2011) The overshoot phenomenon as a function of internal resistance in microbial fuel cells. *Bioelectrochemistry* [online]. 81 (1), pp. 22–27. doi:10.1016/j.bioelechem.2011.01.001
- Winfield, J., Ieropoulos, I., Rossiter, J., Greenman, J. and Patton, D. (2013b) Biodegradation and proton exchange using natural rubber in microbial fuel cells. *Biodegradation* [online]. 24 (6), pp. 733–739. doi:10.1007/s10532-013-9621-x
- Wu, S., He, W., Yang, W., Ye, Y., Huang, X. and Logan, B.E. (2017) Combined carbon mesh and small graphite fiber brush anodes to enhance and stabilize power generation in microbial fuel cells treating domestic wastewater. *Journal of Power Sources* [online]. 356 pp. 348–355. doi:10.1016/J.JPOWSOUR.2017.01.041
- Xu, J., Chou, S.-L., Gu, Q., Liu, H.-K. and Dou, S.-X. (2013) The effect of different binders on electrochemical properties of $\text{LiNi}_{1/3}\text{Mn}_{1/3}\text{Co}_{1/3}\text{O}_2$ cathode material in lithium ion batteries. *Journal of Power Sources* [online]. 225 pp. 172–178. doi:10.1016/j.jpowsour.2012.10.033.
- Xu, J., Sheng, G.P., Luo, H.W., Li, W.W., Wang, L.F. and Yu, H.Q. (2012) Fouling of proton exchange membrane (PEM) deteriorates the performance of microbial fuel cell. *Water Research* [online]. 46 (6), pp.

1817–1824. doi:10.1016/j.watres.2011.12.060.

You, J., Greenman, J., Melhuish, C. and Ieropoulos, I. (2016) Electricity generation and struvite recovery from human urine using microbial fuel cells. *Journal of Chemical Technology & Biotechnology* [online]. 91 (3), pp. 647–654. doi:10.1002/jctb.4617.

You, J., Preen, R.J., Bull, L., Greenman, J. and Ieropoulos, I. (2017) 3D printed components of microbial fuel cells: Towards monolithic microbial fuel cell fabrication using additive layer manufacturing. *Sustainable Energy Technologies and Assessments* [online]. 19 pp. 94–101. doi:http://dx.doi.org/10.1016/j.seta.2016.11.006.

You, J., Santoro, C., Greenman, J., Melhuish, C., Cristiani, P., Li, B. and Ieropoulos, I. (2014) Micro-porous layer (MPL)-based anode for microbial fuel cells. *International Journal of Hydrogen Energy* [online]. 39 (36), pp. 21811–21818. doi:10.1016/j.ijhydene.2014.07.136 [Accessed 4 March 2016].

You, J., Walter, X.A., Greenman, J., Melhuish, C. and Ieropoulos, I. (2015) Stability and reliability of anodic biofilms under different feedstock conditions: Towards microbial fuel cell sensors. *Sensing and Bio-Sensing Research* [online]. 6 pp. 43–50. doi:10.1016/j.sbsr.2015.11.007.

Yousaf, S., Anam, M., Saeed, S. and Ali, N. (2017) Electricigens: source, enrichment and limitations. *Environmental Technology Reviews* [online]. 6 (1), pp. 117–134. doi:10.1080/21622515.2017.1318182

Yousefi, V., Mohebbi-Kalhari, D. and Samimi, A. (2017) Ceramic-based microbial fuel cells (MFCs): A review. *International Journal of Hydrogen Energy* [online]. 42 (3), pp. 1672–1690. doi:10.1016/j.ijhydene.2016.06.054.

- Zhang, F., Liu, J., Ivanov, I., Hatzell, M.C., Yang, W., Ahn, Y. and Logan, B.E. (2014) Reference and counter electrode positions affect electrochemical characterization of bioanodes in different bioelectrochemical systems. *Biotechnology and Bioengineering*. 111 (10), pp. 1931–1939. doi:10.1002/bit.25253.
- Zhang, X., He, W., Ren, L., Stager, J., Evans, P.J. and Logan, B.E. (2015) COD removal characteristics in air-cathode microbial fuel cells. *Bioresource Technology* [online]. 176 pp. 23–31. doi:10.1016/j.biortech.2014.11.001.
- Zhao, C., Wang, C., Gorkin, R., Beirne, S., Shu, K. and Wallace, G.G. (2014) Three dimensional (3D) printed electrodes for interdigitated supercapacitors. *Electrochemistry Communications* [online]. 41 pp. 20–23. doi:10.1016/j.elecom.2014.01.013
- Zheng, S., Yang, F., Chen, S., Liu, L., Xiong, Q., Yu, T., Zhao, F., Schröder, U. and Hou, H. (2015a) Binder-free carbon black/stainless steel mesh composite electrode for high-performance anode in microbial fuel cells. *Journal of Power Sources* [online]. 284 pp. 252–257. doi:10.1016/J.JPOWSOUR.2015.03.014
- Zheng, S., Yang, F., Chen, S., Liu, L., Xiong, Q., Yu, T., Zhao, F., Schröder, U. and Hou, H. (2015b) Binder-free carbon black/stainless steel mesh composite electrode for high-performance anode in microbial fuel cells. *Journal of Power Sources*. 284 pp. 252–257. doi:10.1016/j.jpowsour.2015.03.014.
- Zhou, M., Chi, M., Luo, J., He, H. and Jin, T. (2011) An overview of electrode materials in microbial fuel cells. *Journal of Power Sources* [online]. 196 (10), pp. 4427–4435. doi:10.1016/j.jpowsour.2011.01.012.
- Zhu, X., Tokash, J.C., Hong, Y. and Logan, B.E. (2013) Controlling the

occurrence of power overshoot by adapting microbial fuel cells to high anode potentials. *Bioelectrochemistry*. 90 pp. 30–35. doi:10.1016/j.bioelechem.2012.10.004.

Ziv, N., Brandt, N.J. and Gresham, D. (2013) The use of chemostats in microbial systems biology. *Journal of visualized experiments : JoVE* [online]. (80), pp. 1–10. doi:10.3791/50168.

UWE Bristol (2018) *PEE POWER® to light up more sites after Africa school trial success* [Press release]. 23 April 2018. Available at: <https://info.uwe.ac.uk/news/uwenews/news.aspx?id=3790>

Appendix A

A.1 Details of the evolutionary algorithm

- **Algorithm:** CMA-ES
- **Variables:** percentage of acetate, $a \in [0,100]$, casein, $c \in [0,100]$, and urine $u \in [0,100] \quad \forall a, c, u: a + c + u = 100$
- **Representation:** vector of three real numbers $\{a, c, u\} \forall a, c, u: a + c + u = 1 / a, c, u \in \mathbb{R} \wedge a, c, u \in [0,1]$; individuals are normalized to guarantee that the sum of the three components is 1.
- **Initial population:** randomly generated from the a normal distribution centred at (0.5, 0.5, 0.5) and standard deviation of 0.2
- **Population size:** 8
- **Generations:** 12
- **Evaluation time:** 4 hours (all the population is evaluated in parallel)
- **Fitness:** average voltage of three MFCs, divided by the average voltage of the same MFCs with a recipe of 1/3 acetate, 1/3 casein and 1/3 urine.

$$fitness = \frac{\frac{\sum_1^N V_{mcf1t}}{N} + \frac{\sum_1^N V_{mcf2t}}{N} + \frac{\sum_1^N V_{mcf3t}}{N}}{3 * V_{base_mfc1-3}},$$

where V_{mcfi_t} is the voltage of MFC i at sample t ,

$$V_{base_mfc1-3} = \frac{\frac{\sum_1^N V_{mcf1t}}{N} + \frac{\sum_1^N V_{mcf2t}}{N} + \frac{\sum_1^N V_{mcf3t}}{N}}{3} \quad \text{measured with a recipe}$$

(1/3, 1/3, 1/3) just before the evolutionary experiment started,

and N is the number of samples taken during the experiment ($N=240$, voltage sampled every minute)

A.2 EcoBot-II 2018 edition

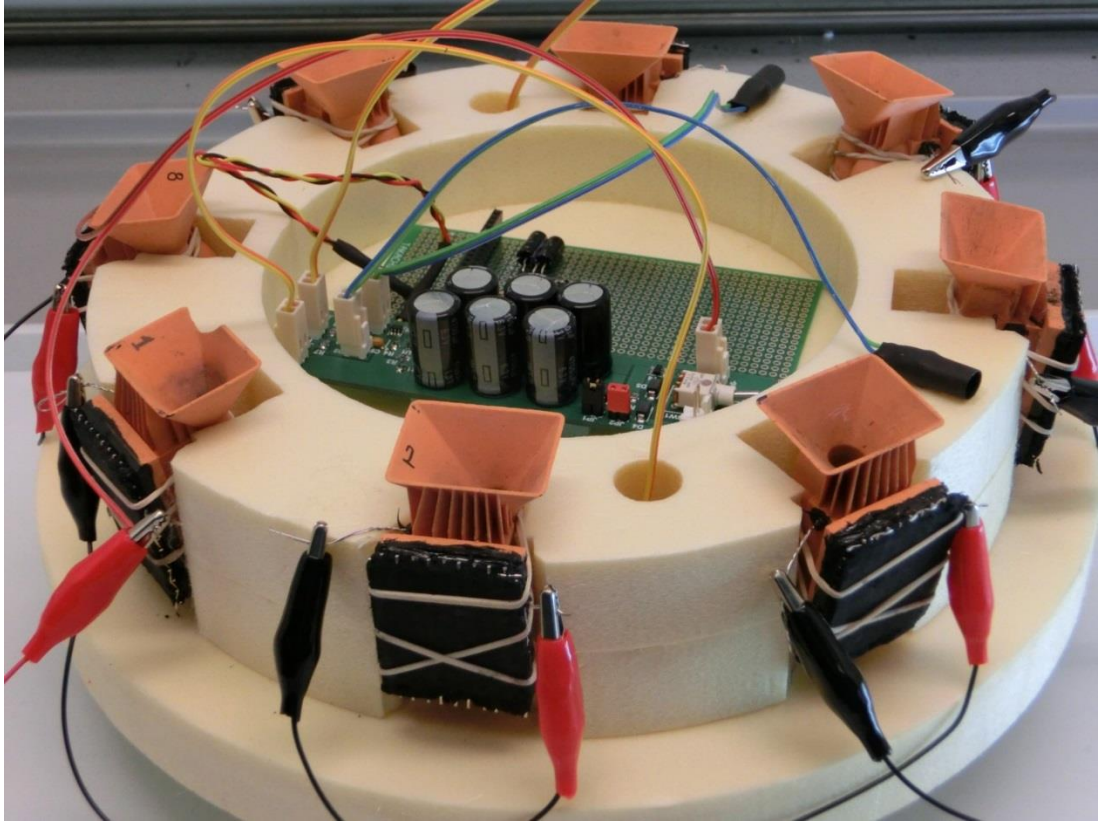


Figure A.1 Close-up photo of EcoBot-II 2018 edition.

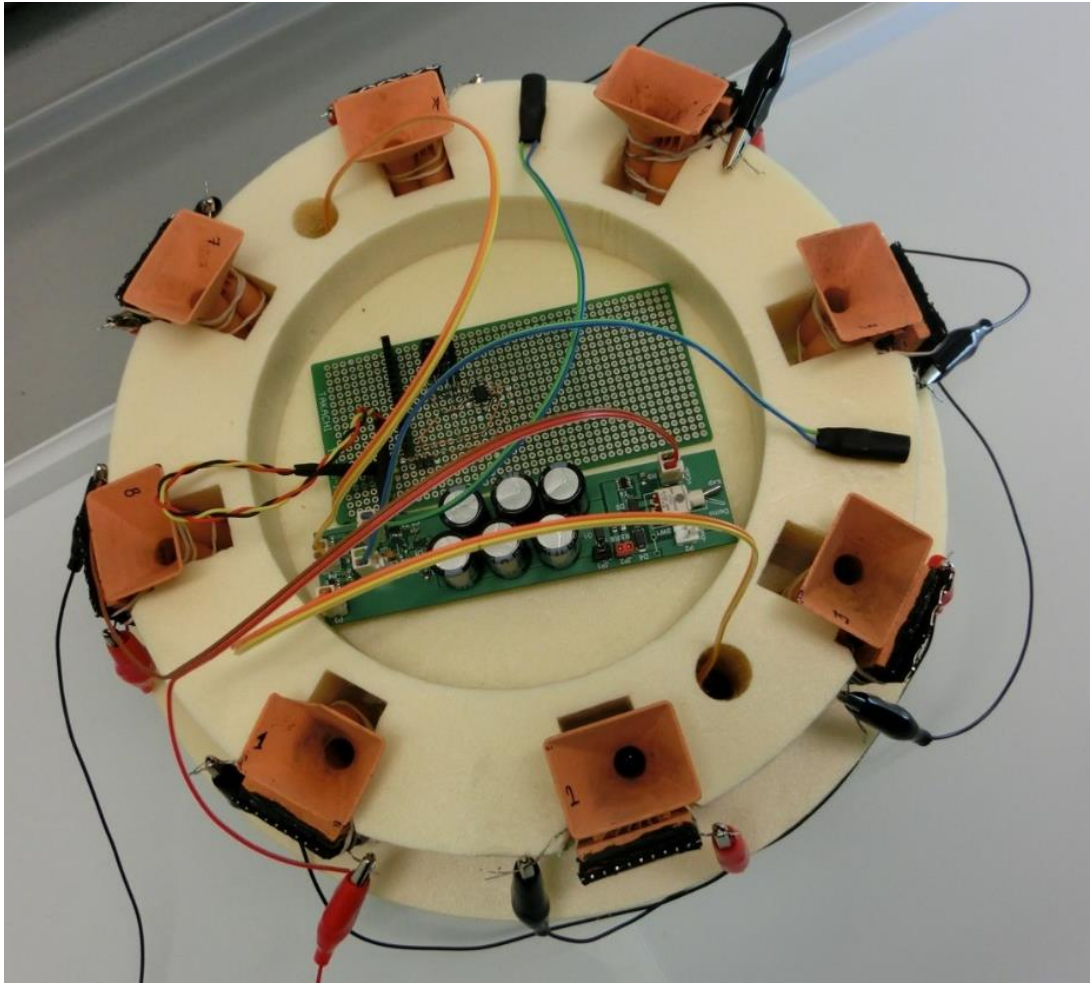


Figure A.2 Close-up photo of EcoBot-II 2018 edition from above.

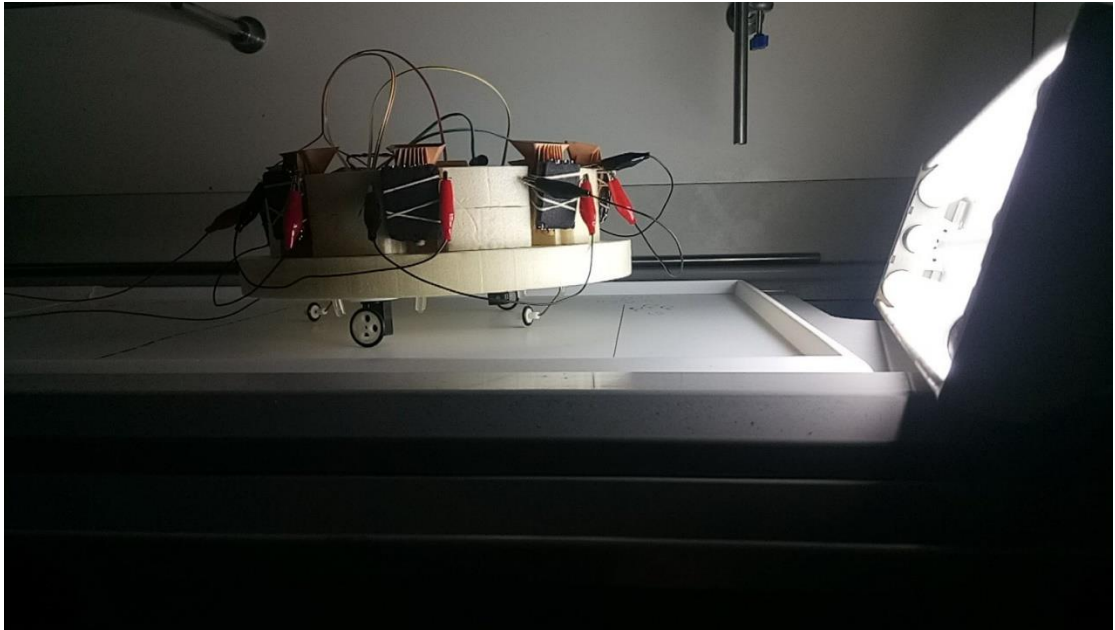


Figure A.3 Photo of EcoBot-II 2018 edition (from the side) performing phototaxis.

ⁱ Beveridge, T.J., Chang, I.S., Kim, B.H., Kim, S., Culley, D.E., Reed, S.B., Margaret, F., Saffarini, D.A., Hill, E.A., Shi, L., Dwayne, A., Gorby, Y.A., Yarina, S., Mclean, J.S., et al. (2009) Electrically conductive bacterial nanowires produced by *Shewanella oneidensis* strain MR-1 and other microorganisms. *Proceedings of the National Academy of Sciences*. 106 (23), pp. 9535–9535. Copyright (2006) National Academy of Sciences, U.S.A.

ⁱⁱ Credits to *Shewanella oneidensis* image by Rizlan Bencheikh and Bruce Arey, Environmental Molecular Sciences Laboratory, DOE Pacific Northwest National Laboratory. Permission to use this image was not needed but the publisher asked to credit the U.S. Department of Energy Genomic Science program and the website <https://genomicscience.energy.gov>.

ⁱⁱⁱ Reprinted with permission from Logan, B. E., Hamelers, B., Rozendal, R., Schröder, U., Keller, J., Freguia, S., Aelterman, P., Verstraete, W. and Rabaey, K. (2006) 'Microbial fuel cells: Methodology and technology', *Environmental Science and Technology*, 40(17), pp. 5181–5192. doi: 10.1021/es0605016. Copyright (2006) American Chemical Society.

^{iv} Reprinted from Ieropoulos, I., Greenman, J. and Melhuish, C. (2010) 'Improved energy output levels from small-scale Microbial Fuel Cells.', *Bioelectrochemistry* (Amsterdam, Netherlands), 78(1), pp. 44–50. Copyright (2010), with permission from Elsevier.

^v Reprinted from Ieropoulos, I. a., Greenman, J. and Melhuish, C. (2013) 'Miniature microbial fuel cells and stacks for urine utilisation', *International Journal of Hydrogen Energy*. Elsevier Ltd, 38(1), pp. 492–496. Copyright (2013), with permission from Elsevier.

^{vi} Reprinted from Papaharalabos, G., Greenman, J., Melhuish, C. and Ieropoulos, I. (2015) 'A novel small scale Microbial Fuel Cell design for increased electricity generation and waste water treatment', *International Journal of Hydrogen Energy*, 40(11), pp. 4263–4268. Copyright (2015), with permission from Elsevier.

^{vii} Used with permission of the "Winfield, J., Chambers, L. D., Rossiter, J., Stinchcombe, A., Walter, X. A., Greenman, J. and Ieropoulos, I.. Copyright (2015), with permission from John Wiley and Sons.

^{viii} Reprinted from Ieropoulos, I., Greenman, J. and Melhuish, C. (2013) 'Miniature microbial fuel cells and stacks for urine utilisation', *International Journal of Hydrogen Energy*. Elsevier Ltd, 38(1), pp. 492–496. Copyright (2013), with permission from Elsevier.

^{ix} Used with permission of the Jung Rae Kim, Giuliano C. Premier, Freda R. Hawkes, Richard M. Dinsdale and Alan J. Guwy. Copyright (2009), with permission from Elsevier.

^x Reprinted with permission from Logan, B. E., Hamelers, B., Rozendal, R., Schröder, U., Keller, J., Freguia, S., Aelterman, P., Verstraete, W. and Rabaey, K. (2006) 'Microbial fuel cells: Methodology and technology', *Environmental Science and Technology*, 40(17), pp. 5181–5192. doi: 10.1021/es0605016. Copyright (2006) American Chemical Society.

^{xi} Reprinted with permission from Rabaey, K., Clauwaert, P., Aelterman, P. and Verstraete, W. (2005) Tubular Microbial Fuel Cells for Efficient Electricity Generation. *Environmental Science and Technology*. 39 (20), pp. 8077–8082. Copyright (2005) American Chemical Society.

^{xii} Reprinted with permission from Liu, H., Ramnarayanan, R. and Logan, E.B. (2004) Production of Electricity during Wastewater Treatment Using a Single Chamber Microbial Fuel Cell. *Environmental Science & Technology*. 38 (7), pp. 2281–2285. Copyright (2004) American Chemical Society.

^{xiii} Reprinted with permission from Liu, H. and Logan, B.E. (2004) Electricity Generation Using an Air-Cathode Single Chamber Microbial Fuel Cell in the Presence and Absence of a Proton Exchange Membrane. *Environmental Science & Technology*. 38 (14), pp. 4040–4046. Copyright (2004) American Chemical Society